RETROFITTING OF REINFORCED CONCRETE BEAM - COLUMN JOINTS USING BONDED LAMINATES

A thesis

Submitted in fulfillment of the requirements

for the award of the degree of

DOCTOR OF PHILOSOPHY

IN

CIVIL ENGINEERING

VARINDER SINGH

Registration No. 950902002

DEPARTMENT OF CIVIL ENGINEERING
THAPAR UNIVERSITY,PATIALA -147004
PUNJAB-INDIA

2015

RETROFITTING OF REINFORCED CONCRETE BEAM - COLUMN JOINTS USING BONDED LAMINATES

A thesis

Submitted in fulfillment of the requirements

for the award of the degree of

DOCTOR OF PHILOSOPHY

IN

CIVIL ENGINEERING

VARINDER SINGH

Registration No. 950902002

DEPARTMENT OF CIVIL ENGINEERING
THAPAR UNIVERSITY,PATIALA -147004
PUNJAB-INDIA

2015

CERTIFICATE

Certified that the work presented in the thesis entitled **"RETROFITTING OF REINFORCED CONCRETE BEAM- COLUMN JOINTS USING BONDED LAMINATES"** which is being submitted by Mr. Varinder Singh (Registration No. 950902002) in fulfillment of the requirements for the award of the degree of Doctor of Philosophy in Civil Engineering of Thapar University, Patiala is an authentic record of the candidate's own independent research work carried out by him under our supervision and guidance. The matter embodied in this thesis has not been submitted in part or full to any other university or institute for the award of any other degree.

Dr. S.K. Kaushik
Formerly, Professor and Head
Department of Civil Engineering
Indian Institute of Technology
ROORKEE-247667

Dr. Prem Pal Bansal
Assistant Professor
Department of Civil Engineering
Thapar University
PATIALA-147004

Dr.Maneek Kumar
Professor
Department of Civil Engineering
Thapar UNiversity
PATIALA-147004

DECLARATION

I hereby certify that the work which is being presented in this thesis, entitled "Retrofitting of Reinforced Concrete Beam- Column Joints Using Bonded Laminates", in fulfillment of the requirements for the award of degree of 'Doctor of Philosophy' in Civil Engineering submitted to Civil Engineering Department of Thapar University, Patiala is an authentic record of my own work carried out under the supervision of Dr. S.K. Kaushik, Dr. Maneek Kumar, Dr. Prem Pal Bansal, and wherever other research work is referred it is indexed in the list of references.

The matter presented in this thesis has not been submitted in part or full to any other university or institute for the award of any degree in India or abroad.

(Varinder Singh)

ACKNOWLEDGEMENT

God has provided me a cherished opportunity to express my grateful thanks to all who helped me in the completion of my doctoral thesis work. This acknowledgement is intended to be thanks giving to all those people who have been involved directly or indirectly with my dissertation work.

First and foremost, I would like to express my thanks and indebtedness to my guides Dr. Maneek Kumar, Professor, Dr. Prem Pal Bansal, Assistant Professor of Civil Engineering, Thapar University, Patiala and Dr. S.K. Kaushik, Formerly, Professor and Head Department of Civil Engineering, Indian Institute of Technology Roorkee, Roorkee for their deep involvement, invaluable and continuous motivation throughout this work. I am highly obliged to them for being there always whenever I needed them.

I would like to thank Dr. Naveen Kwatra, Head, Civil Engineering Department, Thapar University, Patiala who has been a constant source of inspiration for me throughout this work.

I do not find enough words with which I can express my feeling of thanks to the entire faculty and staff of Civil Engineering Department, Thapar University Patiala for their help, inspiration and moral support, which went a long way in the successful completion of my thesis.

The cheerful support of my friends Dr. Lakhvider Singh, Mr. Ravi Kant Pareek, Mr. Rachit Goyal, Mr. Ajayveer Sidhu and colleagues is sincerely appreciated. Special words of appreciation go to Sh. Varinder Kumar and other laboratory staff, who helped me in the experimental work.

Above all, I thank my parents, Sh. Satnam Singh and Smt. Kamlesh Kumari, whose love and affectionate blessings have been a constant source of inspiration in making this thesis a reality.

My wife Yogita Joshi, has borne the pains and distress of daily routine. My daughter Alankrita V.S. and son Bhavya Pratap Singh always kept my morale high with their ever smiling and cheerful faces. They always were a great source of support and encouragement, especially in all my academic endeavors and deserve all admiration.

Finally, I wish to express my thanks to all those who remained behind the scene but whose work has been consulted and quoted in the present research.

In the end, I am thankful and grateful to the Almighty for bringing this day in my life.

(Varinder Singh)

ABSTRACT

Reinforced concrete is one the most abundantly used construction material, not only in the developed world, but also in remotest parts of the developing world. Thousands of reinforced concrete structures are constructed annually and a large number of these deteriorate or become unsafe before the end of their design life. Strengthening of existing reinforced concrete structures is now a major component of construction activity. The RCC structures constructed across the world are often found to exhibit distress and suffer damage, even before service life is over, due to several causes such as earthquakes, corrosion, overloading, improper design, faulty construction, explosions, fire etc. With the mandate to go vertical, due to rising population and space crunch, most of the structures which have come up over the last three or more decades are all framed structures. In such structures, the most important link for transferring loads and stresses are the beam-column joints. The structural design of these joints is usually neglected. Unsafe designs and detailing within the joint region is dangerous for the entire structure, even though the structural members themselves may conform to the design requirements. It is well known that the joint regions in reinforced concrete framed structures are very critical as they transfer the forces and bending moments between the beams and columns. In most cases, during extreme loading, the beam-column joints, if not designed properly are the most vulnerable component. With the advent of revised design and detailing codes and increase in the earthquake vulnerability level of many regions, the existing structures need strengthening to conform to the revised codal provision.

The strengthening and enhancement of the performance of deficient structural elements in a structure or the structure as a whole is referred to as retrofitting. Retrofitting of a structure is not the same as repair or rehabilitation. Repair refers to partial improvement of the degraded strength of a structure after an earthquake, in fact, it is only a cosmetic treatment. Rehabilitation is a treatment of the structure aimed at achieveing the original strength of the structure after it has deteriorated and suffered damage. Retrofitting means structural strengthening of a structure to a predefined performance level irrespective of whether the structure is damaged or not.

The repair or strengthening of an existing structure is a greater challenge for a civil engineer compared to designing or constructing a new one. A specfic technology has to be designed and developed to re-establish the strength of damaged structures, and to improve the performance for new functions of old undamaged structures. Thus, the technique to be used should be simple in implementation; offer better performance when handled by less experienced workers and must use materials that are readily available, durable, strong and economical. Retrofitting of individual members is referred to as 'local retrofitting'. For this, a large number of techniques are being used including replacement technique, removal, injection technique, shotcreting and plate bonding etc. Amongst all the above techniques the plate bonding technique is found to be the most efficient and suitable method for retrofitting purposes. In the plate bonding technique, Ferrocement Plates, Fiber Reinforced Polymer (FRP) Plates, Polymer modified concrete and mortar (PMC/PMM) and Steel plates are most commonly used for retrofitting. Of this techniques the use of Fiber Reinforced Polymer (FRP) Plates has gained significant popularity in the last two to three decades. But this technique is costly and requires skilled labour. Various authors have suggested the use of ferrocement jacketing as a more attractive choice in place of FRP plate bonding technique due to its easy application, lesser weight, higher impermeability, improved tensile strength, economical use, and long life term performance.

In the present study, an effort has been made to study the effect of ferrocement jacketing on the strength of retrofitted beam-column joints. The studies have been carried out for various parameters like number of wire mesh layers and their orientation in the ferrocement jackets and initial stress levels of the beam-column joints. The effect of these parameters on the strength of reinforced concrete beam-column joints initially stressed to pre-determined levels, and subsequently retrofitted with ferrocement jackets was investigated. A similar set of beam-column joints was also retrofitted using two layers of CFRP jackets with an orientation of 45° to the longitudinal axis of the joint, to study the behavior of such beam-column joints.

Subsequently, a 3D nonlinear finite element (FE) model using software ATENA-3D was used to validate the experimental results. Comparison between the finite element and experimental results confirms a reasonable accuracy of the proposed model.

The test results showed that retrofitting beam-column joints with different layers of wire mesh in the ferrocement jackets and two layers of CFRP jacketing significantly increased the ultimate and yield load carrying capacity, stiffness of all the joints stressed to various levels, establishing

the efficacy of using the material for retrofitting. The use of ferrocement and CFRP jacketing for retrofitting of initially stressed beam-column joints helped to regain full strength even if stressed to 85% of the ultimate load. Due to the strengthening of beam-column joints of control specimens, the failure of the retrofitted beam-column joint specimens shifted from the joint region to the beam ends in the retrofitted specimens. This would help in preventing progressive collapse of the structure. The retrofitting of the beam-column joints may thus shift the failure from the joint to the beam end to obtain a weak beam- strong joint failure pattern. The comparison between the load-deflection results obtained from ATENA 3D and the experimental study shows that the ATENA 3D results agree reasonably with the experimental results. The variation of experimental and FEM (ATENA 3D) load results for the control as well as retrofitted specimens was within ± 10%. The element modeling (ferrocement and CFRP) showed higher values as compared to the experimentally obtained values.

CONTENTS

LIST OF TABLES

LIST OF FIGURES

LIST OF PLATES

Plate No. **Title** **Page No.**

CHAPTER – 1

INTRODUCTION

1.1 GENERAL

In various parts of the world, the behavior of reinforced concrete (RC) moment resisting frames during recent earthquakes has highlighted the consequences of poor performance of reinforced concrete (RC) beam-column joints. Reinforced concrete beam-column joints in a RC moment resisting frame are crucial zones for effectively transferring loads between the connecting beams and columns in the structure. The RC structures, constructed in the developed world, are often found to exhibit distress and suffer damage even before service life is over due to several causes, such as improper design, faulty construction, overloading, earthquakes, explosions, corrosion, wear and tear, flood, fire, etc. The majority of the houses, which are still being constructed using indigenous techniques, do not follow the codal provisions due to lack of knowledge and guidance. Such non - engineered constructions are mostly prevalent in earthquake prone areas of the developing world, which include countries like India, Pakistan, Turkey and Iran.

In Indian structural design practice, the beam-column joint is generally neglected for specific design. As per the existing codes the concentration is limited only to providing sufficient anchorage for the longitudinal reinforcement of the beam reinforcement in the columns. This may not be acceptable under seismic effects. There have been many severe failures reported in the past earthquakes, in particular during the Turkey and Taiwan earthquakes due to the faulty design of beam-column joints. The two major failure modes for the joints are (a) joint shear failure and (b) end anchorage failure (Figure 1.1). A typical example of a beam-column joint failure during the 1999 Turkey earthquake is shown in (Figure 1.2).

(a) Joint Shear Failure

(b) Inadequate Reinforcement Anchorage

Figure 1.1: Major Failure Modes for a RC Beam-Column Joints

(Ghobarah et al; 2002)

Figure 1.2: Typical Beam-Column Joint Failures (1999 Turkey earthquake)

(Ghobarah et al; 2002)

1.2 BEAM-COLUMN JOINTS

The beam-column joint is defined as the portion of the column within the depth of the deepest beam that frames into the column Three types of the beam-column joints can be identified in the moment resisting frames i.e. an exterior joint, interior joint and a corner joint (Figure 1.3). When all the vertical faces of the column are framed by four beams, the joint is called the interior joint. When two adjacent faces of a column are framed by a beam, then the beam-column joint is called a corner joint. When one beam frames into a column and two more beams frame into the joint orthogonally, it is called an exterior joint.[ACI-ASCE 352R-02].

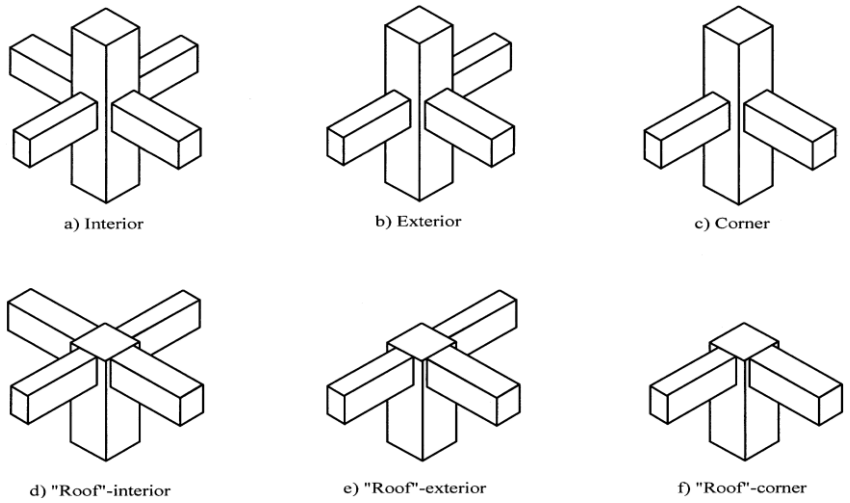

Figure 1.3: Types of Beam-Column Joints [ACI-ASCE 352R-02]

The reinforced beam-column joints are known as the most vulnerable and critical region of a reinforced concrete moment resisting structure specially when subjected to seismic loads. The way the structure behaves during an earthquake is mainly governed by the behavior of beam-column joints. If beam-column joints behave in a brittle manner then the structure will display a brittle behavior and if beam-column joints behave in a ductile manner, the behavior of structures will be a ductile one. The RC beam-column joints are subjected to large shear stresses in the joint region under the action of seismic forces. High bond stresses are also forced on reinforcement bars going into the joint. These difficulties have been highlighted in the past years too by the damage observed during earthquakes in different countries.

Unsafe design and detailing within the joint region destroy the entire structure, even if other structural members conform to the design requirements. In the past three decades, extensive research has been carried out on studying the behavior of joints under seismic conditions through experimental and analytical studies. Various international codes of practices have been undergoing periodic revisions to incorporate the research findings and put them into practice.

Generally, a three phase approach (*Sasmal; 2009)* is followed to describe a structure under seismic loading, which is underlined below;

(1) The structure must have adequate lateral stiffness to control the inter-storey drifts such that no damage would occur to non- structural elements during minor but frequently occurring earthquakes.
(2) During moderate earthquakes, some damage to non- structural elements is permitted, but the structural element must have adequate strength to remain elastic so that no damage would occur.
(3) During rare and strong earthquakes, the structure must be ductile enough to prevent collapse by aiming for repairable damage which would ascertain economic feasibility.
The design of beam-column joints is an important part of the earthquake resistant design of reinforced concrete moment-resisting frames, due to the difficulty in repairing and retrofitting of the buildings damaged at beam-column joints due to the seismic attack. Recent building codes for reinforced concrete buildings provide for allowable joint shear stresses to preclude premature failure of beam-column joints before the beam sway mechanism is developed.

Many theoretical and experimental studies have been carried out regarding beam-column joints since the 1970's. Especially, three-country joint research efforts (America, Japan and New Zealand) did make remarkable improvements in the joint design. Reflecting the results of these studies, ACI Recommendations divide joints into two categories (ACI 352-R02)

i) Type 1 for structures in a non-seismically hazardous area
ii) Type 2 for structures in a seismically hazardous area

In spite of the cooperative research efforts, the three countries have proposed different views on shear mechanisms and joint shear strength of beam-column joints. As per ACI recommendations and AIJ guidelines (AIJ 1999), the prediction of joint shear strength is based on the concrete arch mechanism, while according to the NZS (New Zealand Standard) code *(NZS,1982)*, joint shear

strength is evaluated by both arch and truss mechanisms. Furthermore, although the three country codes agree that the concrete compressive strength and the joint area are two of the most important factors to evaluate joint shear strength, they have different opinions on the effect of reinforcement ratio on joints.

Beam-column joints are critical regions of reinforced concrete frames designed for an inelastic response to seismic attack. Inadequately detailed joints, especially exterior beam-column joints, may fail prematurely in a brittle manner due to high shear stresses. In earthquake prone regions, the joints of Ductile Moment Resisting (DMR) frames must be designed and detailed to allow large energy dissipation in adjacent plastic hinges without a significant loss of strength and ductility. Designing beam-column joints is considered to be a complex and challenging task for structural engineers and careful design of joints in RC frame structures is crucial to the safety of the structure, although the size of the joint is controlled by the size of the frame members. Joints are subjected to a different set of loads from those used in simply designing beams and columns. As a result, it is necessary to pay special attention to the detailing of reinforcement within a joint region. When frames are not designed properly, the possibility of a plastic hinge formation in the columns increases. This is not desirable for two reasons: firstly, the collapse mechanism associated with hinges in the columns has a lower ultimate load and secondly, the energy absorption of plastic hinges within the columns is normally less due to the reinforcement arrangement and the axial load. Engineers can avoid this when designing DMR frames by employing the principle of strong-column weak-beam design. According to this the columns and beams are designed so that the joint region and the column remain essentially elastic under the action of high lateral loads, which may occur due to earthquakes and high pressure winds, while the main energy dissipation occurs within the plastic hinges formed in the beams. Special care also should be taken to make sure that plastic hinges within the beam are sufficiently distanced away from the joint. This is to ensure that penetration of plasticity to the joint core will not occur, as this may trigger a brittle failure within the core.

In each of the following two scenarios, rehabilitation may become necessary within the beam region adjacent to a joint:

i) Repair, when after a moderately large earthquake, visibly significant cracks remain open in the beam end of the joints indicating that some residual plastic deformation is present.

ii) Retrofit, when detailing of the beam reinforcement is not done adequately at the design/construction stage and subsequently there is a danger of potential plastic hinge cracks penetrating to the joint core *(Paulay et al; 1992)*.

Such unserviceable structures require immediate assessment or inquiry into the cause of distress, and suitable remedies and measures need be taken to avoid collapse, which can bring about huge loss of human lives and economy. In the last few decades or so, several attempts have been made in India and abroad to study these problems and to increase the life of such structures by suitable retrofitting and strengthening techniques.

1.3 BEHAVIOUR OF BEAM-COLUMN JOINTS

The basic understanding of the mechanics of shear transfer within a joint is required before a suitable retrofitting technique can be suggested. It is also necessary to evaluate the seismic performance of the joint in as- built condition. The model of forces acting on a joint depends upon the design of the joint and the type of loads acting on it. With reference to stresses the effects of loads on the three types of beam-column joints are discussed herein along with the related crack patterns which can develop in the joints. Figure 1.4.1 (a) shows the forces on an interior beam-column joint subjected to gravity loading. From the beam ends, the compression and tension, and the axial loads from the columns can be transmitted straight through the beam-column joint. Diagonal tensile and compressive stresses within the joint increases in case of lateral loading as shown in Figure 1.4.1(b). Development of cracks will be perpendicular to the tension diagonal A-B in the beam-column joint and at the faces of the beam-column joint where the beams frame in the joint. The struts in compression side are shown by dashed lines and tension ties are shown by solid lines. As concrete is weak in tension, so transverse reinforcements are provided in such a way that they cross the plane of failure to resist the diagonal tensile forces. Figure 1.4.2 shows the forces acting on the exterior beam-column joint. The development of diagonal cracks is due to the shear force so it requires reinforcement at the joint. The efficiency of the joint directly depends on the longitudinal reinforcements details. Figure 1.4.2 (b) and Figure 1.4.2 (c) shows typical reinforcement detailing for exterior beam-column joints. It was observed that detailing as per 1.4.2 (b) results in efficiencies in the

range of only 25 to 40 % when the bars are bent away from the joint core where as 85- 100% more efficiency is achieved by passing the bars through and anchoring them in the joint core as shown in Figure 1.4.2 (c). To confine the concrete a core within the joint the stirrups have to be provided [Uma et al; 2003].

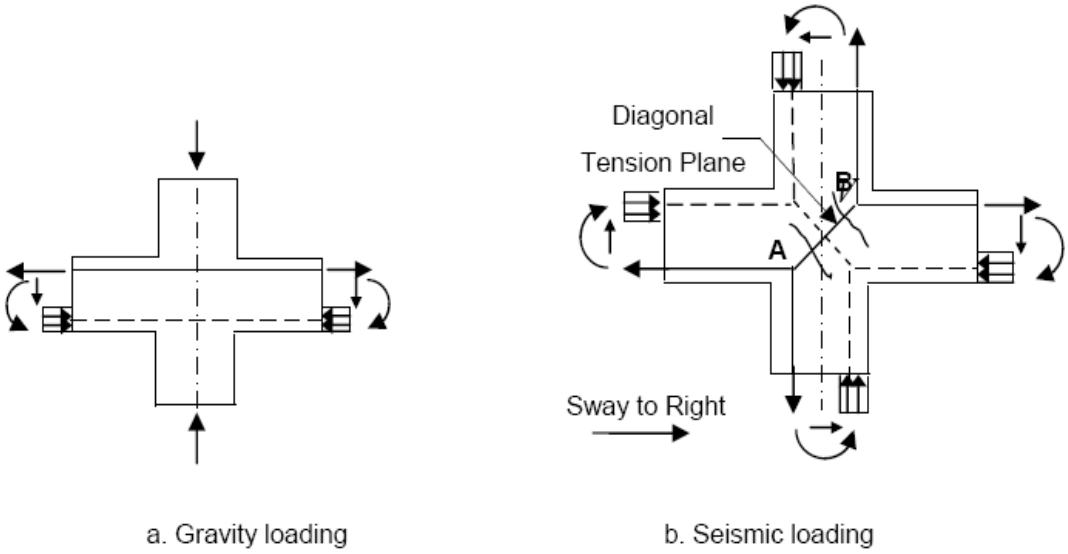

Figure: 1.4.1 Interior Joint

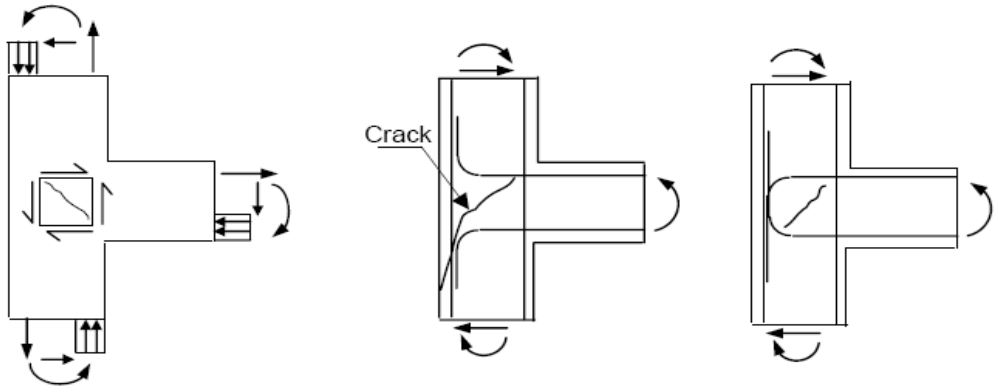

Figure: 1.4.2 Exterior Joint

Figure 1.4.3 (c) shows the forces in a corner beam-column joint having a continuous column above the joint. The other type of joints are wall type corner joints in which the applied moments are likely to either close or open the corners. They may be known as either knee joints or L-joints. Opening corner beam-column joints are likely to develop rising cracks at the reentrant corner and this type of failure is noticeable by the development of a diagonal tensile crack. The longitudinal reinforcement detailing extensively affects the joint behavior. In a closing joint the forces developed are exactly opposite to those in an opening corner joint and they show better effectiveness than the opening joints. The reversal of forces is expected to develop during seismic actions, so the corner beam-column joints have to be conventionally designed as opening joints with proper detailing.

From the framing elements the stress resultants are transferred into the joint through bond forces beside the longitudinal steel bars passing during the joint. The beam-column joints must have adequate strength to oppose the induced stresses and enough stiffness to control excessive deformations [Uma et al; 2003].

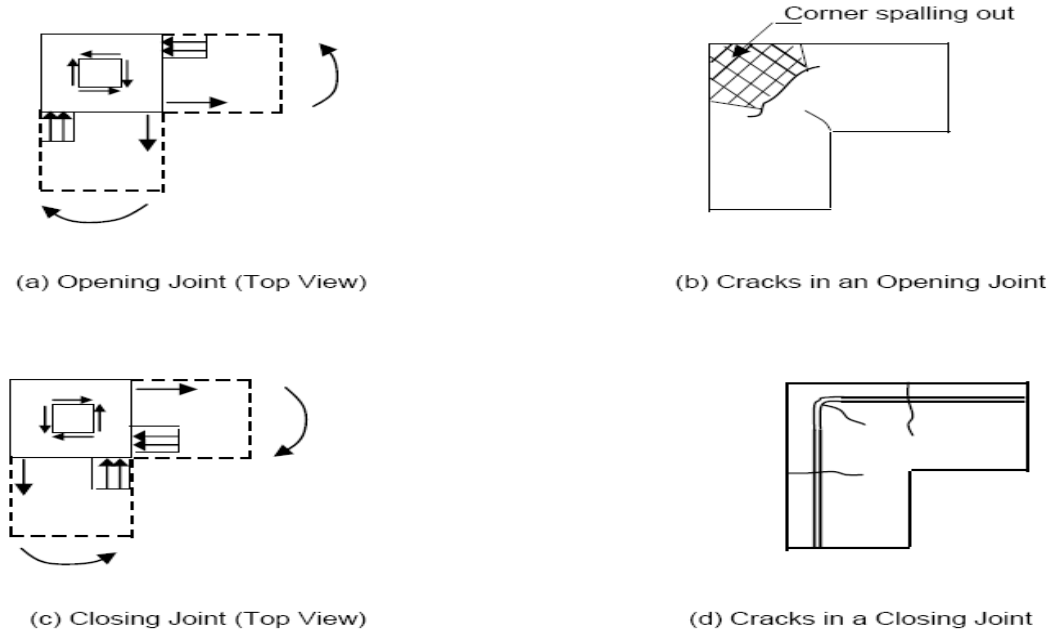

Figure 1.4.3 Corner Joints

Figure 1.4: Behavior of Joints [Uma et al; 2003]

1.3.1 Earthquake Behavior of Joints

In a beam-column joint, the beams adjacent to the joint develop the moments in clockwise or anticlockwise direction during the earthquakes as shown in Figure 1.5, indicating that the top and opposite bars tend to get pulled in opposite directions as shown in Figure 1.6 (i). The bond stress developed between the concrete and steel in the joint region try to balance these forces. If the beam-column joints are not properly designed, the steel will slip inside the concrete and the load carrying capacity of beams will be reduced and beam-column joints will suffer geometric distortion during the action of pull-push forces at top and bottom ends of the joint. Also the beam-column joint will compress and elongate the diagonal length as shown in Figure 1.6(ii) [Robert S; 2009].

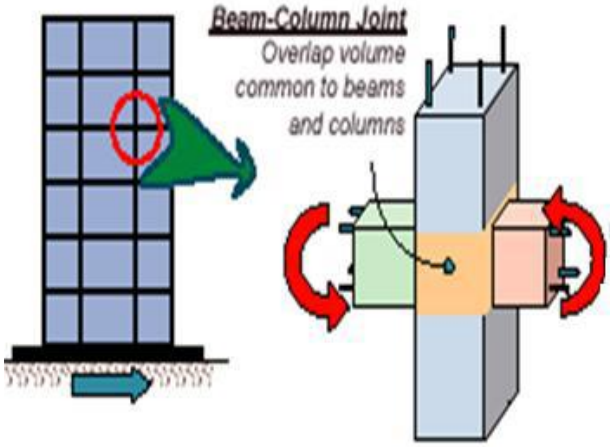

Figure 1.5: Beam-Column Joints Critical Parts of a Structure [Robert S; 2009]

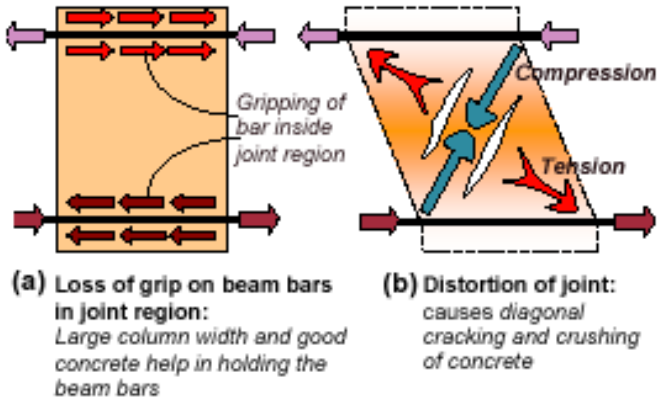

Figure 1.6(i) Pull-Push Forces on Joints [Robert S; 2009]

Problems of diagonal cracking and crushing of concrete in the joint region can be controlled by either providing large column sizes and/or by providing closely spaced closed-loop steel ties around column bars in the joint region. The ties hold together the concrete in the joint and also resist shear forces, thereby reducing the cracking and crushing of concrete. Indian Standard IS: 13920-1993 recommends continuing the transverse loops around the column bars through the joint region. In practice, this is achieved by preparing the cage of the reinforcement (both longitudinal bars and stirrups) of all beams at a floor level on top of the beam formwork of that level and lowering it into the cage. However, this may not always be possible particularly when the beams are long and the entire reinforcement cage becomes heavy.

The gripping of beam bars in the joint region is improved first by using columns of reasonably large cross-sectional size. The Indian Standard IS: 13920-1993 requires building columns in seismic zones III, IV and V to be at least 300 mm wide in each direction of the cross-section when they support beams that are longer than 5m or when these columns are taller than 4m between floors (or beams). The American Concrete Institute recommends a column width of at least 20 times the diameter of the largest longitudinal bar used in adjoining beam. [Senthil et al; 2010].

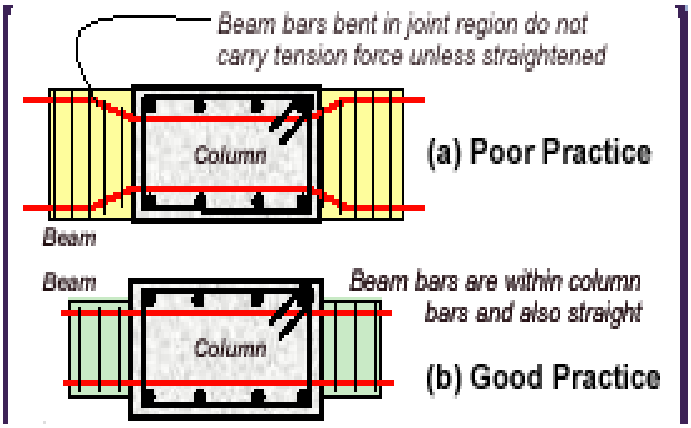

Fig 1.6 (ii): Anchorage of Beam Bars in Interior Joints [Robert S; 2009]

1.4 RETROFITTING

A significant number of structures in India were designed according to older versions of seismic codes. Although, these types of structures, in light of the revised codal provisions, were very vulnerable to unexpected earthquakes, some modifications to their structural configuration and material properties showed improvement in their seismic performance. Thus, retrofitting was suggested to be carried out and practitioners started to apply various interventions to the structures to make them earthquake resistant. In general terms, whereas partial improvement of degraded strength of a structure is known as repairing, retrofitting is the strengthening of structure to a pre-defined level.

Thus the strengthening and enhancement of the performance of deficient structural elements in a structure or the structure as a whole is referred to as retrofitting. Retrofitting of a structure is not the same as repair or rehabilitation; repair refers to partial improvement of the degraded strength of a structure after an earthquake. In fact, it is only a cosmetic enhancement. Rehabilitation is a fictional improvement, wherein the aim is to achieve the original strength of a structure after it has deteriorated and suffered damage. Retrofitting means structural strengthening of a structure to a predefined performance level irrespective of whether the structure is damaged or not. A survey of existing residential buildings reveals that many buildings are not adequately designed to resist earthquakes. In the latest revision of the Indian earthquake code, IS1893-2002, many regions of the country were placed in higher seismic zones. As a result many buildings designed prior to the revision of the code are not likely to perform adequately as per the provisions of the new code. It is, therefore, recommended that the existing deficient structure be retrofitted to improve their performance in the event of an earthquake and to avoid large scale damage to life and property (*Dowrick,(2003)*.Thus, the main objectives of retrofitting, as per IS: 13935: 1993 and White (1995), can be categorized as

- To achieve the desired act most successfully and inexpensively.
- To increase the stiffness and load carrying capacity.
- To remove the feeble points, where stress consideration is possible.
- To improve the energy dissipation and energy absorption capacity.

1.4.1 Retrofitting Steps

According to Basu (2002) the retrofitting plan involves the following steps.

(a) Assessment

Assessment means inspection of the aptness of an existing structure for the preferred purpose as per the most up-to-date codal provisions. The evaluation process includes collection of data related to the structure, preparation of on site drawings, structural design and drawings according to the changed provision of code (if any), manual inspection of the structure, finding test values as per site requirement. The building is analyzed and designed after the collection of the data as per the codes. In any case if the structure fails to attain the target code level or if the need to capacity ratios of the structure is greater than 1, then retrofitting becomes essential. According to an identified deficiency in the structure, the economic feasibility and probable performance of the structure after retrofitting, is carried out as this helps to decide whether to destroy, retrofit, repair or rebuild the structure.

(b) Retrofit Scheme

Depending upon the deficiencies of the structure the retrofit scheme is selected and the members of the structure to be strengthened are identified. The various retrofit schemes possible are discussed in the subsequent section.

(c) Selection of Retrofit Scheme

By using the structural analysis and design of the structure to be retrofitted, the selection of a particular retrofitting method is finalized. After retrofitting the possible types of failure are also studied.

(d) Construction and Monitoring

The selected technique should be easily executable at the site. The efficiency of the retrofit technique wholly depends on the quality and effectiveness of execution. It is imperative to find any defect or deficiency by monitoring the performance of the retrofitting technique. This monitoring may lead to alteration of the design strategy and arrangement for future retrofit projects.

1.4.2 Retrofitting Plan

The retrofitting plan may be classified into the following three categories.

I. Global Retrofitting
II. Local Retrofitting
III. Base Isolation and Energy Dissipation

I. Global Retrofitting

If the structure is retrofitted as a whole the retrofitting known as global retrofitting. This type of retrofitting is used to recover the overall behavior of the structure. Global retrofitting strategies are adopted when an estimate of the structure shows larger demand to capacity ratios in the components throughout the structure than normal. It may occupy providing extra elements like braced frames, shear walls, decrease in the vertical irregularities, decrease in the mass, improving the links between elements.

II. Local Retrofitting

If the individual elements are retrofitted the type of retrofitting is known as local retrofitting. In cases where a few members of a structure are found deficient then this technique is preferable. This retrofitting technique includes the retrofitting of beam-column joints, all type of beams, columns, walls and footings. The different local retrofitting plans are discussed in details in the next section.

III. Base Isolation and Energy Dissipation

Base isolation and energy dissipation devices are used for improving the behavior of the structure during an earthquake. During an earthquake energy dissipation devices such as viscous fluid dampers, yielding plates / friction pads are used for energy dissipation in the structure. According to Tsai and Lin (1993) during a earthquake, to satisfy any undesirable vibration a turned mass damper having a spring mass, viscous damper attached. A damper is tuned to natural frequency to a near the natural frequency of the main scheme; due to this the damper shakes in tune, dissipating the vibrating energy due to the damping in the turned mass damper.

1.4.3 Retrofitting Techniques

Before the discussion of retrofitting techniques it is necessary to discuss the repair techniques. Some of the repair techniques are as discussed below:

(a) Epoxy Injection Technique

To fill the voids and rebinding the cracked structure, injection of high strength epoxy is used in this technique. Repair of fine cracks, filling large cracks and surface coating, depend on the viscosity of the epoxy. Drilling holes at close centers along the cracks and installing entry ports and injecting epoxy under pressure is used in the technique.

(b) Mortar Injection Technique

Pre-mixed mortar is injected in this method. This method is used to repair older works where the usual introduction of concrete is difficult. Retaining walls, piers, are repaired by this method. Compacted accumulation of dirt free and fine graded aggregates injected grout into the voids with uninterrupted operation in this technique.

(c) Epoxy Mortar Filling Technique

In this technique, epoxy mortar is made using low or high viscosity epoxy mixed with fine aggregate. Cement concrete has higher modulus of elasticity and lower compressive and tensile strengths as compared with epoxy. Larger voids are filled using this technique.

(d) Shotcreting Technique

This technique is suitable for repair works where concrete is to be positioned among existing elements where a close surface is desired. The concrete mix which sprayed in-situ is generally called shortcrete. It may be placed either dry mix or wet mix method. To amend the structural properties of concrete/mortar, fibers of steel, polypropylene or additional material may be used jointly with the admixture to be placed in position.

(e) Removal and Replacement method

In this method loose and broken concrete is replaced with new concrete. Extra steel may be provided by welding it to existing steel. The epoxy, sand, mortar may also be other replaced.

(f) Repair with Steel Fibrous Concrete

In this method the broken portion of concrete is removed and recast using steel fibrous concrete. SFC shows better shear strength, better ductile behavior, and better stiffness as compared to normal concrete.

(g) Plate Bonding Techniques

The concept of plate bonding technique is mainly based on the information that concrete is having high compressive strength and poor tensile strength. In arranging to increase the strength of the concretes plates of special materials are bonded on the web faces of the structural elements by any of the following;

i. Epoxy Adhesives
ii. Cement Slurry
iii. Shear Connectors
iv. Combination of Epoxy Adhesives and Cement Slurry with Shear Connectors

The following types of plates are most commonly used in this technique;

i. Ferrocement Plates
ii. Fiber Reinforced Polymer (FRP) Plates
iii. Polymer modified concrete and mortar PMC/PMM
iv. Steel plates

The salient characteristic of each of these techniques are discussed below:

(i) Ferrocement Plates

Ferrocement plates are lean walled reinforced concrete usually constructed with cement mortar which is reinforced with intimately spaced layers of constant and quite small size wire mesh. Ferrocement is able to resisting high tensile, shear, impact and fatigue stresses with outstanding maintance to corrosion and access of water. The load carrying capacity may be increased using

ferrocement plates by casting-in-situ or gluing to the surface of the element by a suitable bonding agents. FRP and steel plates has more cost as compared to the ferrocement, so ferrocement plates are the perfect choice to the FRP and steel plates.

(ii) Fiber Reinforced Polymer Plates

A group of materials collected with inorganic and organic fibers implanted in a resin matrix is known as Fiber Reinforced Polymers. Fiber Reinforced Polymers have tremendous properties such as high tensile strength and stiffness. FRPs are light in weight, non-magnetic, and offer superior resistance to corrosion, which make FRPs particularly appropriate for the treatment and strengthening works. High strength to weight ratio and high corrosion resistance is the main advantage of FRP. FRP plates are two to ten times stronger than steel plates, while their weight is just 20% of that of steel, though, in the market their cost is high. Fiber Reinforced Polymer composites are shaped by embedding a constant fiber matrix in resin matrix. The resin matrix binds the fiber together and also provides bond between concrete and fiber reinforced polymer. Generally, Glass Fiber Reinforced Plastics (GFRPs), Carbon Fiber Reinforced Plastics (CFRPs) and Aramid Fiber reinforced plastics (AFRPs) are used in the construction industry. FRP is are instinctively different from steel because it is anisotropic. It is elastic linearly and has generally high strength with inferior modulus of elasticity than steel. The sheets of Fiber Reinforced Polymers are light, flexible, and thin sufficient to be inserted following the pipes, cables, and other service ducts thus are easy in their fitting. The main drawback is FRPs vulnerability to moisture and refuse of properties at higher temperatures. FRP can also be used as reinforcing bars. FRP bars can also be attached to web of a beam for shear strengthening (Lorenzis and Nanni, 2001, 2002).

(iii) Polymer Modified Concrete and Mortar PMC/PMM

Built with a grouping of single units called monomers having long molecule hydrocarbons, are known as Polymers, are made in a process called polymerization. The particles with small diameter of polymers emulsified with water are known as polymer latexes. These polymer latexes shape a continuous film when drying. In the dry cement aggregate mix these types of polymers can also be used in the form of dispersible powder. When water is added in the dry cement aggregate mix, the development is like that described above. The PMC/PMM shows

superior workability and water preservation properties to normal concrete/mortar. The main benefit of PMC/PMM is its enhanced adhesion and bonding with existing cement concrete and considerably reduced permeability.

(iv) Steel Plates

This retrofitting technique was originated in South Africa, wherein steel plates were used to strengthen the concrete elements as some of the steel had been accidentally misplaced in the structures. The steel plates considerably increased the strength, ductility, stability and stiffness of the structural elements. Steel plates also reduce the clear crack width. The bonding of steel plates is very easy to apply, even when structural element is in the use. The steel plating may be bonded on the tension face or on the side faces of the structural elements. Higher increase in stiffness and in flexural strength has been achieved in tension face plates. Shear capacity and the flexural strength increases mainly for side-face plating, up to a restricted level. A U-shaped retrofitting may also be done using a combination of the above two methods. This method shows good results but having some drawbacks such as jeopardy of corrosion. Due to limited transportation of the length steel plates might need the lengthening using welding methods.

From the techniques discussed above, plate bonding techniques are one of the most successful and suitable methods for jacketing. Amongst these plate bonding techniques FRP plates are fairly accepted these days. Although, it is noted that the use of FRPs is limited to developed countries or urban areas of the developing countries as they have higher initial cost and its application requires skilled persons for the purpose. Thus, there is a need to develop another technique, which is cheap and can be executed with the help of semi-skilled persons present at the site. Ferrocement jacketing has established itself to be one such striking technique due to its properties of being lightweight, economic, good tensile strength, water tightness, trouble-free application and longer life span. Thus it was proposed to use ferrocement jackets for carrying out the current study due to its valuable properties of having low thermal conductivity, lightweight, durable, ease of being cast into any form. Ferrocement jacketing is economical and does not require any specifically skilled persons for execution. It was also proposed to use CFRP Jackets for comparison purposes. A review of the earlier carried out work using ferrocement and FRPs is presented in the succeeding chapter.

1.5 OBJECTIVE AND SCOPE OF THE RESEARCH

1.5.1 Gap in the Research Area

The main drawbacks which limit the use of ferrocement for retrofitting of beam-column joints are firstly, the agent used for bonding the ferrocement laminates to the affected reinforced cement concrete element, requires skilled labour for application and secondly, is very uneconomical. Thus, there is a need for developing a technology, which is not only economical but can also be easily used in the field. The studies done so far on the retrofitting of RCC beam-column joints also do not include the effect of wire mesh layers and their orientation on the strength and other related parameters, the type of wire mesh commonly available in the market, and the effect of retrofitting beam-column joints at different stress levels. Normally epoxy has been used for bonding ferrocement plates with the existing stressed beam-column joints. No study has been done for other possible bonding materials and methods. Also, due to the non availability of a specific design methodology, there is a need to develop the same for retrofitting of beam-column joints.

From the literature survey presented in the preceding section it is observed that very little work has been done on **retrofitting of reinforced concrete beam- column joints using bonded laminates**, specifically the use of ferrocement for the purpose. Keeping this in view, the objectives of the proposed work are laid down in the succeeding section.

1.5.2 Objective of the Research Work

Keeping in view the gap in the research area, the objectives of the present study are as follows:

1.) Study the effect of initial damage level and type of loading on strength characteristics of reinforced concrete orthogonal beam-column joints retrofitted using ferrocement jackets and fiber reinforced polymer plates.

2.) Study the effect of the number of wire mesh layers and their orientation on orthogonal beam-column joints retrofitted using ferrocement laminates.

3.) To develop an analytical model for predicting the behavior of beam-column joints strengthened using ferrocement laminates.

1.5.3 Scope of the Research Work

The scope of the present work includes determining the effect of ferrocement repair jackets on maximum and safe load carrying capacity, deflection ductility ratio, energy absorption and stiffness of exterior beam-column joints retrofitted with different layers and orientation of wire mesh under static loading. In the second part the effect on maximum and safe load carrying capacity, deflection ductility ratio and stiffness of exterior beam-column joints retrofitted two CFRP layers and having a different orientation under static loading. In the third part test results are compared with the analytical results obtained by modeling of beam-column joint using ATENA 3D, FEM software**.** To achieve this a pilot study is proposed to finalize the parameters for the detailed investigations. The pilot studies undertaken are as follows;

- To study the effect of wire mesh layers on the strength of the beam-column joints retrofitted using ferrocement jackets.
- To study the effect of wire mesh orientation on the strength of the beam-column joints retrofitted using ferrocement jackets.

From the pilot studies an efficient number of wire mesh layers and orientation of wire mesh is finalized for the final study. In the detailed final testing program the effect of the number of wire mesh layers and their orientation on the maximum and safe load, deflection ductility and stiffness is studied on the prototype exterior beam-column joints. In conclusion an analytical model is proposed for calculating the maximum and safe load carrying capacity of retrofitted beam-column joints using ferrocement jackets. The analytical model so developed is validated with the experimental results obtained from the test programme undertaken.

1.6 ORGANIZATION OF THE THESIS

The thesis consists of seven chapters:

Chapter 1 introduces the concept of retrofitting, defines beam-column joints and presents their behavior, identifies the need of retrofitting, outlines various retrofitting steps, the retrofitting plan, and techniques and the objectives of the present work.

Chapter 2 reviews the existing literature by presenting the work done by various researchers in the field of ferrocement**,** experimental studies on retrofitting of beam-column joints using

ferrocement and FRP, finite element modeling (FEM) of concrete structures, analytical modeling and design of retrofitted concrete structures.

Chapter 3 details the materials used in the study along with their properties, the concrete mix used for casting of specimens, casting of specimens for studying various properties, their curing and testing, and methodology for retrofitting of beam-column joints.

Chapter 4 details the various pilot studies undertaken for finalization of the parameters for carrying out further detailed studies on prototype beam-column joints.

Chapter 5 presents the results of the prototype beams tested, analysis and discussion of the results obtained from the experimental data on beam-column joints retrofitted using ferrocement and CFRP jacketing. The results are presented both in tabular as well as in graphical form.

Chapter 6 deals with the FEM modeling of beam-column joints. To start with a beam-column joint model is set up using a commercial finite element analysis package ATENA 3D and validated with an experimental study from the literature. Subsequently, the beam-column joint retrofitted with externally bonded ferrocement is analyzed. These results are then compared with experimentally obtained data.

Chapter 7 summarizes and concludes the results of the study. Recommendations for further studies are also presented and discussed.

A list of references, referred to in the work is placed at the end.

CHAPTER – 2

LITERATURE REVIEW

2.1 GENERAL

Reinforced concrete is one the most abundantly used construction materials, not only in the developed world, but also in the remotest parts of the developing world. Concrete, as is well known, is brittle in behavior, has low tensile strength when compared with its high compressive strength, and is also heterogeneous in nature. By using steel reinforcement the inherent low tensile strength of concrete can be improved, but not the cracks, which are very thin and are invisible, although the propagation of such cracks can be delayed by reinforcing steel. Various efforts have been made to overcome such deficiencies of concrete by developing two-phase composite materials, wherein the presence of one phase improves the basic properties of the other phase and each phase is used to its best advantage (Bansal, 2008).

Thousands of reinforced concrete structures are constructed annually and a large number of these deteriorate or become unsafe before the end of their design life. This may be attributed to changes in loading conditions, codal provisions, improper design, faulty construction, etc. Such unserviceable structures require immediate attention, enquiry into the cause of distress and suitable remedial measures, so as to bring the structures back to their functional use again. Various field retrofitting techniques can be used for this purpose and out of them the plate bonding technique is considered as the most appropriate. In this technique, the plates of different materials viz. CFRP, GFRP, Ferrocement etc. can be bonded to the surface of a member to improve its structural properties. Ferrocement sheets are most commonly used as retrofitting material these days due to their easy availability, economy, durability, and property of being cast into any shape without needing significant formwork. In the last few decades or so, ferrocement has gained popularity, not only as a standalone material but also as a retrofit composite, due to its superior performance and versatility of use. It is being used not only just in housing repair but its use is being continuously explored in retrofitting and strengthening of damaged structural members as well (Singh and Kaushik et al., 1998). The flexural strength and ductility of beams

repaired by ferrocement has been reported to be greater than the corresponding original beams (Andrew and Sharma, 1998). At Ahmedabad (India), an underground ferrocement shell structure, which was built in 1993, has not only withstood the earthquake in 2001 but is also crack free till date (Doshiet al., 2011). Ductility requirements are the main feature of an efficient earthquake resistant design process, and ferrocement being a highly ductile material has led to its application in the rehabilitation of houses damaged during earthquakes. The effectiveness of its use has been reported by many a researcher (Wastt and Erberiket al., 1998; Desia, 1999). Ferrocement construction technology is being popularized throughout the world in countries like China, Canada, Indonesia, USA, Brazil, Australia, New Zealand, United Kingdom, Mexico, Russia, Thailand, India, and other developing countries due to its uniqueness and versatility (Shannag and Ziyyad, 2007). Ferrocement can be fabricated into any desired shape or structural configuration which is generally not possible with RCC Steel a standard masonry (Robles Austriaco, 2006; Dongyenet al., 2006; Kondraivendhan and Pradhan, 2009). Ferrocement is now being used as building materials substituting beams, columns, slabs, floors, walls, roofs, retaining walls etc. (Divekar2011). Composite construction with ferrocement gives more versatility to delicate looking thin walled construction elements. Its path for the future as a laminated cementitious composite combining advanced cement based matrices, high performance reinforcing meshes and fibers, and new construction techniques promises to be very bright (Naaman, 2001). Many structures like water tanks, silos, housing units, biogas digesters, swimming pools, shell roofs, food storage units and some specialized applications such as floating marine structures for which reinforced concrete is too heavy, ferrocement is a preferred choice now-a-days (Naaman, 2000; Hagoet al., 2005; Abasoloet al., 2009).

The bonding of fiber reinforced plastic (FRP) laminates to the tension face of concrete girders is becoming an attractive solution to the rehabilitation and retrofit of damaged structural systems (Al-Farabiet al., 1993). While investigating the effectiveness of fiberglass-bonded plates for capacity enhancement, an increase in strength and reduction in ductility was also reported. Premature failure by plate separation was also identified as a potential problem at the plate curtailment location (Basunbul et al., 1993). Rehabilitation techniques using CFRP were effective in avoiding the brittle joint shear and bond slip failure (Ghobarah and El-Amoury, 2005). Externally bonded composites, CFRP or GFRP, improved the moment capacity of damaged concrete beams (Karunasena et al., 2002), whereas an experimental investigation

clearly demonstrated that the effectiveness of the repair primarily depends upon how effectively the diagonal tension cracks in the shear-damaged beams were trapped (Neelmani, 2013).

2.2 LITERATURE RELATED TO DEVELOPMENT OF FERROCEMENT

In 1848 Joseph Louis Lambotan a horticulturist living at Miraval, near Brignoles in Varregion, experimented with plant pots, seats and tubs made of meshes hand plastered with sand/cement mortar and replaced his rotting rowing boat. He called this material as 'Ferciment' in a patent, which he took in 1852. The patent reads as follows which is translated from French

"My invention is a new product that can replace timber where it is endangered by wetness, as in wood flooring, water containers, plant pots etc. the new substance consists of a metal net of wire or sticks which are connected or formed like a flexible oven mat. I give this net a form, which looks in the best possible way, similar to the articles, i want to create. Then I put in hydraulic cement or similar bitumen tar or mix, to fill up the joints".

Lambot's construction consisted of a mesh or grid reinforcement made of two layers of small diameter bars at right angles and plastered with cement mortar with a thin cover to reinforcement. Lambot's rowing boats were 3.66m long, 1.22m wide and 25mm to 38mm thick. These were reinforced with grid and wire netting. One of the boats built by him, still in good condition and is now available in Brignoles museum in France. There was very little application of true ferrocement construction between 1888 and 1940. In the early 1940's an Italian engineer Pier Luigi Nervi began a series of experiments on ferrocement, rescuing the original idea of lambot, wherein, he observed that reinforcing concrete with layers of wire mesh produced a material possessing the mechanical characteristics of an approximately homogeneous material and great resistance to impact. Narvi called this material as 'ferro-cemento', nearly a hundred years after lambot originally patented it. There was very little application of true ferrocement construction between 1888 and 1942 when Pier Luigi Nervi began a series of experiments on ferrocement. After the Second World War Nervi demonstrated the utility of ferrocement as a boat building material. In 1945, Pier Luigi Nervi built the 165-ton Motor Yatch "Prune" on a supporting frame of 6.35mm diameter rods spaced 106 mm apart with 4 layers of wire mesh on each side of the rods with total a thickness of 35 mm. It weighed 5% less than a comparable wooden hull and cost 40% less at that time. In 1947, Nervi built the first terrestrial ferrocement

structure, a storage warehouse of about 10.7 m x 21.3 m size. The strength of the structure was due to the corrugations of the wall and the roof which were 44.45 mm thick and in 1948, he used ferrocement in the first public structure, the tutrin exhibition building. The central hall of the building, which spans 91.4 m, was built of prefabricated elements connected by reinforced concrete arches at the top and bottom of the undulations. In 1958, the first ferrocement structure, a vaulted roof over shopping centre was built in Leningrad in the Soviet Union. In 1970, a prototype prefabricated ferrocement home was constructed in the U.S.A. The house was found to be much lighter in weight and higher in resistance to dynamic load than the conventionally built brick or blockhouse. In 1971, a ferrocement trawler named "Rosy in I" was built in Hong Kong with an overall length of 26 m and it was claimed to be the longest ferrocement fishing boat in the world. In 1972, under the chairmanship of Prof. James P. Romualdi of Carnegie-Mellon University, U.S.A., the National Academy of Sciences of the United States of America set up an ad-hoc Panel on the utilization of ferrocement in developing countries. In early 1973, the report of the panel was first published. As a result of the report society became aware of this material and started using it. A 'Workshop on Introduction of Technologies in Asia-Ferrocement': A Case Study' sponsored by the AIT and the U.S. National Academy of Sciences (NAS), was held in Bangkok, Thailand, in November 1974. In 1975, two ferrocement aqueducts were designed and built for rural irrigation in China. In 1976, the International ferrocement Information Centre (IFIC) was founded at the Asian Institute of Technology, Bangkok, Thailand. In 1977, the American Concrete Institute (ACI) had set up Committee 549 on ferrocement to review and formulate a code of practice for this material. In its first report published in 1980, ACI Committee 549 first explains the definition of ferrocement, which was subsequently revised in 1988, 1993 and 1997. The international ferrocement society (IFS) formed a Committee (1FS-10-01), the recommendations of which were published as "Ferrocement Model Code" (FMC) in January 2001. Earlier in 1979, RILEM (International Union of Testing and research Laboratories of materials and structures) established a Committee (48-FC) to evaluate testing methods for ferrocement. In 1984, at the state university of New York at Buffalo, ferrocement was used in the construction of a shaking table at the large-scale earthquake simulation facility. Recently, it has been reported that the Chinese have been building ferrocement boats. It is estimated that they have built 2000 boats. Most of these boats are 12 m to 15 m long and are mainly used in carrying goods. The journal of ferrocement, which was originally published by the New Zealand

Ferrocement Marine Association (NZFCMA), was handed over to the international ferrocement Information Center. The Journal of Ferrocement is now the main propagation tool regarding any information concerning ferrocement.

2.3 LITERATURE RELATED TO RETROFITTING OF BEAM-COLUMN JOINTS – EXPERIMENTAL STUDIES

Lee et al. (2010) retrofitted the beam-column joint using carbon fiber reinforced polymer (CFRP) to enhance the strength and stiffness of the beam-column joints. A total of three interior beam-column joints were tested for the purpose. They were designated as JI0 (prototype), and JI1- JI2 (strengthened specimens). Retrofitting method for specimens JI1 and JI2 are shown in Figure 2.1**.** To avoid the de-bonding of the CFRP laminate, anchorage was used for one of the specimens, JI2 only but it was not used in specimen JI1.

The experimental results showed that the behavior of the specimen JI1 strengthened with CFRP was similar to that of specimen JI0 with only a 4% increase in ultimate strength. This indicates that the CFRP retrofitting without anchoring did not significantly improve the shear resistance of the retrofitted beam-column joint. While in JI2 specimen, with appropriate anchoring, it was found that anchoring had an important role in preventing the premature de-bonding of CFRP and thus upgrading the shear resistance of the retrofitted beam-column joint.

Bousselham (2010) presented a review of published experimental studies on the seismic retrofitting of reinforced concrete beam-column joints using FRP. In total fifty-four tests carried out worldwide were considered for the review. The author observed that, the test results showed enhancement, due to FRP bonding, in terms of strength, ductility, and energy dissipation, whereas a degradation in stiffness was observed with FRP retrofitting. The experimental results clearly show the important role of mechanical anchorage systems in the mode of failure. In comparison to the effectiveness of carbon versus glass fibers, the study concluded that glass fibers sheets proved marginally more effective than carbon fiber sheets.

Sharma et al. (2010) tested full scale reinforced concrete structures to failure and then repaired and retrofitted using a combination of GFRP and CFRP as shown in Figure 2.2. The structure shown in the figure was tested earlier using pushover loads till failure, then retested after retrofitting. It was reported that the structure was not able to reach 90% of the base shear in comparison to original the structure shown in Figure 2.3 and the stiffness of the retrofitted

structure was reduced. De-bonding was quite obvious due to unevenness of the surface. Although, due to prevention of spalling of concrete, the joint behavior did improve but the failure of the structure could not be prevented.

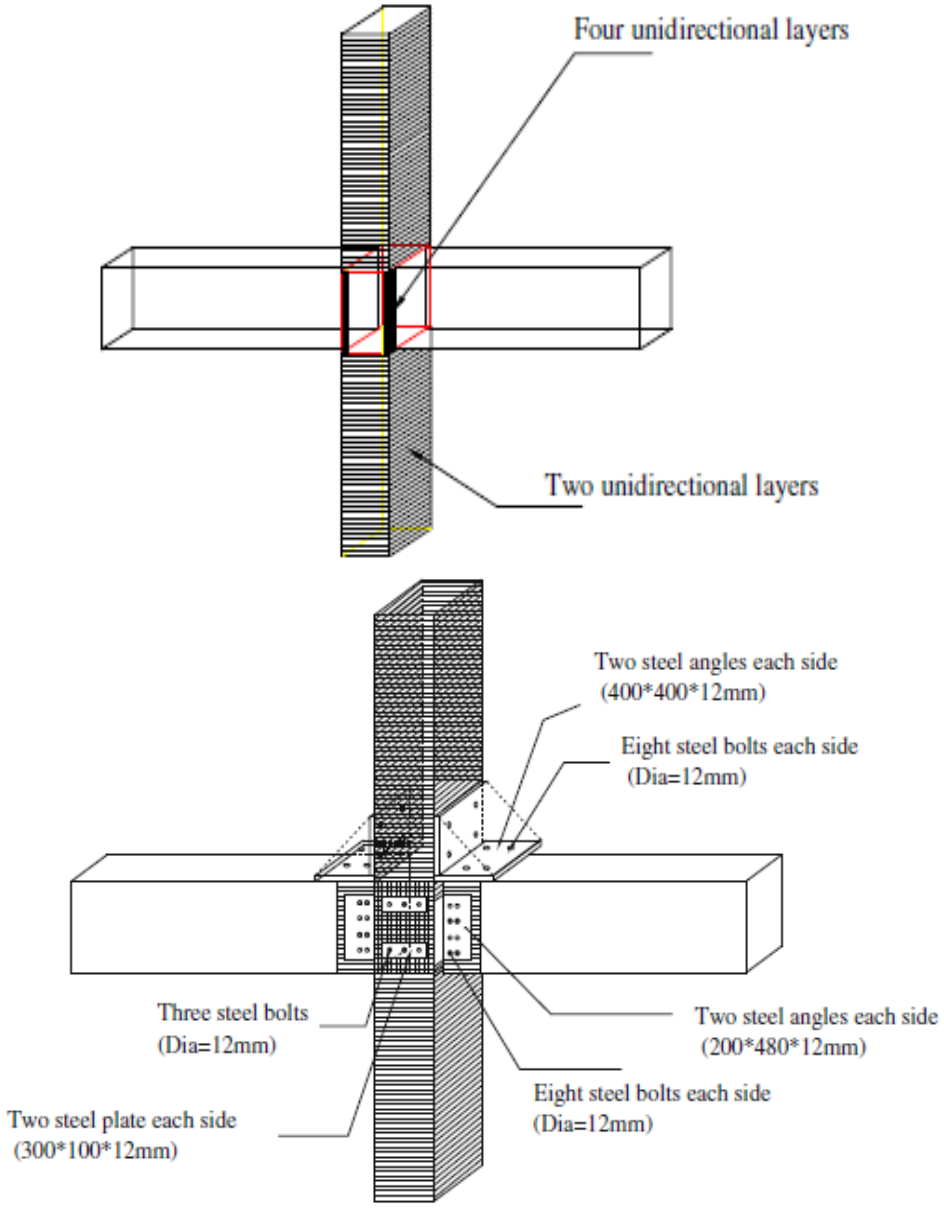

Figure 2.1: **Rehabilitation Scheme for Specimen JI1and JI2**

Lee et al. (2010)

(a) **(b)**

Figure 2.2: Full Scale Structure (a) As-built (b) Retrofitted Sharma et al. (2010)

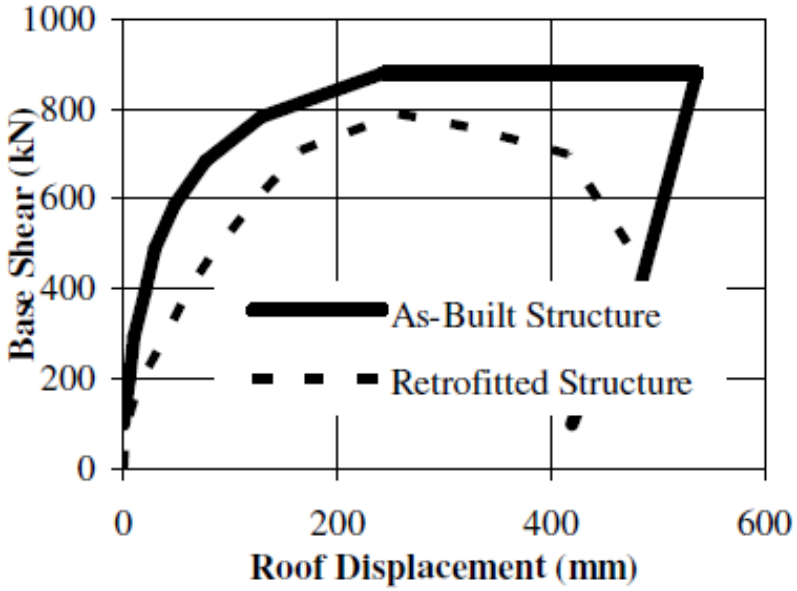

Figure 2.3: Base Shear vs Roof Displacement Curves by Sharma et al. (2010)

Li and Chua (2009) studied the experimental results of the effects of different methods of wrapping of the CFRP and GFRP sheets for strengthening non-seismically designed interior beam-column joints, subjected to seismic loadings. Figure 2.4 shows the proposed FRP strengthening methods.

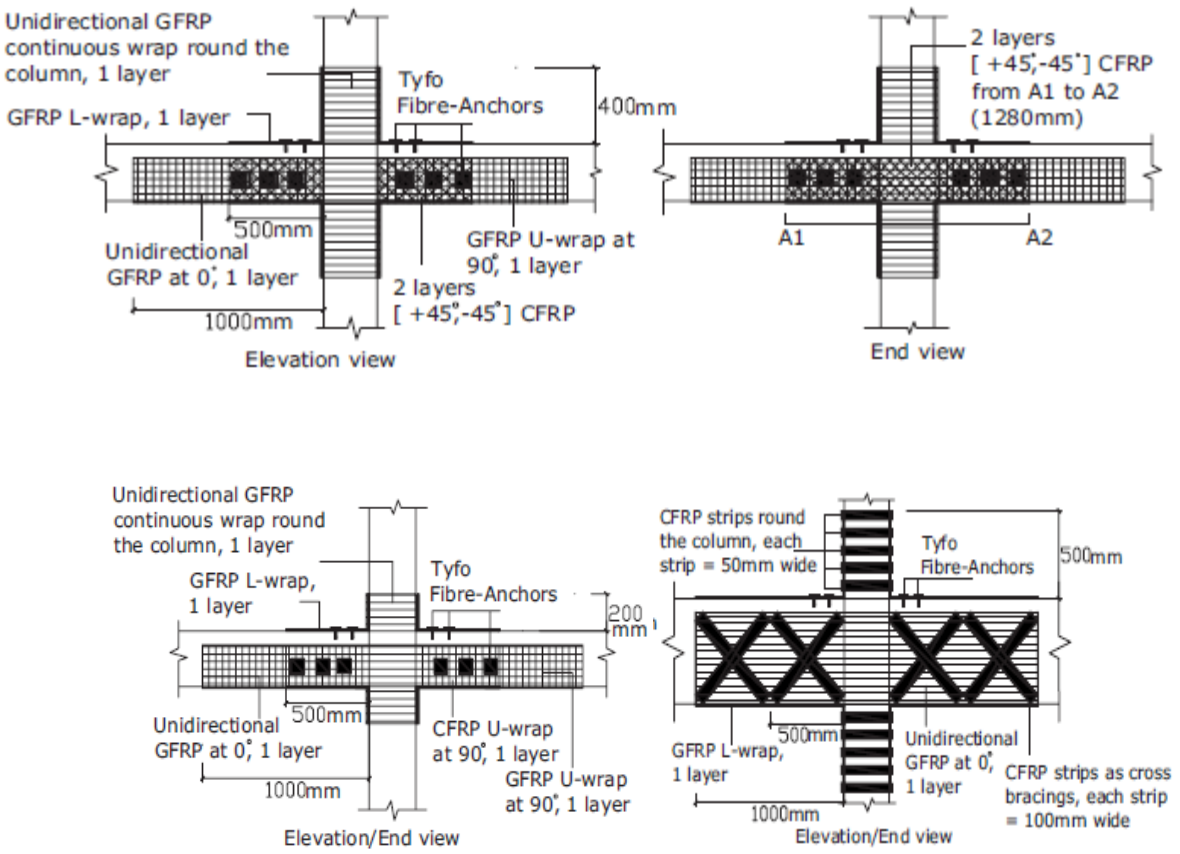

Figure 2.4: Different Wrapping Methods, Li and Chua (2009)

A comparison of strength, stiffness and energy dissipation capacity of retrofitted ones showed a tremendous increase as compared to control specimens and it was found that the use of CFRP strips on strong-column weak-beam it was effective in improving the flexural strength. It was also noted that beam retrofitting in the form of FRP U-wrapping was necessary in preventing shear failure in the beam. These proposed strengthening schemes were very helpful in eliminating or delaying the shear mode of failure. The ductile mode of failure occurred in the form of cracks near the joint corners, instead of flexural hinging of the beam for specimen SE1C and near joint core region de-lamination of FRP strips was observed at beam-column interface for specimen SC1C and specimen SC2C.

Ludovico et al. (2008) performed experimental tests on the seismic behavior of a full-scale reinforced concrete structure retrofitted by GFRP laminates to find the effectiveness of different retrofit methods. The structure was designed for typical housing building in earthquake-prone areas of Europe, wherein, the structures designed had poor detailing, lacked a sufficient number

of rebars, and had insufficient confinement with weak joints Figure 2.5 (a). In order to prevent brittle shear failure of the beam-column joints due to increased ductility of the columns, further FRP retrofit was designed on beam-column joints according to the approach proposed by Antonopoulos and Triantafillou in 2002 Figure 2.5(b)**.** It was observed that the retrofitted beam-column joints were almost undamaged after the testing, while the original beam-column joints (without retrofit) showed significant damage on columns. At the seismic level intensity of 0.3 *g*, the maximum displacement recorded on the retrofitted beam-column joints was significantly increased confirming the effectiveness of the jacketing technique.

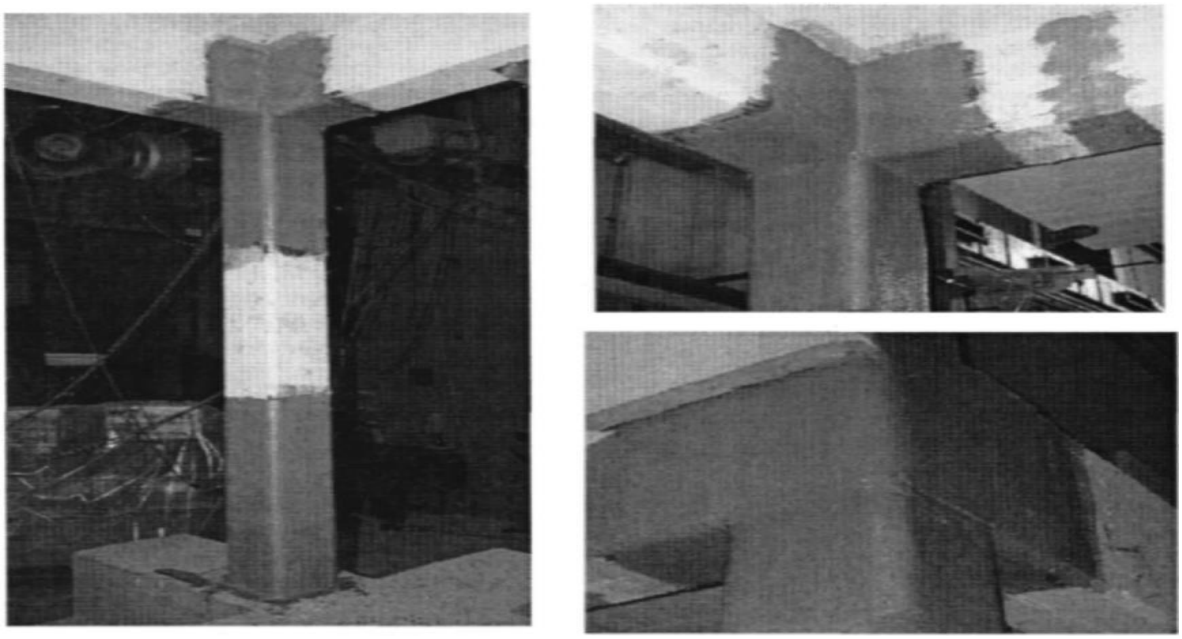

(a) **(b)**

Figure 2.5: GFRP Retrofit of the Structure: (a) Column Confinement; (b) Unconfined Joint Retrofit, Ludovico et al. (2008)

Gergely et al. (2000) showed the experimental results of fourteen 1/3-size scale RC concrete T-joints with FRP composite materials. Four specimens were tested in as-built condition and the other were externally reinforced with CFRP sheets as shown in Figure 2.6. It was observed that the failure of the control specimens was identical and diagonal tension cracks in the joint region were also observed. The FRP retrofitted specimens showed an increase in the maximum composite capacity but this load level could not be sustained. This showed the failure of specimens at lower loads with bending moments more than the element's capacity. Excellent performance was shown by water jetting the concrete surface with high strength adhesive, but

there was no evidence of better joint shear improvement by using an elevated temperature cure system. Debonding of the inclined FRP sheets was also observed from the top and bottom of the joint. Debonding occurred at stress levels of only $1/5^{th}$ of the composite's capacity. Because the concrete in the joint could resist the diagonal compression forces, there were no significant compression stresses in the inclined composite layers.

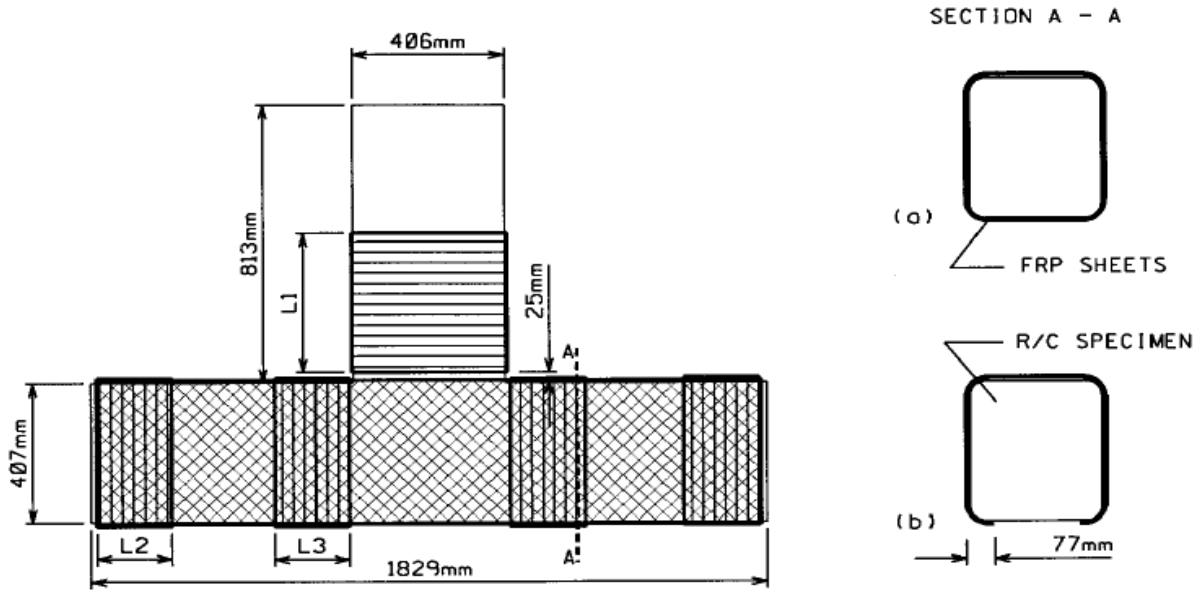

Figure 2.6: **CFRP Layout on: (a) Four Sides of Beam; (b) Three Sides of Beam Gergely et al. (2000)**

Akguzel and Pampanin (2010) tested the effects of axial load with variation on the column due to lateral sway of the frame on the performance of jacketed RC beam-column joints. For this purpose, four 2/3-scale exterior RC beam-column joints, including one as-built and three retrofitted with different configurations, were tested under changeable axial load. RC joints were retrofitted using GFRP sheets as per the configuration given in Figure 2.7. On testing the GFRP retrofitted specimen under axial load, a few hairline cracks were observed in both the column faces as well as in the joint area. No debonding or damage in the joint of the GFRP sheet was observed. In other specimens which were tested under the varying axial load systems, a hybrid failure mechanism was observed. A gradual debonding of the GFRP sheet in the joint area and damage to the joint concrete core was observed. The failure mode shifted from ductile to brittle.

Thus, it was concluded that the GFRP retrofitting designed under constant load conditions can be inadequate under varying axial load conditions.

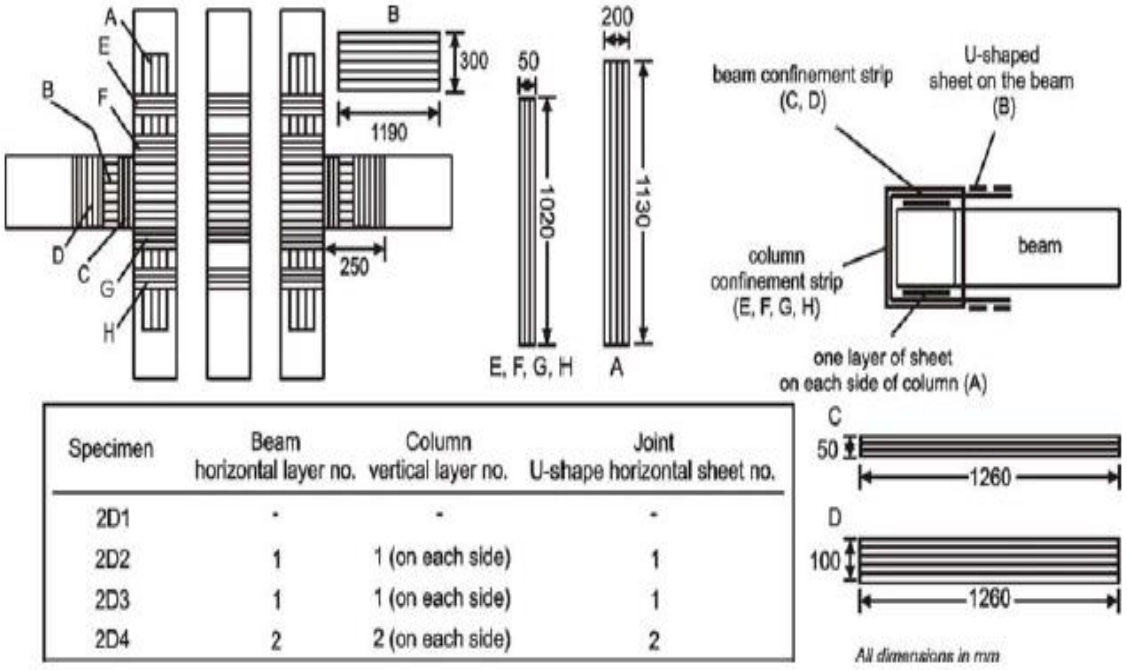

Specimen	Beam horizontal layer no.	Column vertical layer no.	Joint U-shape horizontal sheet no.
2D1	-	-	-
2D2	1	1 (on each side)	1
2D3	1	1 (on each side)	1
2D4	2	2 (on each side)	2

Figure 2.7: GFRP Retrofit Configuration with Top View Layout
Akguzel and Pampanin (2010)

Mukherjee and Joshi (2005) examined the performance of FRP in up progression of RC joints, with adequate and deficient reinforcements, after rehabilitation of damaged joints. Two sets of joints, one with adequate steel reinforcement and proper detailing of reinforcement at the critical sections known as ductile specimens and an other set of specimens with deficient bond lengths of the beam reinforcements at the joint with the columns, known as non-ductile specimens, were tested. All the specimens were strengthened by using carbon and glass FRP materials as given in Figure 2.8(a) and Figure 2.8 (b). The control specimens were used after testing to evaluate the rehabilitation of joints with FRP known as rehabbed specimens. It was observed that the ductile specimens showed higher load at yield in the FRP reinforced specimens than the control specimen and, for the same tip load, the tensile force in steel was lower in the CFRP retrofitted specimen than in the GFRP specimens. The displacement at yield was much lesser than the load due to FRP retrofitting. All the FRP retrofitting specimens showed higher peak loads than the control specimen and FRP retrofitting specimens also showed a total loss of stiffness at a higher

displacement level than the control specimen. The energy dissipation of the FRP retrofitted specimens was close to that of the control specimen. The FRP retrofitting increased the ultimate deformation of the structure to a large extent. The load versus displacement curves for the retrofitted specimens showed that the use of FRP not only restored the original capacity of damaged specimen, but also upgraded the ultimate load capacity by 55% with 30 % increase in displacement at ultimate load. Also a 57% increase in the energy dissipation capacity was observed in the structure after the rehabilitation

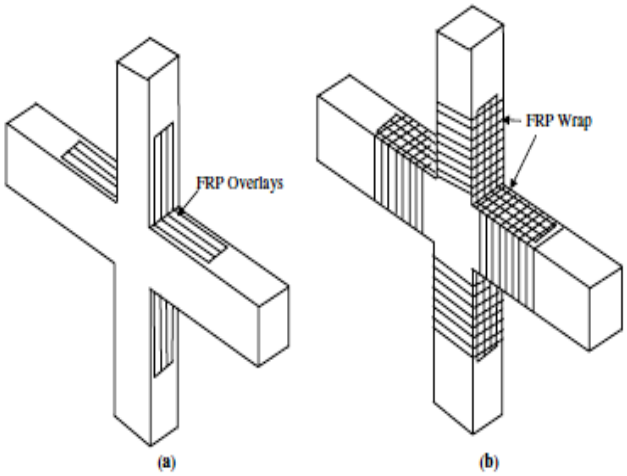

Fig. 2.8(a) Type A Strengthening System (Use of composite overlays)
Mukherjee and Joshi (2005)

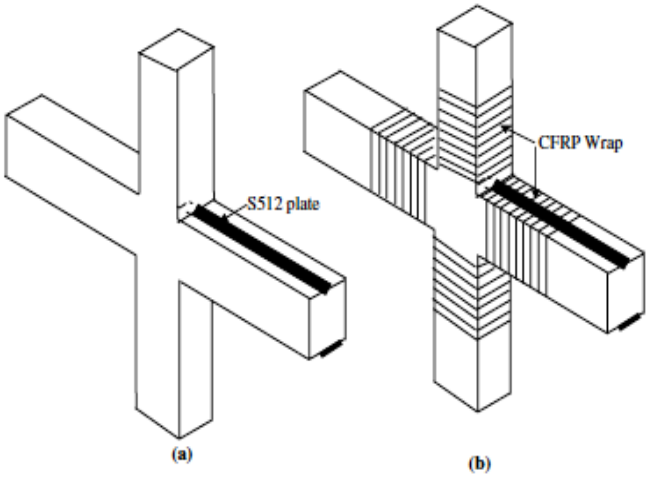

Figure 2.8: (b) Type B Strengthening System (Use of pre-cured carbon plate)
Mukherjee and Joshi (2005)

Ghobarah and El-Amoury (2005) compared the results of retrofitted RC beam-column joints with existing joints designed as per the pre-seismic codes to assess the efficacy of the proposed retrofitting techniques. A total of six RC joints, cast with non-ductile reinforcement detailing, were subjected to replicate seismic forces. Specimens T-B12 and T-B11, having as inadequate anchorage length of the bottom beam bars, were retrofitted with CFRP sheets attached to the bottom beam face as shown in Figure 2.9 (a) and Figure 2.9 (b). Specimen T-SB8- TSB7 having no steel ties installed in the joint region in addition to inadequate anchorage length of the beam bars were retrofitted by GFRP sheets at the joint zone with steel rods or plates as shown in Figure 2.9(c) and Figure 2.9(d). The retrofitted techniques shown excellent results for eliminating the brittle joint shear and steel bar bond-slip failure modes. In the cases of specimens TB-12 and TB-11, CFRP sheets were very effective in replacing the anchorage deficient beam bars when an adequate anchorage system of these sheets was provided. In case of specimen T-SB8 andT-SB7, GFRP retrofitting was found to be an effective system to provide confinement with shear strength to shear-deficient joints. External steel tie-rods welded to the existing deficient beam reinforcement was found to be an excellent technique to improve the anchorage conditions of the bars so that the tensile strength can be fully developed.

Prota et al. (2004) tested eleven one-way interior RC beam-column joints with three different levels of axial load and used CFRP rods in combination with externally bonded sheets as shown in Figure 2.10 in an attempt to shift the failure first from the column to the joint, then from the beam-column joint to the beam. The CFRP sheets were placed in epoxy-filled grooves prepared near the surface. The failure modes could not be controlled as planned so ductile beam failure cannot be achieved. In the case of Type-2 joints design moved the failure from the compression to the tension side of the column for low column axial load and a combined column-joint failure occurred. In case of Type-3 the addition of CFRP sheets as flexural reinforcement along the column led to a beam-column joint shear failure. In the case of Type-4, when the joint panel was also retrofitted the beam column-joint interface failed, which was attributed to extinction of the CFRP sheet reinforcement at the joint to account for the presence of a floor system. The Type-5 scheme with U-wrapping of the beam and beam-column joint showed in a failure mode similar to that of Type- 4.

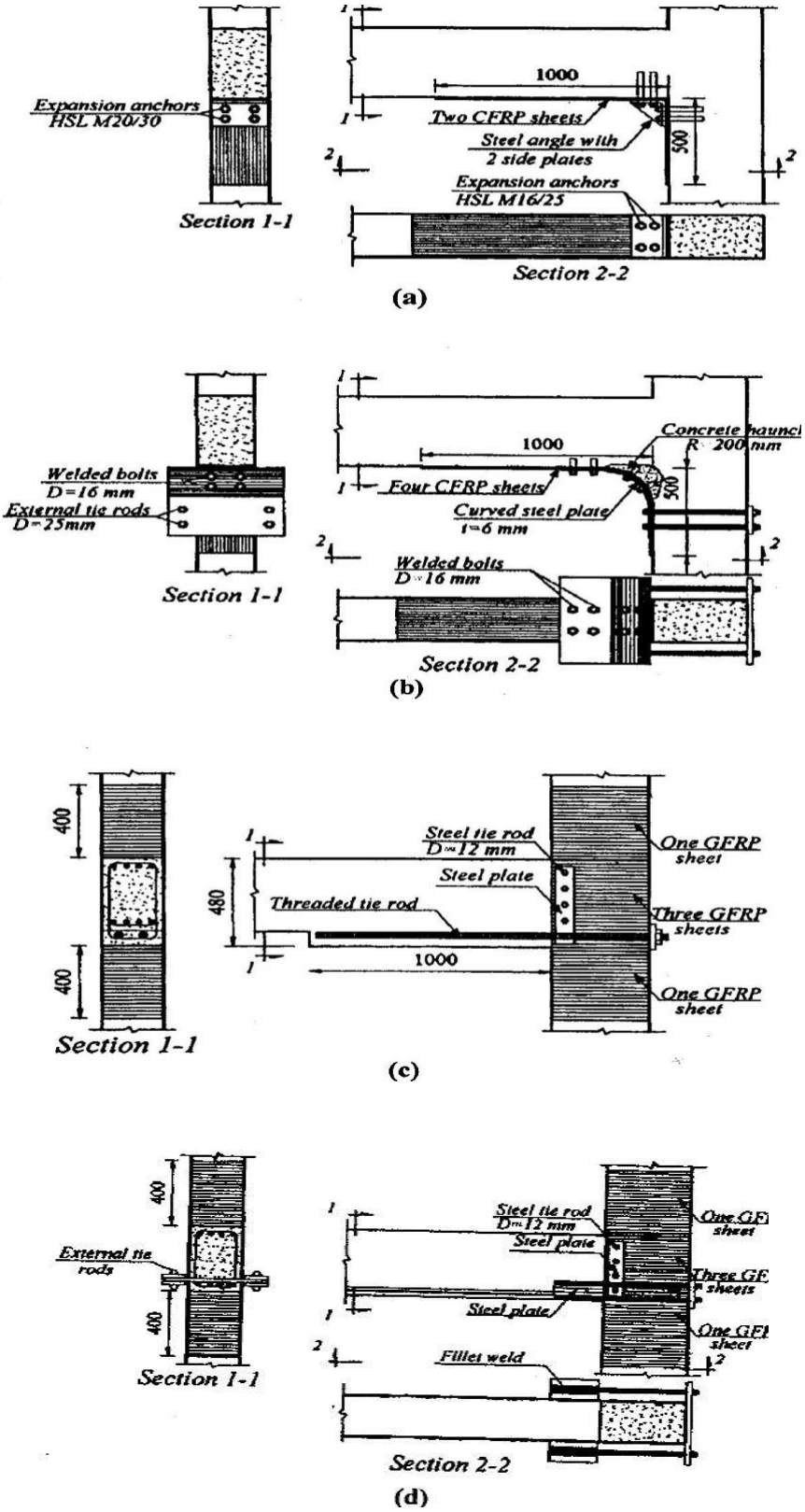

Figure 2.9: Strengthening Joint (a) T-B12; (b) T-B11; (c) T-SB8; (d) T-SB7 Ghobarah and El-Amoury (2005)

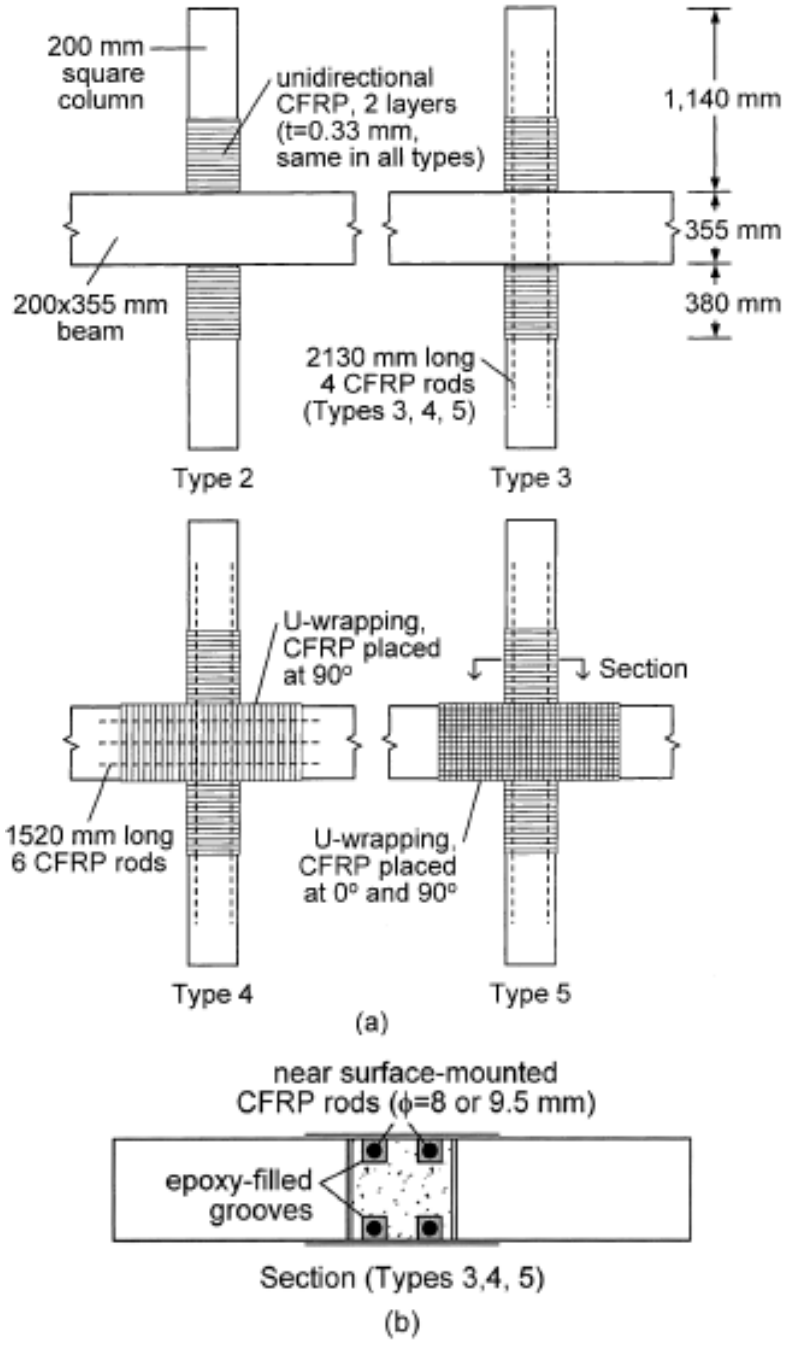

Figure 2.10: Specimens Retrofitted with CFRP Sheets and Rods Tested: (A) Elevation; (B) Plan, Prota et al. (2005)

Antonopoulos and Triantafillou (2003) examined tests on eighteen exterior beam-column joints of 2/3-scale retrofitted with different configurations of pultruded carbon strips and with GFRP sheets. The examined variables were distribution of FRP, area fraction, column axial load, joint

reinforcement (internal), initial damage level, comparative of CFRP and GFRP, sheets versus strips, and effect of transverse stub beams. All the eighteen specimens were designed to fail at joint shear, before and after retrofitting so that the contribution of FRP retrofitting could be evaluated. The result showed an increase in column axial load from 4% to 10% of its initial load capacity, 65% to 85% increase in strength and 50% to 70% increase in energy, and a 100% increase in stiffness 100% of which varied in each loading cycle. The conclusions shown are better performance of flexible sheets over strips, the need for mechanical anchorage, positive effect of increased column axial load on shear capacity of FRP-retrofitted joints, better energy dissipation due to GFRP than CFRP, and the negative effect of transverse stubs on the efficiency of FRP.

El-Amoury and Ghobarah (2002) modified the GFRP methods used by Ghobarah and Said (2002), as shown in Figure 2.11, for strengthening of beam-column joints using both inadequate anchorage of beam bottom bars with no hoop shear reinforcement.

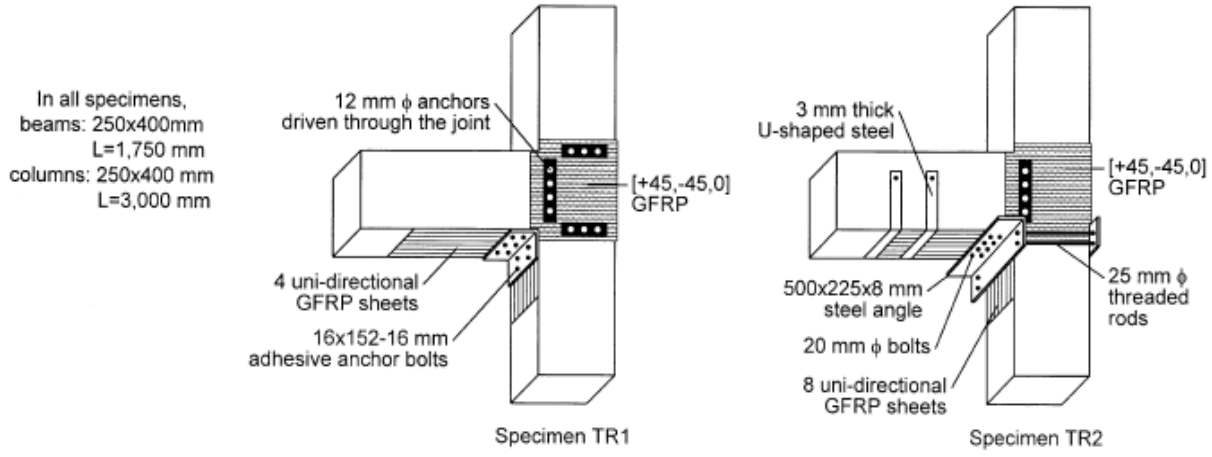

Figure 2.11: **GFRP Retrofitted Specimens**
El-Amoury and Ghobarah (2002)

Both methods showed approximate by a 100% increase in load carrying capacity; specimen TR1 and TR2 dissipated three and six times the energy dissipated by the reference specimen, respectively. In the case of specimen TR1 the failure was due to complete debonding of GFRP from the beam and column surfaces with pullout of the bottom bars in the beam led by fracture of the weld around the bolt heads. In the case of specimen TR2 debonding was eliminated with the use of two U-shaped steel plates of the GFRP and it failed in joint shear.

Ghobarah and Said (2002) examined 4 one-way exterior joints shown in Figure 2.12, originally designed to fail in joint shear with or without retrofitting by unidirectional or bi directional GFRP sheets inclined at 45 degrees.

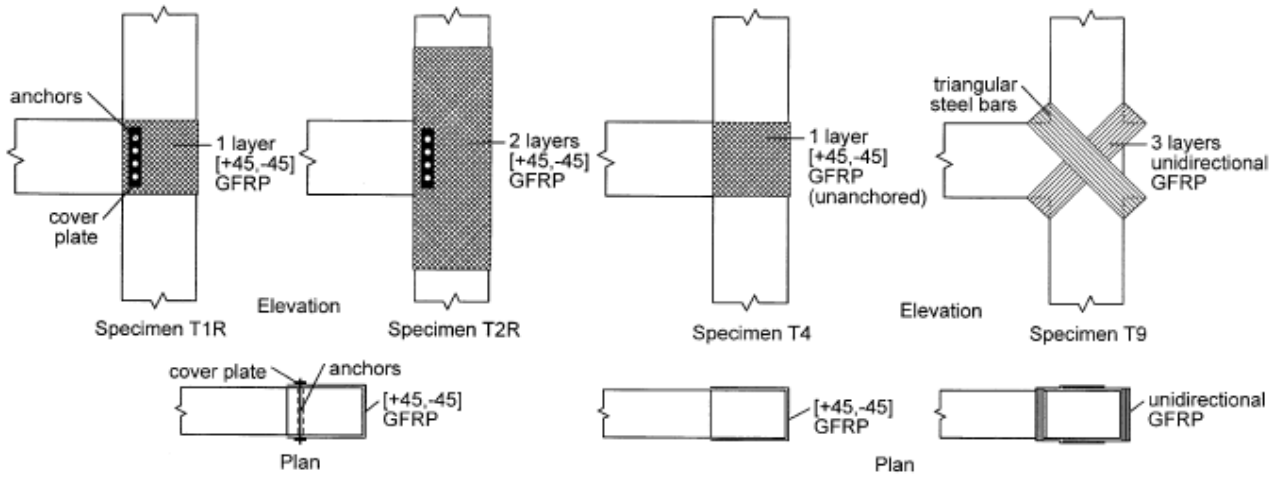

Figure 2.12: GFRP Retrofitted Specimens

Ghobarah and Said (2002)

Previously damaged specimens T1R and T2R were retrofitted with mechanical anchorage provided by steel plates and threaded rods core-drilled through the joint. The GFRP sheet anchored through the joint in the case of specimen T1R was efficient until it failed in tension, but same showed no improvement in the case of specimen T4 due to a lack of threaded rod anchorage showing early de-lamination. The failure in the beam was due to the formation of a plastic hinge. No debonding or joint shear cracking was observed in the case of specimen T2R. The placement of the diagonal unidirectional strips in case of specimen T9 could not prevent expansion of the joint concrete which led to de-lamination. In general this study tinted the significance of anchorage of composite sheets in developing the full fiber strength in a small joint area.

Ghobarah and Said (2001) used FRP to upgrade the shear capacity of beam-column joints and allowed the ductile flexural hinge to form in the beam. The RC joint T1 (control specimen) with no transverse reinforcement tested and retrofitted with one layer of bidirectional GFRP laminate

in the form of a U is shown in Figure 2.13. The free ends of the U were tied together using threaded steel rods and a steel plate driven through the joint section being re-designated as T1R.

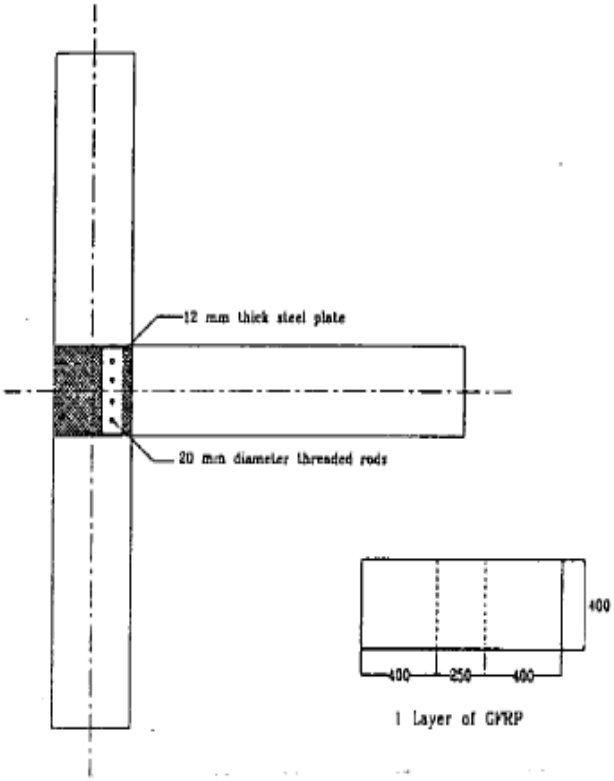

Figure 2.13: Proposed Joint Rehabilitation Scheme Using FRP

Ghobarah and Said (2001)

Specimen T1R showed a slightly higher yield load as compared to specimen T1. Specimen T1R also showed a lower rate of decline of strength, a higher ductility (increased by 60% up to failure) with slightly higher initial stiffness. The total energy dissipation was also three times higher than that of specimen T1. For specimen T1 storey shear-joint shear deformation showed that the joint shear deformation increased with increasing storey drift.

2.4 LITERATURE RELATED TO FINITE ELEMENT MODELLING OF CONCRETE STRUCTURES

Ravi and Arulraj (2010) modelled three exterior RC beam-column joint specimens retrofitted with CFRP using the package ANSYS**.** Out of the three, two were used as control specimens. Both the specimen had different reinforcement with one provided with reinforcement as per code

IS 456: 2000and the other had detailing as per IS 13920-1993. The CFRP retrofitted specimen had reinforcement as per IS 456:2000. The beam-column joint as shown in Figure 2.14 was considered for analysis with column cross section of 200 mm x 200 mm having overall length 1500 mm and beam cross section of 200 mm x 200 mm with the length of 600 mm. Solid65 elements was used for concrete modeling. Link8 element was used for modelling the reinforcement. Solid45 element was used as the retrofitting material. The control as well as retrofitted RC beam- column joint models was tested under static loading at a regular interval of 5kN. The results showed 23.5% more deflection as compared to specimen detailed as per code IS 13920-1993 and CFRP retrofitted specimen showed 75.3% less deflection for the specimen detailed as per code IS 456: 2000. Specimen detailed as per code IS 13920-1993 showed 42.9% more energy absorption capacity as compared to specimen detailed as per code IS 456: 2000 and CFRP retrofitted specimen showed 114.3% more energy absorption as compared specimen detailed as per code IS 456: 2000.

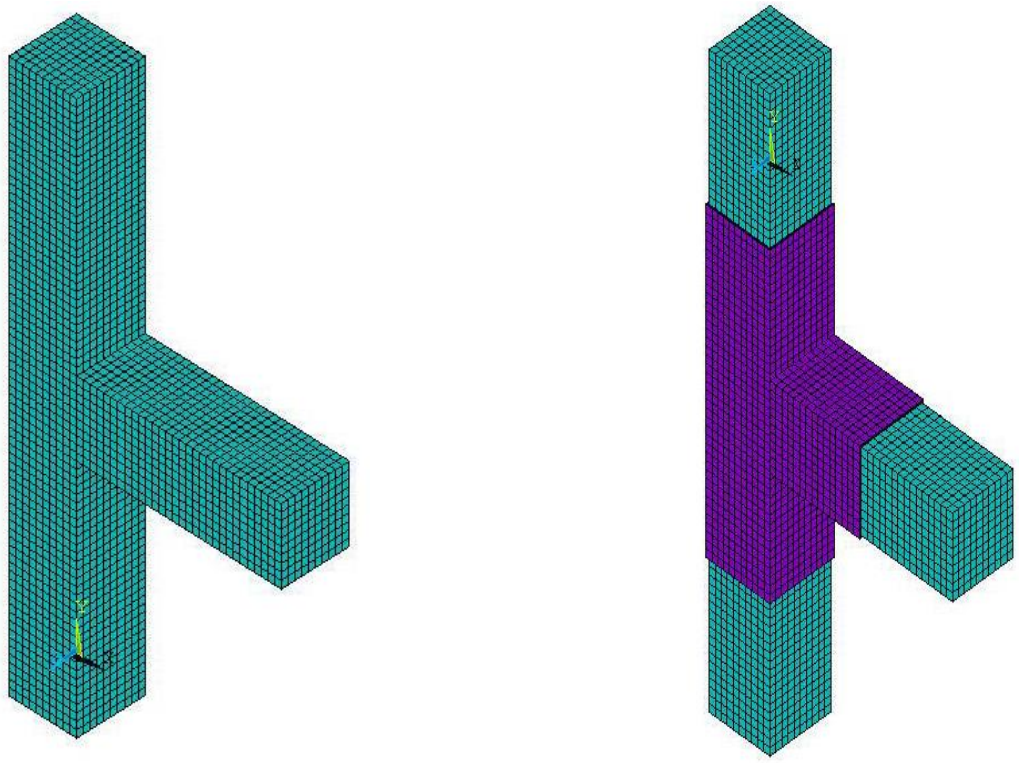

Figure 2.14: (a) Control Specimen; (b) Retrofitted Specimen

Ravi and Arulraj (2010)

Ibrahim and Mahmood (2009) analyzed six beams with different conditions using ANSYS. An FEM model for RC beams retrofitted with fiber reinforced polymer (FRP) laminates using finite elements method was presented. The analytical results obtained from ANSYS were compared with the experimental data from the literature. The concrete Solid65 element was used for modeling. For steel reinforcement the Link8 element was used to model the reinforcement. For FRP models a Solid46 layered element was used for modeling purposes. The crack pattern was recorded at each applied load using ANSYS. The end conditions, loading and FE mesh are shown in Figure 2.15. The failure modes of the FEM using ANSYS showed good agreement with observations. The FRP retrofitting of the control beams shifted shear failure near the boundaries of the beam to flexure failured at the mid span.

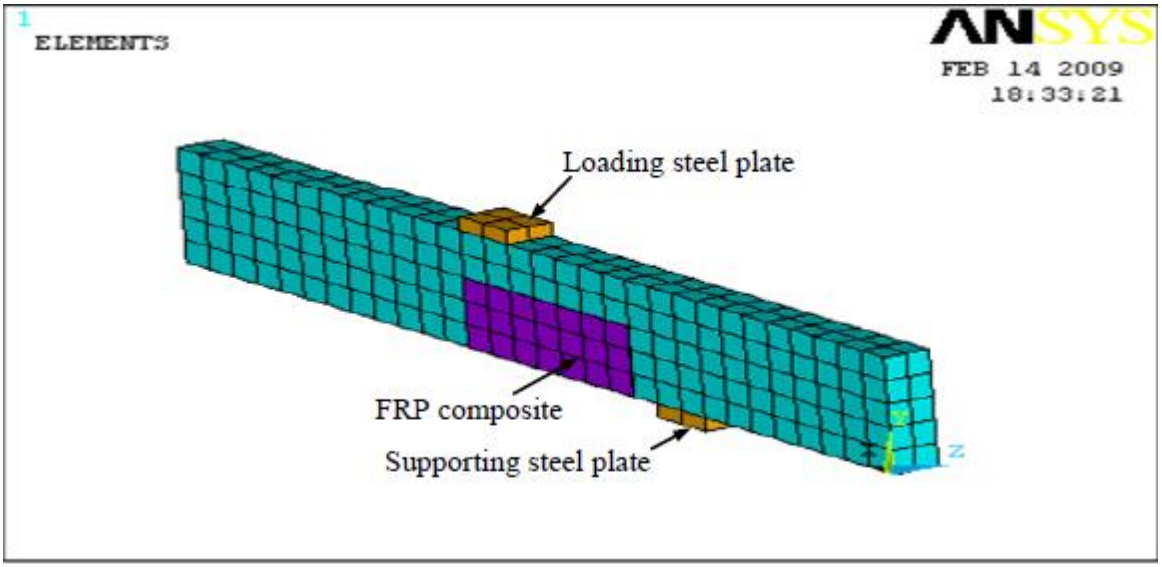

Figure 2.15: Finite Element Modeling by Ibrahim and Mahmood (2009)

The failure load shown by the ANSYS solution for the beams was slightly less than the experimental loads.

Haach et al. (2008) studied the performance of exterior RC joints under the control of column axial loads through numerical simulations using ABAQUS software. A comparison of the experimental and numerical results was presented. For concrete a two-dimensional planar solid elements with 2 active degrees of freedom was used for numerical simulation. Truss elements were modeled as longitudinal and transversal bars whose nodes were embedded in the concrete

elements. A monotonic loading was applied in two steps. (i)The column axial load was applied up to the necessary level. (ii) A vertical displacement (δ) was applied at the beam edge. Beam-column joint behavior was studied under different conditions (1) for different levels of column axial load (v): 0.0, 0.2, 0.4, 0.6 and 0.8; (2) for eccentricity of column axial load (e): -50 mm to 50 mm; and (3) for stirrup ratio variation (ρw): 0.0%, 0.1%, 0.3%, 0.4% and 0.5%. Figure 2.16 and Figure 2.17 showed the numerical and experimental result for the behavior of the stirrup in the joint and for the tensioned bars of the beam, for specimens with v = 0.85 and v = 0.64, respectively. In experimental observations, at the maximum value of the loading a delay in the load resisting mechanism occurred. When one of the load resisting mechanisms reached its maximum, the delay occurred again and the load decreased. The ABAQUS modeling could not represent this occurrence, so near to this maximum loading, numerical analysis showed instabilities in some areas of the mesh so the model could not continue converging.

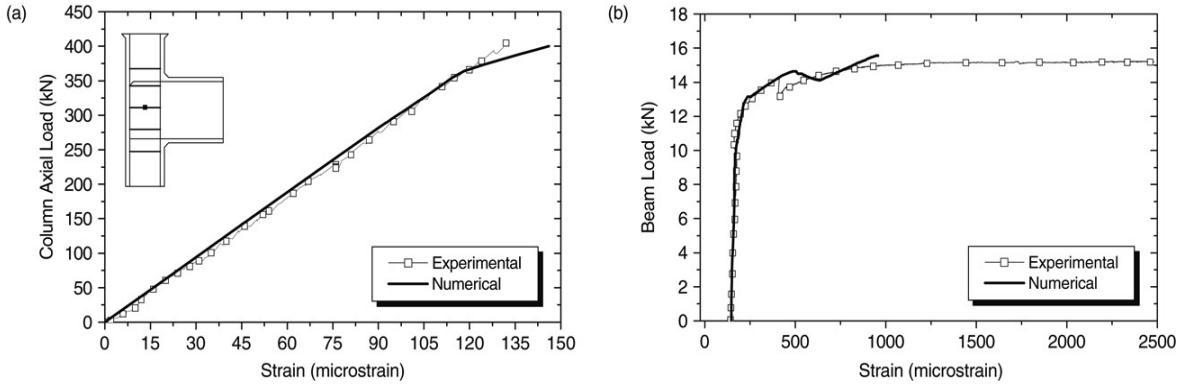

Figure 2.16: Strain of Stirrup Inside the Joint for Specimen with v = 0.85: (a) Column Load (b)Beam Load, Haach et al. (2008)

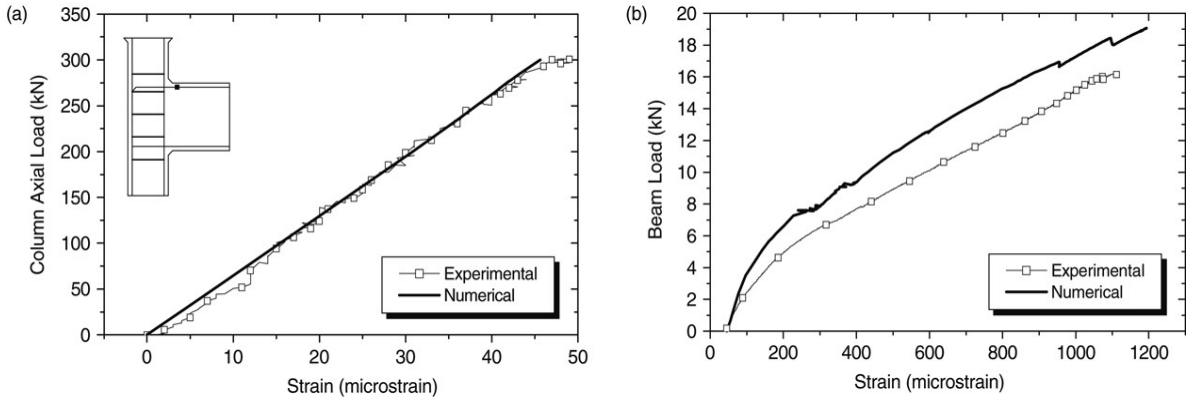

Figure 2.17: Strain of Tensioned Bar of Beam for Specimen with v = 0.64: (a) Column Load (b)Beam Load,Haach et al. (2008)

Inside the joint region a significant strain in stirrups was observed, earlier in specimens at low column axial loads than in specimens with high column axial loads. Upper region stirrups located in the joint region absorbed part of the tension beam longitudinal reinforcement and improved anchorage.

Mahini et al. (2008) experimentally tested two exterior beam-column connections, which were subsequently modelled using FEM (nonlinear) software. The experimental results were then compared with the hysteretic curves of these connections.

The authors studied the capability of nonlinear quasistatic FEM in simulating the hysteretic behavior of CFRP jacketed reinforced concrete exterior beam-column joints under cyclic loads with displacement control. The Solid65 element was used to model the concrete characteristics.

For fracture modeling in concrete the Willam-Warnke criterion was used and the Hognested model was used for modeling the compressive strength of concrete. Link8 and Solid45 elements were used to model the longitudinal reinforcement and the FRP composites, respectively. As in the experimental study, the plastic hinge was formed at the column face in the analytical modelling for the control specimen. Experimental and analytical studies showed reasonably similar hysteresis curves for the control specimens. In the case of CFRP jacketed specimens the results were similar to the experimental results i.e. the plastic hinge was created beyond the end point of the CFRP.

Hegger et al. (2004) investigated the behavior of interior and exterior beam-column joints using nonlinear finite element analysis using ATENA. The analytical model was validated by the author's experimental data. The study was conducted to investigate the behavior and find the critical parameter that affected the shear capacity of these connections. Nine-node iso-parametric shell elements were used for concrete modelling and reinforcement was modeled with discrete bars. Meshes for interior and exterior joints are shown in Figure 2.18. Coarser mesh was used for the beam and the column. The ATENA program assumes full bond between the concrete and reinforcement. In some of the connections, the beam tensile reinforcement was anchored by anchor plates at their ends. The theoretical and experimental load-deflection curves showed good agreement for both the interior and exterior joints. Also, it was concluded that the finite element modeling is capable of distinguishing between the failures types of the joints.

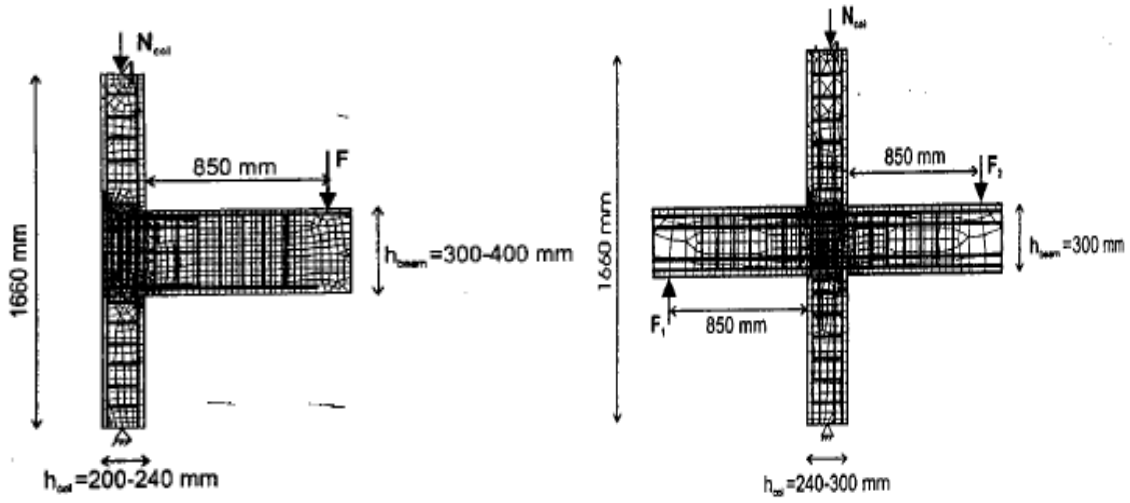

Figure 2.18: Exterior and Interior Beam-Column Joint used in FEM Analysis Hegger et al. (2004)

Wolanski (2004) investigated the use of the FEM for the analysis of RC and pre-stressed concrete beams. Experimental results of Buckhouse (1997) was compared with a mild-steel reinforced concrete beam with shear and flexural reinforcement, which was analyzed to failure to calibrate the parameters in ANSYS 2003.

In FEM modelling (ANSYS) only one quarter of the beam was modelled as the section was symmetrical in cross-section and loading. The RC beam model was 2.36m long, with a cross-section of 125 x 450 mm. A rectangular mesh was adopted for FE model of the beam. For concrete Solid65 element and for the steel reinforcement Link8 element were used in modeling. Boundary conditions, loading and supports were applied at points of symmetry, similar to the experimental beam. The finite element analysis of the beam model was carried out to study three different behaviors: strength of the beam by limit state, initial cracking, and yielding of the steel reinforcement. Incrementally load was applied up to failure of the beam. The FE analysis of the beam within the linear region was done to make sure deflections and stresses were steady in the beam before cracking, as deflections and stresses become difficult to predict once cracking sets in. Finite element model values and hand calculations are shown in Table 2.1.

Table 2.1: Stress and Deflection Comparisons at First Cracking by Wolanski (2004)

Model	Extreme Tension Fiber Stress (psi)	Reinforcing Steel Stress (psi)	Centerline Deflection (in.)	Load at First Cracking (lbs.)
Manual Calculations	530	3024	0.052	5118
ANSYS	536	2840	0.053	5216

The above provided results of FE analysis indicated that earlier cracking was acceptable. For the non-linear area, succeeding cracking occurred when more load was applied to the beam. It was observed that in the constant moment region cracking increased and at a load of 8000 lbs. The beam began to crack towards the supports. At 12000 lbs flexural cracking occurred in the beam and a diagonal tension crack was also observed in the model. At a load of 13400 lbs yielding of steel reinforcement was found to have occurred.

Table 2.2:Ultimate Load vs Deflections by Wolanski (2004)

Beam	Load (lb.)	Centerline Deflection (in.)
Buckhouse (1997)	16310	3.6
ANSYS	16310	3.5

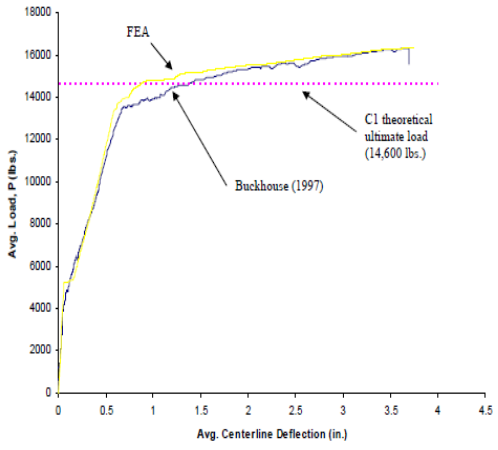

Figure 2.19: Load vs. Deflection Curve Comparison of Buckhouse and ANSYS

The maximum load taken up by the beam was 16,382 lbs., as indicated by an insoluble convergence failure in the beam. The results of FEM analysis and control beam deflections at the failure load are shown in Table 2.2. The difference in the deflections as obtained by FEM analysis and the control beam was only 2% at the same load at which the control beam failed.

Kachlakev et al. (2001) did the FEM analysis of Horsetail Creek Bridge retrofitted using FRP sheets for the Oregon Department of Transportation. Behavior of four full size beams was studied using the ANSYS program (1998). Experimental and FEM results were compared. It was observed that the load-carrying capacity increased using FRP retrofitting. CFRP sheets were fixed to the bottom side of the beam with the fibers oriented along the length of the beam for flexural strengthening. GFRP sheets were wrapped around the beam with fibers perpendicular to the length of the beam. The concrete solid65 element, steel reinforcement Link8 element, and FRP Solid46 element, were used in the model. A good agreement in the form of load-deflection curves of FEM was observed. The crack patterns were similar for the FEM as observed in the experimental results.

2.5 LITERATURE RELATED TO RETROFITTING OF CONCRETE STRUCTURES – ANALYTICAL MODELLING AND DESIGN

Akguzel and Pampanin (2012) developed an analytical model for the control and FRP retrofitted reinforced concrete beam-column joints. Firstly, the in-built beam-column (BC) joint components were assessed. The shear strength of the FRP jacketed beam-column joints was calculated with sum of the as- built BC joints and the composite material attached to the plain concrete. A schematic illustration with the nomenclature used in the design of the average stresses are shown in Figure 2.20 and Figure 2.21.

An iterative procedure using equations 2.1 to 2.4, was developed by the authors to evaluate the joint shear capacity after FRP retrofitting,

The input included a) Geometric data*:* b_c , b_w ,h_b, h_c b) Material properties*:* elastic modulus of concrete, E_c*;* compressive strength of concrete, *fc';* tensile strength of concrete, f_{ct}; FRP thickness per layer, t_f*;* elastic modulus of the fibers, E_f and design rupture strain in the FRP, $\varepsilon_{fu.}$ c) FRP application scheme details*:* depth of FRP sheet on beam surface, $d_{f\,b}$*;* depth of FRP sheet on column surface, d_{fc}*;* number of sheet on the beam, n_{fb}*;* number of sheets on column, n_{fc}; number of beam sides covered with FRP , $n_{sf\,,}b$; number of column sides covered with FRP, $n_{sf\,,}c$.

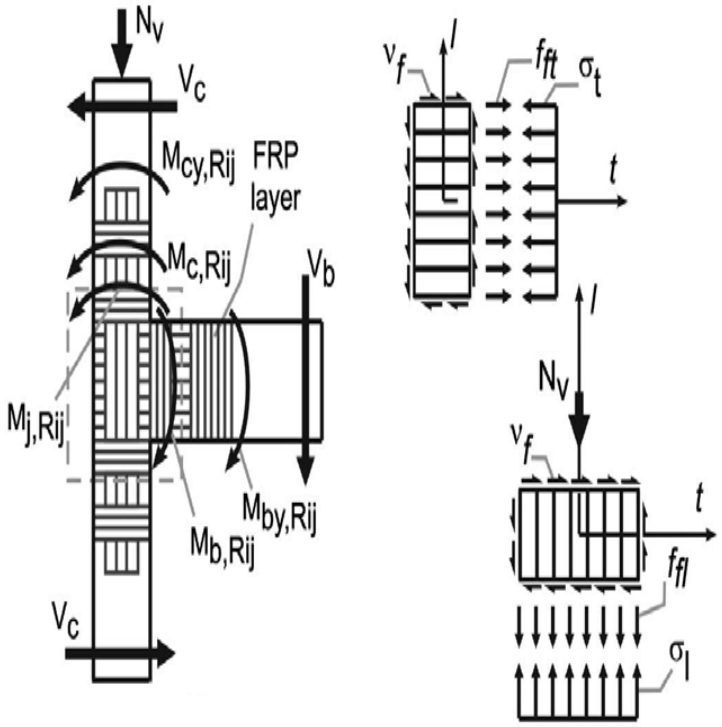

(a) (b) and (c)

Figure 2.20: RC Beam-Column Joint with Shear Resisting Mechanisms

a) Forces acting on a retrofitted joint b) Horizontal force equilibrium c) Vertical force equilibrium

Akguzel and Pampanin (2012)

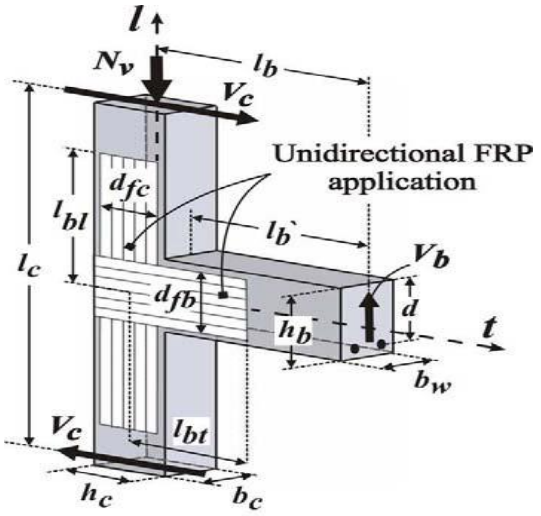

Figure 2.21: RC Beam-Column Joint Retrofitted with FRP: Figure of Proposed Dimensions

Akguzel and Pampanin (2012)

FRP reinforcement ratio in the transverse or longitudinal direction was found as follows:

$$\rho_{ft} = \frac{n_{fb} n_{sf,b} t_f d_{fb}}{h_b b_w} \quad (2.1)$$

$$\rho_{ft} = \frac{n_{fc} n_{sf,c} t_f d_{fc}}{h_c b_c} \quad (2.2)$$

At the end of each iteration step, two failure conditions were checked;

i) *Failure of FRP*: Tensile fracture was the main reason for the fail use of FRP when tensile stress of FRP reaches the tensile strength, f_{fu} or the corresponding ultimate strain, $\varepsilon_{fu.}$ The maximum tensile stress in an FRP strip of thickness, t_f, in mm when failure occurs was given by

$$f_f, max = f_f, deb = C_1 \sqrt{\frac{E_f f_{ct}}{t_f n_{fb}}} \quad (2.3)$$

for $l_b \geq l_b$, max, where C_1=0.64 (empirical coefficient) for CFRP and l_{bt}=development length along the direction taken in mm

$$l_{b,max} = \sqrt{\frac{E_f t_f}{C_2 f_{ct}}} \quad (2.4)$$

where C_2 is taken as 2 in order to satisfy capacity design considerations.

ii) *Diagonal compression failure of the concrete in the joint panel zone:* The diagonal compression stress in the joint sheet region was to be restricted ($\rho_c \leq 0.3 fc'$) to prevent early brittle failure of the compression bar especially after the progress of multiple diagonal cracks in the region. By applying the above mentioned relationships, the FRP contribution to the increase in the joint shear capacity of weakly detailed external beam-column joints could be sufficiently predicted in terms of principal tensile stresses, $p_{tf.}$ The experimental test results available from the past literature were compared with the analytical model predictions, and the authors confirmed the legitimacy of the proposed design procedure.

Mahini and Ronagh (2010) developed an analytical model to calculate the ultimate load, yield load and ductility of beams using FRP retrofitting. Compression failure, tension failure, de-bonding and FRP rupture of FRP retrofitted beams were considered in the flexural failure. In derivation de-bonding was not considered as it was not observed in experimental tests. Moment and curvature graphs were drawn using a trial and error procedure for three stages of cracking i.e. pre-cracking, cracking and post-cracking. For the small differences between the two values only estimated values were established or else these values were customized by the bisection method till convergence occurred using equations (2.5) and (2.6). Figure 2.22 shows a reinforced concrete beam cross-section retrofitted using FRP, where b is the width and h is the height of the section, $t_{f\ was}$ considered as the thickness of FRP with ff as stress. A_s is the area of steel reinforcement with stress $f_{s,}$ and reinforcement in compression having an area A'_s with stress f'_s and f'_c considered as the concrete compressive strength.

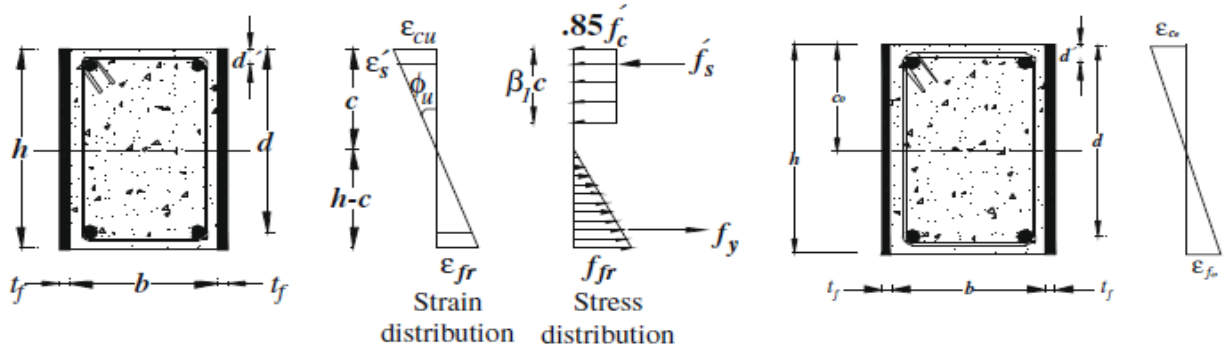

Figure 2.22: **(a) Stress- Strain Diagram of FRP Strengthened Beam; (B) Strain Diagram of Beam before Retrofitting By Mahini &Ronagh (2010)**

It was seen that if $\varepsilon_{fr} + \varepsilon_{fo} > \varepsilon_{cu}$ ((h-c) / c) then tension failure occurred and a

if $\varepsilon_{fr} + \varepsilon_{fo} < \varepsilon_{cu}$((h-c) / c), then the failure was due to FRP rupture.

ε_{fr} and ε_{fo}, the ultimate strain of the fiber and the initial strain of the un-retrofitted beam at the extreme tensile level of the reinforced concrete section, respectively and the ultimate compressive strain in the concrete was given by ε_{cu}.

The total strain at the extreme tensile level of the FRP wrap was given by

$$\varepsilon_{ft} = \varepsilon_{fr} + \varepsilon_{fo} \quad (2.5)$$

and the neutral axis depth was considered as c, shown in equation (2.6), at the ultimate load condition.

c was obtained from equilibrium as

$$c = \frac{A_s f_s - A'_s f'_s + f_f (h-c) t_f}{0.85 f'_c \beta_1 b} \quad (2.6)$$

By considering both modes of failure the ultimate flexural capacity of the FRP retrofitted beam was calculated. The maximum possible curvature of the FRP retrofitted beam was expressed as $\Phi = \varepsilon_{cu} / c$ with the maximum permissible concrete compression strain in the extreme fiber, ε_{cu}= 0.003, for normal strength concrete.

Antonopoulos and Triantafillou (2002) offered analytical models for analysis of RC joints retrofitted with externally bonded composite materials in the form of unidirectional strips. Stress and strain were provided in the models for the various stages. The Pantazopoulou and Bonacci (1992) model was extended by the authors in the study. The stress-strain equations were provided for various stages defined by FRP debonding and concrete crushing. The developed models provided valuable information on the shear capacity of FRP retrofitted joints in terms of the quantity and design of the externally bonded fiber. Good agreement of experimental results and analytical models was found in the form of shear-strength predictions found in the literature.

Ghobarah and Said (2001) proposed a design methodology for upgrading the joint shear capacity with fiber retrofitting of existing RC joints in moment resisting frames. In the joints the missing transverse reinforcement was replaced with the fiber. By using the expression (2.7) given by Park and Paulay (1974) the joint shear force V_j, was calculated using

$$V_j = 1.25 A_s f_y - V_{col}, \quad (2.7)$$

where, V_{col} = shear force in the column

A_s =area of the longitudinal tension steel reinforcement

f_y= yield strength of the steel

The total joint shear resistance of the improved joint was given by

$V_j = V_c + V_s + V_f$

where

V_c = concrete shear resistance

V_s = transverse reinforcement

V_f. = fiber resistance

As there was no transverse reinforcement in the RC joint so V_s, was taken as zero.

Then, the shear resistance of concrete using equation (2.8) considering the applied axial stress is

$$V_c = 0.2 \sqrt{f'_c} \left(1 + \frac{3 f_{col}}{f'_c}\right) b d_j \qquad (2.8)$$

where,

f_{col}= nominal stress in the column,

b= *width* of the joint, and

d_j= effective depth of the joint.

The required area of fiber in the joint

$$A_f = \frac{V_f S}{\Phi_f d_j f_u} \qquad (2.9)$$

where,

A_f= area of fiber reinforcement required over the jointregion,

f_u= tensile strength of the fiber,

s = joint height, and

Φ_f= resistance factor (0.8).

Gergely et al. (2000) proposed design equations (2.10) and (2.11) for the strengthened RC joints based on the experimental results. To calculate the horizontal and vertical shear forces in the joint region the forces acting at the face of the column and the beam were considered.
The joint shear forces and composite properties are given by

$$V_f = nt\varepsilon_f E_f d_e \frac{sin\beta}{cos\beta} \qquad (2.10)$$

where,

V_f =increase in the joint shear force,

n =total number of composite layers,

t = calculated thickness of the composite sheets,

ε_f = average axial strain in the fiber,

E_f= elastic modulus of the composite material, and

d_e = effective joint depth

The column cap beam joint details with the composite layer perpendicular to the crack are shown in Figure 2.23. Crack direction is similar to the principal compression stresses. The inclination of the principal planes and dimension of the joint control the value of the joint effective depth, d_e. The magnitude of the force *F* is given by

$$F = nt\varepsilon_f E_f \frac{d_e}{cos\beta} \qquad (2.11)$$

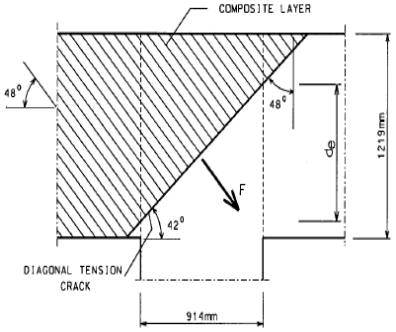

Figure 2.23: Composite Forces (Tensile)

Gergely et al. (2000)

The value of the force *F* was divided by the width of the joint and by the inclined length for finding the principal tensile stress in the composite, bordered by the effective depth.

2.6 SUMMARY

Based upon the published literature, it can be said that very limited work has been done in the area of retrofitting of beam-column joints using ferrocement. Only a few studies have been reported on strengthening of exterior beam-column joints using ferrocement. The RCC structures, which require retrofitting, are already stressed to a particular level due to the loads experienced by the structure in its life span, and therefore, it is imperative to study the effect of the initial stress levels on the behavior of such structures after retrofitting.

Therefore, the present study undertaken is very important and its results shall be very useful in designing the bonded laminate for retrofitting. The studies herein present the effect of initial stress level on the various parameters such as maximum load carrying capacity, safe load carrying capacity, toughness and ductility of reinforced concrete exterior beam- column joints retrofitted with ferrocement jackets, which are reinforced with different layers of woven wire mesh.

CHAPTER – 3

EXPERIMENTAL PROGRAM AND TEST PROCEDURE

3.1 GENERAL

The experimental program in the investigation was designed to study the effect of various parameters on the strength characteristics of predetermined initially stressed reinforced concrete exterior beam-column joints retrofitted with bonded laminates. Thirty seven prototype exterior beam-column joints were cast as shown in Plate 3.3. The beam- column joint specimens had a column cross-section of 225 mm x 125 mm with an overall length of 1000 mm and the cantilever beam part of the joint had a cross- section of 125 mm x 225 mm with a length of 500mm. For all the thirty seven specimens, four deformed bars of 10mm diameter were used as longitudinal reinforcement and 6mm diameter mild steel lateral ties at a spacing of 100mm c/c were provided in the columns. The beam was designed as an under reinforced section with two deformed bars of 10mm diameter as tension reinforcement and two deformed bars of 8 mm diameter as compression reinforcement, and vertical stirrups of 6mm diameter at 100mm c/c which is less then 0.75d i.e. 138.75mm, so that beam should not fail in shear. The cross sectional dimensions of the beam were decided to achieve a shear span / effective depth ratio of the beam (*a/d)* greater than 2, so that it did not act as a corbel/bracket. In the current case, the shear span *a*, which is the distance of the point of application of the load from the support, is 450mm and effective depth of the beam *d* is 195mm. So *a/d* ratio for the present study was to be 2.3 which is greater than 2. Eleven RC exterior beam-column joints were cast to be tested under each stress level, and in addition four beam-column joints were cast and tested to failure for deciding the stress levels (control specimens).

For the purpose of investigation, out of the two sets of RC beam-column joints, one set was retrofitted with ferrocement jackets incorporating two, four and six layers of wire mesh at 45 degree w.r.t. longitudinal axis of the beam and in L-shape to the longitudinal axis of the beam.

The variation in these parameters was finalized considering gaps in the available literature and on the basis of pilot testing carried out in the laboratory.

The other set of the six exterior beam-column joints, were retrofitted using Carbon Fiber Reinforced Polymer (CFRP) jackets with fibers orientated at 45 degree and in L-shape to the longitudinal axis of the beam.

Figures 3.1 and 3.2 show the flow chart of the experimental program on testing of the beam-column joints.

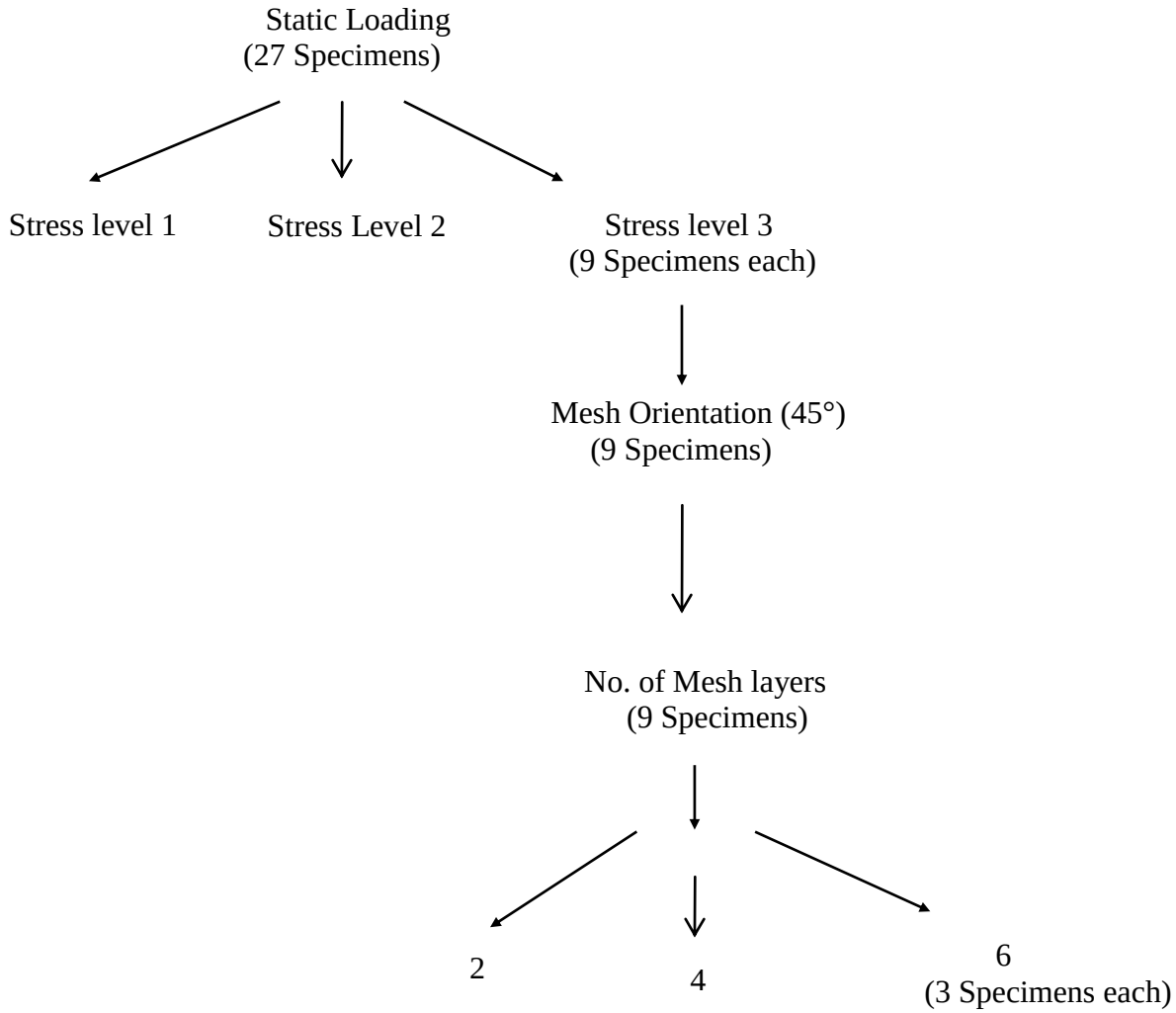

Figure 3.1: Flow Diagram for Retrofitting of Beam-Column Joints Using Ferrocement Jackets

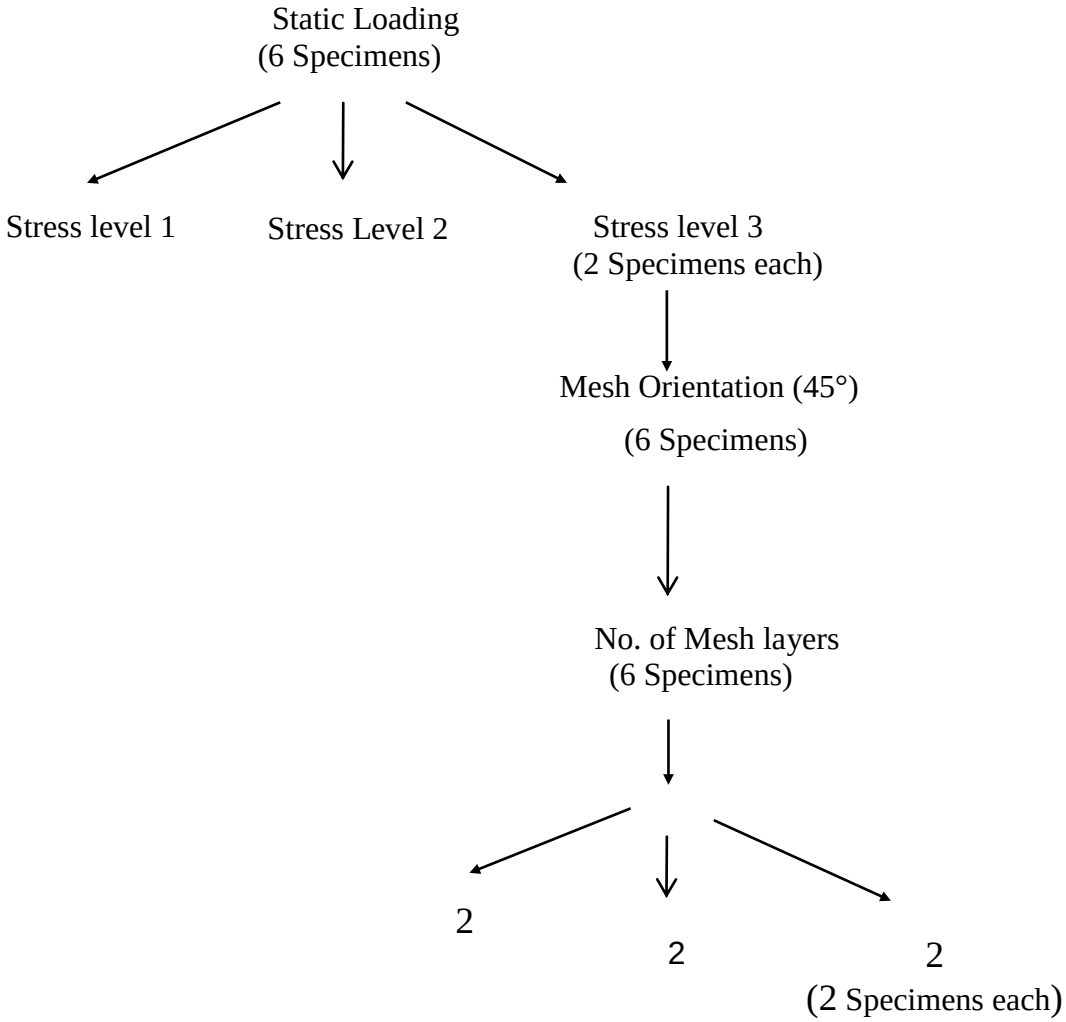

Figure 3.2: Flow Diagram for Retrofitted Beam-Column Joints CFRP Jacket

3.2 MATERIALS

All the material used in the investigation were tested in accordance with the relevant Indian standard codes of practice, to determine their physical properties. The same sets of materials were used in the pilot study for casting the beam-column joints. The details of materials used along with their properties are discussed below.

3.2.1 Cement

Portland Pozzolana Cement of UltraTech made from a single lot was used in the study. The physical properties of the cement obtained from various tests are listed in Table 3.1. All the tests were carried out in accordance with the procedure laid down in IS 1489 (Part 1):1991.

3.2.2 Fine Aggregate

The aggregate passing through 4.75mm IS sieve is classified as fine aggregate as per IS: 383-1970. Locally available riverbed sand was used in the present study. The physical properties are presented in Table 3.2. The percentage of fine aggregate passing through 600 micron was 61.6, which indicates that the sand conforms to grading zone – III as per IS 383-1970.

3.2.3 Coarse Aggregate

The aggregate retained on the 4.75 mm IS sieve is termed as coarse aggregate. Two types of crushed aggregate with different maximum sizes were used in the present study i.e.

CA-I Aggregate passing through 20 mm sieve and retained on 10 mm sieve.

CA-II Aggregate passing through 10 mm sieve and retained on 4.75 mm sieve.

The physical properties and sieve analysis results of the coarse aggregates used are listed in Table 3.3.

3.2.4 Water

Fresh and clean potable water was used for casting and curing the specimens in the study. The water was relatively free from organic matter, silt, oil, sugar, chloride and acidic material as per Indian standard IS: 456-2000.

3.2.5 Reinforcing Steel

HYSD steel of grade Fe- 415 conforming to IS: 1786 – 1985 was used in the study. Deformed bars of 10mm and 8mm diameter and mild steel bars of 6mm diameter were used in the experimental program. The 10mm diameter deformed bars were used as tension reinforcement and 8mm diameter deformed bars were used as compression steel in the cantilever beams, and 8mm diameter deformed bars were used as reinforcement in the column part of the joint. The 6mm diameter mild steel bars were used as shear stirrups and lateral ties in the beam and column parts of the joints, respectively. The properties of these bars are presented in Table 3.4.

3.2.6 Wire Mesh

GI woven steel wire mesh of 0.5 mm diameter wires with a 10mm x 10mm opening was used as the reinforcement in the ferrocement jackets. The salient properties of the wire mesh used are given in Table 3.4.

3.2.7 Concrete Mix

M20 grade concrete mix was designed as per Indian standard recommended guidelines IS: 10262:2009, using the materials with properties laid down in Tables 3.1 to 3.3. The water cement ratio achieved in the design was 0.48. The mix proportion of materials adopted was 1: 1.44: 2.09: 0.88 by weight (cement: sand: coarse aggregate CA-1: coarse aggregate CA-2). The quantities of materials per cubic meter of concrete along with the strength results of 150mm cubes cast for the proportioned design mix are listed in Table 3.5 (a) and 3.5 (b), respectively. Plates 3.1- 3.2 shows setup for testing the of steel bars, testing of wire mesh, preparation of wire mesh sample for testing, and test result recording of steel and wire mesh.

Test Setup for Beam- Column Joints Subjected to Static Load at Beam Tip with LVDT'S At Beam Tip And at 50mm From Column Face

Plate 3.1

(a) Testing of Steel Bars

(b) Preparation of Wire Mesh Sample for Testing

(c) Testing of Wire Mesh

(d) Test Result Recording of Steel and Wire mesh

Plate 3.2: Test Setup for Steel Bars and Wire Mesh

Table 3.1: Physical Properties of Portland Pozzolana Cement

Sr. No.	Characteristics	Test Values	Value specified by IS :1489 (Part 1) - 1991
1.	Standard Consistency (%)	32	---
2.	Fineness of cement as percentage retained on 90 micron sieve (%)	0.7	Maximum 10
3.	Setting time (minutes) Initial Final	 105 255	 Minimum 30 Maximum 600
4.	Specific gravity (Specific gravity bottle)	3.1	-
5.	Compressive Strength (MPa) 7 days 28 days	 23.5 34.5	 Minimum 22.0 Minimum 33.0
6	Soundness (by Le- Chatelier's method), mm	3.0	Maximum 10 (fresh Cement)

Table 3.2: Physical Properties of Fine Aggregate

Sr. No.	Characteristics	Test Value
1.	Specific gravity (oven dry basis)	2.7
2.	Bulk density loose (kg/lt)	1.3
3.	Fineness modulus	2.3
4.	Water absorption (%)	2.3
5.	Grading Zone (based on percentage passing 600 µm sieve)	Zone III

Table 3.3: Physical Properties of Coarse Aggregate

S.No.	Characteristics	Values	
		CA-I	CA-II
1.	Type	Crushed	Crushed
2.	Maximum Nominal Size (mm)	20	10
3.	Specific gravity	2.6	2.7
4.	Total water absorption (%)	1.9	1.8
5.	Fineness modulus	6.8	6.3

Table 3.4: **Physical Properties of Steel Bars and Steel Mesh Wires**

S.No.	Diameter of Bars/ Wire Mesh (mm)	Yield Strength (MPa)	Ultimate Strength (MPa)	Elongation (%)
1.	10	554.0	670.0	20.5
2.	8	557.0	676.2	25.8
3.	6	442.4	612.7	32.7
4.	0.5(wire)	665.0	950.0	18.2

Table 3.5 (a): Mix Proportion for M20 Grade Concrete (kg/m^3)

Water	Cement	Fine Aggregate	Coarse Aggregate -1 (20mm)	Coarse Aggregate -1I (10mm)
189.9	395.6	571.6	814.6	349.1
0.48	1	1.44	2.09	0.88

Table 3.5 (b) Compressive Strength of Cubes for M20 Concrete

S.No.	Age (Days)	Compressive Strength (MPa)
1.	7	18.5
2.	28	21.5

3.2.8 Mortar Mix for Ferrocement Jackets

The range of mix proportion (cement : sand) by weight recommended for common ferrocement application is between, 1:1.5 to 1: 1.25, but not greater then 1:3 in any case, and water cement ratio (by weight) ranges between 0.35 to 0.5 (*ACI Committee 549 Report*). The higher the sand content the higher is the water content required for the desired workability. The fineness modulus of the sand, water-cement ratio and sand-cement ratio are generally varied and trial batches are cast to ensure a mix that can infiltrate the mesh and develop a strong and dense matrix. For the present study, the proportion of cement mortar used for applying ferrocement jackets was 1:2 (cement: sand). The water-cement ratio for mortar was 0.4 to ensure a homogeneous mix of desired workability. A compressive strength of 29.5MPa achieved for the cement sand mortar after a curing period of 28 days.

3.2.9 CFRP Fabric

Unidirectional CFRP sheets 500 mm wide and 0.117mm thick were used for retrofitting purposes. The CFRP sheets were obtained from BASF construction chemicals and building systems. Under stress, the deformation of the matrix transfers the load to the fiber mesh which results in high strength and a high modulus composite. The adhesive used for bonding CFRP sheets with concrete was a compatible epoxy system provided by the manufacturer. It was blue pigmented epoxy resin for saturation of MBrace fiber sheet to formed in-situ CFRP Composite. It was made by mixing the base saturant and hardner in the ratio 100:40. Mixing of the saturant and hardner was done thoroughly for five minutes until components were thoroughly dispersed. The typical properties of the materials as provided by the manufacturer are listed in the Tables 3.6 -3.7.

Table 3.6: Properties of Carbon Fibers used for Retrofitting

Sr. No.	Physical Properties	Value
1.	Tensile Strength (MPa)	3800.0
2.	Modulus of Elasticity (GPa)	240.0
3.	Density (gm/cm^3)	1.7
4.	Weight of CFRP mesh before stiching (gsm)	200.0
5.	Weight of CFRP mesh, after stiching (gsm)	230.0
6.	Thickness (mm)	0.12

Table 3.7: Properties of Epoxy Resin

Aspect	Translucent Blue Liquid
Volume solids	100 %
Mix Density	1.13±0.03
Mixing Ratio Epoxy: Hardener (by weight)	100 : 40
Mixed viscosity (cps at 25^0)	4000±500
Pot life	25 minutes at 25^o C
Setting Time	< 3 hrs. at 25^o C
Full Cure	7 Days at 18^oC
Compressive Strength	>40MPa at 1 day >60 MPa at 7 days
Tensile Strength	>17 MPa
Flexure Strength	>35 MPa
Density	0.8 to 1.0 kg/m^3

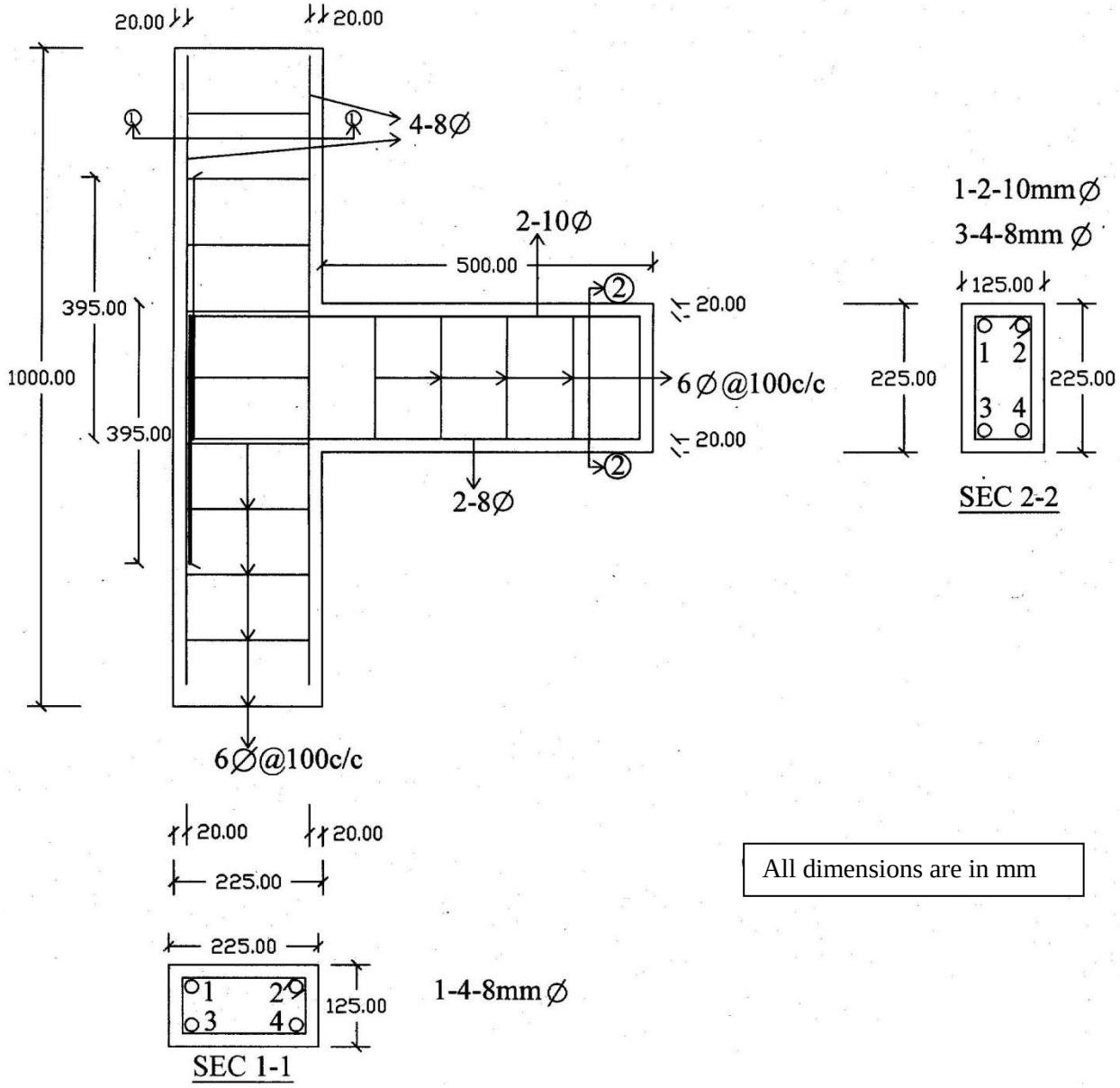

Figure 3.3: Details of Beam- Column Joints

3.3 TESTING ARRANGMENT

All the controlled as well as retrofitted beam-column joint specimens were tested using a servo- controlled hydraulic jack with load control facility. The testing system in the laboratory had the capability to do a load control test only the arrangement for the testing being shown in the Plate 3.1. The specimens were fixed to a triangular frame with the help of nuts and bolts, and a point load was applied on the cantilever beam tip. The value of the deflection and corresponding load at beam tip were recorded. The load was read from the data acquisition system connected to the jack having a least count of 0.1 kN. The deflection at specific points corresponding to the applied load was measured with the help of LVDT's (Linear Variable Differential Transducers) having a least count of 0.01mm. Two LVDT's were used, one was placed at the tip of the beam and the other at 50mm from the face of the column as shown in Figure 3.4.

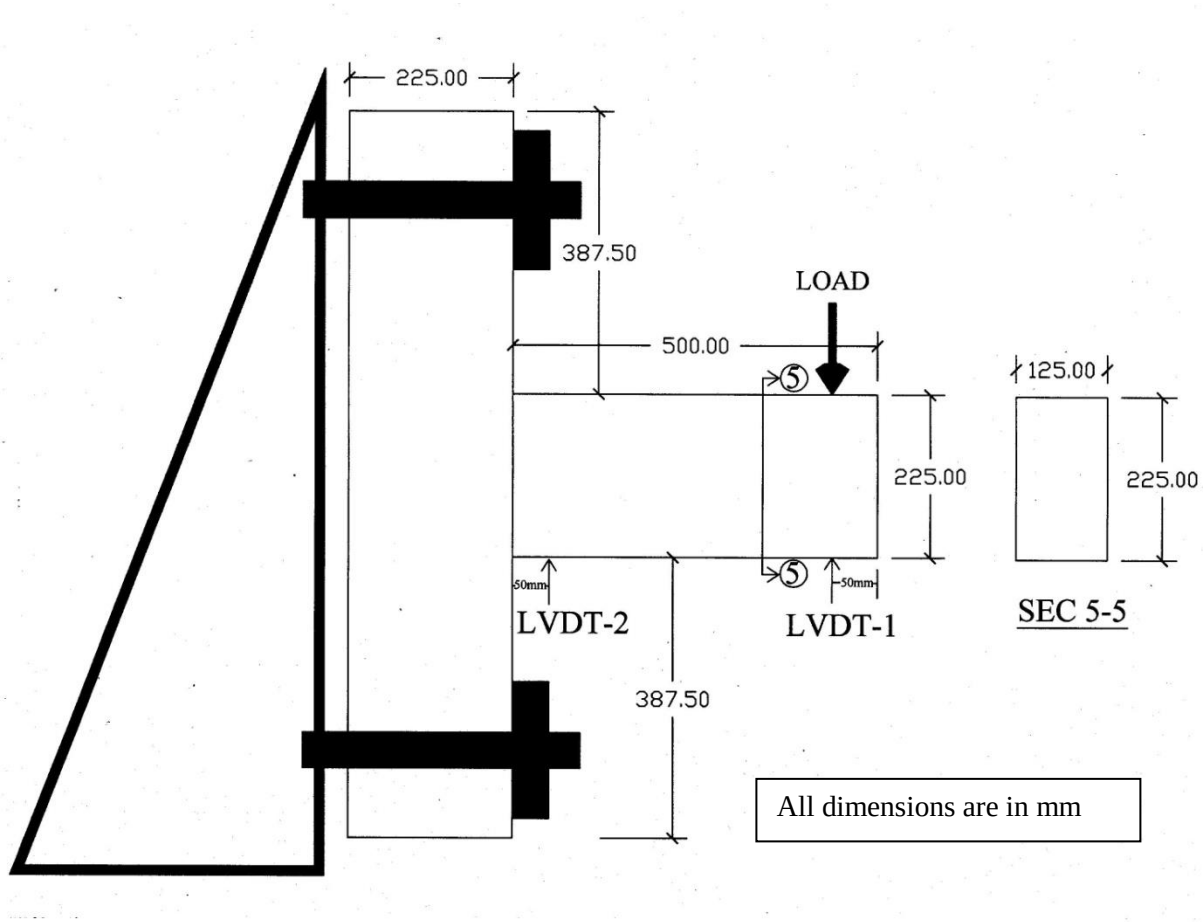

Figure 3.4: Loading Arrangements for Testing of Beam-Column Joints

3.4 CASTING OF REINFORCED BEAM-COLUMN JOINTS

The prototype RC beam-column joint specimens, both for the pilot studies as well as for the experimental program of column cross-section of 225 mm x 125 mm with an overall length of 1000 mm and the cantilever beam had a cross- section of 125 mm x 225 mm with a length of 500mm were cast as explained in section 3.1 of this chapter. The steel mould was made with dimensions 125mm x 225mm for the beam portion and length of 500mm and 225mm x 125mm for the column portion with a length of 1000mm. Cover blocks of 20mm were placed under the reinforcement cage to provide a uniform cover as shown in Plate 3.3 (a). The coarse aggregates, fine aggregate, cement and water were mixed manually as per proportion obtained form the design concrete mix. The beam-column joint as cast dimensions/ reinforcement details are shown in Figure 3.3. The moulds were oiled before concreting to ease the demoulding process. The concrete mix was poured into the moulds and compacted using a needle vibrator as shown in Plates 3.3 (d) and 3.3 (e). The vibration was done until the mould was completely filled. The beam-column joints were demoulded after forty eight hours. After demoulding the beam- column joints were cured for 28 days using fully wet jute bags as shown in Plates 3.3 (f) and 3.3 (g). The beam-column joints were cast corresponding to the parameters fixed based on the pilot study program to study the effect of variation on strength characteristics of the beam-column joints as presented in Figures 3.1 - 3.2.

(a) Cover Blocks

(b) Preparation of Moulds

(c) Reinforcement Cage in Moulds

(d) Compaction of Concrete Using Needle Vibrator

(e) Beam-column Joint

(f) Curing of Samples

(g) Stack of Cast Specimens

Plate 3.3: Casting of Beam- Column Joints

3.5 PROCESS OF RETROFITTING

The retrofitting of RC exterior beam-column joints was done with two types of jackets, namely ferrocement jackets and CFRP jackets. The method of retrofitting for each of the two cases is presented below.

3.5.1 Retrofitting Using Ferrocement Jackets

For the purpose of investigation of beam-column joints, retrofitted using ferrocement jackets, twenty seven exterior RC beam-column joint specimens were cast. Nine beam-column joints were cast for each stress level i.e stress level-1(ultimate load), stress level-2 (85% of ultimate load) and stress level-3 (50% of ultimate load). Firstly, the stressed beam-column joints were chipped grooves and the surface was subsequently cleaned with a metallic brush using potable water. After wrapping the specimen with the wire mesh the cement slurry was applied as the bonding agent to the surface of the beam- column joints. One coat of cement slurry was applied

on the cleaned surface before placing the wire mesh cage on it, without repairing the initial cracks. The cage was properly placed ensuring a tight fit with the help of mild steel wire and 1**:**2 cement sand mortar with a water cement ratio 0.4. The process of ferrocement jacketing is shown in Plate 3.4.

(a) Fixing of Wire Mesh

(b) Application of Cement Slurry

Plate 3.4: Application of Ferrocement Jacket

Out of these nine specimens, three beam-column joint specimens were retrofitted with two layers, three beam-column joint specimens were retrofitted with four layers; three beam-column joint specimens were retrofitted with six layers, with woven wire mesh, for each stress level.

3.5.2 Retrofitting Using CFRP Jackets

For the second part of the investigation six prototype beam-column joints were cast, two each for stress level-1 (ultimate load), stress level-2 (85% of ultimate load) stress level-3 (50% of ultimate load). These beam-column joints were subsequently retrofitted using CFRP sheets, obtained from BASF construction chemicals and building system, to study their effect on the strength of the stressed beam-column joints. The surface of these stressed beam-column joints was first cleaned and dried, and cavities, if any, were removed by repairing the surface with cement paste. The surface of beam-column samples was smoothened with the help of a grinder having diamond plates. Subsequently the edges of the beam-column joints were rounded, as shown in Plates 3.5 and 3.6. A compatible epoxy adhesive provided by the manufacturer was used for bonding CFRP sheets with concrete.

The adhesive used was a blue pigmented epoxy resin used for saturation of MBrace fibre sheet to form an in-situ FRP Composite. It was made by mixing base saturant and hardner in a ratio of 100:40. Mixing of the saturant and hardner was done thoroughly for five minutes until components were thoroughly dispersed. Two layer sheets of CFRP were then wrapped on the surface of the stressed beam-column joint specimens in a L-shape and at 45^0 to the longitudinal axis of the beam- column joint as shown in Plates 3.7- 3.8. A special type of roller for impregnating the adhesive substance to the fiber and to the beam was used as a part of the retrofitting process.

(a) Surface Preparation

(b) Rounding of Edges

(c) Surface Preparation

Plate 3.5: Surface Preparation for Retrofitting of Beam-Column Joints for CFRP Jacket

(a) Prepared Surface for Stress Level- 1

(b) Prepared Surface for Stress Level-2

(c) Prepared Surface for Stress Level-3

Plate 3.6: Prepared Surfaces for Retrofitting of Beam-Column Joints for CFRP Jacket

(a) CFRP Used for Jacket

(b) Mbrace Saturant: Resin and Hardener

(c) Application of Epoxy

(d) Application of CFRP

Plate 3.7: Application of Resin and CFRP to Surface of Beam-Column Joints

(a) Application of CFRP

(b) CFRP jacketed Joints

Plate 3.8: Application of CFRP and CFRP Jacketed Beam-Column Joints

3.6 IDEALIZATION OF LOAD DEFLECTION CURVE

The load deflection data obtained from the testing of the beam-column joint specimens was plotted and the plot was idealized as a trilinear curve for the purpose of calculating the ductility ratio and toughness of the beam- column joints. The ductility ratio is defined as the ratio of deflection at the ultimate load (defined as 85 % of the maximum load) to the deflection at the yield point, whereas, toughness is the area under the idealized load deflection curve up to the ultimate load.

The idealized load deflection curve is obtained by linearly joining three points starting from the origin. Each of these three points are located on the curve as explain below.

1. Elastic load point is the load up to which the load deflection curve is linear.
2. Yield load point is the load at which yielding of the beam-column joint specimen starts, which is obtained by drawing a tangent to the elastic load point and maximum load point on the curve.
3. Ultimate load point, defined as the point at which the load drops to 85 % of the maximum load.

3.7 SUMMARY

In this chapter various physical properties of the materials (cement, fine aggregate coarse aggregate, steel bars, steel mesh wires, CFRP, epoxy resin) that were used in the present investigation, are presented. Ingredients of M20 Grade of concrete mix were determined in accordance with the Indian standard. After casting and testing of these specimens the beam-column joints were retrofitted using ferrocement and CFRP, after finalizing the retrofitting technique from the pilot study, and tested in the laboratory.

CHAPTER – 4

PILOT STUDY

4.1 GENERAL

A review of related literature shows that the behavior of ferrocement depends upon various parameters like type of wire mesh, cement-sand ratio, orientation of wire mesh, number of wire mesh layers and water cement ratio. Thus the behavior of beam-column joints retrofitted using ferrocement jackets will also vary depending upon such parameters. Thus, to understand and optimize the parameters for use in the main program, pilot studies were carried out for studying the effect on the retrofitted beam-column joints. The studies were carried out to identify the technique most suitable for retrofitting the joints using ferrocement jacketing. Four number of prototype beam-column joints were cast for pilot testing as control specimens as per the procedure laid out in section 3.4

4.2 RETROFITTING USING FERROCEMENT JACKETS

The four beam-column joints were first stressed to the ultimate load. The surface of the beam-column joints were prepared as per the procedure laid down in the section 3.5.1.

For the pilot studies, two types of retrofitting scheme were used for wrapping of the GI wire mesh designated as Type-A and Type-B. In Type-A retrofitting, two L-shaped wire mesh pieces of appropriate size wire mesh were cut and wrapped on the lower and upper faces of the beam at the joint with a 25mm thick cement mortar (1:2) layer as shown in Figure 4.1. In type-B retrofitting, again two L-shaped wire mesh pieces of appropriate size were wrapped on the lower and upper faces of the beam at the joint, with extra mesh of appropriate size diagonally at 45 degree to the joint using 25mm thick cement mortar (1:2) as the bonding agent, as shown in Figure 4.2. The retrofitted specimens are shown in Figure 4.3.

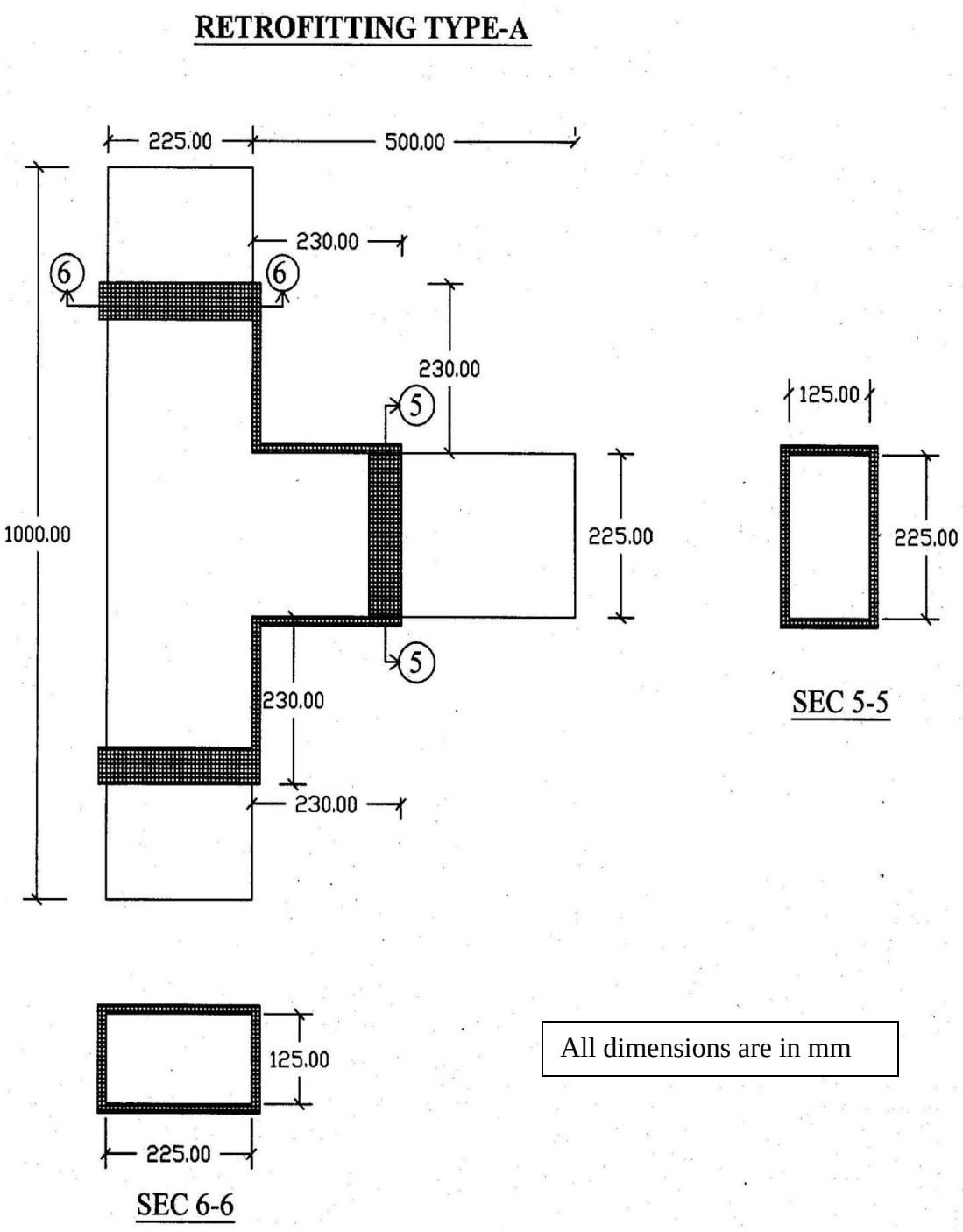

Figure 4.1: Wire Mesh Wrapping Method in Type-A Retrofitting

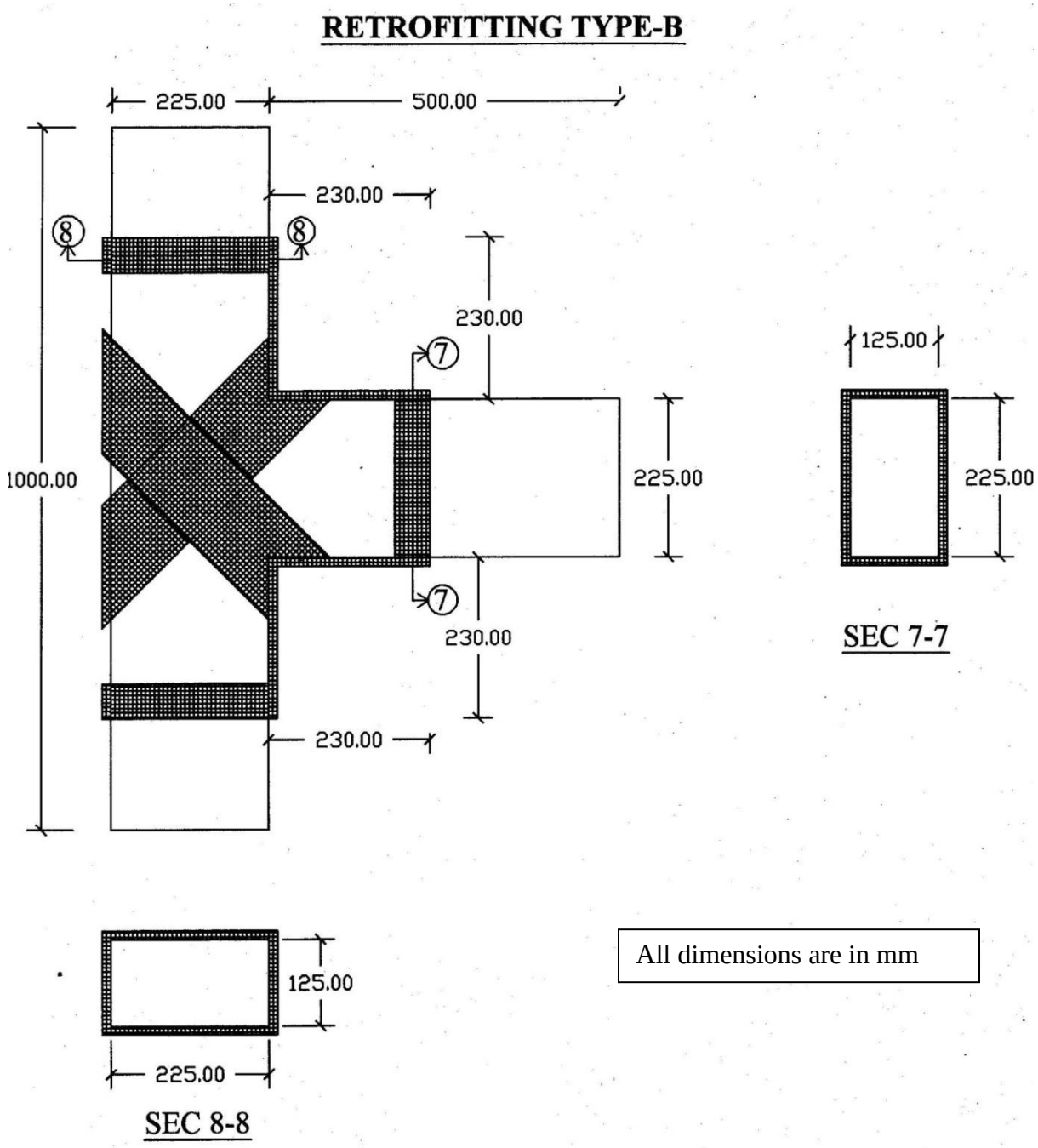

Figure 4.2: Wire Mesh Wrapping Method in Type-B Retrofitting

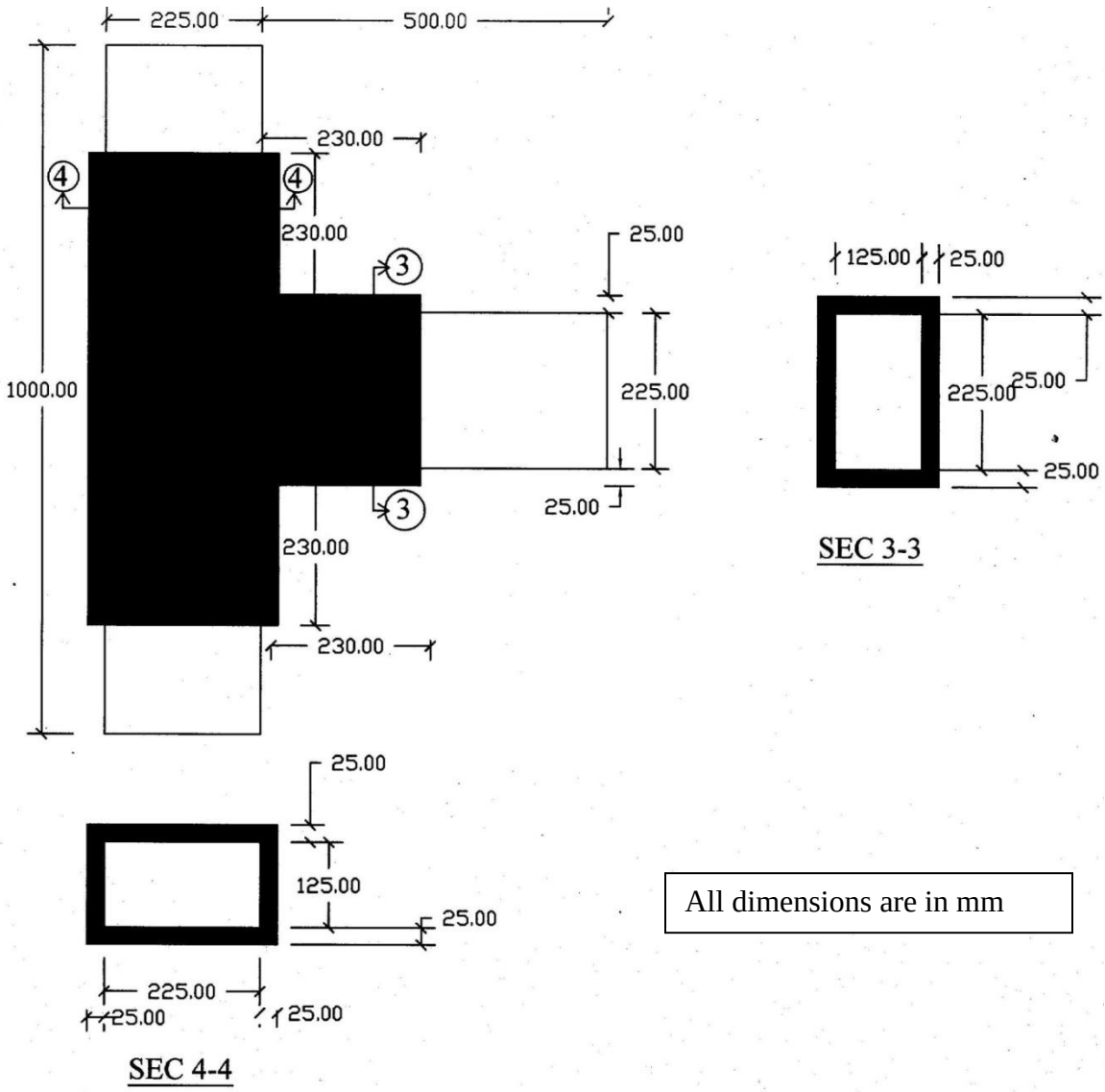

Figure 4.3: Retrofitted Beam-Column Joint with Details

4.3 EFFECT OF WRAPPING TECHNIQUE ON STRENGTH OF BEAM-COLUMN JOINTS RETROFITTED USING FRROCEMENT JACKETS

The pilot studies were carried out to study the effect of the method of wrapping technique on strength of beam- column joints using ferrocement jackets. In this, two methods of wire mesh the wrapping were adopted on the distressed beam- column joints, as explained in the preceding section.

For the purpose of pilot testing, all the four prototype beam-column joints were stressed up to ultimate load. Out of these four beam-column joints two specimens R1 and R2, were retrofitted using Type- A jacketing technique and the remaining two specimens R3 and R4, were retrofitted using Type- B jacketing technique. Based on the testing of the three control specimens the three stress levels were decided as ultimate load (stress level 1), 85 percent of ultimate load (stress level 2), 50 percent of ultimate load (stress level 3).

4.3.1 Testing of Beam-Column Joints

All the four beam-column joint specimens, control as well as retrofitted, were tested as per arrangement explained earlier in section 3.3 and shown in Figure-3.4.

4.3.2 Results and Discussion

It was observed from the experimental data and corresponding graph of Type-A retrofitted specimen (R1), that retrofitting leads to a marginal increase in the ultimate load carrying capacity from 22.7kN to 24.6kN, whereas the deflection corresponding to ultimate load of 24.6kN was 20.5mm as compared to 23.3mm for the control specimen at 22.7kN. For Type-A retrofitted sample (R2), exactly similar trend was observed. The increase in load was of the same order i.e. from 22.7kN (control specimen) to 23.8kN (retrofitted specimen) with a deflection of 18.7mm compared to 23.3mm for control specimen at 22.7kN. Thus Type- A retrofitted beam-column joint specimens showed an average 6.7 percent increase in the ultimate load carrying capacity with a 15.7 percent decrease in deflection as compared to control beam-column joint specimens.
In case of Type- B retrofitted specimens (R3), it was observed that retrofitting leads to a marginal increase in the ultimate load carrying capacity from 22.7kN to 27.6kN, whereas the

deflection corresponding to the ultimate load of 27.6kN was 14.7mm as compared to 23.3 mm for the control specimen at 22.7kN. However, there was a marginal increase in the yield load from 22kN (control specimen) to 24kN (retrofitted specimen). For Type-B retrofitted specimen (R4) a trend similar to retrofitted specimen R3 was observed. The increase in load was almost of the same order i.e. from 22.7kN (control specimen) to 28kN (retrofitted specimen) with a deflection 10.3mm compared to 23.3mm for the control specimen at 22.7kN. Also there was a considerable increase in the yield load from 22kN (control specimen) to 24kN (retrofitted specimen). Thus on average, Type-B retrofitted beam-column joint specimens showed 22.6 percent increase in the ultimate load carrying capacity with a 46.3 percent decrease in deflection as compared to the control beam-column joint specimens.

From a comparative point of view it was observed from Figure 4.4, that the beam- column joints with different wrapping techniques showed different behavior. Specimens with Type-B retrofitting scheme showed the maximum improvement in the ultimate load carrying capacity as compared to Type-A retrofitting. However, the ductility ratio and energy absorption (Table 4.5) decreased with higher stiffness in beam- column joints retrofitted with Type-B retrofitting. The smaller average spacing and lesser number of cracks observed in the retrofitted beam-column joints indicated a better distribution of the stress after retrofitting.

4.4 CONCLUSION FROM PILOT STUDIES

Based upon the discussion and analysis of test results of the pilot study undertaken the following conclusions were drawn.

1. The load carrying capacity of retrofitted beam-column joints, for both types of retrofitting techniques, increased by 6.7% and 22.6%, respectively, as compared to the control beam-column joints.
2. Type-B retrofitted specimens (i.e. diagonally wrapped beam-column joint specimens) showed more improvement in their ultimate load carrying capacity and stiffness as compared to Type-A retrofitted specimens.

Thus, considering the overall results, the Type-B retrofitting technique was adopted for further investigations.

Table 4.1

Load vs Deflection Data for Control Beam- Column Joints and Beam- Column Joints Retrofitted with Ferrocement Jackets Using Type - A Retrofitting

S.No.	Average Control Beam-Column Joint (CS)		Type-A Retrofitted Beam- Column Joint (R1)		Type-A Retrofitted Beam- Column Joint (R2)		Type-A Retrofitted Beam- Column Joint Average = (R1+R2)/2	
	Load (kN)	Deflection (mm)	Load (kN)	Deflection (mm)	Load (kN)	Deflection (mm)	Load (kN)	Deflection (mm)
1	0.0	0.0	0.0	0.0	0.0	0.0	0.0	0.0
2	2.0	0.4	2.0	0.5	2.0	0.4	2.0	0.5
3	4.0	0.8	4.0	0.8	4.0	0.9	4.0	0.9
4	6.0	1.5	6.0	1.6	6.0	2.1	6.0	1.9
5	8.0	2.5	8.0	2.9	8.0	3.5	8.0	3.2
6	10.0	3.0	10.0	3.3	10.0	4.0	10.0	3.7
7	12.0	4.8	12.0	3.9	12.0	4.8	12.0	4.3
8	14.0	5.6	14.0	4.9	14.0	6.4	14.0	5.6
9	16.0	6.1	16.0	5.5	16.0	6.9	16.0	6.2
10	18.0	7.0	18.0	5.9	18.0	8.0	18.0	6.9
11	20.0	8.4	20.0	6.8	20.0	9.5	20.0	8.1
12	22.0	19.4	22.0	15.9	22.0	14.6	22.0	15.3
13	22.7	23.3	24.6	20.5	23.8	18.7	24.2	19.6

Table 4.2

Load vs Deflection Data for Control Beam-Column Joints and Beam-Column Joints Retrofitted with Ferrocement Jackets Using Type- B Retrofitting

S.No.	Average Control Beam-Column Joint (CS)		Type-B Retrofitted Beam- Column Joint (R3)		Type-B Retrofitted Beam- Column Joint (R4)		Type-B Retrofitted Beam- Column Joint Average = (R3+R4)/2	
	Load (kN)	Deflection (mm)	Load (kN)	Deflection (mm)	Load (kN)	Deflection (mm)	Load (kN)	Deflection (mm)
1.	0.0	0.0	0.0	0.0	0.0	0.0	0.0	0.0
2.	2.0	0.4	2.0	0.9	2.0	0.5	2.0	0.7
3.	4.0	0.8	4.0	1.6	4.0	1.7	4.0	1.6
4.	6.0	1.5	6.0	1.9	6.0	2.5	6.0	2.2
5.	8.0	2.5	8.0	2.5	8.0	3.6	8.0	3.0
6.	10.0	3.0	10.0	3.2	10.0	4.5	10.0	3.9
7.	12.0	4.8	12.0	4.3	12.0	5.9	12.0	5.1
8.	14.0	5.6	14.0	5.2	14.0	6.2	14.0	5.8
9.	16.0	6.1	16.0	5.9	16.0	6.2	16.0	6.0
10.	18.0	7.0	18.0	7.0	18.0	6.6	18.0	6.8
11.	20.0	8.4	20.0	8.4	20.0	6.9	20.0	7.7
12.	22.0	19.4	22.0	9.8	22.0	7.2	22.0	8.5
13.	22.7	23.3	24.0	10.1	24.0	8.9	24.0	9.5
			26.0	12.2	26.0	9.8	26.0	11.0
			27.6	14.7	28.0	10.2	27.8	12.4

Table 4.3

Test Results of Beam-Column Joints Using Ferrocement Jacket having Different Types of Retrofitting

S.NO.	Beam Type	Pmax (kN)	Mmax (kN-m)	Ductility Ratio* (ΔU/ ΔY)	Energy Absorption** (kN.mm)	Stiffness P_u / Δ_U kN/mm
1	ACS	22.7	11.3	2.7	412.7	0.9
2	Avg. Type-A	24.2	12.1	2.4	377.6	1.2
3	Avg. Type-B	27.8	13.9	1.6	250.3	2.2

**Ductility Ratio of beam -column joints is defined as ratio of deflection at ultimate load to the yield load calculated from idealized trilinear load deflection curve*

*** Area under the load deflection curve upto ultimate load*

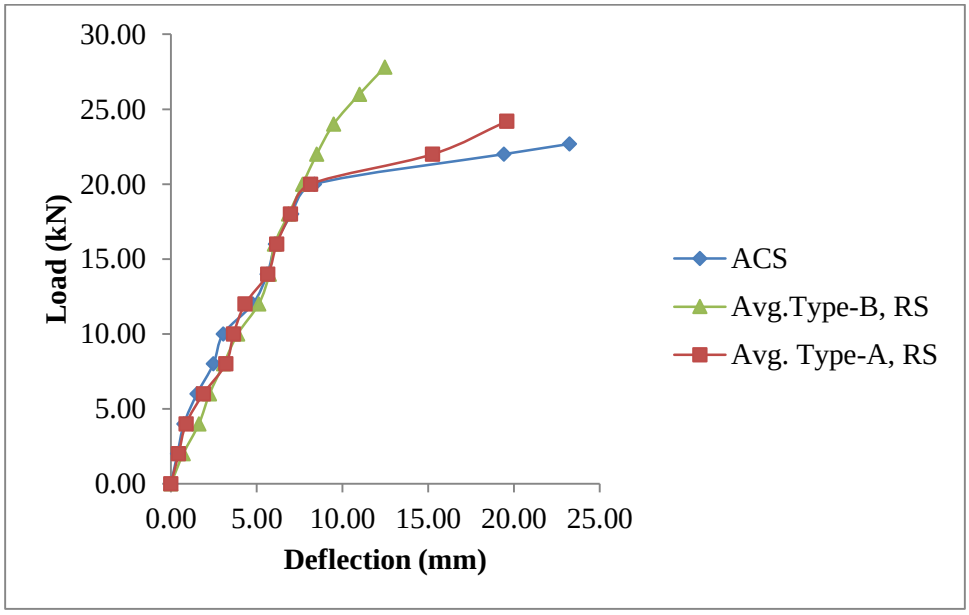

Figure 4.4: Load vs Deflection Curves for Different Types of Retrofitting using Ferrocement

ACS = Control / un-retrofitted beam -column joints, Avg. Type-A, RS= Type-A retrofitted beam -column joints

Avg. Type-B, RS = Type-B retrofitted beam -column joints

4.5 SUMMARY

In this chapter, pilot studies highlighting the effect of the method of wrapping technique on strength of beam- column joints using ferrocement jackets finalized for the present investigation are presented. Type-B retrofitting technique showed better results as compared to Type-A retrofitting technique, and hence is adopted for further detailed investigation.

CHAPTER – 5

RETROFITTING OF BEAM-COLUMN JOINTS

5.1 GENERAL

In this chapter the data obtained from testing of retrofitted beam-column joints is presented, analyzed and discussed. Prior to finalizing the retrofitting parameters a pilot study was carried out as shown in the Chapter 4. In the first section the test results of beam-column joints retrofitted using ferrocement jackets reinforced with two, four and six layers of woven wire mesh, stressed to stress level-1, stress level-2 and stress level-3, are presented and discussed. The retrofitting of the beam-column joints using ferrocement jacketing was carried out in two phases. In the first phase the beam-column joints were stressed to ultimate load. As earlier enumerated, three stress levels, in terms of percentage of the ultimate load viz. 100%, 85%, and 50% of ultimate load were taken up for studying the effect of retrofitting, with different number of woven wire mesh layers. In the second phase, two, four and six layers of GI woven wire mesh were provided in L-shape and at 45 degree to the longitudinal axis of the beam as shown in Figure 4.2 and subsequently a 25mm thick layer of cement mortar (1:2) was applied to the beam-column joints. The retrofitted beam-column joints were then cured for ten days and tested as per procedure presented in section 3.3.

Out of the total of twenty seven beam- column joints cast for the purpose, nine beam-column joints were retrofitted with ferrocement jacketing having two layers of GI woven wire mesh, nine were retrofitted with ferrocement jacket having four layers of GI woven wire mesh and the remaining nine were retrofitted with ferrocement jacket having six layers of GI woven wire mesh, three to be tested for each stress level i.e. stress level-1, stress level-2 and stress level-3, respectively.

The experimental load deflection results for the control beam-column joints and beam-column joints retrofitted using ferrocement jackets with two, four and six layers of GI woven wire mesh, bonded to the surface of beam-column joints using cement slurry as a bonding agent, are given in Appendix in Tables 5.1- 5.20. The average load vs deflection data for all the three stress levels with two four and six layers of wire mesh is tabulated in Table 5.21. The load deflection curves for the data obtained from experimental program are shown in Figures 5.1- 5.13**.** For further analysis, these curves were idealized as trilinear curves as explained in section 3.6. The parameters such as ultimate load carrying capacity, ductility ratio, energy absorption and stiffness are calculated and are tabulated in Table 5.22. The effect of different layers of GI woven wire mesh, at different stress levels, on various parameters listed above are studied and a detailed discussion is presented in the succeeding section.

The second section presents the test results of beam-column joints retrofitted using two layers of CFRP (Carbon Fiber Reinforced Polymer) jackets, stressed to predefined stress level-1, stress level-2 and stress level-3. The parameters such as ultimate load carrying capacity, ductility ratio, energy absorption and stiffness are calculated and same are tabulated in Table 5.29.

5.2 BEHAVIOR OF BEAM-COLUMN JOINTS RETROFITTED USING FERROCEMENT

For the purpose of investigation, firstly three beam-column joints were tested as the control specimens, as per the procedure presented in section 3.3. The load deflection data obtained from the testing of the beam-column joint specimens was plotted and the plot was idealized as a trilinear curve for the purpose of calculating the ductility ratio and toughness of the beam-column joints, as explained in the section 3.6 of previous chapter. The experimental load deflection results for the control beam-column joints are shown in Appendix in Tables 5.1-5.2 and in Figure 5.1. After testing of control specimens, the other retrofitted specimens were tested as per the procedure explained in the section 5.1.

It was noted both ultimate load and yield load carrying capacities of beam-column joints increased after retrofitting. This increase can be attributed to increase in the stiffness of the beam-column joints after retrofitting. The highest increase in ultimate load carrying capacity was of the range of 100 percent and it was observed in case of six layer retrofitting with GI woven

wire mesh as reinforcement. Further it was observed that the percentage increase in strength increases as the initial stress level increases from 50 percent to 85 percent of ultimate load. The reduced increase in the load carrying capacity with initial stress levels can be attributed to loss in stiffness of the beam-column joints due to initial stressing. It was also observed that with increase in the percentage of reinforcement in the ferrocement jackets the load carrying capacity of the exterior RC beam-column joints increases. This trend was observed for all the stress levels, i.e. for stress level-1, stress level-2 and stress level-3.

All the retrofitted beam-column joints shown similar type of load deflection behavior however, due to higher stiffness, all the retrofitted beam-column joints exhibited reduced deflection as compared to control beam-column joints. The crack pattern for the beam-column joints at various stages of loading was also noted and shown in Plates 5.1- 5.6.

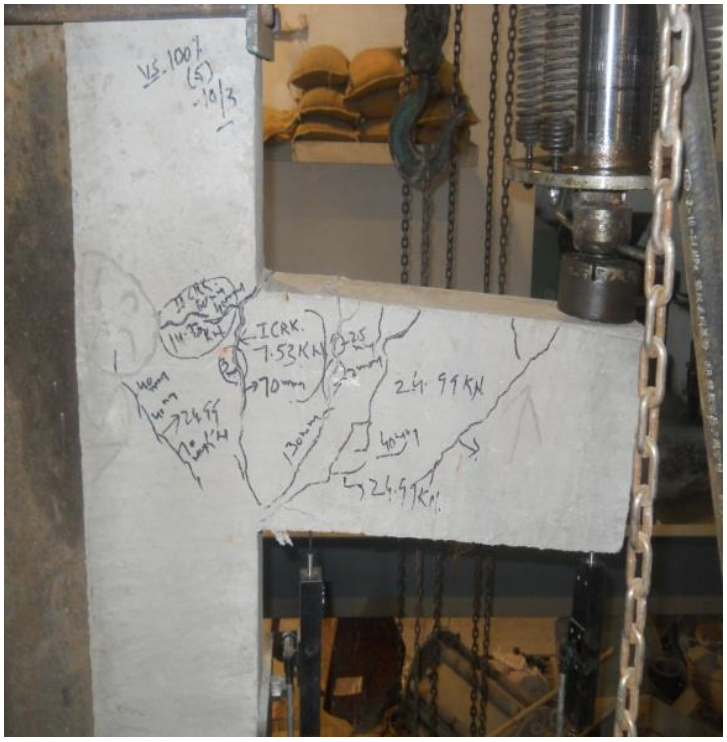

Plate 5.1: Crack Patterns in Control Beam-Column Joints Stressed to Ultimate Load i.e. Stress Level-1

Crack Pattern in Two Layers Retrofitted Joint

Crack Pattern in Four Layers Retrofitted Joint

Crack Pattern in Six Layers Retrofitted Joint

Plate 5.2: Crack Patterns in Beam-Column Joints Retrofitted With Ferrocement Jacketed Reinforced With Two Layers, Four Layers and Six Layers of GI Woven Wire Mesh Stressed to Ultimate Load, Stress Level-1

Plate 5.3: Crack Patterns in Control Beam-Column Joints Stresed to 85 Percent of Ultimate load i.e. Stress Level-2

Plate 5.4: Crack Patterns in Control Beam-Column Joints Stresed to 50 Percent of Ultimate Load i.e. Stress Level-3

Crack Pattern in Two Layers Retrofitted Joint

Crack Pattern in Four Layers Retrofitted Joint

Crack Pattern in Six Layers Retrofitted Joint

Plate 5.5: Crack Patterns in Beam-Column Joints Retrofitted With Ferrocement Jacket Reinforced With Two Layers, Four Layers and Six Layers of GI Woven Wire Mesh for Joints Already Stressed to 85 Percent of Ultimate Load, Stress Level-2

Crack Pattern in Two Layers Retrofitted Joint

Crack Pattern in Four Layers Retrofitted Joint

Crack Pattern in Six Layers Retrofitted Joint

Plate 5.6: Crack Patterns in Beam-Column Joints Retrofitted With Ferrocement Jacket Reinforced With Two Layers, Four Layers and Six Layers of GI Woven Wire Mesh for the Joints Already Stressed to 50 Percent of Ultimate Load, Stress Level-3

The cracks observed during the test can be classified into two types: flexural cracks (perpendicular to the axes of the beam or column) and shear cracks (diagonal to the beam, column or the joint axes). The shear cracks on the beam surface near the joint occurred first and got wider significantly during the test as shown in Plates 5.4, 5.3 and 5.1. In case of all twenty seven beam-column joint specimens which were tested to various load levels before retrofitting, the cracks in the joint surface were first visible at an average load of 6.85kN, 6.78kN and 6.40kN, for stress level-1, stress level-2 and stress level-3, respectively. These cracks widened as the testing proceeded. For most beam-column joint specimens, the flexure cracks almost did not appear as shown in Plate 5.1, on the beam and column surface. The shear cracks in the joint region were the widest at the ultimate loading and were the main reason for failure of the control beam-column joint specimens as shown Plates 5.1, 5.3, and 5.4. In case of ferrocement jacketed beam-column joint specimens with different layers, the formation of cracks could not be observed in the joint region. However, none of the specimen failed due to de-bonding, indicating a good joint of ferrocement with the existing surface as shown in Plates 5.2, 5.5 and 5.6. They were also observed to show lesser deflections at higher loads. The ferrocement jacketed beam-column joint specimens failed due to formation of cracks in the beam portion only. Thus, due to strengthening of beam-column joints, the failure was shifted from joints (control specimens) to beam ends (retrofitted specimens) as is observed from the cracking pattern of the specimens. This indicates that after retrofitting, the failure pattern of a weak beam strong column joint is achieved. Obviously, the addition of wire mesh layers was an effective way to enhance the joint shear capacity of the beam-column joint specimens and considerably influenced in prevention of shear failure.

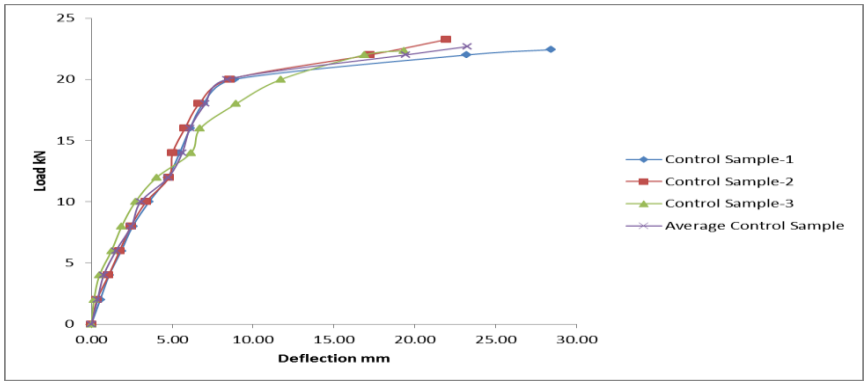

Figure 5.1: Load vs Deflection at Cantilever Beam Tip for Control Beam- Column Joints Stressed to Ultimate Load

5.3 BEAM-COLUMN JOINTS RETROFITTED WITH FERROCEMENT JACKETS AND EFFECT OF STRESS LEVEL WITH TWO LAYERS OF GI WOVEN WIRE MESH

The testing results of individual beam-column joints in the form of loads and deflections at the tip of the beams are presented in the Appendix in Tables 5.3 - 5.8. Figures 5.2 - 5.3 shows the load and deflection plots of the beam-column joints retrofitted with ferrocement jackets having two layers of GI woven wire mesh. Table 5.21 shows the load vs deflection data for ferrocement jacketed joints with two layers of wire mesh at all the three stress levels. The Table 5.22 presents the values of parameters like deflection ductility ratio, energy absorption and stiffness which have been derived from the trilinear curves, which are superimposed on the load and deflection curves to get the values of elastic point (Pe), yield point (Py) and ultimate load (Pu). The ductility ratio is defined as the ratio of deflection at ultimate load to the yield load calculated corresponding to the above values. Energy absorption or toughness is defined as the total area under the trilinear curve.

5.3.1 Effect on Load Carrying Capacity of Beam-Column Joints

The average ultimate load carrying capacity obtained from experimental data was 22.7kN for control beam-column joints whereas, it was found to be 26.7kN, 27.6kN, 26.8kN for the retrofitted beam-column joints initially stressed to ultimate load, 85 percent and 50 percent of ultimate load respectively, indicating that after retrofitting the ultimate load carrying capacity and moment increased by 17.7 percent, 21.7 percent and 18.2 percent for stress level-1, stress level-2 and stress level-3 respectively. The corresponding deflection at ultimate load reduced to 15.4mm, 13.5mm and 12.5mm shows 33.8 percent, 41.7 percent, 46.1 percent decrease in deflection, and 40 percent decrease in rotation, as compared to the control specimen for the same stress levels. Similarly the obtained average yield load value of beam-column joints was 20kN for control sample whereas it was found to be 26kN each for the retrofitted beam-column joints initially stressed to ultimate load, 85 percent and 50 percent of ultimate load, indicating that after retrofitting. The yield load carrying capacity increased by 30 percent each for stress level-1, stress level-2 and stress level-3.

So it can be concluded that in all cases when beam- column joints were retrofitted with ferrocement jackets reinforced with two layers of GI woven wire mesh the ultimate load carrying capacity, and moment of the beam-column joints increases and rotation decreases appreciably.

However, increases in ultimate load carrying capacity in beams were more in the case of stress level-2 as compared to stress level-1 and stress level-3, because after retrofitting of all the three stress levels by the same type of jackets the percentage increase in stiffness of the stress level 1, stress level-3 of the beam- column joints was less than that of stress level-2. It was observed from Figure 5.2 and 5.3 that the behavior of load deflection curve for stress level-1 was different from stress level-2 and stress level-3. The average load deflection curve for stress level-1 showed more deflections in comparison to stress level-2 and stress level-3 curves at the same loads. Because the control samples were tested upto ultimate load and were fully cracked in stress level-1 hence, the steel reached its maximum yield load in stress level-1(100%) which were not in other stress levels. In addition to that the two layers of wire mesh in ferrocement jacketing does not showed much differences in deflections in comparison to control samples upto yield load for SL-1.

5.3.2 Effect on Deflection Ductility Ratio, Energy Absorption and Stiffness of Beam-Column Joints

As the testing was carried out under load controlled conditions, the load deflection curves for the controlled as well as retrofitted specimens were obtained up to ultimate load only. By using tri-linear idealized (elastic load point, yield load point, ultimate load point shown in figure 5.1) curves the deflection ductility ratio, i.e. the ratio of deflection at ultimate load to yield load and energy absorption (i.e. the area under the curve up to ultimate load) were calculated shown in the Table 5.22. It is generally expected that after failure of the ferrocement jacket the load-deflection curve will follow the path similar to that of the controlled specimen and the total energy absorption at failure will be higher than that of un-retrofitted specimen. From the Table 5.22 it is concluded that deflection ductility ratio and energy absorption decreases for the retrofitted specimens for all the three stress levels as compared to the control specimens. This may be attributed to the testing of the specimens under load controlled conditions, due to which the curve beyond the ultimate load could not be achieved, indicating that the retrofitted joints tend to become brittle early once the yield point was reached. It was also observed from the Table- 5.22 that the stiffness of ferrocement jacketed beam-column joint specimens increased by 70%, 100%, 110% for stress level-1, stress level-2 and stress level-3, respectively, as compared to control specimens. From the experimental results, given in Table 5.22 noted that the stiffness for all the

initial stress levels increases with increase in the percentage of reinforcement in the ferrocement jackets therefor, will improve the behavior of beam-column joints during earthquakes.

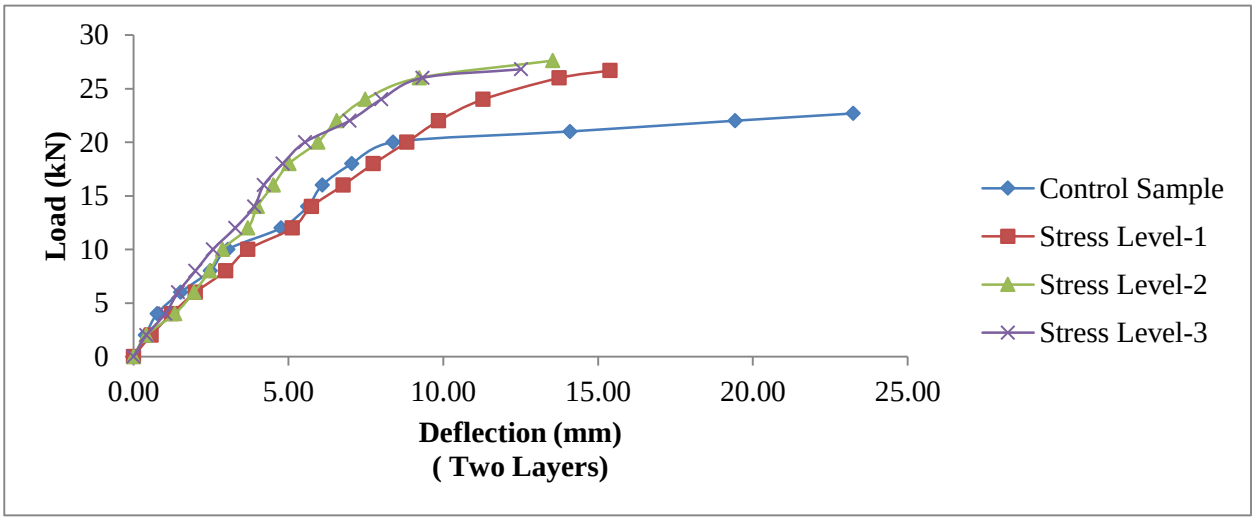

Figure 5.2: Load vs Deflection at Cantilever Beam Tip for Beam- Column Joints Retrofitted with Ferrocement Jacketing with Two Layers of Wire Mesh Stressed to Different Levels

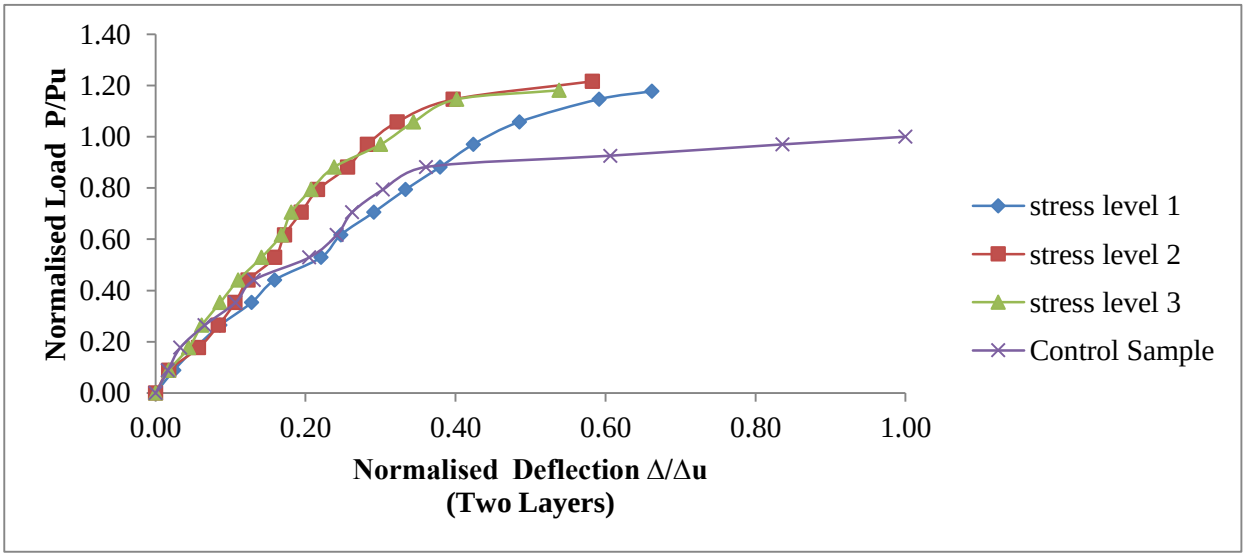

Figure 5.3: Normalized Load v/s Normalized Deflection at Cantilever Beam Tip for Beam- Column Joints Retrofitted with Ferrocement Jacketing with Two Layers of Wire Mesh Stressed to Different Levels

5.4 BEAM-COLUMN JOINTS RETROFITTED WITH FERROCEMENT JACKETS AND EFFECT OF STRESS LEVEL WITH FOUR LAYERS OF GI WOVEN WIRE MESH

The experimental results of individual beam-column joints in the form of loads and deflection at the free end of beam are presented in the Appendix in Tables 5.9- 5.14. Figures 5.4- 5.5 show the load and deflection plots of the beam-column joints retrofitted with ferrocement jackets having four layers of GI woven wire mesh. Table 5.21 shows the load vs deflection data for ferrocement jacketed joints with four layers of wire mesh at all the three stress levels. The Table-5.22 presents the values of parameters like deflection ductility ratio, energy absorption and stiffness, which have been derived from the trilinear curves, which are superimposed on the load and deflection curves to get the values of elastic point (Pe), yield point (Py) and ultimate load (Pu).

5.4.1 Effect on Load Carrying Capacity of Beam-Column Joints

The average ultimate load carrying capacity obtained from experimental data was 22.7kN for control beam-column joints whereas it was found to be 30.2kN, 29.4kN, 28.4kN for the retrofitted beam-column joints initially stressed to ultimate load, 85 percent and 50 percent of ultimate load respectively, indicating that after retrofitting the ultimate load carrying capacity and moment increased by 33.2 percent, 29.6 percent and 25.2 percent for stress level-1, stress level-2 and stress level-3 respectively. The corresponding deflection at ultimate load reduced to 14.4mm, 10.5mm, and 11.3mm shows 38.2 percent, 54.8 percent, 51.4 percent decrease in deflection, and 60 percent decrease in rotation, as compared to the control specimen for the same stress levels. Similarly the obtained average yield load value of beam-column joints was 20kN for control sample whereas, it was found to be 28kN, 28kN and 27kN for stress level-1, Stress level-2 and stress level-3, respectively for the retrofitted beam-column joints initially stressed to ultimate load, 85 percent and 50 percent of ultimate load respectively, indicating that after retrofitting, the yield load carrying capacity increased by 40 percent, 40 percent and 35 percent, for stress level-1, stress level-2 and stress level-3, respectively.

So, it can be concluded that in all cases when beam-column joints were retrofitted with ferrocement jackets reinforced with four layers of GI woven wire mesh the ultimate load

carrying capacity, and the moment capacity of the beam-column joints increases and rotation decreases appreciably. However, it can be concluded from Table 5.22 that an increase were more in the case of stress level-1 as compared to stress level-2 and stress level-3. Herein, it is noted from Figures 5.4-5.5, that the load deflection curves for all the stress levels showed same behavior but in Figure 5.2-5.3 load deflection curve for stress level-1 showed the different behavior then other stress levels. This may be due to that in Figures 5.4- 5.5 four layers retrofitted beam-column joints having more confinement and stiffness showed better results in the form of load and deflection and in comparison to two layers retrofitting for SL-1.

5.4.2 Effect on Deflection Ductility Ratio, Energy Absorption and Stiffness of Beam-Column Joints

The load vs deflection curves for the control and retrofitted specimens were obtained up to ultimate load only because the testing of the samples was done under load controlled conditions only. For the analysis, deflection ductility ratio and energy absorption were calculated using tri-linear idealized curves which as shown in the Table 5.22 and it is concluded that deflection ductility ratio and energy absorption decreases for the retrofitted joint specimens, with four layers of wire mesh for stress level-1, stress level-2 and stress level-3, as compared to the control specimens. This may be credited to the testing of the specimens was done under load controlled conditions, due to which the curve additional than the ultimate load could not be achieved. So, it may be concluded that the ferrocement jacketed beam-column joints be inclined to turn out to be brittle early once the yield point was reached. It was observed that the stiffness of ferrocement jacketed beam-column joint specimens increased by 110%, 180%, 150% for stress level-1, stress level-2 and stress level-3, respectively, as compared to control specimens. From the Table- 5.22 it is also concluded that the increase in the percentage of reinforcement in the ferrocement jackets shows the increase in the stiffness for stress level-1, stress level-2 and stress level-3, which may improve the strength of the structural elements during damaged conditions.

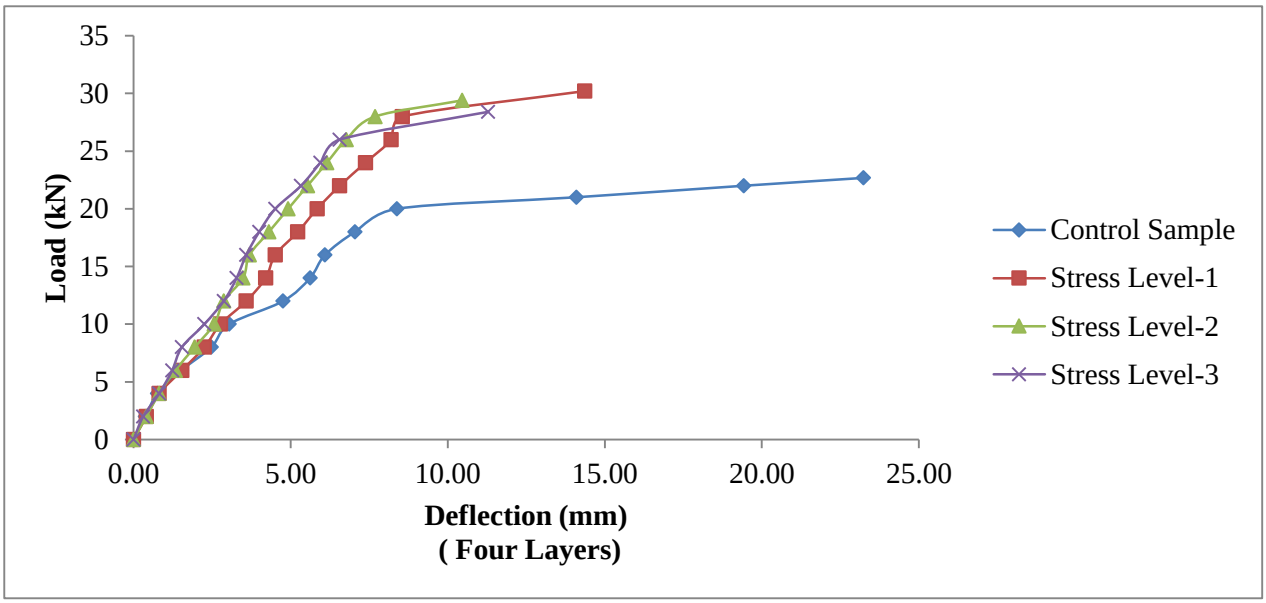

Figure 5.4: Load vs Deflection at Cantilever Beam Tip for Beam- Column Joints Retrofitted with Ferrocement Jacketing with Four Layers of Wire Mesh Stressed to Different Levels

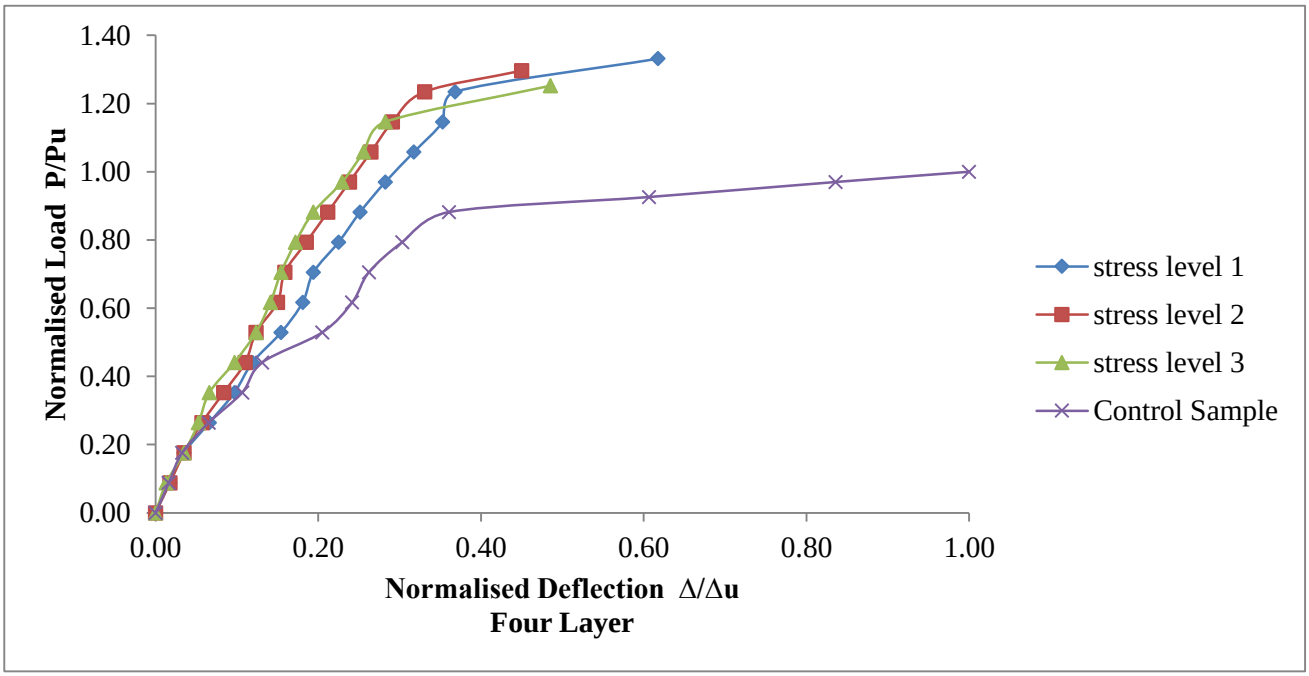

Figure 5.5: Normalized Load vs Normalized Deflection at Cantilever Beam Tip for Beam- Column Joints Retrofitted with Ferrocement Jacketing with Four Layers of Wire Mesh Stressed to Different Levels

5.5 BEAM-COLUMN JOINTS RETROFITTED WITH FERROCEMENT JACKETS AND EFFECT OF STRESS LEVELS WITH SIX LAYERS OF GI WOVEN WIRE MESH

The experimental load vs deflection results of individual beam-column joints at tip of the beam are presented in the Appendix in Tables 5.15- 5.20. Figures 5.6- 5.7 show the load and deflection plots of the beam-column joints retrofitted with ferrocement jackets having six layers of GI woven wire mesh. Table 5.21 shows the load vs deflection data for ferrocement jacketed joints with six layers of wire mesh at all the three stress levels. The Table 5.22 presents the values of parameters like ductility ratio, energy absorption and stiffness of ferrocement jacketed joints using four layers of wire mesh. These are derived from the trilinear curves, which are superimposed on the load and deflection curves to get the values of elastic point (Pe), yield point (Py) and ultimate load (Pu). Ductility ratio and Energy absorption is already explained in section 5.3.

5.5.1 Effect on Load Carrying Capacity of Beam-Column Joints

The average ultimate load carrying capacity obtained from experimental data was 22.7kN for control beam-column joints whereas, it was found to be 32kN, 31kN, 30.2kN for the retrofitted beam-column joints initially stressed to ultimate load, 85 percent and 50 percent of ultimate load respectively, indicating that after retrofitting the ultimate load carrying capacity and moment increased by 41.1 percent, 36.7 percent and 33.2 percent for stress level-1, stress level-2 and stress level-3 respectively. The corresponding deflection at ultimate load reduced to 19.3mm, 18.5mm, and 13.5mm shows 17 percent, 20.3 percent, 41.9 percent decrease in deflection, and 40 percent decrease in rotation as compared the control specimen for the same stress levels. Similarly the obtained average yield load value of beam-column joints was 20kN for control sample whereas, it was found to be 29kN, 30kN and 28kN for stress level-1, Stress level-2 and stress level-3, respectively for the retrofitted beam-column joints initially stressed to ultimate load, 85 percent and 50 percent of ultimate load respectively, indicating that after retrofitting, the yield load carrying capacity increased by 45 percent, 50 percent and 40 percent, for stress level-1, stress level-2 and stress level-3.

So it can be concluded that in all cases when beam-column joints were retrofitted with ferrocement jackets reinforced with six layers of GI woven wire mesh the ultimate load carrying

capacity, moment of the beam-column joints increases and rotation decreases appreciably. However, an increase was more in the case of stress level-1 as compared to stress level-2 and stress level-3.

5.5.2 Effect on Deflection Ductility Ratio, Energy Absorption and Stiffness of Beam-Column Joints

All the testing was conceded out under load controlled conditions, the load deflection curves for all the specimens (controlled as well as retrofitted) was obtained up to ultimate load only. The deflection ductility ratio, i.e. ratio of deflection at ultimate load to yield load and energy absorption i.e. area under the curve up to ultimate load were calculated using tri-linear idealized curves shown in the Table 5.22. It is predictable that after failure of the ferrocement jacket the load-deflection curve will follow the path alike to that of controlled specimen and the total energy absorption at failure will be higher than that of un-retrofitted specimen. From the Table 5.22 it was observed that deflection ductility ratio and energy absorption decreases for the retrofitted specimens for all the three stress levels as compared to the control specimens. This may be credited to the testing of the specimens under load controlled conditions, due to which the curve beyond the ultimate load could not be achieved, indicating that the retrofitted joints tend to become brittle early once the yield point was reached. It was observed that the stiffness of ferrocement jacketed beam-column joint specimens increased by 70%, 70%, 120%, for stress level-1, stress level-2 and stress level-3, respectively, as compared to control specimens. From Table 5.22 noted that the stiffness for all the three stress levels increases with increase in the percentage of reinforcement in the ferrocement jackets.

Table 5.21: Load vs Deflection Data for Control and Retrofitted Beam-Column Joints with Different Layers at Different Stress Levels

Control Joint		Stress Level 1 (100%)		Stress Level 2 (85%)		Stress Level 3 (50%)		Stress Level 1 (100%)		Stress Level 2 (85%)		Stress Level 3 (50%)		Stress Level 1 (100%)		Stress Level 2 (85%)		Stress Level 3 (50%)	
		TL		TL		TL		FL		FL		FL		SL		SL		SL	
P	Δ	P	Δ	P	Δ	P	Δ	P	Δ	P	Δ	P	Δ	P	Δ	P	Δ	P	Δ
0.0	0.0	0.0	0.0	0.0	0.0	0.0	0.0	0.0	0.0	0.0	0.0	0.0	0.0	0.0	0.0	0.0	0.0	0.0	0.0
2.0	0.4	2.0	0.6	2.0	0.4	2.0	0.4	2.0	0.4	2.0	0.4	2.0	0.3	2.0	0.3	2.0	0.4	2.0	0.4
4.0	0.8	4.0	1.2	4.0	1.3	4.0	1.0	4.0	0.8	4.0	0.8	4.0	0.8	4.0	0.7	4.0	1.0	4.0	0.8
6.0	1.5	6.0	2.0	6.0	2.0	6.0	1.4	6.0	1.5	6.0	1.3	6.0	1.2	6.0	1.2	6.0	1.6	6.0	1.4
8.0	2.5	8.0	3.0	8.0	2.5	8.0	2.0	8.0	2.3	8.0	2.0	8.0	1.5	8.0	2.1	8.0	2.2	8.0	1.8
10.0	3.1	10.0	3.7	10.0	2.9	10.0	2.6	10.0	2.8	10.0	2.6	10.0	2.3	10.0	2.8	10.0	2.7	10.0	2.3
12.0	4.8	12.0	5.1	12.0	3.7	12.0	3.3	12.0	3.6	12.0	2.9	12.0	2.9	12.0	3.5	12.0	3.3	12.0	2.7
14.0	5.6	14.0	5.7	14.0	4.0	14.0	3.9	14.0	4.2	14.0	3.5	14.0	3.3	14.0	4.0	14.0	4.0	14.0	3.2
16.0	6.1	16.0	6.8	16.0	4.5	16.0	4.2	16.0	4.5	16.0	3.7	16.0	3.6	16.0	4.4	16.0	4.5	16.0	3.4
18.0	7.1	18.0	7.7	18.0	5.0	18.0	4.8	18.0	5.2	18.0	4.3	18.0	4.0	18.0	5.1	18.0	5.2	18.0	3.9
20.0	8.4	20.0	8.8	20.0	6.0	20.0	5.5	20.0	5.9	20.0	4.9	20.0	4.5	20.0	5.6	20.0	6.0	20.0	4.4
21.0	14.1	22.0	9.9	22.0	6.6	22.0	7.0	22.0	6.6	22.0	5.5	22.0	5.3	22.0	6.2	22.0	6.6	22.0	5.0
22.0	19.4	24.0	11.3	24.0	7.5	24.0	8.0	24.0	7.4	24.0	6.2	24.0	6.0	24.0	6.8	24.0	7.6	24.0	5.7
22.7	23.2	26.0	13.7	26.0	9.2	26.0	9.3	26.0	8.2	26.0	6.8	26.0	6.6	26.0	7.4	26.0	8.4	26.0	6.5
		26.7	15.4	27.6	13.5	26.8	12.5	28.0	8.6	28.0	7.7	28.4	11.3	28.0	8.0	28.0	9.5	28.0	7.4
								30.2	14.4	29.4	10.5			30.0	8.6	30.0	10.7	30.2	13.5
														32.0	19.3	31.0	18.5		

Table 5.22: Comparison of Experimental Loads, Deflections, Ductility Ratio, Stiffness and Energy Absorption of Control and Ferrocement Jacketed Beam- Column Joint Specimens

S. No	Stress Level	Beam-Column Design.	P_{CR} (kN)	P_Y (kN)	P_U (kN)	Percentage increase in load on strengthening (%)			ΔCR (mm)	ΔY (mm)	ΔU (mm)	Stiffness P_u / Δ_U kN/mm	Ductility ratio (ΔU/ ΔY)	Energy Absorption (kN.mm)
						P_{CR}	P_Y	P_U						
1	**____**	**Control Sample**	**6.9**	**20.0**	**22.7**	**-**	**-**	**-**	**1.6**	**8.8**	**23.2**	**1.0**	**2.6**	**412.7**
2	**100%**	SL1-TL*	9.3	26.0	26.7	35.8	30.0	17.7	3.2	9.0	15.4	1.7	1.7	255.2
		SL1-FL#	9.5	28.0	30.2	39.3	40.0	33.2	2.6	8.6	14.4	2.1	1.7	293.2
		SL1-SL**	9.8	29.0	32.0	42.6	45.0	41.1	2.6	9.8	19.3	1.7	2.0	408.4
3	**85%**	SL2-TL	9.8	26.0	27.6	43.1	30.0	21.7	2.8	9.2	13.5	2.0	1.5	253.7
		SL2-FL	11.4	28.0	29.4	66.4	40.0	29.6	2.9	7.7	10.5	2.8	1.4	251.7
		SL2-SL	13.8	30.0	31.0	101.2	50.0	36.7	3.2	10.7	18.5	1.7	1.5	397.6
4	**50%**	SL3-TL	10.5	26.0	26.8	52.6	30.0	18.2	2.6	9.3	12.5	2.1	1.3	229.0
		SL3-FL	11.1	27.0	28.4	62.0	35.0	25.2	2.7	6.6	11.3	2.5	1.7	221.0
		SL3-SL	13.8	28.0	30.2	101.9	40.0	33.2	3.1	7.4	13.5	2.2	1.8	281.1

P_{CR} – first crack load, P_Y – yield load, P_U – ultimate load; ΔY – deflection at yield point, ΔU – deflection at ultimate load; * - Two layer, # - Four Layer, ** - Six Layer; SL-1, SL-2, SL-3, means Stress level-1, Stress Level-2 and Stress Level-3, respectively, *** Area Under load deflection graph using tri-linear curves.

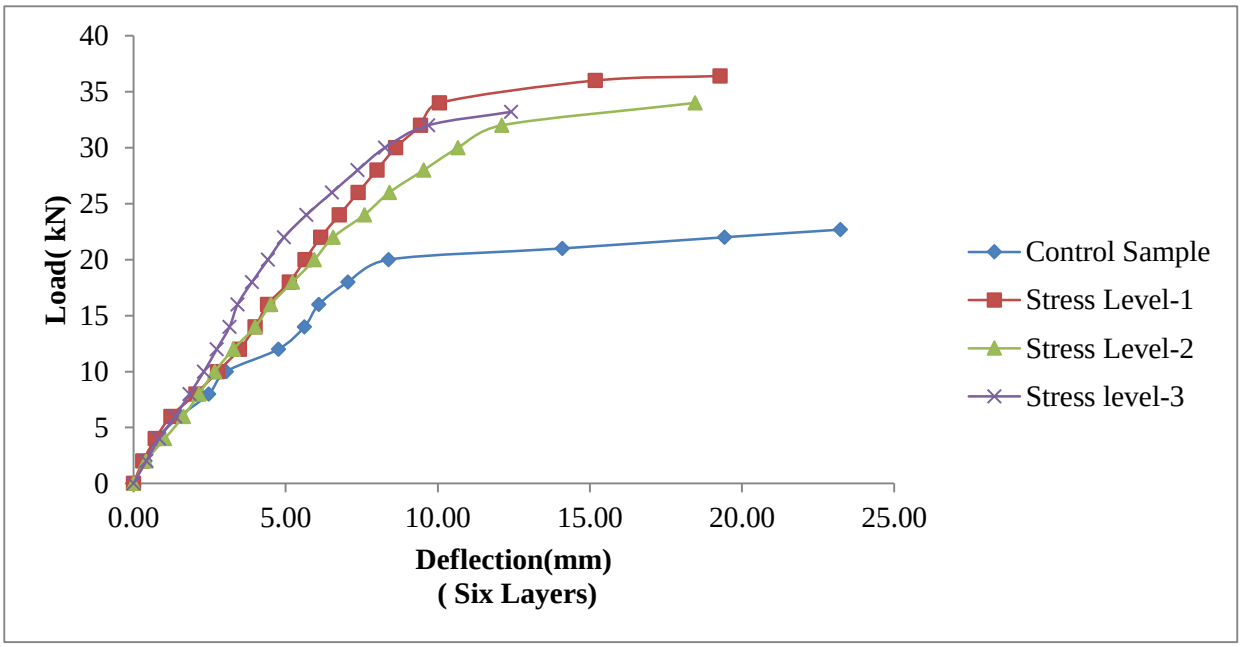

Figure 5.6: Load vs Deflection at Cantilever Beam Tip for Beam- Column Joints Retrofitted with Ferrocement Jacketing with six Layers of Wire Mesh Stressed to Different Levels

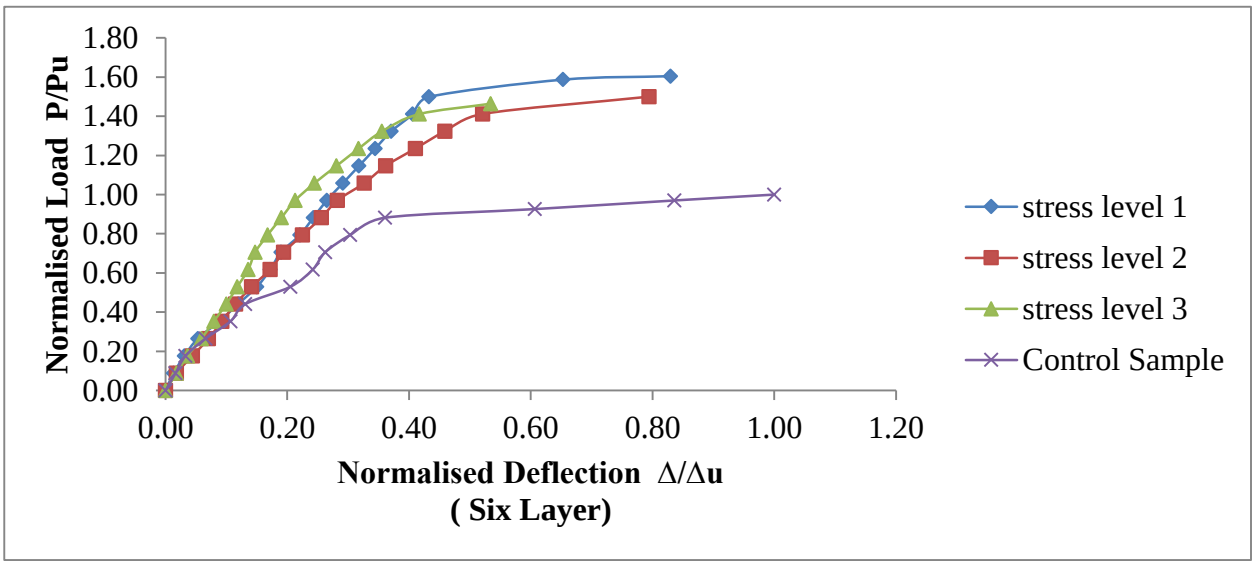

Figure 5.7: Normalized Load vs Normalized Deflection at Cantilever Beam Tip for Beam- Column Joints Retrofitted with Ferrocement Jacketing with Six Layers of Wire Mesh Stressed to Different Levels

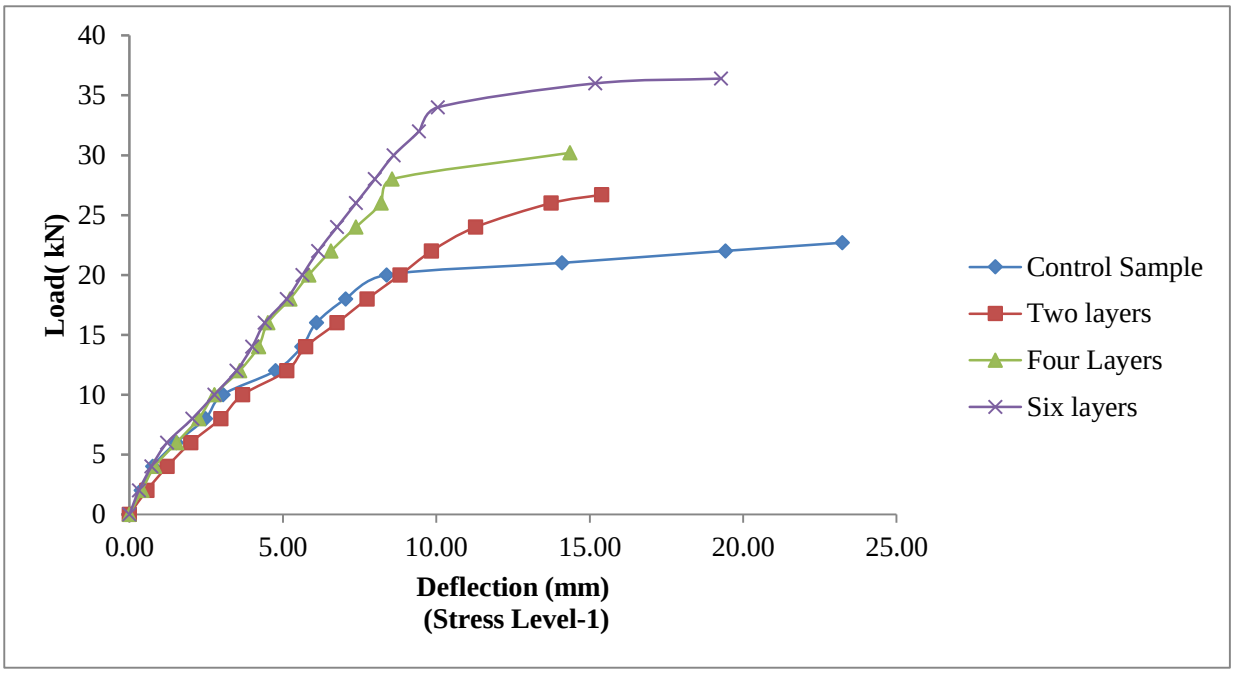

Figure 5.8: Load vs Deflection at Cantilever Beam Tip for Beam- Column Joints Retrofitted with Ferrocement Jacketing with Different Layers of Wire Mesh Stressed to Ultimate Load i.e Stress Level-1

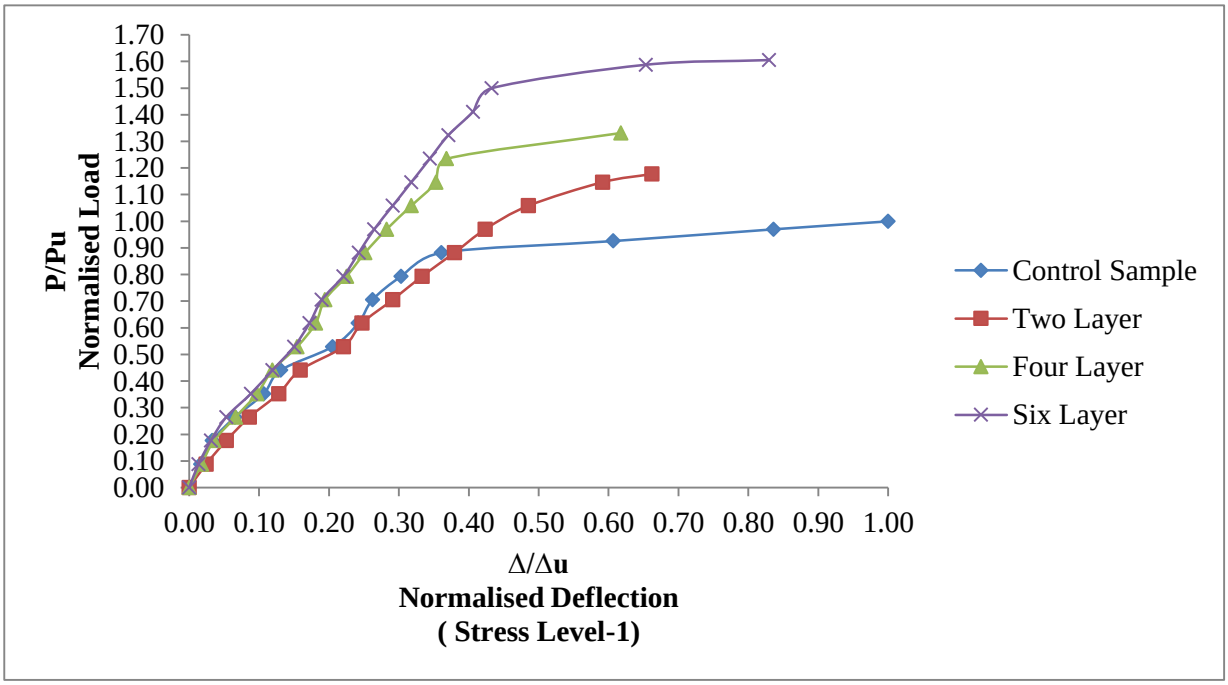

Figure 5.9: Normalised Load vs Normalised Deflection at Cantilever Beam Tip for Beam- Column Joints Retrofitted with Ferrocement Jacketing with Different Layers of Wire Mesh Stressed to Ultimate Load i.e. Stress Level-1

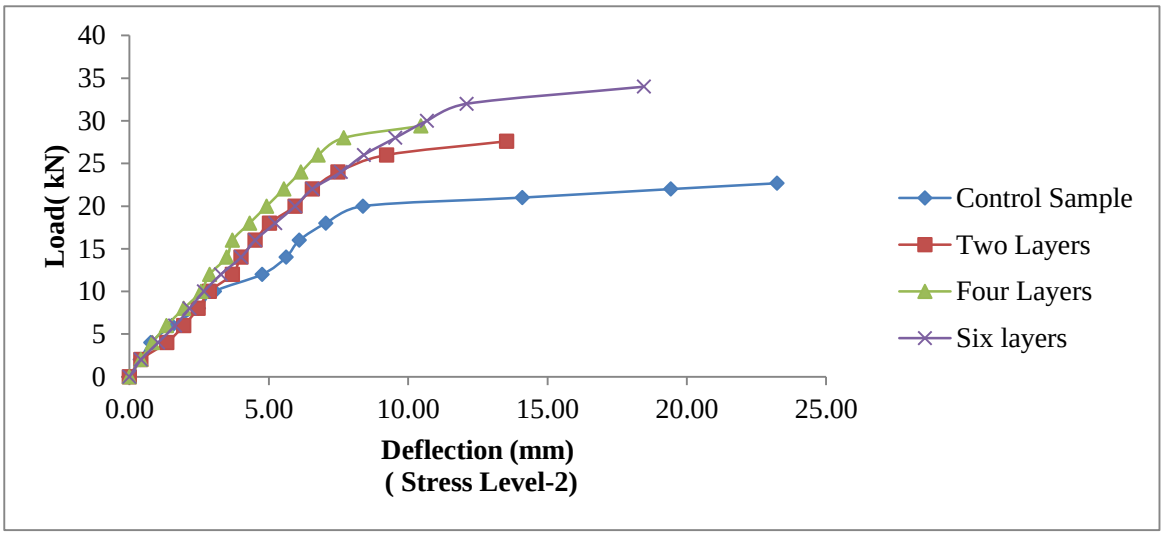

Figure 5.10: Load vs Deflection at Cantilever Beam Tip for Beam-Column Joints Retrofitted with Ferrocement Jacketing with Different Layers of Wire Mesh Stressed to 85 percent of Ultimate Load of Control Sample i.e. Stress Level-2

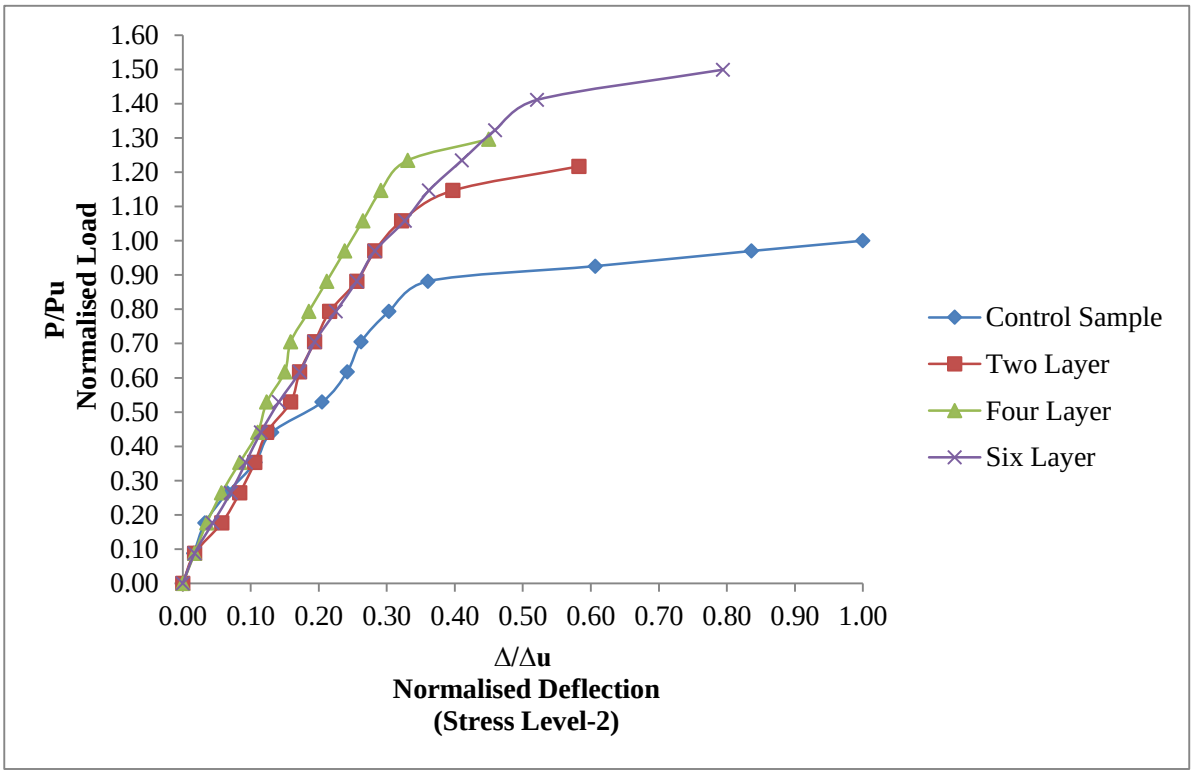

Figure 5.11: Normalised Load vs Normalised Deflection at Cantilever Beam Tip for Beam-Column Joints Retrofitted with Ferrocement Jacketing with Different Layers of Wire Mesh Stressed to 85 percent of Ultimate Load of Control Sample i.e. Stress Level-2

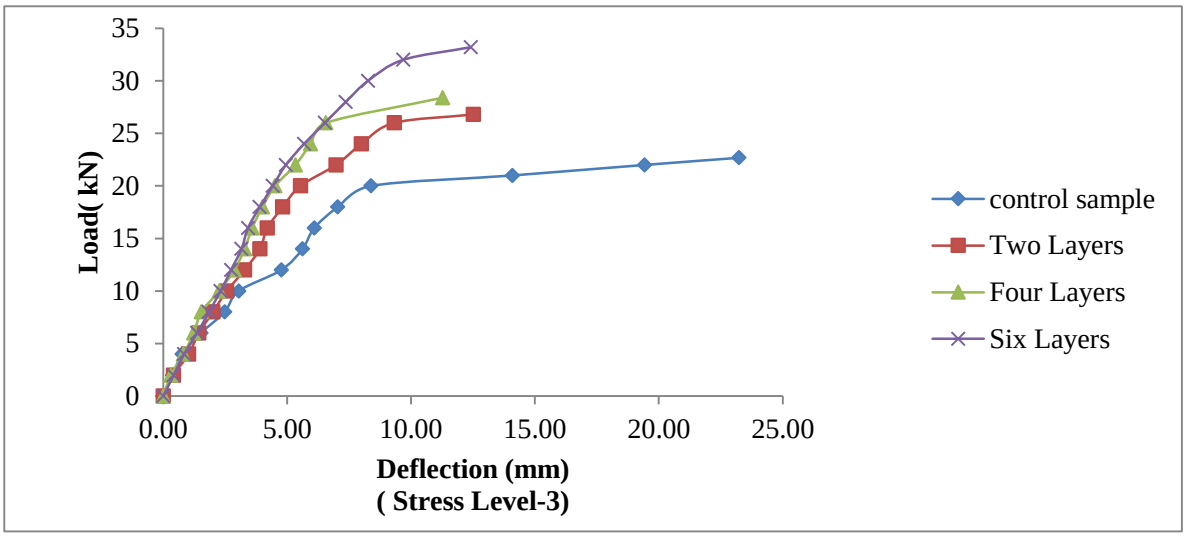

Figure 5.12: Load vs Deflection at Cantilever Beam Tip for Beam-Column Joints Retrofitted with Ferrocement Jacketing with Different Layers of Wire Mesh Stressed to 50 percent of Ultimate Load of Control Sample i.e. Stress Level-3

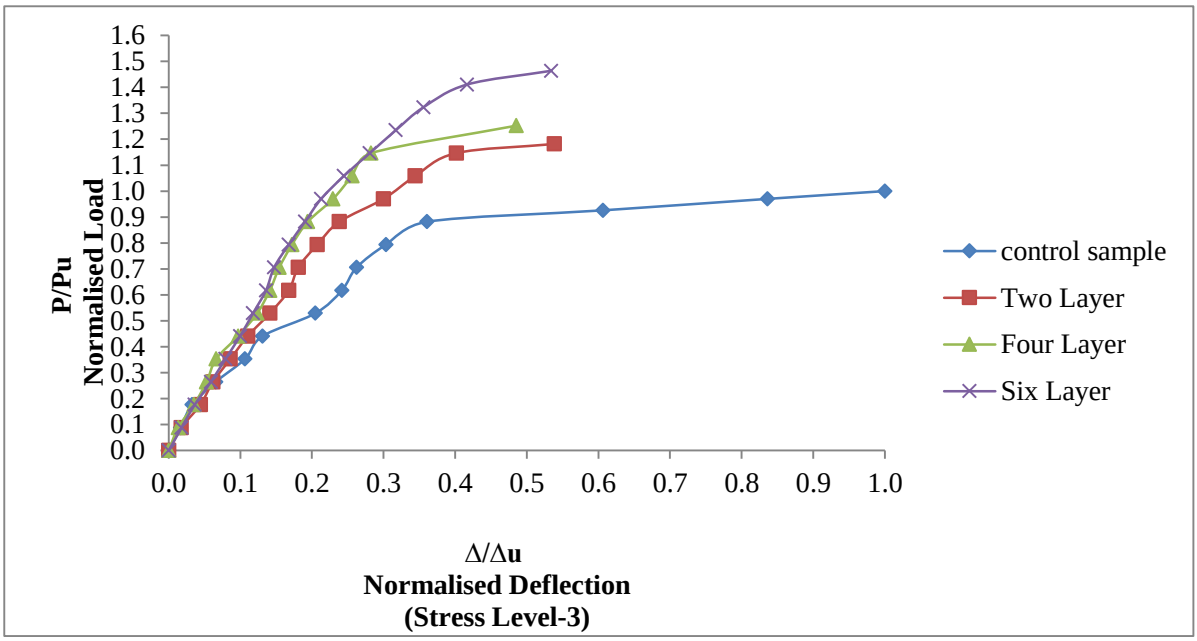

Figure 5.13: Normalised Load vs Normalised Deflection at Cantilever Beam Tip for Beam-Column Joints Retrofitted with Ferrocement Jacketing with Different Layers of Wire Mesh Stressed to 50 percent of Ultimate Load of Control Sample i.e. Stress Level-3

5.6 COMPARATIVE ANALYSIS OF FERROCEMENT JACKETED JOINTS

A comparative analysis of the effect of different layers of woven wire mesh used for the retrofitting of initially stressed beam-column joints on the ultimate load carrying capacity, deflection ductility and energy absorption and stiffness, is presented in this section. It was found from the discussion in the preceding sections that the ultimate load carrying capacity, stiffness, moment increases and ductility ratio, energy absorption, rotation decreases considerably irrespective of stress level and number of layers of GI woven wire mesh.

On comparison, the effect of change in the initial stress levels on all the parameters was observed. This can be attributed to the fact that during retrofitting, extra steel was provided in the joint region in the form of wire mesh which results in its failure by crushing of concrete rather than yielding of the reinforcement. The increase in the number of layers of wire mesh in the ferrocement jacket also affects the observed properties. It was observed from Table 5.22 that with an increase in the number of layers from two to four and six, the average percentage increase in the ultimate load carrying capacity of beam- column joints after retrofitting increased from 17.7 percent, 33.2 percent and 41.1 percent for stress level-1 to 21.7 percent, 29.6 percent and 36.7 percent for stress level-2. While for stress level-3 the corresponding values were 18.2 percent, 25.2 percent and 33.2 percent respectively. It was observed from the experimental data that there was no increase in energy absorption for all the layers in all stress levels. This may be attributed to the testing of the specimens under load controlled conditions, due to which the curve beyond the ultimate load could not be achieved. But also for a given deflections, the energy absorption is higher for larger number of layers. It was observed that the stiffness of ferrocement jacketed beam-column joint specimens increased by 70%, 110%, 70% with two layers, four layers and six layers respectively, in case of stress level-1. Similar trend was observed for stress level- 2, i.e. significant increase in stiffness by 100%, 180%, 70%, for joints retrofitted with two layers, four layers and six layers respectively. A fairly similar trend was observed for stress level- 3, i.e. significant increase in the stiffness increased by 110%, 150% and 120%, for joints retrofitted with two layers, four layers and six layers respectively. It was also observed from Table 5.22 that the deflection ductility ratio decreased for the retrofitted specimens as compared to control specimens for all stress levels, indicating that the retrofitted

joints tend to become brittle early once the yield point has been reachedshowed their higher strength.

The cracks observed during the test can be classified into two types: flexural cracks (perpendicular to the axes of the beam or column) and shear cracks (diagonal to the beam, column or the joint axes). The shear cracks on the beam surface near the joint occurred first and got significantly wider during the test as shown in plates 5.1-5.3 and 5.4. In case of all twenty seven beam-column joint specimens which were tested at various load levels before retrofitting, the cracks in the joint surface were first visible at an average load of 6.8kN, 6.7kN and 6.4kN, for stress level-1, stress level-2 and stress level-3. It was observed from Table 5.22, the load at which first crack was observed, for two, four and six layers layers, ferrocement jacketed beam-column joint specimens increased from 34.7 percent to 42 percent, for stress level-1, 42 percent to 100 percent, for stress level-2 and 52.1 percent to 100 percent, for stress level-3, as compared to the control specimen. These cracks were widened shown in figures 5.4, 5.3 and 5.1, as the testing proceeded. For most beam-column joint specimens, the flexural cracks almost did not appear on the beam and column surface. The shear cracks in the joint region were the widest at the ultimate loading (Figure-5.1), and were the main reason for failure of the control beam-column joint specimens. In the cases of ferrocement jacketed beam-column joint specimens with different layers, the formation of cracks could not be observed. However, none of the specimens failed due to de-bonding, indicating a good joint of ferrocement with the existing surface and ferrocement jacketed beam-column joint specimens failed due to formation of cracks in the beam portion only as shown in Figure 5.5-5.6. It was also observed from Table-5.22 that the ferrocement jacketed joints showed lower deflection at higher loads. Thus, due to strengthening of the beam-column joints, the failure shifted from the joint region in the control specimens to the beam in the retrofitted specimens. This indicates that after retrofitting, the failure pattern of weak beam strong column joint is achieved. Obviously, the addition of wire mesh layers was an effective way to enhance the joint shear capacity of the beam-column joint specimens and considerably influenced the prevention of shear failure. Hence from the Table- 5.22 it may be concluded that the ultimate load carrying capacity, first crack load, yield load and stiffness, increases but ductility and energy absorption decreases of ferrocement retrofitted exterior RC beam-column joints with two layers, four layers and six layers of wire mesh at three different stress levels.

5.7 CFRP RETROFITTED BEAM-COLUMN JOINTS

This section presents the experimental results of testing for control exterior beam-column joints and beam-column joints retrofitted using CFRP with fibers orientated in L-shape and at 45° to the joint in two layers. The data obtained from laboratory testing is analyzed and discussed. The entire section is divided into two parts; in the first part the beam-column joints retrofitted using CFRP jackets for stress level-1 i.e. ultimate load, stress level-2 (85 percent of ultimate load) and stress level-3 (50 percent of ultimate load) and the second section presents the comparative details of the effect on strength of CFRP retrofitted beam-column joints with two layers, when joints are stressed to different stress levels. The retrofitting of the beam-column joints using CFRP jacketing was carried out in two phases. In the first phase the beam-column joints were stressed to ultimate load. As earlier enumerated, three stress levels of stressing viz. ultimate load, 85 percent of ultimate load and 50 percent of ultimate load were taken up for studying the effect of retrofitting with two layers. In the second phase, two layers of CFRP were provided in an L-shape and at 45 degree to the longitudinal axis of the beam as shown in Figure 4.2 The retrofitted beam-column joints were then cured for seven days and tested as per the procedure presented in section 3.3.

The experimental load deflection results for the control beam-column joints are shown in the Appendix in Tables 5.1-5.2, and for the beam-column joints retrofitted using CFRP with two layers at different stress levels are also shown the Appendix in Tables 5.23-5.28. The load deflection curves for the data obtained from experimental program are plotted in Figures 5.14-5.21. These curves were idealized as trilinear curves as explained in section 3.6. The parameters such as ultimate load carrying capacity, ductility ratio, energy absorption and stiffness are calculated and are tabulated in the Table 5.29. The effect of the various parameters is studied and discussed in the succeeding section.

5.7.1 BEHAVIOR OF CFRP RETROFITTED BEAM-COLUMN JOINTS

It was observed during testing that, near the joint, the shear crack on the beam surface occurred first and become wider significantly during the test. The cracks in the joint surface were first visible at an average load of 6.67kN for all the three stress levels for control beam-column joint specimens. As the testing preceded these cracks widened going up to the ultimate load. At the

ultimate loading the shear cracks in the joint region were the largest one. The main reason for failure of the control beam-column joint was due to shear cracking in the joint region which were the widest at the ultimate loading. The flexural cracks did not appear on the beam and column surface. A typical crack pattern for control beam-column joint samples is shown in the Plates 5.1-5.3 and 5.4. Formation of cracks could not be observed in joint portion for CFRP jacketed beam-column joint specimens, however, none of the CFRP retrofitted specimens failed due to de-bonding, indicating a good joint of CFRP with the existing surface shown in Plates 5.7 - 5.10. They were also observed to show less deflection at higher loads. The results indicate that the beam-column joints retrofitted with CFRP jackets show extra enhancements in the ultimate load carrying capacity and a decrease in deflection at ultimate load as compared to the control beam-column joint specimens. Thus, due to strengthening of beam-column joints, the failure was shifted from joints (control specimens) to beam ends (retrofitted specimens) as was observed from the cracking pattern of the specimens. It was also observed that failure was sudden and brittle in the case of the CFRP retrofitted specimens. This indicates that, after retrofitting, the failure pattern of weak beam strong column joint is achieved. Obviously, the application of CFRP was an effective way to enhance the joint shear capacity of the beam-column joint specimens and considerably influenced the prevention of shear failure.

Plate 5.7: Brittle failure of Beam-column Joints Retrofitted with CFRP Jacket Using Two Layers for Stress Level-1

Plate 5.8: Brittle failure of Beam-column Joints Retrofitted with CFRP Jacket Using Two Layers for Stress Level-2

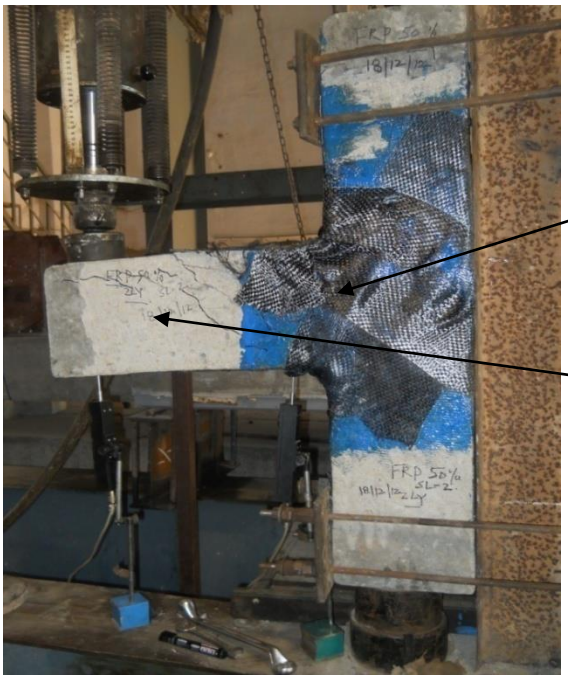

Plate 5.9: Failure of Beam-column Joints Retrofitted with CFRP Jacket with Two Layers for Stress Level-3

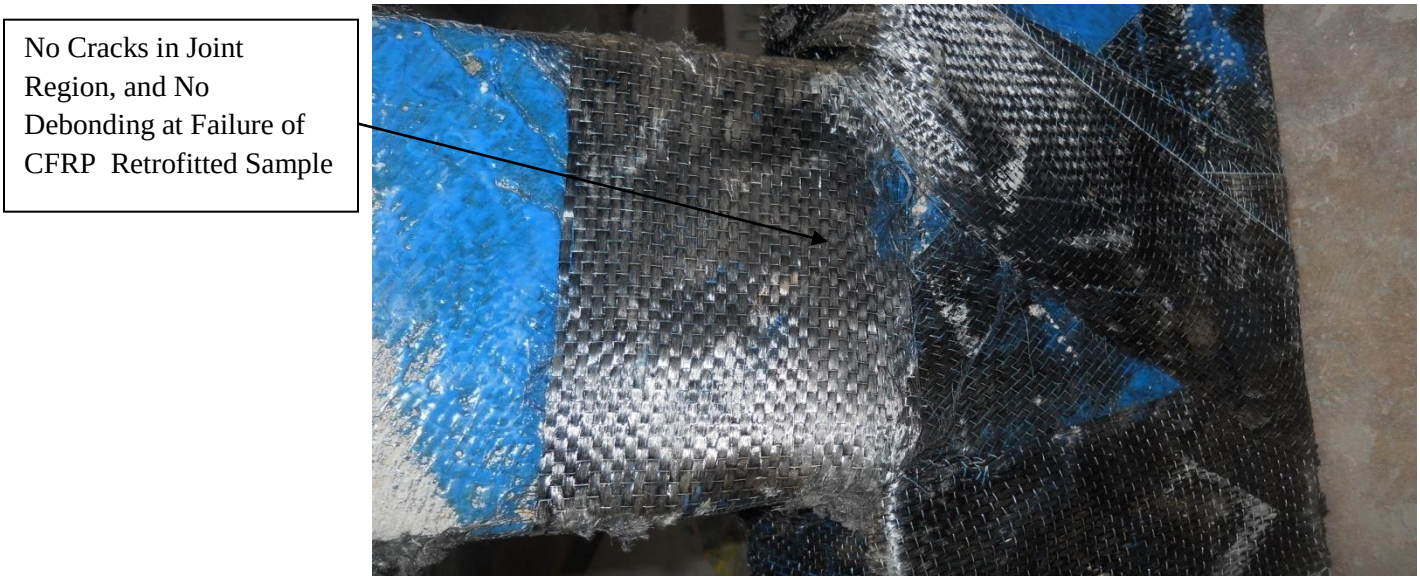

Plate 5.10: Failure of Beam-Column Joints without Debonding

5.7.2 BEAM-COLUMN JOINTS RETROFITTED USING CFRP JACKETS WITH FIBER IN L-SHAPE AND AT FORTY FIVE DEGREES TO THE JOINT IN TWO LAYERS

Out of a total of thirty seven beam-column joints, six were retrofitted using CFRP jackets with fibers orientated in an L-shape and at forty five degree to the joint. Two specimens were stressed up to ultimate load i.e. stress level-1, two specimens were stressed up to 85% of the ultimate load i.e. stress level-2, and two specimens were stressed up to 50% of the ultimate load i.e. stress level-3. The set of beam-column joint specimens was divided into three categories depending upon the stress levels. These were designated SL-1, stressed upto ultimate load; SL-2, stressed upto 85% of ultimate load; SL-3, stressed upto 50% of ultimate load; whereas the beam- column joints retrofitted with CFRP were designated as SL1-CFTL for stress level-1; SL2-CFTL for stress level- 2; SL3-CFTL for stress level- 3, where CFTL means Carbon fiber reinforced polymers with two layers. After testing the average ultimate load of the control specimens was taken as an ultimate stress level. The load deflection data obtained from the laboratory testing of

beam-column joints are plotted and presented separately in the curves shown in Figures 5.14 - 5.21.

5.7.2.1 Effect on Load Carrying Capacity of Beam-Column Joints

It can be observed from the Table 5.29, for stress level-1 and corresponding figures 5.14-5.21 that CFRP retrofitting leads to a marginal increase in the ultimate load carrying capacity. The ultimate load carrying capacity increased from 22.7kN (control specimen) to 24.8kN, (9.2% increase), for joints retrofitted with two layers of CFRP. The corresponding deflection at ultimate load reduced to 22mm, as compared to 23.2mm for the control specimen (5.2% decrease). A considerable increase in the yield load carrying capacity was observed, with a 15 percent increase for beams under stress level-1. In the case of stress level- 2, there was also a marginal increase in the ultimate load carrying capacity. The ultimate load carrying capacity increased from 22.7kN in the control specimen to 25.4kN, (11.9% increase), for joints retrofitted with two layers of CFRP. The corresponding deflection at ultimate load reduced to 22.7mm, as compared to 23.2mm for the control specimen (2.1% decrease). A considerable increase in the yield load carrying capacity was observed, with a 15 percent increase for beams under stress level-2. In Table- 5.29 a fairly similar trend was observed for stress level- 3 i.e. the ultimate load carrying capacity increased from 22.7kN control specimen to 24.4kN, (7.7% increase), for joints retrofitted with two layers of CFRP. The corresponding deflection at ultimate load reduced to 20.1mm, as compared to 23.2mm for the control specimen (13.3% decreases). A considerable increase in the yield load carrying capacity was observed, a significant increase from 20kN (yield load for control specimen) to 23kN showing a 15 percent increase for stress level- 3. Furthermore, as can be observed from Table 5.29 there was an increase in yield as well as ultimate load carrying capacity and in stiffness at ultimate load in the retrofitted specimens with two number of layers, as well. This may be due to the vertical alignment of unidirectional carbon fibers in polymers. Due to the strengthening of beam-column joints, the failure of the retrofitted specimens shifted from columns to the beams as was observed from the cracking pattern of the specimens as shown in Plate 5.9. This indicates that, after retrofitting, the failure pattern of a weak beam strong column joint was achieved.

5.7.2.2 Effect on Energy Absorption, Deflection Ductility Ratio and Stiffness of Beam-Column Joints

The load deflection curves for the controlled and CFRP retrofitted specimens was obtained up to ultimate load only as the testing was carried out under load controlled conditions. By using tri-linear idealized curves the deflection ductility ratio and energy absorption were calculated and are presented in the Table 5.29. It is generally expected that after failure of the CFRP jacket the load-deflection curve will follow the path similar to that of controlled specimen and the total energy absorption at failure will be higher than that of an un-retrofitted specimen. However, it was observed from Table 5.29 that the energy absorption ductility decreases for CFRP retrofitted specimens for all the stress levels. This may be attributed to the testing of the specimens under load controlled conditions, due to which the curve beyond the ultimate load could not be achieved. It was also observed from Table 5.29 that deflection ductility ratio decreased for retrofitted specimens as compared to control specimens for all the three stress levels, indicating that the retrofitted joints tend to become brittle early once the yield point was reached. It was also observed from Table 5.29 that the stiffness of CFRP retrofitted beam-column joints increases by 22.2 percent, 22.2 and 33.3 percent, for stress level-1, Stress level-2 and stress level-3 respectively. This may be due to the vertical alignment of unidirectional carbon fibers in polymers, which confine the joint region of the cracked beam results the increase in the strength of the beam-column joints.

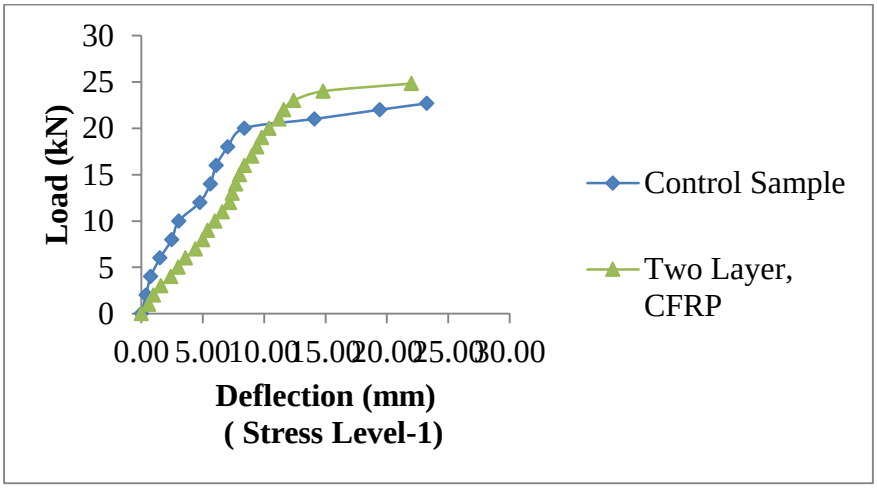

Figure 5.14: Load vs Deflection at Cantilever Beam Tip for Beam- Column Joints Retrofitted with CFRP Jacketing with Two Layers of CFRP for Stress Level-1

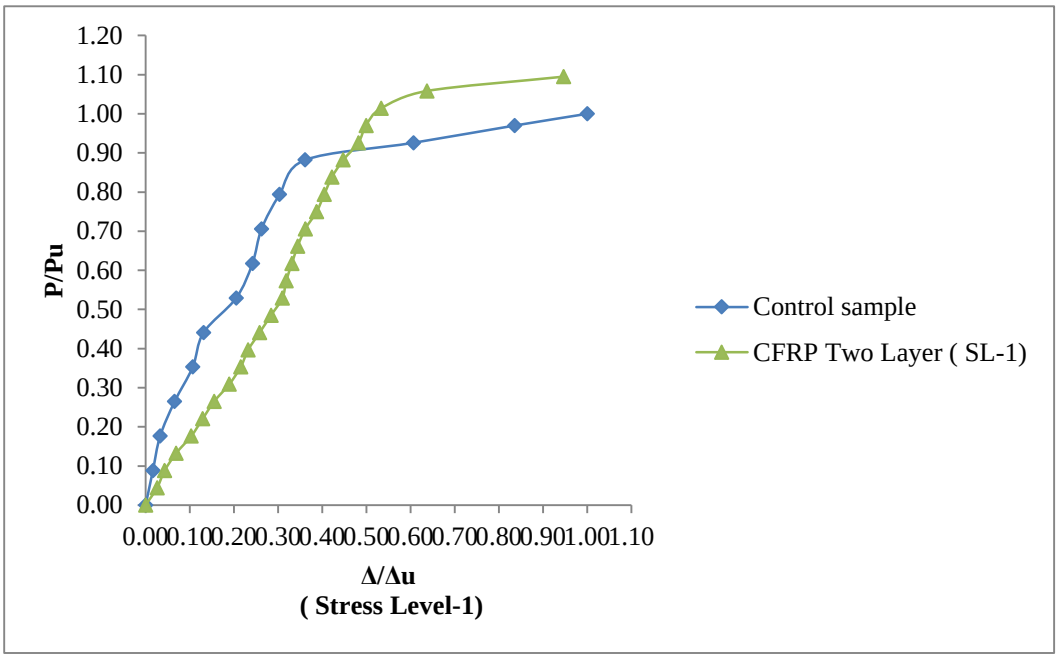

Figure 5.15: Normalized Load v/s Normalized Deflection at Cantilever Beam Tip for Beam- Column Joints Retrofitted with CFRP Jacketing with Two Layers for Stress Level-1

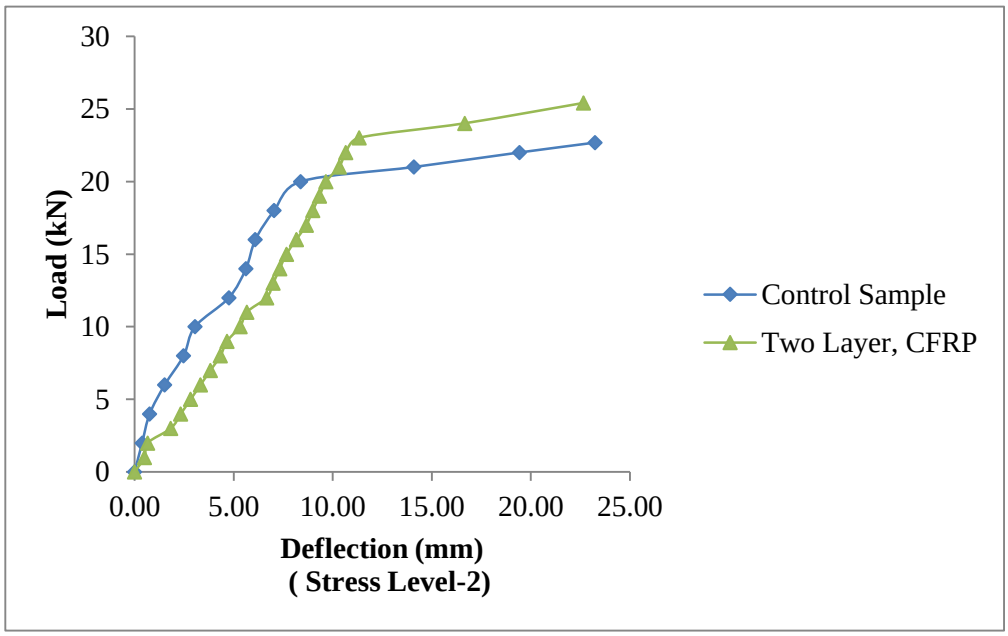

Figure 5.16: Load vs Deflection at Cantilever Beam Tip for Beam- Column Joints Retrofitted with CFRP Jacketing with Two Layers of CFRP for Stress Level-2

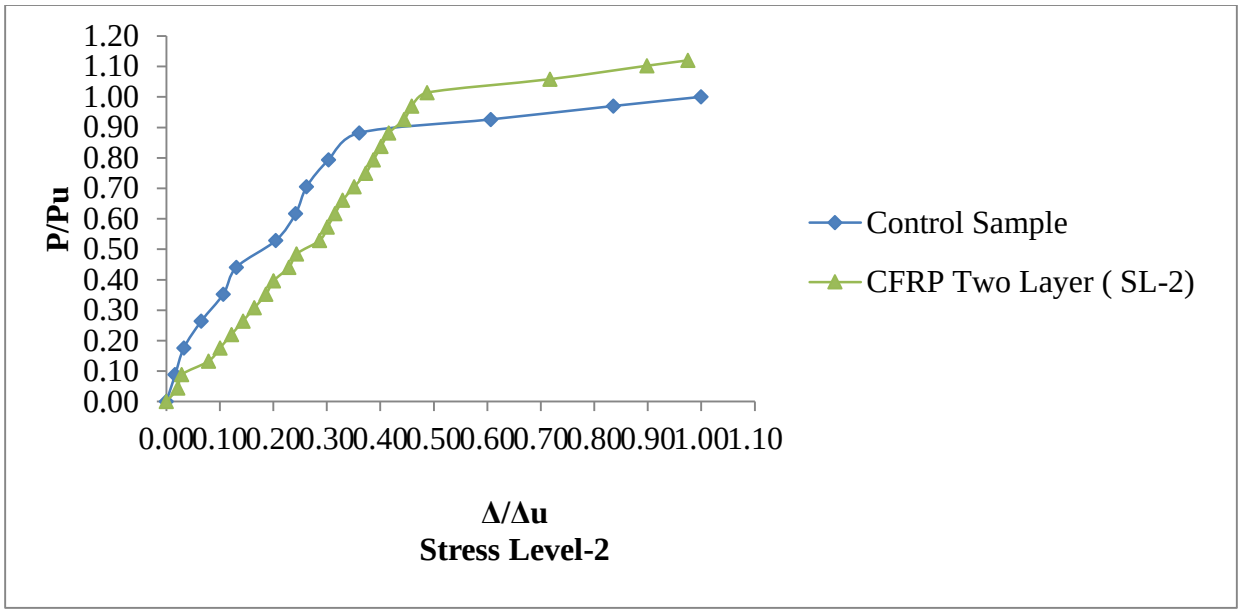

Figure 5.17: Normalized Load v/s Normalized Deflection at Cantilever Beam Tip for Beam- Column Joints Retrofitted with CFRP Jacketing with Two Layers for Stress Level-2

Table 5.29: Comparison of Experimental Loads, Deflections, Ductility Ratio, Energy Absorption and Stiffness of Control and CFRP Jacketed Beam- Column Joint Specimens

S.No.	*Stress Level*	*Beam-Column Design.*	*Pcr (kN)*	*Py (kN)*	*Pu (kN)*	*Percentage Increase In Load on Strengthening (%)*			ΔCR (mm)	ΔY (mm)	ΔU (mm)	Stiffness (Pu/Δu)	Ductility ratio (Δu/ Δy)	Energy Absorption (KN.mm) **
						P_{cr}	P_y	P_u						
1.	**____**	**Control Sample**	**6.9**	**20.0**	**22.7**	**-**	**-**	**-**	**1.6**	**8.4**	**23.2**	**0.9**	**2.8**	**412.7**
2.	**100%**	SL1-CFTL*	9.0	23.0	24.8	31.1	15.0	9.5	5.4	12.4	22.0	1.1	1.8	371.5
3.	**85%**	SL2-CFTL	9.1	23.0	25.4	33.1	15.0	12.0	4.7	11.3	22.7	1.1	2.0	380.3
4.	**50%**	SL3-CFTL	10.0	23.0	24.4	46.0	15.0	7.8	4.7	12.5	20.1	1.2	1.6	371.7

CFTL*- *Carbon fiber reinforced polymer with two layers,* ***P_{CR} –*** *First crack load,* ***P_Y –*** *Yield load* ***, P_U –*** *Ultimate load,* ***ΔCR –*** *Deflection at first crack,* ***ΔY –*** *Deflection at yield point,* ***ΔU –*** *Deflection at ultimate load,* ***SL-1, SL-2, SL-3, means*** *Stress level-1, Stress Level-2 and Stress Level-3, respectively, ** Area Under load deflection graph using tri-linear curves.*

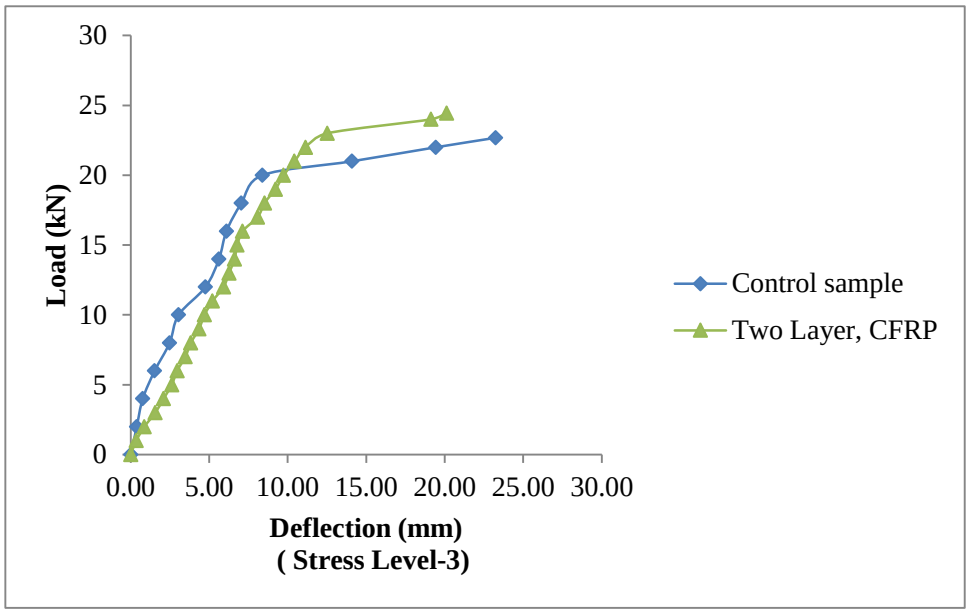

Figure 5.18: Load vs Deflection at Cantilever Beam Tip for Beam- Column Joints Retrofitted with CFRP Jacketing with Two Layers of CFRP for Stress Level-3

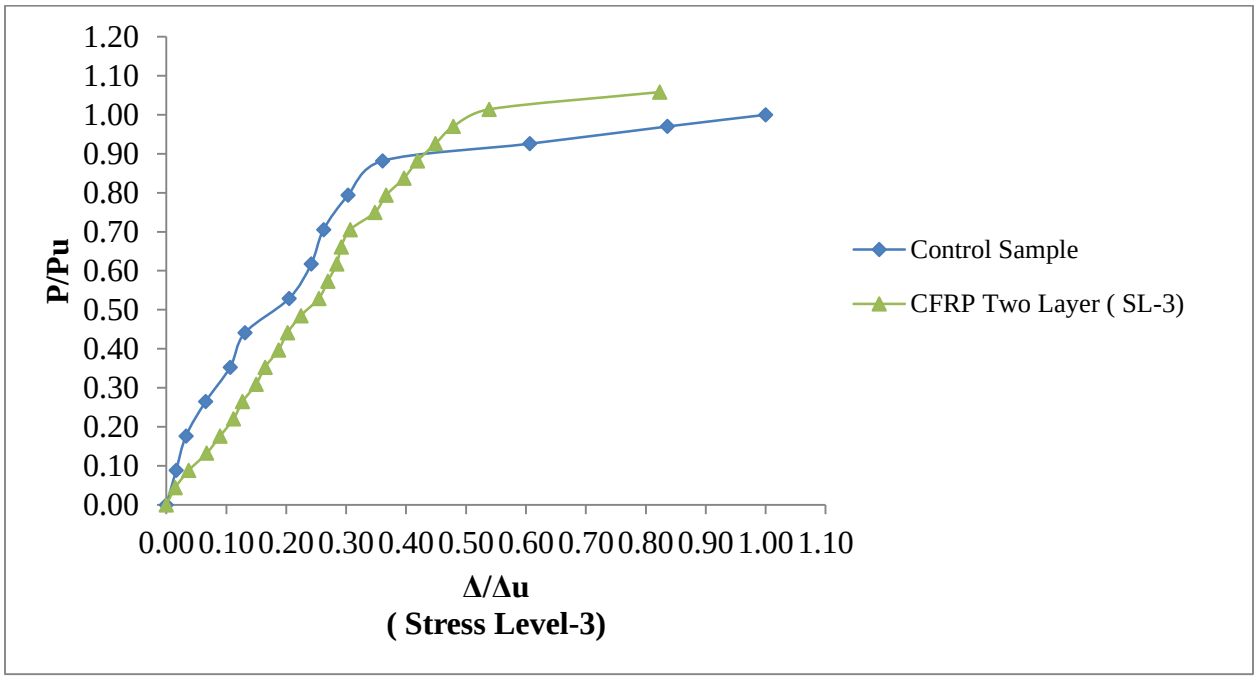

Figure 5.19: Normalized Load v/s Normalized Deflection at Cantilever Beam Tip for Beam- Column Joints Retrofitted with CFRP Jacketing with Two Layers for Stress Level-3

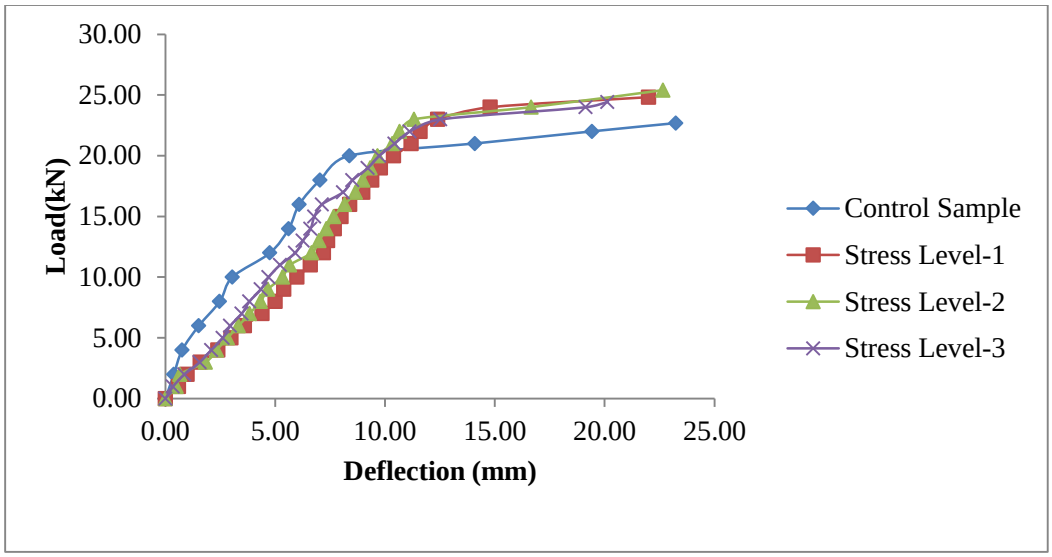

Figure 5.20: Load vs Deflection at Cantilever Beam Tip for Beam- Column Joints Retrofitted with CFRP Jacketing with Two Layers of CFRP for All The Stress Levels

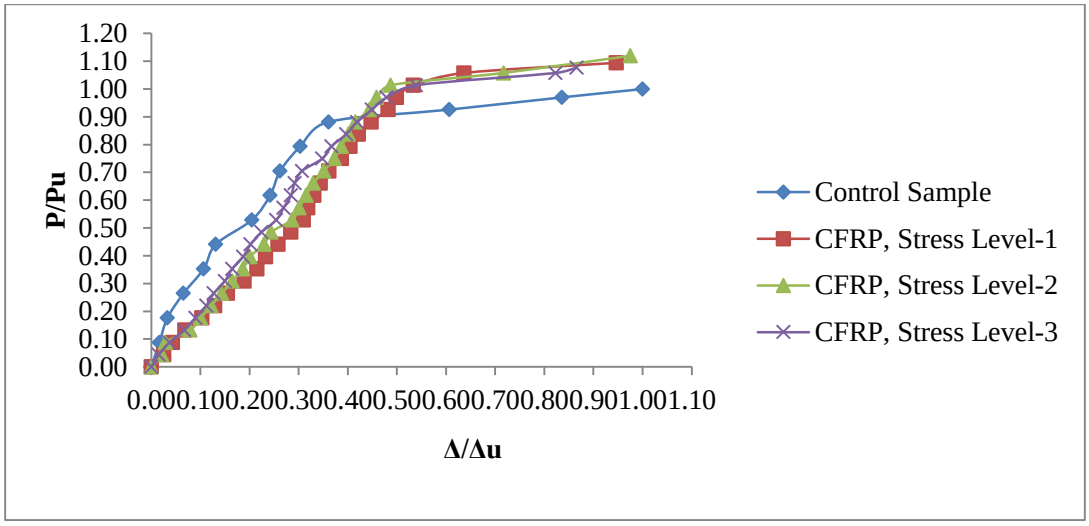

Figure 5.21: Normalized Load v/s Normalized Deflection at Cantilever Beam Tip for Beam- Column Joints Retrofitted with CFRP Jacketing with Two Layers for All the Stress Levels

It is observed from the figures 5.14- 5.21 that the two layers CFRP jacketed beam-column joint specimens was initially less stiff then control joints, this may be due to that the samples which were retrofitted using CFRP were already reached to its yield load hence they showed more deflection or less stiffness upto yield load. Once CFRP jacketed samples reached to the yield load they showed more load carrying capacity and stiffness upto ultimate load.

5.8 COMPARATIVE ANALYSIS OF CFRP JACKETED JOINTS

A comparative analysis of the effect of two layers of CFRP for retrofitting of initially stressed beam-column joints on the ultimate load carrying capacity, deflection ductility and energy absorption and stiffness is presented in this section. It was found from the discussion in the preceding that the ultimate load carrying capacity and stiffness at ultimate load increased considerably irrespective of the stress levels.

A comparison of the ultimate load carrying capacity, deflections at ultimate loads, results showed the higher ultimate load carrying capacity, lesser deflections with change in initial stress levels on all the parameters. It was observed that with two number of layers the average percentage increase in ultimate load carrying capacity of beam- column joints after retrofitting increases from 9.5 percent, 12 percent and 7.8 percent for stress level-1, stress level-2 and stress level-3 respectively as compared to the control specimens. It is generally expected that after failure of the CFRP jacket the load-deflection curve will follow the path similar to that of controlled specimen and the total energy absorption at failure will be higher than that of un-retrofitted specimen. From the Figures 5.14-5.21 and Table 5.29 it is concluded that deflection ductility ratio and energy absorption decreases for the retrofitted specimens for all the three stress levels as compared to the control specimens. This may be attributed to the testing of the specimens under load controlled conditions, due to which the curve beyond the ultimate load could not be achieved, indicating that the retrofitted joints tend to become brittle early once the yield point was reached. It has been observed that the stiffness of CFRP jacketed beam-column joint specimens increased by 22.2%, 22.2%, 33.3% for stress level-1, stress level-2 and stress level-3, respectively, as compared to the control specimens. The load at which first crack was observed to form for CFRP jacketed beam-column joint specimens increased to 30.4 percent, 31.8 percent and 44.9 percent for stress level-1, stress level-2 and stress level-3 respectively, as compared to the control specimens. For most beam-column joint specimens, the flexural cracks almost did not appear on the beam and column surface. The shear cracks in the joint region were the widest at the ultimate load and were the main reason for failure of the control beam-column joint specimens. In comparison to control specimens the CFRP jacketed joints showed more deflection upto the yield point because of the specimens which were retrofitted were already reached to their yield point and CFEP jacketing showed strength after yield point. In comparison

to SL-1 and SL-3, SL-2 showed better increase in ultimate load carrying capacity, ductility ratio and energy absorption. In case of CFRP jacketed beam-column joint specimens the formation of cracks could not be observed. However, none of the specimen failed due to de-bonding, indicating a good joint of CFRP with the existing surface. The specimens showed less deflection at higher loads. The CFRP jacketed beam-column joint specimens failed due to formation of cracks in the beam portion only. Thus, due to strengthening of beam-column joints, the failure pattern shifted from joint region in the control specimens to beam ends in retrofitted specimens, as shown in Plates 5.7- 5.10. This indicates that after retrofitting, the failure pattern of a weak beam strong column joint is achieved. Obviously, the addition of CFRP layers was an effective way to enhance the joint shear capacity of the beam-column joint specimens and considerably influenced the prevention of shear failures. These results clearly indicate that after retrofitting, the beam-column joints can absorb much higher loads making this technique eminently suitable for earthquake prone areas.

5.9 SUMMARY

The findings of the experimental investigations are discussed in this chapter. At different stress levels, flexural tests were conducted to determine the effect of the number of wire mesh layers on the ultimate strength, yield strength, ductility ratio, stiffness and energy absorption of ferrocement jacketed beam-column joints. In the case of carbon fiber reinforced polymer (CFRP) joints the load vs deflection tests were conducted at different stress levels. In this investigation it was found that ferrocement jacketing using different layers of wire mesh, and CFRP jacketing using two layers of fiber polymer, showed noticeable improvement in the ultimate strength, yield strength, stiffness of such exterior beam-column joints. Due to strengthening of beam-column joints, the failure pattern shifted from the joint region (control specimens) to the beam ends (retrofitted specimens) in both, cases. This indicates that, after retrofitting, the desired failure pattern of the weak beam strong column joint was achieved.

CHAPTER-6

FINITE ELEMENT MODELLING AND VALIDATION

6.1 GENERAL

In this chapter the validation of experimental results is done by carrying out FEM analysis using the commercial available ATENA-3D software. Herein, a description of finite element modelling of beam-column joint sample, as taken in the experimental study, is presented and analyzed to obtain the pushover curve analytically. The control specimen under static loading was taken and analyzed using the by finite element method (FEM). Subsequently, the specimens retrofitted using ferrocement with different layers of wire mesh and with CFRP using two layers, are analyzed using the same software. All the necessary steps, from the creation of the model to generating the analytical load-deformation response are explained and discussed in detail. A total of five reinforced concrete beam-column joints were modelled, one as a control joint, one each as a joint retrofitted with ferrocement using two layers, four layers and six layers of wire mesh, respectively and the fifth one as a joint retrofitted using two layers of CFRP. A static load was applied. Wire mesh wrapping is used for ferrocement retrofitting of damaged joints with cement mortar as an epoxy.

6.2 FINITE ELEMENT MODELLING OF CONTROL SAMPLE

6.2.1 Assumptions

The assumptions for the finite element modelling of the control specimen are as enumerated as below:

1. Concrete and steel are modelled as an isotropic and homogeneous materials.
2. The maximum compressive strain in the concrete is assumed to be 0.0035 as per IS 456: 2000.
3. A perfect bond exits between steel reinforcement and concrete.
4. The tensile strength of the concrete is ignored.
5. Steel is assumed to be an elastic-perfectly plastic material and identical in tension and compression.

6. Initially plane sections remain plane after loading (that is, the strain in the concrete and the reinforcement is proportional to the distance from the neutral axis).

6.2.2 Failure Criteria for Concrete

According to Willam and Warnke (1975), the assumed model is capable of predicting failure for concrete materials, wherein, both crushing and cracking failure modes are accounted for. The two input strength parameters i.e. compressive strengths and ultimate uniaxial tensile are required to define a failure surface for the concrete. Consequently, a criterion for failure of the concrete due to a multi-axial stress state can be calculated. A three-dimensional failure surface for concrete is shown in Figure 6.1.

The most considerable non-zero principal stresses are in the *x* and *y* directions, represented by σ_{xp} and σ_{yp}, respectively. Three failure surfaces are shown as the projections on the σ_{xp} -σ_{yp} plane. The mode of failure is a function of the sign of $\sigma_{zp.}$ For example, if σ_{xp} and σ_{yp} are both negative and σ_{zp} is slightly positive, cracking would be predicted in a direction perpendicular to σ_{zp}.

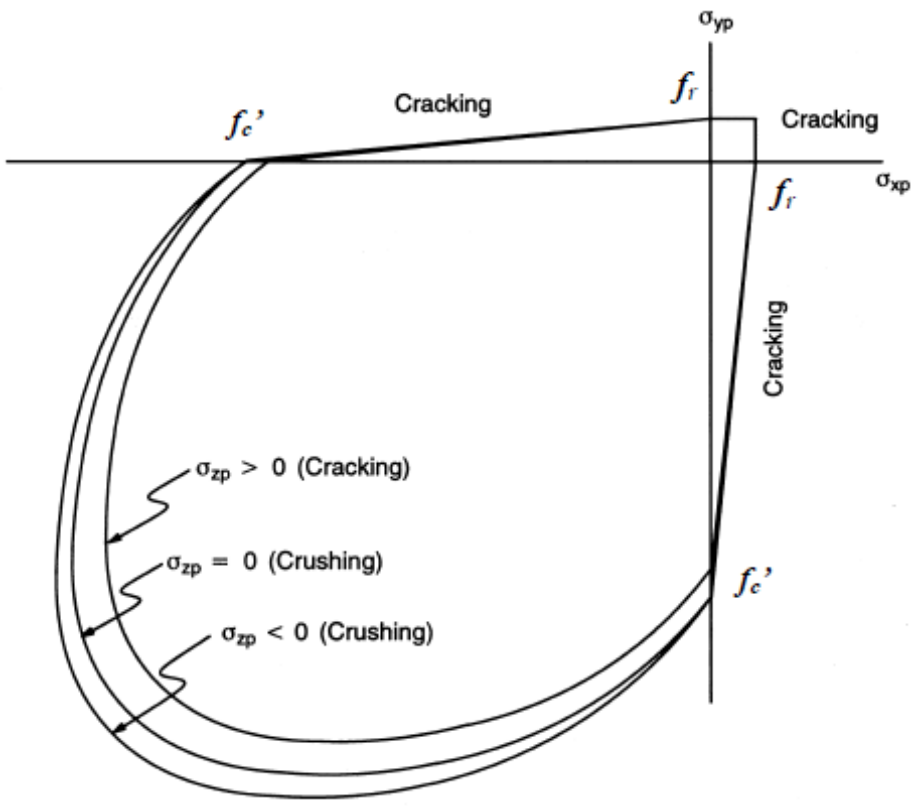

Figure 6.1: 3-D Failure Surface for Concrete (SAS, 2009)

However, if σ_{zp} is zero or slightly negative, the material is assumed to crush (SAS, 2009). During this study, it was found that in a concrete element, cracking occurs when the principal tensile stress in any direction lies outside the failure surface. After cracking, the elastic modulus of the concrete element is set to zero in the direction parallel to the principal tensile stress direction and the crushing occurs when all principal stresses are compressive and lie outside the failure surface; subsequently, the elastic modulus is set to zero in all directions and the element effectively disappears (SAS, 2009).It was also observed that if the crushing capability of the concrete is turned on, the FE beam models fail prematurely. Crushing of the concrete started to increase in elements placed directly under the loads. Subsequently, adjacent concrete elements crushed within several load steps as well, significantly reducing the local stiffness. Finally, the model showed a large displacement, and the solution diverged. Consequently, in this study, the crushing capability was turned off and cracking of the concrete controlled the failure of the FE models. Similar behavior was observed by past researchers such as Kachlakev et al. (2001),Wolanski (2004) and Ibrahim and Mahmood (2009).

6.2.3 Elements Types

For different materials and purposes the program ATENA 3D offers a variety of material models. Concrete and reinforcement are the most important material models in ATENA 3D, for RCC structures. All the important aspects of real material behavior in tension and compression are considered in these advanced models. [ATENA 3D Th. manual].

a) Geometry of the Concrete

A 3D solid brick element with 8 to 20 nodes has been used for element geometric modelling of concrete in ATENA 3D, as shown in Figure 6.2

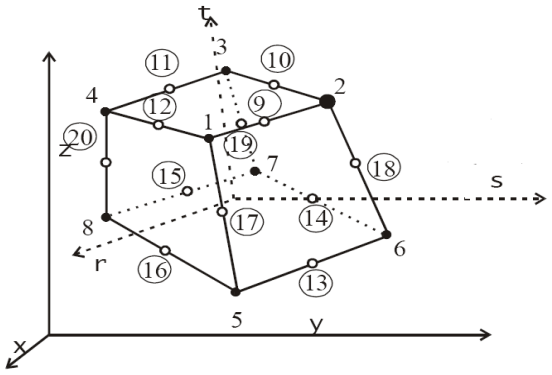

Figure 6.2: Geometry of Brick Element [ATENA 3D Th. manual]

The 3D solid brick element has three degrees of freedom at each node: translations in the nodal x, y and z directions. This is an isoparametric element integrated using Gauss integration at integration points. The element is capable of plastic deformation, cracking in three orthogonal directions, and crushing. The most important aspect of this element is the treatment of non-linear material properties.

b) Geometry of the Reinforcement

In ATENA 3D two types of reinforcement modelling can be done i.e. discrete or smeared. Discrete modelling of reinforcement was done in the present work. Bar element, which is a uniaxial tension-compression element, was used for modelling the reinforcement in analysis using ATENA 3D.The reinforcement steel is a 3D bar element, which has three degrees of freedom at each node; translations in the nodal x, y and z direction. The stress was assumed to be uniform over the entire element and, additionally, plasticity, creep, swelling, large deflection and stress-stiffening capabilities are also included in the element. This element shown in Figure 6.3.

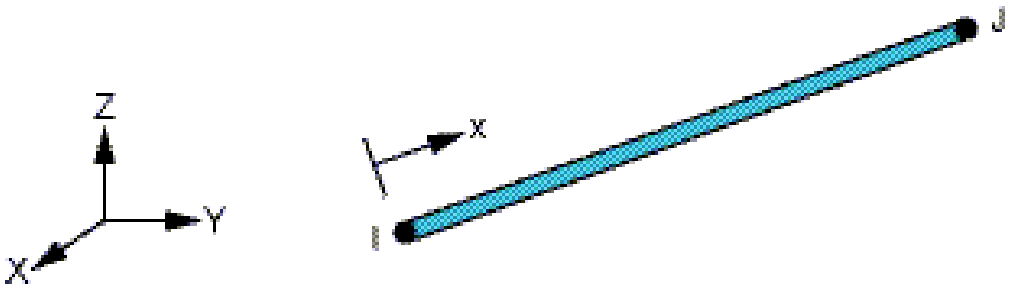

Figure 6.3: Geometry of Steel Reinforcement Element

For application of load homogeneous structural solid with simplified enhanced strain formulation was used to model steel plate. This element is shown in Figure 6.4. Here, the property of steel plate was same as the reinforcement bar except its yield strength. The HYSD steel of grade Fe-415 was used for the steel plate.

6.2.4 Material Properties

The material used for modelling of reinforced concrete was M-20 grade concrete and Fe-415 grade reinforcing steel. Concrete, reinforcement steel, steel plates, ferrocement were used to

model the RC beam-column joint. The specification and the properties of these materials are as under:

1) Concrete

The concrete material was modelled using a '3D nonlinear cementitious2'element in ATENA 3D. The physical properties of '3D nonlinear cementitious2' material, used for FEM analysis are given in Table 6.1.

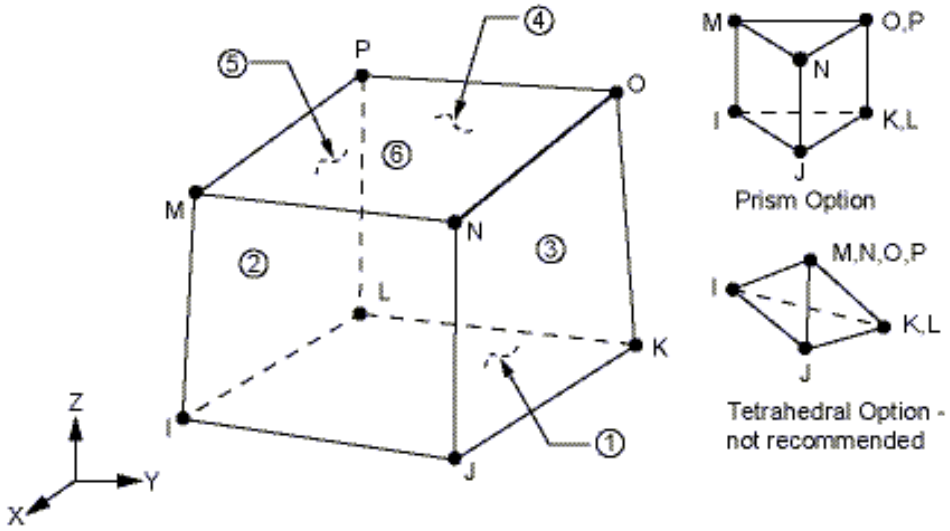

Figure 6.4: Geometry of Steel Plate Element

2) Reinforcement Bars

10mm and 8mm diameter bars of HYSD steel of grade Fe-415 are used as main reinforcing steel while 6mm diameter bars are used as shear reinforcement. The properties of these bars, as used in the FEM analysis model, are shown in Table 6.2.

3) Steel Plate

The steel plate element in the ATENA 3D is used at the location of support and loading. Mild steel of grade Fe-250 was used for modellng the steel plate element.

Table 6.1: Properties of Concrete for FEM

Properties	Values
Elastic Modulus E_C	23184MPa($E_c = 5000\sqrt{f_{ck}}$)
Poisson's Ratio	0.2
Tensile Strength	1.856E+00
Compressive Strength (f_{ck})	21.5MPa
Specific Material Weight	2.300E-02MN/m^3
Coefficient of Thermal Expansion	1.200E-05 1/K
Fixed Crack Model Coefficient	1
Ultimate strain in bending(ε_{cu})	0.0035

Table 6.2: Properties of Reinforcement for FEM

Properties	Values
Elastic Modulus	21,0000MPa
Yield Strength (f_y)	415MPa
Specific Material Weight	0.0785MN/m^3
Coefficient of Thermal Expansion	1.2E-05 1/K

6.2.5 Modelling

The beam-column joint was modelled as a mass concrete element in volume. The dimensions are shown in Figure 3.3. The combined volumes for the control specimen created in ATENA-3D are shown in Figure 6.5.

Height of the column = 1000mm

Length of the cantilever = 500mm

Cross section of the column = 225mm x 125mm

Cross section of the cantilever beam = 125mm x 225mm

Steel Plate =125mm x 100 mm x 25 mm

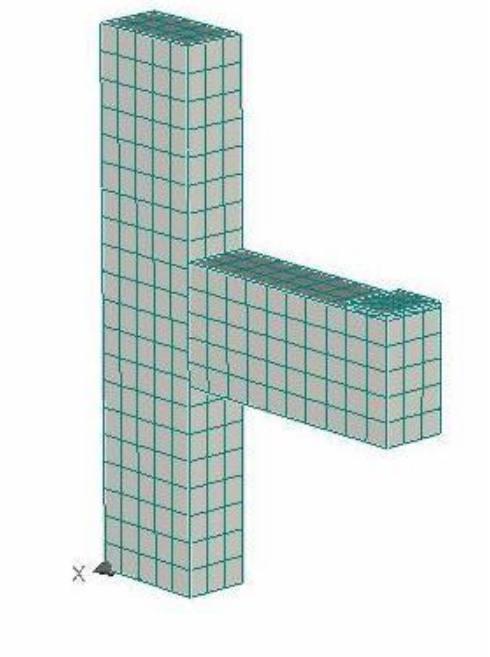

Figure 6.5: Volumes Created in ATENA-3D for the Control Specimen

6.2.6 Meshing

According to Wolanski (2004) and Kachlakev et al. (2001), the use of rectangular mesh elements in modeling have shown to good results. Thus, the mesh set up is such that rectangular elements are created in the model. The overall mesh of the control specimen created in ATENA-3D is Figures 6.6- 6.7 shown and illustrate the reinforcement arrangement modelled in ATENA-3D.

6.2.7 Loads and Boundary Conditions

To get a unique solution in FE analysis, displacement boundary conditions are needed to restrain the FE model. To attain this, the translations at the nodes X, Y and Z are set at a constant value of 0. The support conditions at the bottom of the column are shown in Figures 6.8- 6.9. The same boundary conditions are imposed at the top of the column. The load was applied at a distance of 450mm from the face of the column. Figure 6.10 shows the applied loading in the modelling.

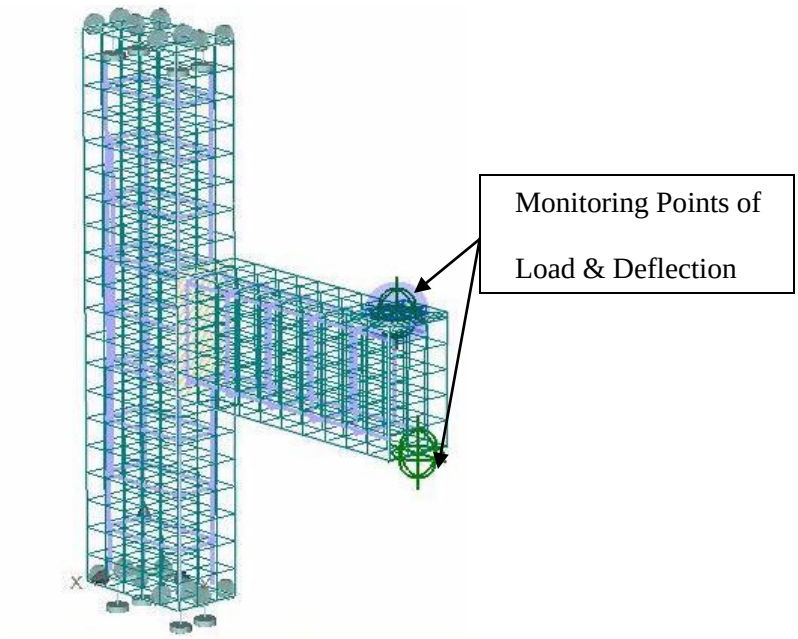

Figure 6.6: Mesh Created in ATENA-3D for the Control Specimen

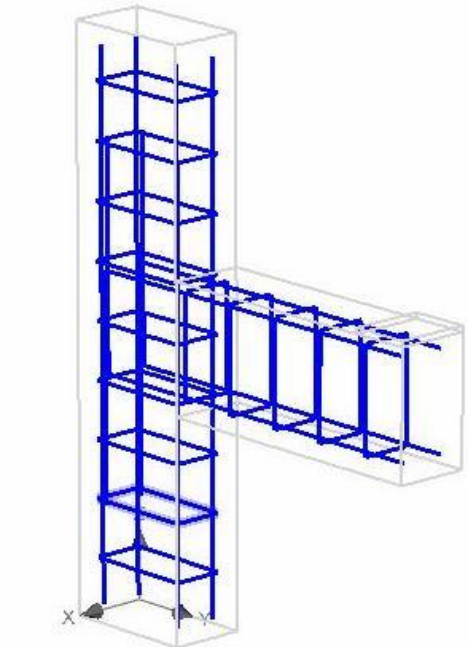

Figure 6.7: Reinforcement Arrangement Modelled in ATENA-3D for the Control Specimen

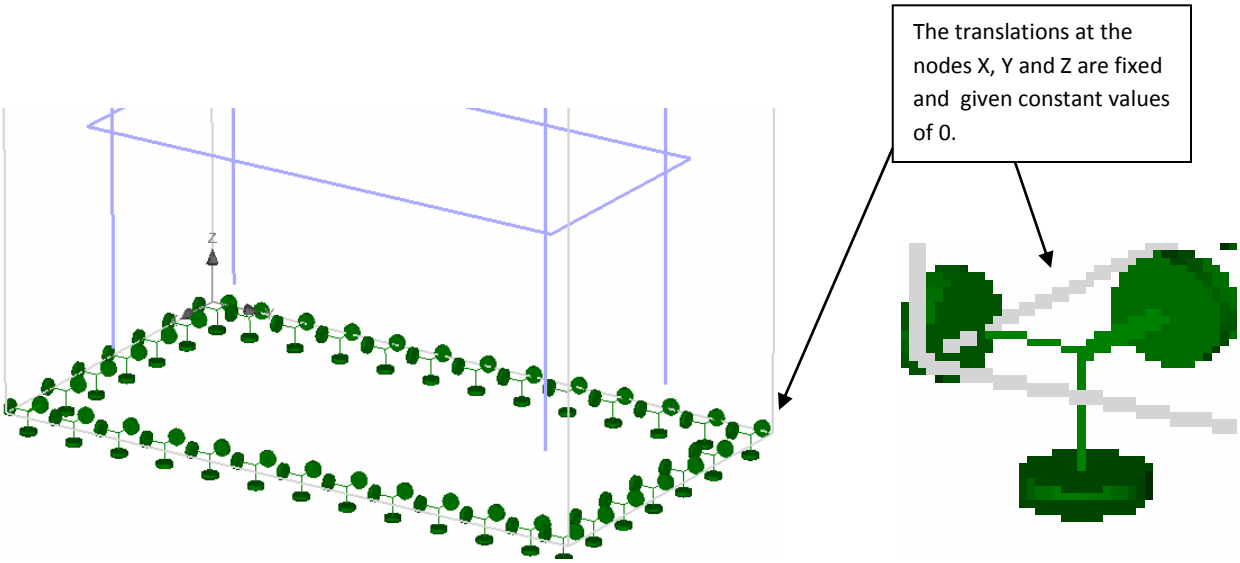

Figure 6.8: Boundary Conditions for the Control Specimen for Bottom of the Column

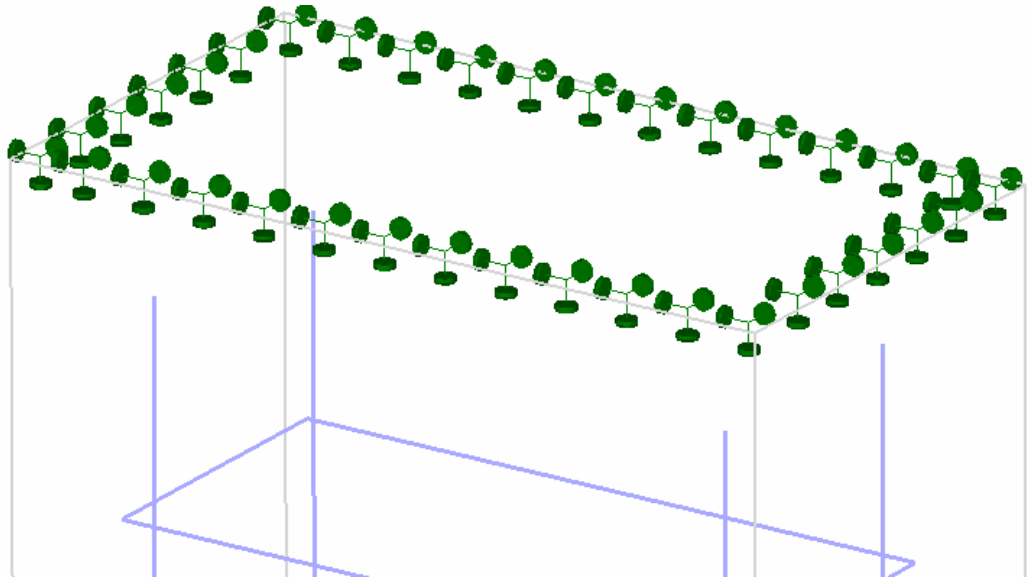

Figure 6.9: Boundary Conditions for the Control Specimen for Top of the Column

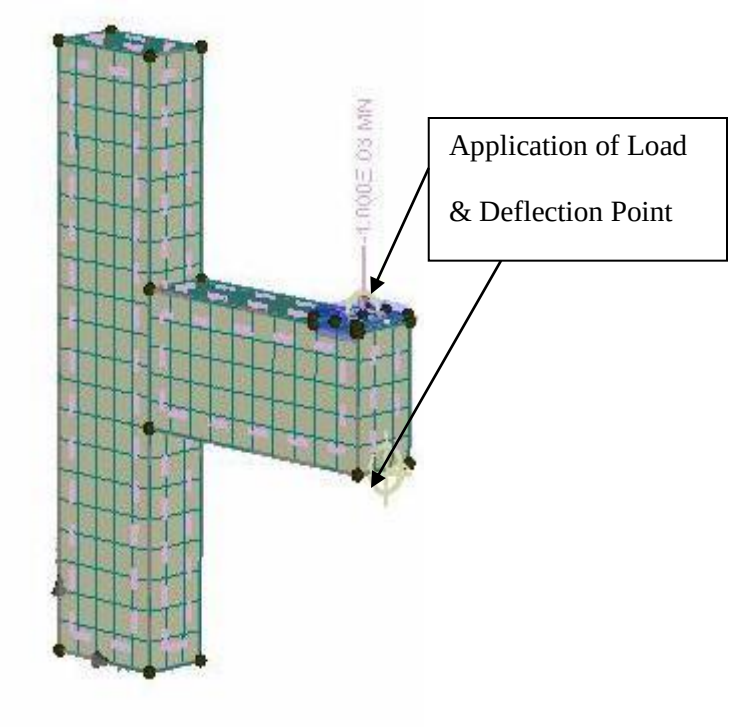

Figure 6.10: Loading Conditions for the Control Specimen

6.2.8 Analysis Process

The ATENA 3D program has three main functions to perform starting with pre-processing, then the loading is applied and analysis is carried out and finally post-processing was done. These function are explained as below:

A. **Pre-processing:** The process involves input of geometrical objects (concrete, reinforcement, interfaces, etc.), loading and boundary conditions, meshing and solution parameters.

B. **Analysis:** This function makes it possible to have a real time monitoring of results during calculations.

C**. Post-processing:** this feature gives a direct access to a wide range of graphical and numerical results.

The detailed step-by-step procedure for FEM analysis envisaged using ATENA 3D is discussed as below:

First and foremost, in the pre-processing window following four steps are performed:

Step 1: Geometry of FE model of beam- column joint is created. (Figure 6.5)

Step 2: Material properties was assigned to the various elements of the RC beam-column joint specimen.

Step 3: Finite element meshing parameters were given and meshing of the model is generated accordingly. (Figure 6.6)

Step 4: Structural element, various supports, loadings and monitoring points was defined (Figure 6.7- Figure 6.10)

Subsequently in the next two steps analysis and post-processing are done.

Step 5: Herein, different analysis steps was defined. The finite element non-linear analysis was completed in the Run window. The finite element non-linear static analysis calculates the effects of steady loading conditions on a structure. A static analysis include steady inertia loads (gravity and rotational velocity), and time-varying loads that can be approximated as a static equivalent. Static analysis was used to determine the stresses, strains, forces and displacements, in structures or components by loads.

Step 6: When the FE nonlinear static analysis was completed then the results can be viewed in the post processing component. The behavior of the elements at every step of loading and deflection, in the form of stress- strain values, crack pattern, cracks propagation at every stage, can be studied in this step.

6.3 FE MODELLING OF RETROFITTED RC BEAM-COLUMN JOINT

After loading and analysis of the control specimen, it was retrofitted with ferrocement and CFRP jackets with a typical retrofitting scheme, as per the experimental program, and analyzed using ATENA-3D software.

6.3.1 Assumptions

The assumptions for finite element modelling of the retrofitted specimen are the same as in Para 6.2.1 in addition to that;

1. The tensile behavior of the ferrocement and CFRP reinforcement is linear-elastic until failure.
2. The ferrocement and CFRP reinforcement is assumed to carry stress along its axis only.

6.3.2 Element Types for Ferrocement Retrofitting

In ATENA 3D, the modelling of concrete element geometry was prepared using 3D solid brick element with 8 up to 20 nodes for the RC structures, as shown in Figure 6.11. This 3D solid brick element has three degrees of freedom at each node: translations in the nodal x, y and z directions. This is an isoparametric element integrated by Gauss integration at integration points. This element is capable of plastic deformation, cracking in three orthogonal directions, and crushing. The treatment of nonlinear material properties is the most important aspect of this element.

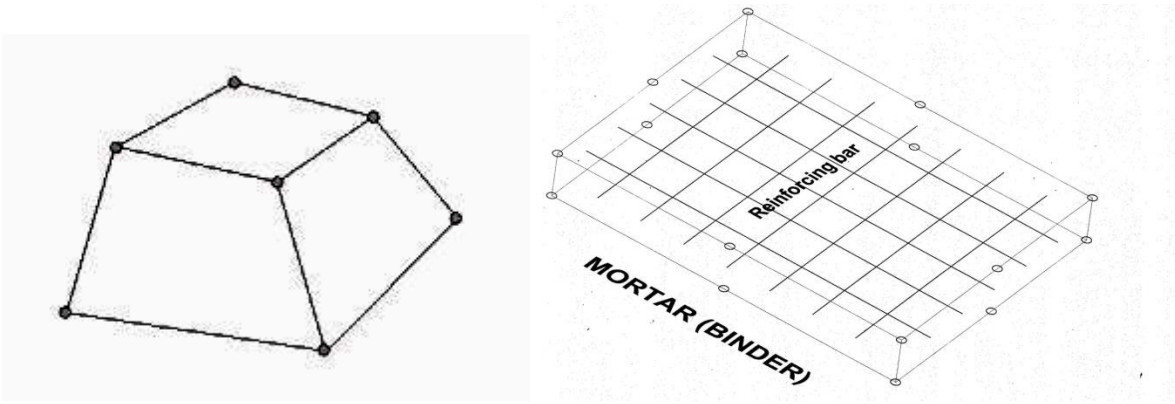

Figure 6.11:Eight Nodes Brick Element Model for Concrete and 20 Nodes Shell Element Model for Ferrocement Composite

In ATENA 3D, the ferrocement can be modelled as a shell element. The shell element is a 20 nodes isoparametric brick element as shown in Figure 6.11. This is needed, in order to be able to use the same pre and post-processors support for the shell and native 3D brick element. After the 1st step of the analysis, the input geometry will automatically change to the external geometry as shown in Figure 6.12. As nodes 17 and 18 contain only, so called, bubble functions, the element was post-processed in the same way as it would be the in isoparametric brick element [ATENA 3D Th. manual]. In the following general shell element theory concept, every node of the element has five degree of freedom, i.e. three displacements and two rotations in planes normal to mid surface of element. In order to facilitate a simple connection of this element with other true 3D elements, the five degrees of freedom are transformed into x, y, z displacement of a top node and x, y displacement of a bottom node degrees of freedom. The two nodes are located on the normal to the mid surface passing through the original mid-surface element node.

6.3.3 Material Properties

Cement Concrete, steel reinforcement, steel plates (as discussed earlier), cement mortar and wire mesh layers have been used to model the retrofitted beam-column joint.

The specification and the properties of mortar and wire mesh are as under:

1. **Concrete:** The concrete was modelled using a '3D nonlinear cementitious- 2' element in ATENA 3D as explained earlier. A damage index of 0.6 is assumed to exist at the final stage. After necessary retrofitting and repair the elastic modulus was assumed to be 0.4 times the initial value. The damage index and elastic modulus is assumed on the basis of previous literature survey of same problems. The other values of concrete were incorporated corresponding to 0.4E in the retrofitted model [Beena & Kwatra, 2013].
2. **Steel Plate:** The steel plate used under the application of load was modelled in the same way as for the control beam-column joint as explained earlier.
3. **Steel Reinforcement:** The steel reinforcement was also modelled in the same way as done in case of control beam-column joint explained earlier, however, with one major difference. As the steel has reached its yield point, the value of yield stress for the retrofitted model was taken to be 210 MPa instead of 415 MPa [Beena & Kwatra, 2013].
4. **Epoxy:** Cement mortar was used as an epoxy in the analysis. The material properties of the epoxy are shown in Table 6.3.

Table 6.3: Properties of Epoxy for FEM

Properties	Values
Elastic Modulus	3465 MPa
Possion Ratio	0.2
Yield Strength	53 MPa
Specific Material Weight	2.300E-02
Coefficient of Thermal Expansion	1.200E-05 1/K

5. **Wire Mesh:** GI woven steel wire mesh of 0.5mm diameter with 10mm x 10mm square grid was used as the reinforcement component in ferrocement retrofitting. The properties used in the modelling are shown in the Table 6.4.

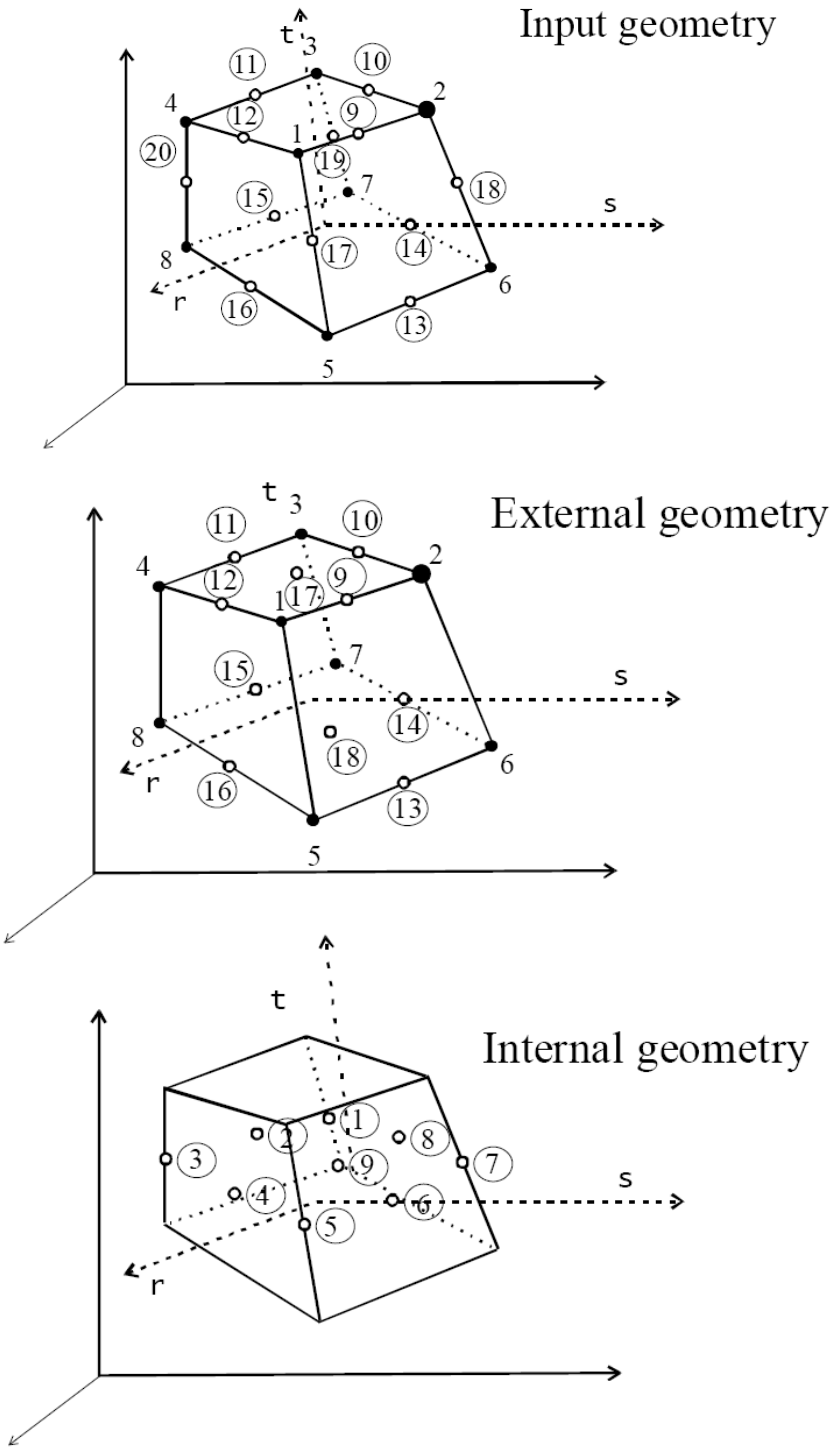

Figure 6.12: Geometry of the Ferrocement [ATENA 3D Th. manual].

Table 6.4: Properties of Wire Mesh for FEM

Properties	Values
Elastic Modulus	2.100E+05 MPa
σy	185 MPa
Coefficient of Thermal Expansion	1.200E-051/°K
Specific Material Weight	7.850E-02 MN/m^3

6.3.4 Modelling of Ferrocement Retrofitting in ATENA 3D

In ATENA 3D, modelling of retrofitting can be done in two ways. In the first method it can be done by making two different construction cases. The material properties of the composite material are taken as negligible when the 1st case is activated. The FEM analysis was done in the same way as done in the case of control frame. After attaining the required load/stress level, construction case 2 was activated in which the full values of the composite materials are incorporated for strengthening and analysis was done as explained earlier. In the second method properties of material corresponding to a particular value of Damage-Index are assigned to the elements and the structure was analyzed. [Beena & Kwatra, 2013].

In the present study, due to the complication of model and software restrictions, as the memory required in previous case is almost double as compared to the second one, the second method was opted for. The properties of wire mesh and epoxy used in the model have already been discussed in detail. The retrofitting method adopted is presented in the Figure 6.13.

The combined volumes created in ATENA-3D are shown in Figure 6.14.

6.3.5 Meshing

For the ferrocement retrofitted specimen, meshing of concrete and reinforcement members was done in the same way as for the control specimen as shown in Figures 6.6- 6.7. Ferrocement layers were meshed as brick elements in such a way that the nodes of the ferrocement layered solid elements are connected to those of adjacent concrete solid elements in order to satisfy the perfect bond assumption.

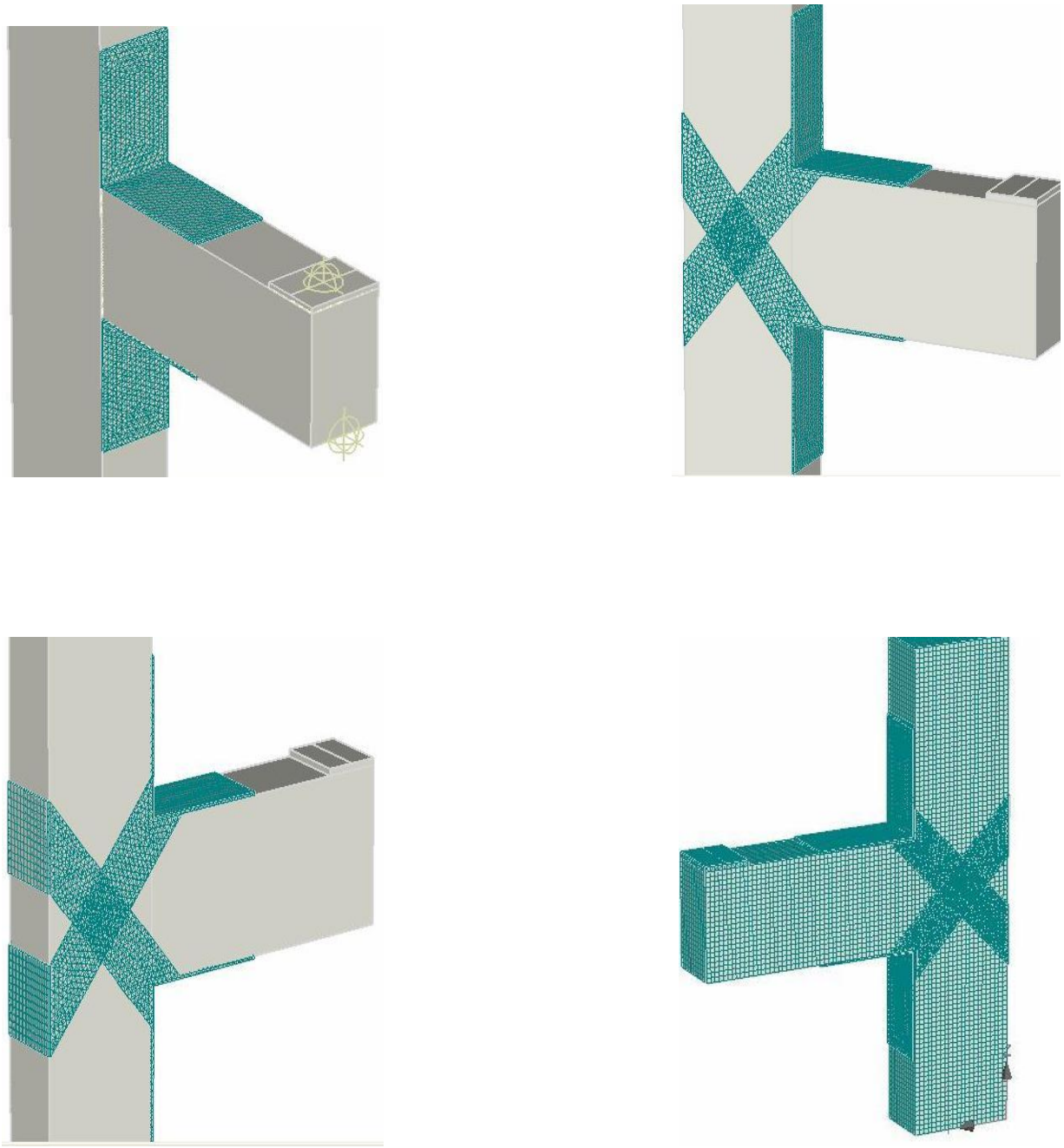

Figure 6.13: Scheme of Modelling of Wire Mesh Wrapping in Ferrocement Retrofitting

6.3.6 Loads and Boundary Conditions

Displacement boundary conditions were applied to restrain the retrofitted beam-column joint model on similar lines as was done in the modelling of the control specimen. The translations at

the nodes X, Y and Z were given constant values of 0. Similar support conditions are given at the top of the column. The load was applied at a distance of 450mm from the face of the column. The modelling of steel plate, supports, meshing and monitoring points of retrofitted sample are shown in Figure 6.15.

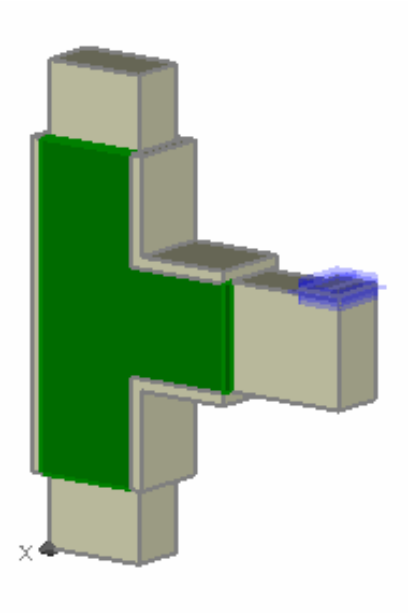

Figure 6.14: Volumes Created in ATENA-3D for the Retrofitted Specimen

Figure 6.15:Modelling of Steel plates, Supports, Meshing and Monitoring Points of Retrofitted Sample in ATENA 3D

6.3.7 Analysis Process

The analysis process for the ferrocement retrofitted FE models was the same as for the control FE model samples as discussed in 6.2.8.

6.4 VALIDATION OF FE MODEL RESULTS

6.4.1 Control Specimen

A non-linear response of the RC beam- column joint was modelled under the static loading as per details in previous discussion. The experimental and finite element analysis results of the control beam-column joint specimens was compared. Finite element analysis of an RC beam column joint under the static incremental loads was performed using ATENA 3D software. This was followed by plotting the load deflection curve and the cracking behavior obtained from the analysis. In the FE analysis, load was applied in terms of prescribed deformation on the beam-column joint at the free end of the cantilever beam and the loads taken by the joint corresponding to the deformations were obtained. The load-deflection values at every step were recorded as shown in Table- 6.5. Further the crack pattern and crack propagation at every step was studied. The load vs deflection curves were plotted for both control specimens under the static load. Subsequently these results were compared with the experimental results. Figures 6.16- 6.18 show the crack pattern and different stresses at ultimate load of the beam-column joint using ATENA 3D software. Figure 6.19 shows the comparison of the FE model using ATENA and the experimental results for the control specimens. The finite element model results showed slightly higher values compared to the experimental values. The difference in experimental and FE results was approximately 10 percent. This may be due to that in FE model the concrete input ideal material values, while in the real specimens the curing / compaction/ temperature history may not been perfect and thus the in-situ strengths are actually lower.

Table 6.5

Load-Deflection Results from ATENA 3D at Free End of Beam for Control Specimens

Load(kN)	Deflection(mm)	Load(kN)	Deflection(mm)
8.0	0.3	20.7	4.2
10.5	0.7	22.8	6.0
12.9	1.9	22.9	8.0
14.5	2.5	23.1	8.9
16.4	3.1	24.8	18.9
18.0	3.5		

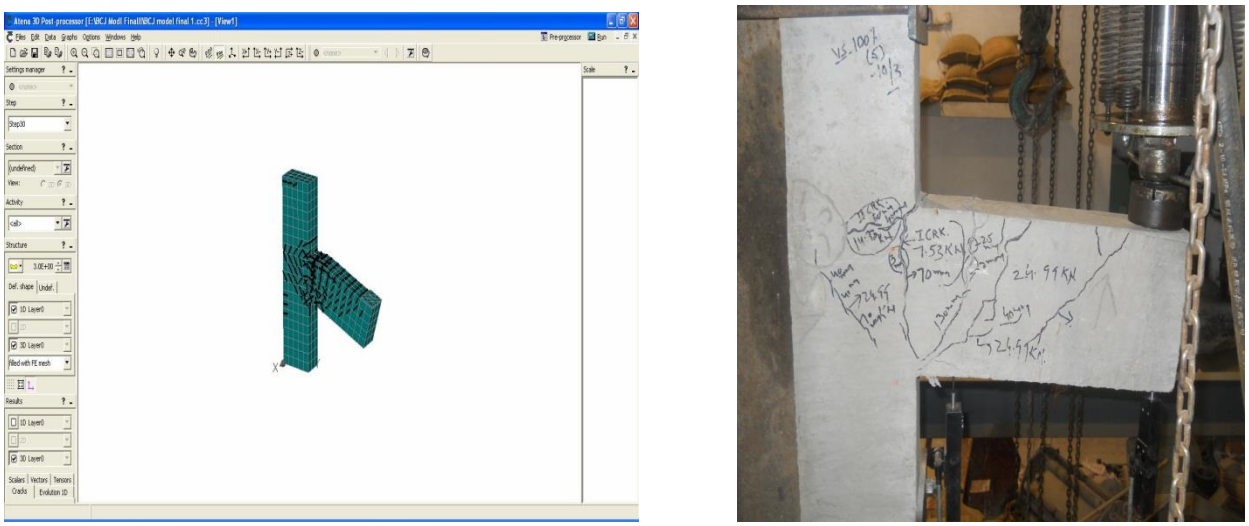

Figure 6.16: Deflected Shape and Cracks of Control Beam-Column Joint at Ultimate Load (FE Model vs Experimental)

Figure 6.17: Stresses in Control Beam-Column Joint at Ultimate Load (FE Model vs Experimental)

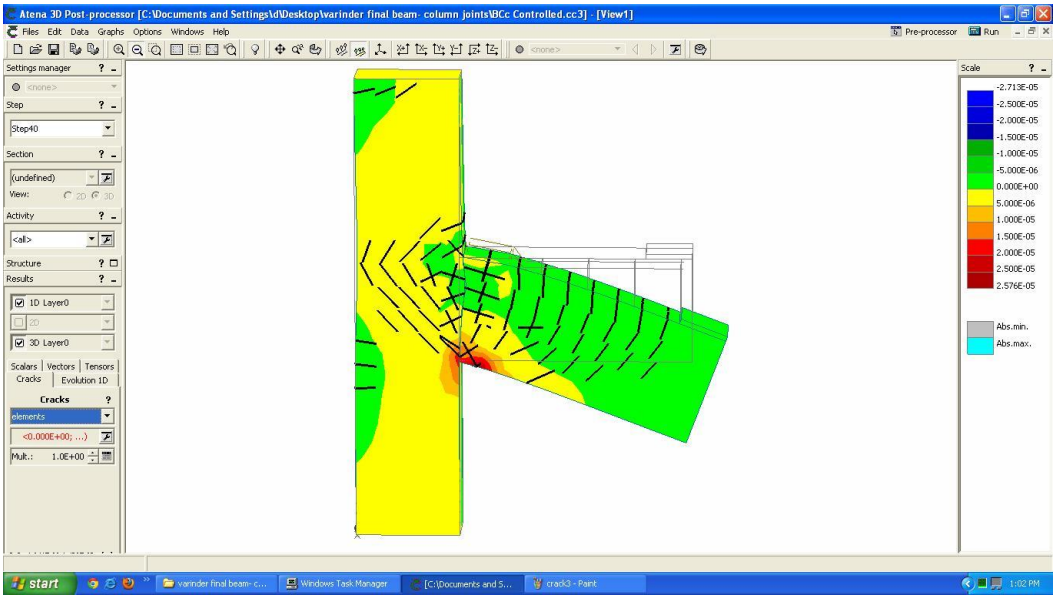

Figure 6.18: Different Stress Values in Control Beam-Column Joint at Ultimate Load

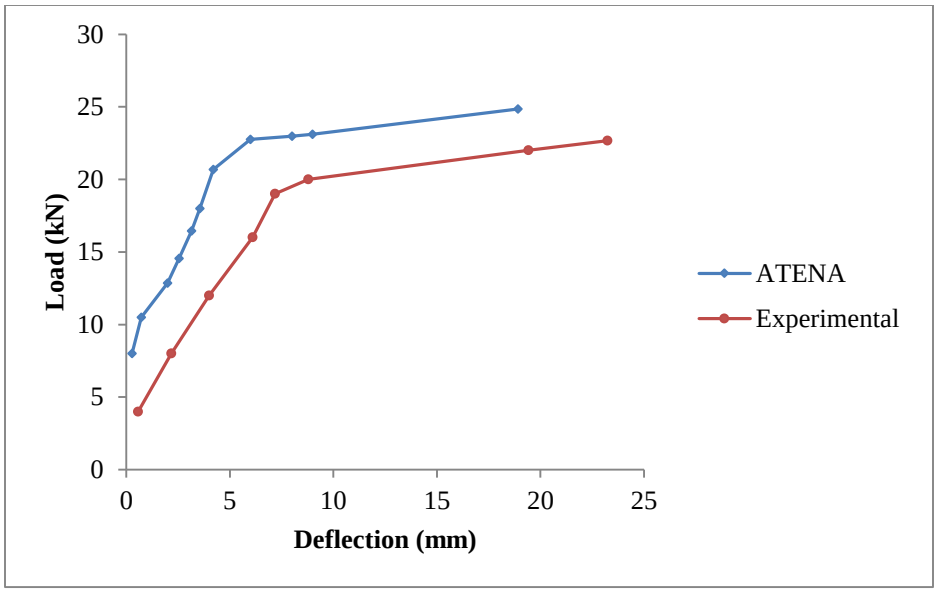

Figure 6.19: Comparison of Experimental and ATENA 3D Load vs Deflection Results at Free End of Beam for Control Specimen

6.4.2 Retrofitted Specimens: The load vs deflection values from the analysis of retrofitted beam-column joint specimens with two, four and six layers of wire mesh in ATENA 3D were noted at the free end of beam. These are presented in Tables 6.6, 6.7 and 6.8 respectively.

Table 6.6
Load-Deflection Results From ATENA 3D at the Free End of Beam for Ferrocement Retrofitted Specimens with Two Layers of Wire Mesh

Load (kN)	Deflection(mm)	Load (kN)	Deflection(mm)
6.5	0.10	20.6	3.3
8.8	0.13	22.5	3.9
10.5	0.9	24.8	4.3
12.1	1.1	26.9	5.1
14.5	1.6	28.9	8.4
15.9	2.2	29.2	11.0
17.5	2.5		
19.4	3.0		

Table 6.7
Load-Deflection Results from ATENA 3D at Beam Free End for Ferrocement Retrofitted Specimen with Four Layers of Wire Mesh

Load (kN)	Deflection(mm)	Load (kN)	Deflection(mm)
6.0	0.04	22.5	3.6
8.0	0.1	25.4	4.1
10.6	0.2	29.4	5.8
12.5	0.9	30.6	7.4
14.1	1.5	32.5	9.9
15.7	2.2		
17.8	2.7		
20.3	3.1		

Table 6.8
Load-Deflection Results from ATENA 3D at the Free End of Beam for Ferrocement Retrofitted Specimen with Six Layers of Wire Mesh

Load (kN)	Deflection (mm)	Load (kN)	Deflection (mm)
8.0	0.1	24.5	3.5
10.0	0.2	26.2	3.9
12.1	0.6	28.0	4.2
14.3	1.2	31.2	5.4
16.5	1.8	33.5	7.1
17.4	2.2	34.8	12.6
19.5	2.5		
22.6	3.1		

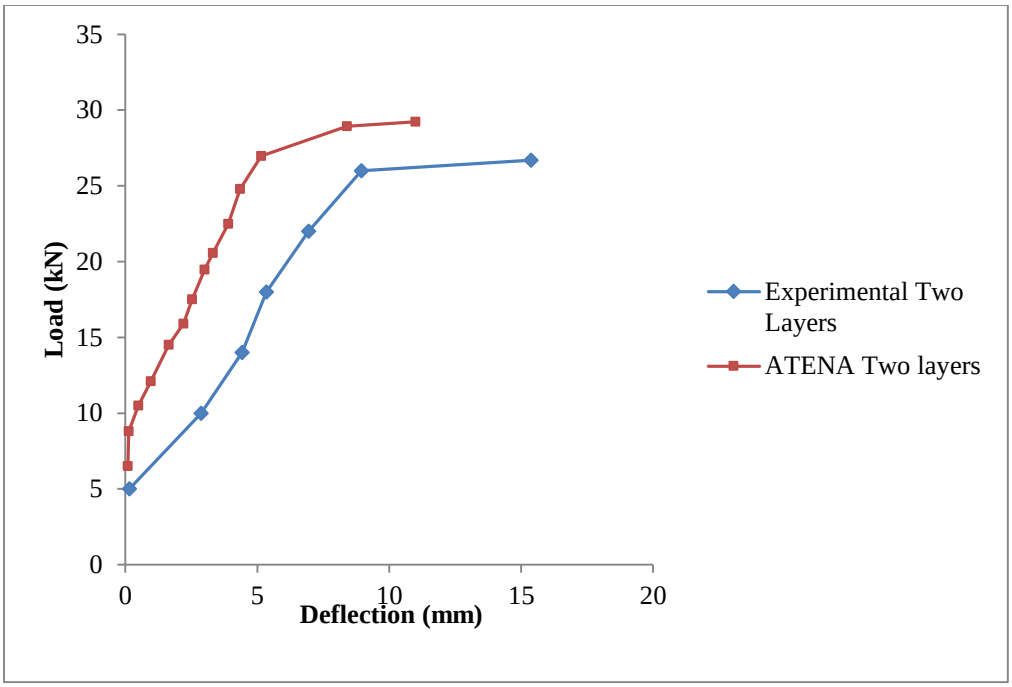

Figure 6.20: Comparison of Experimental and ATENA 3D Load vs Deflection Results at the Free End of Beam for Two Layer Ferrocement Retrofitted Specimen

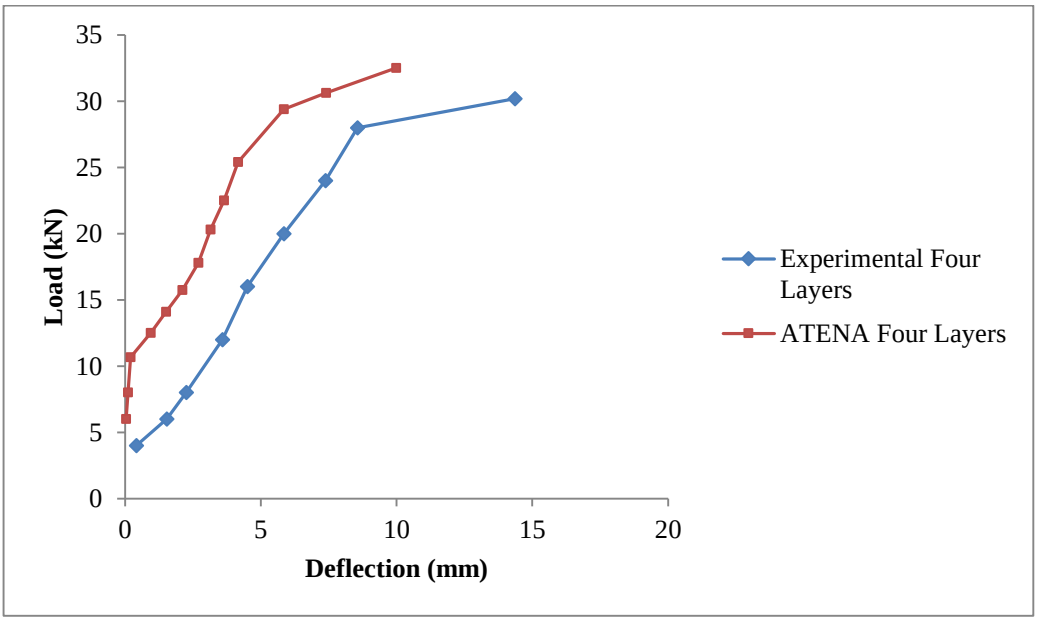

Figure 6.21:Comparison of Experimental and ATENA 3D Load vs Deflection Results at the Free End of Beam for Four Layer Ferrocement Retrofitted Specimen

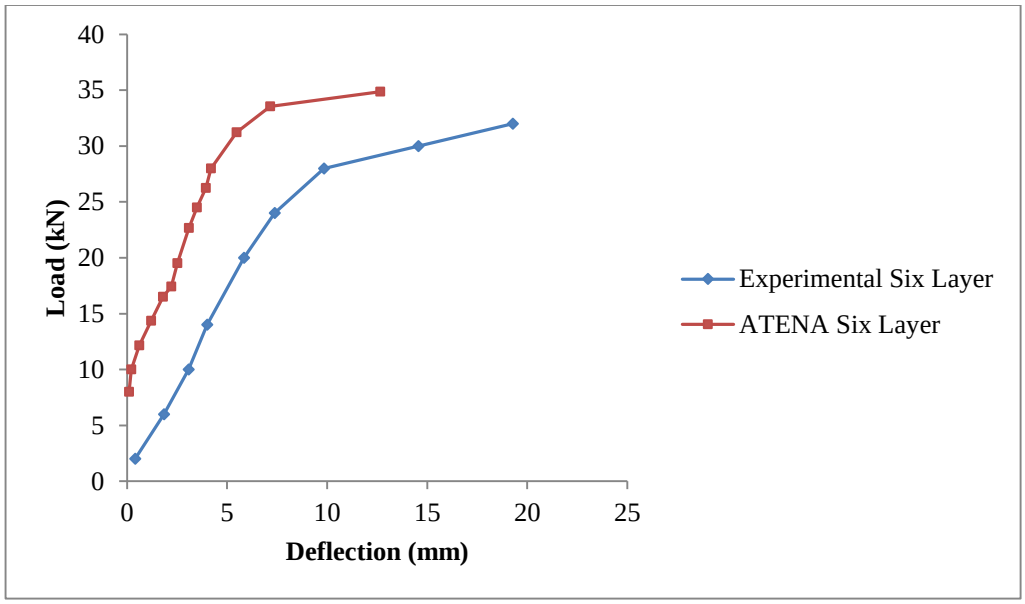

Figure 6.22: Comparison of Experimental and ATENA 3D Load vs Deflection Results at the Free End of Beam for Six Layers Ferrocement Retrofitted Specimen

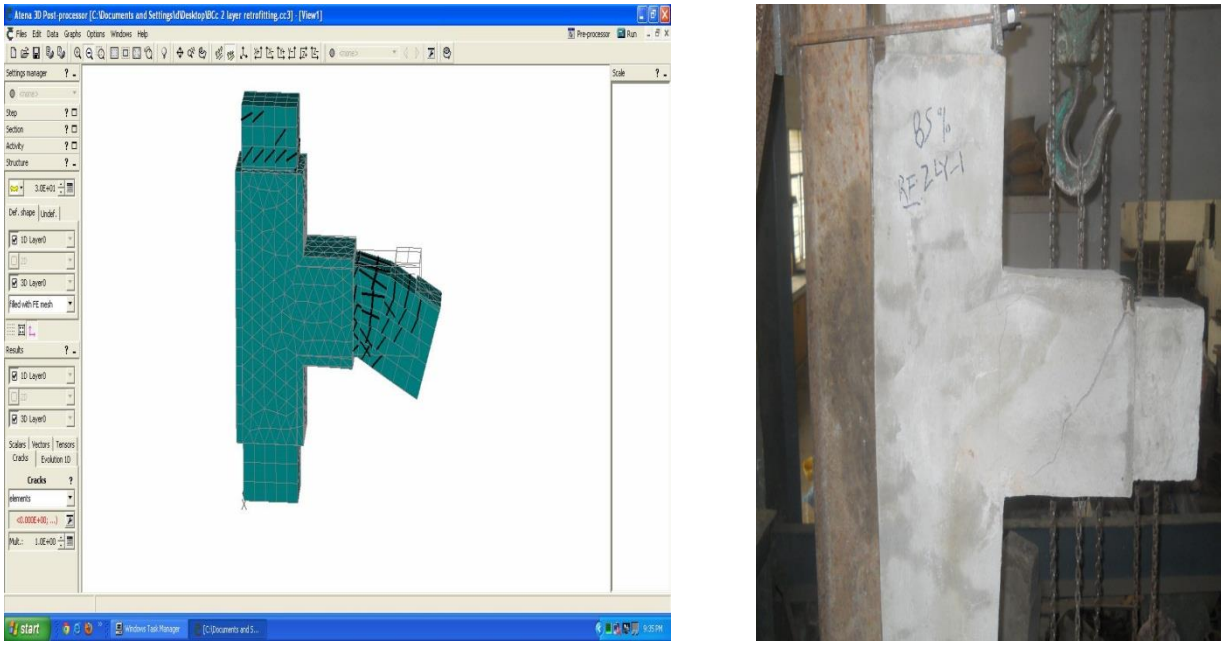

Figure 6.23: Deflected Shape and Cracks of Ferrocement Retrofitted Beam-column Joint at Ultimate Load (FE Model vs Experimental)

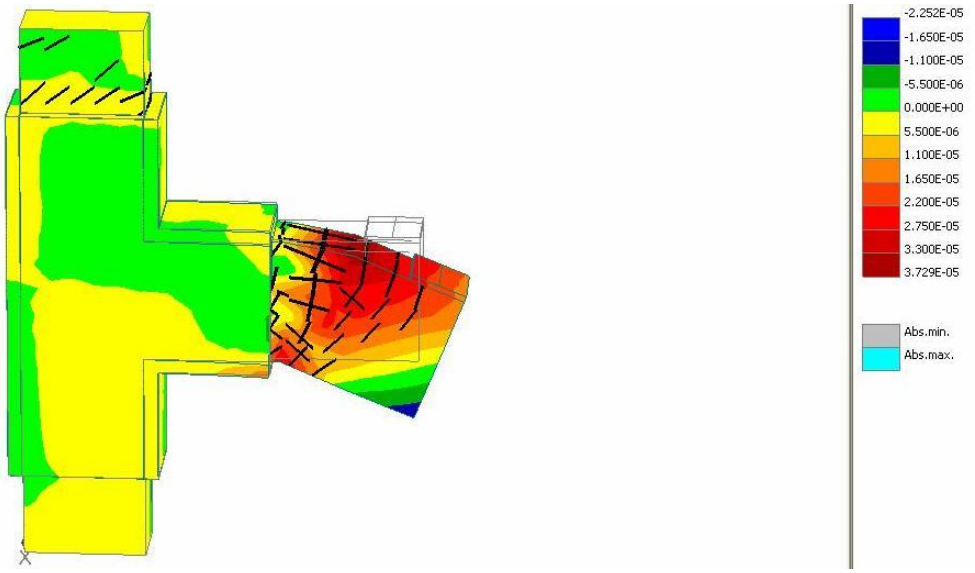

Figure 6.24: Stress Values in Ferrocement Retrofitted Beam-Column Joint at Ultimate Load with Four Layers of Wire Mesh

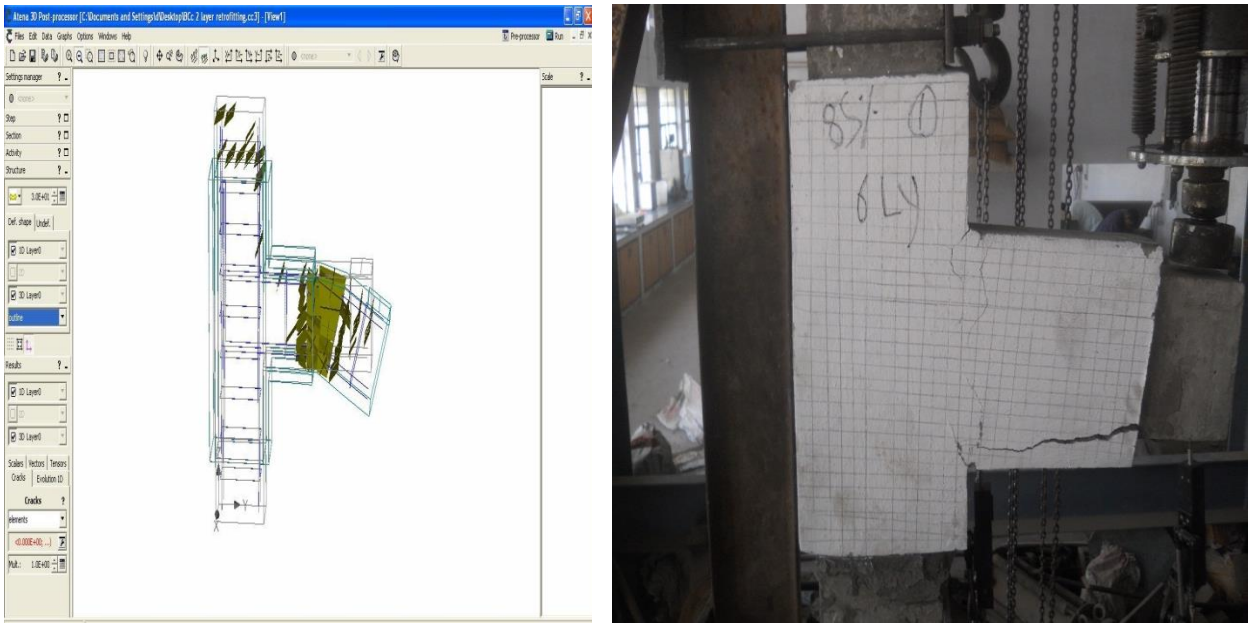

Figure 6.25: Stresses in Ferrocement Retrofitted Beam-Column Joint at Ultimate Load (FE Model vs Experimental)

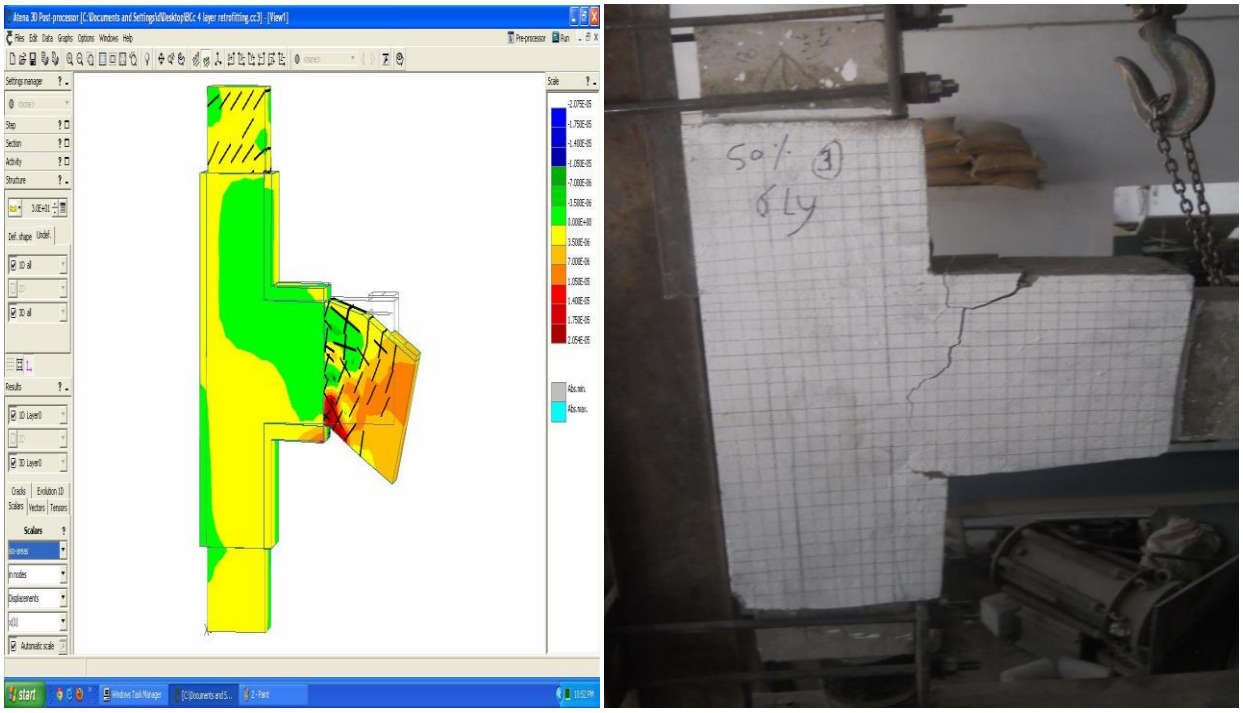

Figure 6.26: Stress Values inFerrocement Retrofitted Beam-Column Joint at Ultimate Load with Six Layers of Wire Mesh

It is observed from the figures 6.19- 6.22, there is a difference in the experimental and FE graphs both for the control and retrofitted specimens. As the FE model graphs showed less deflection and higher loads as compared to experimental tested specimens. This may be due to that in FE models the concrete input ideal material values, while in the real specimens the curing/ compaction/ temperature history may not been perfect and thus the in-situ strengths are actually lower.

6.4.3 Results and Discussion

FE analysis of RC beam-column joints was carried out in two phases. In the first phase, FE analysis of the beam-column joints was performed to obtain the ultimate load, crack pattern, deflected shape, and the load vs deflection curve for the control joints (without retrofit) using software ATENA 3D. In the second phase, FE analysis of the retrofitted beam-column joint was performed to obtain the ultimate load, crack pattern, deflected shape, load vs deflection curves for ferrocement jacketed specimens with two, four and six layers of wire mesh at stress level-1

(100%). The results are presented with the experimental results as already explained in Chapter 5.

The non linear FE analysis of RC beam-column joints under static incremental loads was performed using software ATENA 3D. The load on the beam-column joint was increased step by step till collapse of the beam-column joint. After the completion of the nonlinear analysis, the results were recorded in the third part of the analysis in ATENA 3D i.e. post processing. The load-deflection data at every step was recorded and crack propagation and crack pattern at every step has been studied. Figures 6.16 –6.18 show the crack pattern, stresses and deflected shape of the control joints. Subsequently, these results were compared with the experimental results followed by the load-deflection curves and crack patterns obtained from the analysis. The control beam-column joint specimen models were analyzed up to the ultimate load.

The ultimate load of the finite element control model was observed to be 24.8kN i.e. 9.5% higher then the experimental result. The deflection at ultimate load was18.9mm i.e.18.6% lower the experimental result at the free end of the cantilever beam as the deflection was 23.3mm at the experimentally observed load of 22.7kN. The yield load obtained at the 17^{th} step of FE analysis was22.7kN whereas it was 20kN in the experimental case. The crack pattern was also recorded from the post processor of ATENA 3D. The un-deformed and deformed shape with cracks of FE model beam-column joints are shown in Figure 6.10 and Figures 6.16 –6.18. The shear cracks on the beam surface near the joint occurred first at the 4^{th} step at the load of 8.4kN, which widened significantly during FE analysis. The various cracks at 40^{th} step are shown in Figure 6.16 at ultimate load of 24.8kN. It was observed from the finite element analysis data and corresponding graphs that ferrocement jacketed FE model beam-column joint, leads to a significant increase in the ultimate load carrying capacity. The observed increase in load carrying capacity may be due to the extra steel in different layers provided in the joint region so the beam got stiffer then control FE model joint. The ferrocement jacketed FE beam-column joint models showed 29.2kN ultimate load value (9.4% higher than the experimental value) with the deflection at ultimate load of 11mm (28.4% less then the experimental result) for two layers of wire-mesh reinforcement, 32.5kN ultimate load (7.6% higher than the experimental value) with the deflection at ultimate load of 9.9mm (30.4% less from experimental value) for four layers of wire mesh reinforcement and 34.8kN ultimate load (8.9% higher than the experimental value) with the deflection at ultimate load of 12.6mm (34.3% lower deflection from the experimental

value) for six layers of wire mesh reinforcement for stress level-1. Experimentally these values were observed to be 26.7kN at a deflection of 15.3mm, 30.2kN at a deflection of 14.3mm, and 32kN at a deflection of 19.2mm, for two, four and six layers of wire mesh reinforcement for ferrocement jacketed beam-column joints. The yield loads were observed to be 26.9kN, 29.4kN; 31.2kN for two, four and six layers wire mesh ferrocement jacketed FE models of beam-column joints nearly at 22 to 25 step of FE analysis, whereas it was 26kN, 28kN and 28kN in the experimental results. In case of ferrocement jacketed FE models of beam-column joint specimens with different layers the formation of cracks could not be observed, also they showed lower deflection at higher loads. Therefore, the FE model analysis, showed that the retrofitting of beam-column joints, the failure shifted from the joint region in control FE model to the beam end side of the retrofitted model, as is observed from the cracking pattern of the FE models, similar to the pattern observed in the experimental results. From the figures 6.16-6.26 and from the Table- 6.10 it can be seen that the trends of the crack patterns and load vs deflection curves for the control as well as retrofitted, experimental and FE model joints were same because all the properties of concrete and steel of experimental and FE model were same with same dimensions of the model. But, FE model graphs showed higher loads with less deflection as compared to experimental tested specimens. This may be due to that the input values in the FE models were ideal material values, while in the real specimens there were not the ideal conditions for curing/ compaction/ temperature and thus the in-situ strengths are actually lower.

The comparative results are shown in Figures 6.20- 6.22 and tabulated in Table-6.10.The un-deformed and deformed shapes with cracks and stresses of FE retrofitted beam-column joint models are shown in Figure 6.15 and Figures 6.23-6.26 respectively.

In the case of CFRP retrofitted FE model of beam-column joint, it was observed that it CFRP jacketing leads to a significant increase in the ultimate load carrying capacity. The two layers CFRP jacketed beam-column joint showed an ultimate load of 26.9kN (8.5% higher than the experimental value) with an ultimate deflection of 19.2mm (14.2% less then experimental result).The yield load at the 23^{th} step of FE analysis observed was 22.9kN whereas it was 23kN in the experimental investigation. The formation of cracks could not be observed, also they showed less deflection at higher loads. Therefore, in the FE model analysis, due to retrofitting of beam-column joints, the failure shifted from the joint region, in the control beam-column joint FE model, to the beam ends side in the retrofitted model. The cracking pattern of the FE models

was similar to the experimental results. A comparison of the results is shown in Figure-6.27 and Table-6.10.The cracks, stresses and deflected profile of the FE CFRP retrofitted model beam-column joints are shown in Figures 6.28- 6.30. The variation of experimental and FEM (ATENA 3D) load results for the control as well as retrofitted specimens was within ± 10%. The element modelling (ferrocement and CFRP) showed higher values as compared to the experimentally obtained values.

Table 6.9

Load-Deflection Results from ATENA 3D at Beam Free End for Two Layers CFRP Retrofitted Specimen

Load (kN)	Deflection(mm)	Load (kN)	Deflection(mm)
4.0	0.10	20.1	7.1
6.0	1.1	22.9	8.1
8.8	2.3	25.7	14.5
10.5	3.5	26.9	19.2
12.2	4.2		
14.0	5.3		
16.0	5.8		
19.0	6.3		

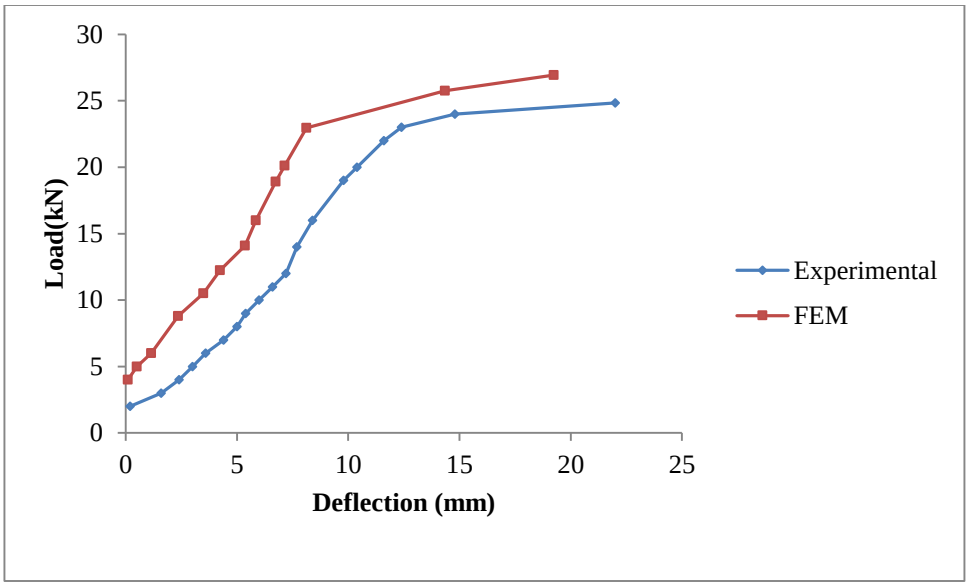

Figure 6.27: Comparison of Experimental and ATENA 3D Loadvs Deflection Curves at the Free End of Beam for Two Layer CFRP Retrofitted Specimen

The comparison between the load-deflection results obtained from FE and the experimental study shows that the FE results agree reasonably with the experimental results. The first crack load, yield load and ultimate load obtained in FE are higher than the values obtained from the experimental study.

Table 6.10

Comparison of Experimental vs ATENA Results

Loads, Deflections, Ductility Ratio, Stiffness and Energy Absorption of Control and Ferrocement/ CFRP Jacketed Beam- Column Joint Specimens

Experimental vs ATENA	Beam-Column Type	P_{CR} (kN)	P_Y (kN)	P_U (kN)	Percentage Variation Experimental vs ATENA (%)			ΔCR (mm)	ΔY (mm)	ΔU (mm)	Stiffness P_u / Δ_U kN/mm	Ductility ratio (ΔU/ ΔY)	Energy Absorption (kN.mm)
					P_{CR}	P_Y	P_U						
Experimental ***(Control / Ferrocement Retrofitted)***	CEJ	6.8	20	22.7	-	-	-	1.5	8.7	23.3	0.9	2.6	412.7
	TLEJ	9.3	26	26.7	-	-	-	3.2	8.9	15.3	1.7	1.7	255.2
	FLEJ	9.5	28	30.2	-	-	-	2.5	8.5	14.3	2.1	1.6	293.1
	SLEJ	9.7	28	32.0	-	-	-	2.6	9.8	19.2	1.6	1.9	408.4
ATENA ***(Control / Ferrocement Retrofitted)***	CFEM	8.4	22.7	24.8	23.5	13.8	9.5	0.3	6.0	18.9	1.3	3.1	375.6
	TLFEM	10.8	26.9	29.2	16.1	3.6	9.4	3.1	5.1	11.0	2.6	2.1	228.6
	FLFEM	11.0	29.4	32.5	15.3	5.0	7.6	3.1	5.8	9.9	3.2	1.6	211.3
	SLFEM	11.2	31.2	34.0	15.1	11.6	6.4	3.1	5.4	12.6	2.6	2.3	322.6
Experimental ***(CFRP Retrofitted)***	TLCFRP	8.9	23.0	24.8	-	-	-	5.3	12.4	22.0	1.7	1.1	371.4
ATENA ***(CFRP Retrofitted)***	TLCFFEM	9.3	22.9	26.9	4.1	- 0.2	8.4	2.8	8.1	19.2	2.3	1.3	370.8

TLEJ- two layer retrofitted experimental beam-column joint, FLEJ-four layer experimental beam-column joint ,SLEJ- six layer experimental beam-column joint, CFEM- control finite element model beam-column joint, TLFEM- two layer finite element model beam-column joint, FLFEM- four layer finite element model beam-column joint, SLFEM-six layer finite element model beam-column joint, P_{CR} – first crack load, P_Y – yield load, P_U – ultimate load; ΔCR – deflection at first crack, ΔY – deflection at yield point, ΔU – deflection at ultimate load. TLCFRP- *two layers CFRP retrofitted experimental beam-column joint,* TLCFFEM- *two layer CFRP finite element model beam-column joint..*

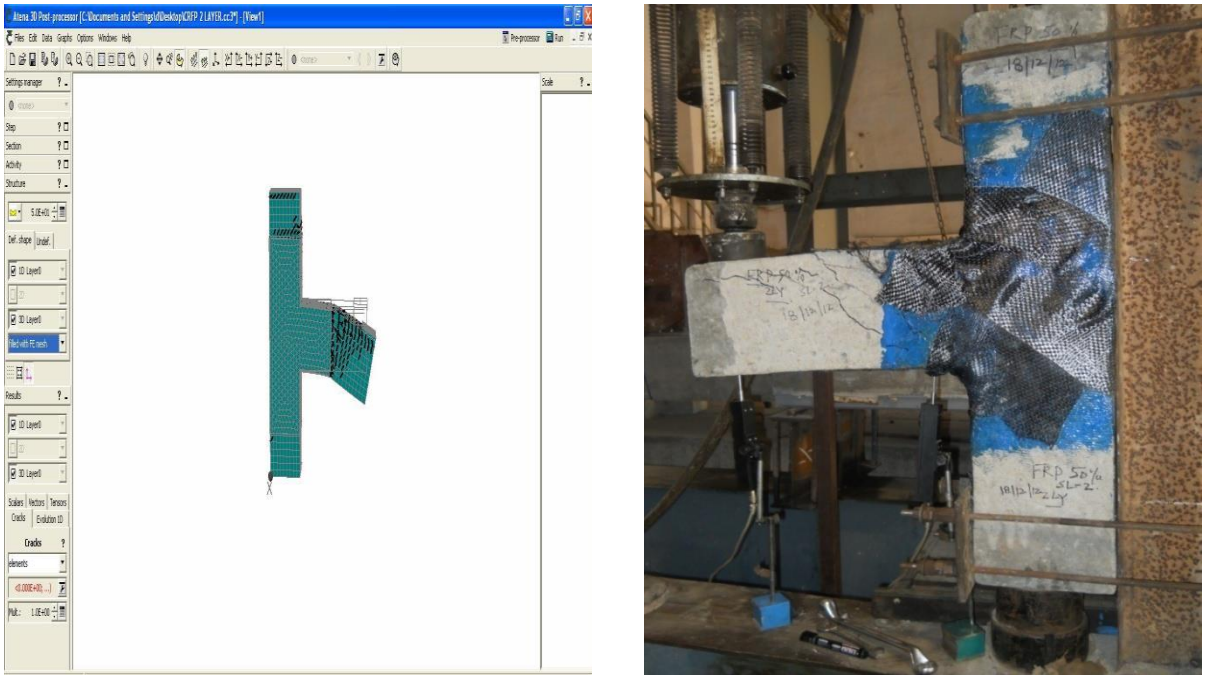

Figure 6.28: Deflected Shape and Cracks of CFRP Retrofitted Beam-Column Joint at Ultimate Load (FEM vs Experimental)

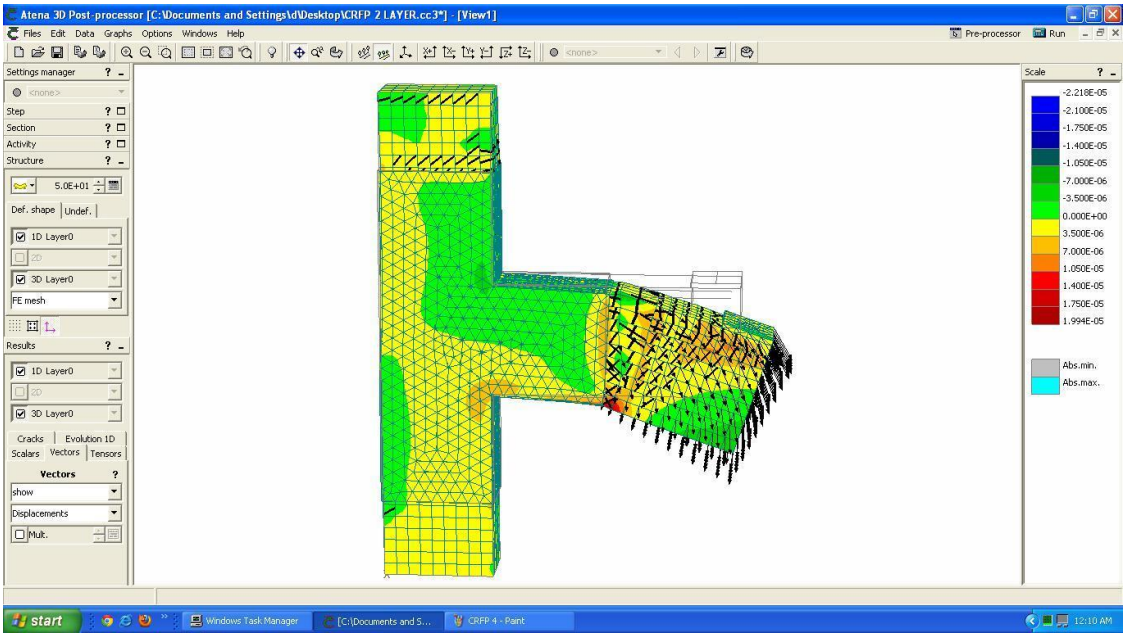

Figure 6.29: Different Stress Values in CFRP Retrofitted Beam-Column Joint at Ultimate Load

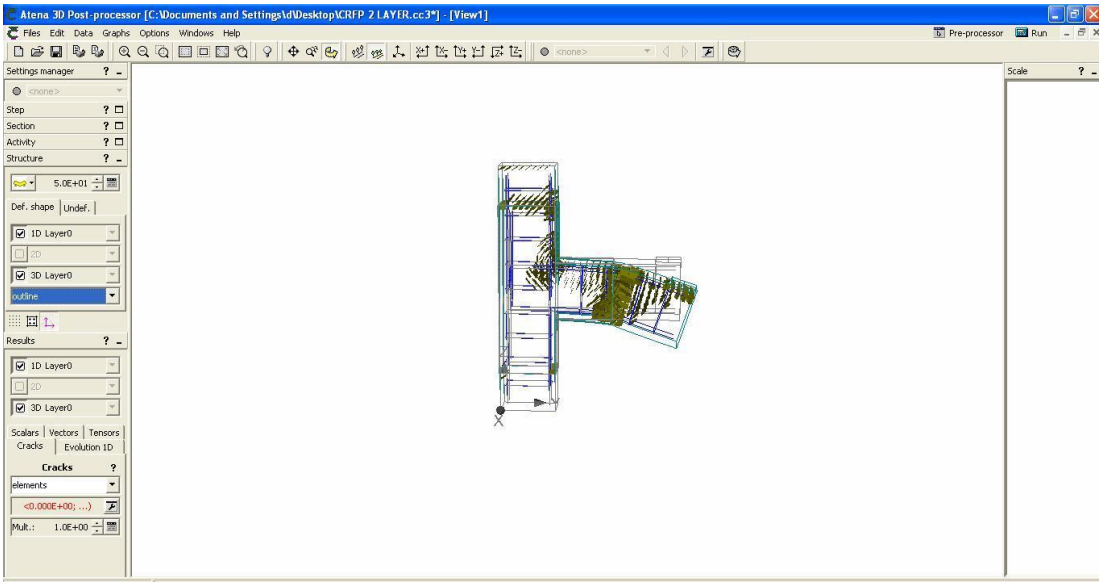

Figure 6.30: Stresses in CFRP Retrofitted Beam-Column Joint at Ultimate Load

6.5 SUMMARY

The finite element modelling using software ATENA 3D, of RC beam-column joints (Control and retrofitted), using ferrocement with different layers of wire mesh and CFRP with two layers of fiber are discussed in this chapter. The necessary steps to create FE models are explained in detail and the steps taken to generate the analytical load-deformation response of the model are presented in detail. The FE results obtained are compared with the experimental results presented in Chapter 5. The ultimate load carrying capacity, yield load, first crack load, and deflection at ultimate load of experimental and FEM (ATENA 3D) for the control as well as retrofitted (Ferrocement and CFRP) were compared. The variation of experimental and FEM (ATENA 3D) load results for the control as well as retrofitted specimens was within ± 10%. The finite element model results showed slightly higher values compared to the experimental values. It may well be that in the FE model the concrete results were input as materials values while in the real specimens the curing/ compaction/temperature history may not have been perfect and thus the insitu strengths are probably actually lower, thus explaining the consistently higher FE results. However, the theoretical behavior observed was the same as that seen in the experimental results.

CHAPTER - 7

CONCLUSIONS

7.1 GENERAL

Beam-column joints retrofitted with ferrocement, using different layers of wire mesh, and carbon fiber reinforced polymer using two layers of fiber, have been studied in the present work. The effect on various parameters like ultimate load carrying capacity, ductility ratio, stiffness, energy absorption of joints stressed at three different levels were obtained. A finite element model has been developed using software ATENA 3D, for the control, ferrocement jacketed and CFRP jacketed beam-column joints and validated with experimental results. On the basis of the present study, the following conclusions may be drawn.

7.2 BEAM-COLUMN JOINTS RETROFITTED USING FERROCEMENT JACKETS

1. Retrofitting of beam-column joints with ferrocement significantly increases the ultimate as well as the yield load carrying capacity for all joints stressed to 50-100% of stress level of control specimens establishing the efficacy of using the material for retrofitting. The ferrocement jacketed exterior beam-column joints with two, four and six layers, showed an increase in ultimate load carrying capacity of 17.7 %, 33.1%, 41.1 % for stress level-1(100% of ultimate load), 21.7 %, 29.6 %, 36.7 % for stress level-2 (85% of ultimate load) and 18.1 %, 25.2%, and 33.1% for stress level-3 (50% of ultimate load), as compared to the control joint specimens.
2. Likewise, the ferrocement jacketed exterior beam-column joints showed an increase in the yield load of 30 % , 40 %, 45 % for stress level-1; 30 %, 40 %, 50 % , for stress level-2 and 30 %, 35%, 40 % for stress level-3 with two, four and six layers respectively, as compared to the control joint specimens.

3. The ferrocement jacketed exterior beam-column joints showed that the stiffness of the retrofitted beam-column joint specimens with two, four and six layers of wire mesh was at least 120.6%, 188.6 %, 130.9% higher than that of the control joint specimens.
4. The ferrocement jacketing of initially stressed beam-column joints stressed to 85% of ultimate load regain full strength for two, four and six layers of wire mesh.
5. Due to the strengthening of beam-column joints, the failure of the retrofitted beam-column joint specimens shifted from the joint region in the control specimens to the beam ends region in retrofitted specimens, preventing progressive collapse of the structure. Retrofitting of the beam-column joints shifted the failure from the joint region to the beam side end to obtain a failure pattern of a weak- beam strong joint.
6. Retrofitted beam-column joint specimens with six layers of wire mesh, for all the three stress levels, showed the maximum improvement in their ultimate load.
7. The beam-column joint specimens retrofitted with four layers of wire mesh showed optimum results as compared to two and six layers of wire mesh retrofitted specimens, for all the three stress levels.
8. The maximum load carrying capacity of the retrofitted beam-column joints is independent of the thickness of the jackets, since the mortar cracks at an early stage.

7.3 BEAM-COLUMN JOINTS RETROFITTED USING CFRP JACKETS

1. Retrofitting of beam-column joints with CFRP significantly increases the ultimate as well as the yield load carrying capacity for all joints stressed to various levels establishing the efficacy of using the material for retrofitting.
2. Two layer CFRP jacketed beam-column joints show an increase in ultimate load carrying capacity of 9.5%, 12.0% and 7.7% for stress level-1, stress level-2 and stress level-3, respectively establishing the efficacy of using the material for retrofitting. This increase in load carrying capacity is less than the ferrocement jacketed beam-column joints because the area of fiber provided was less than the area of steel provided in ferrocement, hence fiber jacketed joints was less stiff then the ferrocement jacketed joints.

3. Two layer CFRP jacketed beam-column joints show an increase of nearly 15% in the yield load carrying capacity for all the initially stressed and retrofitted beams.
4. With the decrease in initial stress level from 100%, 85% and 50%, the stiffness of the two layer CFRP retrofitted beam-column joint at ultimate load increased by 22.2%, 22.2%, 33.3% for stress level-1, stress level-2 and stress level-3, respectively, as compared to the control specimens.
5. The use of CFRP jacketing for retrofitting of initially stressed beam-column joints helps regain full strength even if stressed up to 85% of ultimate load.
6. Due to the strengthening of beam-column joints, the failure of the retrofitted beam-column joint specimens shifted from joints (control specimens) to the beam ends (retrofitted specimens) which will prevent progressive collapse of the structure. Retrofitting of the beam-column joint may shift the failure from the joint to the beam end to obtain a failure pattern of weak beam strong joint.
7. The beam-column joints which were initially stressed up to stress level-2 (85% of ultimate load) showed the best results after two layer CFRP jacketing in comparison to stress level-1(ultimate load) and stress level-3 (50% of ultimate load) two layer CFRP jacketed beam-column joints.

7.4 FINITE ELEMENT MODELLING

1. In the finite element analysis, both ferrocement and CFRP jacketed finite element models of beam-column joints showed an increase in the ultimate as well as the yield load carrying capacity for stress level-1 (100%); this was seen in the experimental results also.
2. The FE models of ferrocement jacketed joints showed an increase of 17.5%, 30.7%, and 40.3%, in the ultimate load carrying capacity for two, four and six layers of wire mesh respectively, as compared to the control finite element model joint sample for stress level-1, whereas this increase was 17.7%, 33.1% and 41.0% in the experimental results.
3. The ferrocement jacketed joints showed an increase of 18.4%, 29.1% and 37.2% in the yield load carrying capacity for two, four and six layers, respectively, as compared to the control FE joint for stress level-1.

4. In the finite element analysis, FE model results of ferrocement jacketed joint show the maximum 115.8% higher stiffness for the four layer retrofitted FE model as compared to FE control model results, whereas this was 116.5% in the experimental results.
5. The CFRP retrofitted finite element (FE) model showed 8.4% higher load as compared to FE control model results, whereas it was 9.4% in the experimental observation.
6. In the both the experimental and FE analysis, retrofitting of the beam-column joint may shift the failure from the joint to the beam end to obtain a failure pattern of weak beam strong joint.

ATENA 3D is able to model the different components of a load-deflection curve i.e. the linear region, initial cracking, the non-linear region, the yielding of steel and failure. The comparison between the load-deflection results obtained from ATENA 3D and the experimental study shows that the ATENA 3D results agree reasonably with the experimental results. The first crack load, yield load and ultimate load obtained in ATENA 3D are higher than the values obtained from the experimental study. It may well be that in the FE model the concrete results were input as materials values while in the real specimens the curing / compaction / temperature history may not have been perfect and thus the in situ strengths are probably actually lower, thus explaining the consistently higher FE results. Comparison between the load-deflection results obtained from experiments and from ATENA 3D for control and retrofitted specimens shows that the yield load and ultimate load has significantly increased for the retrofitted specimen with the higher value of yield load and ultimate load for the retrofitted specimen associated with lower deflections as compared to the control specimen. The variation of experimental and FEM (ATENA 3D) load results for the control as well as retrofitted specimens was within ± 10%. The element modelling (ferrocement and CFRP) showed higher values as compared to the experimentally obtained values.

7.5 SUMMARY

This chapter deals with the conclusions based on the findings of strength properties of exterior beam-column joints retrofitted with ferrocement jacketing using different numbers of wire mesh layers and CFRP using two layers of fiber, at three different stress levels. Comparison between finite element and experimental results confirms excellent accuracy of the proposed FE model.

The variation of experimental and FEM (ATENA 3D) load results for the control as well as retrofitted specimens was ± 10%. The element modelling (ferrocement and CFRP) showed higher values as compared to the experimentally obtained values.

7.6 FUTURE SCOPE OF WORK

In the present study, the experimental studies on exterior beam-column joints using ferrocement jacketing with two layers, four layers and six layers and CFRP jacketing with two layers, at three different stress levels have been done and analytical model using ATENA-3D software have been developed to validate the experimental results. Further work can be directed towards same studies on the interior beam-column joints or with different materials like glass fiber reinforced polymer (GFRP) or by changing the number of layers and stress levels and comparative studies among different FEM software to know the preciseness and efficiency of each of them. Retrospective studies can be performed by collecting actual field data from sites where ferrocement/ CFRP/ GFRP retrofitting has been done.

LIST OF PUBLICATIONS FROM PRESENT WORK

1. **Varinder Singh***, PremPal Bansal, Maneek Kumar, S.K. Kaushik (2014) "Experimental studies on strength and ductility of CFRP jacketed reinforced concrete beam-column joints". ***Construction and Building Materials,*** 55, 194–201. **(Elsevier), Science Direct.** ***Impact Factor 2.265, ISSN: 0950-0618***

2. **Varinder Singh***, PremPal Bansal, Maneek Kumar, S.K. Kaushik (2014) **"**Finite Element Modeling of CFRP Retrofitted RC Beam-Column Joints". ***International Journal on Emerging Technologies 5(2): 31-39(2014) Scientific Journal Impact Factor 3.393, ISSN No. (Online): 2249-3255, ISSN No. (Print): 0975-8364***

3. **Varinder Singh***, PremPal Bansal, Maneek Kumar, S.K. Kaushik (2014) "Effect of Wire Mesh Orientation on Strength of Exterior RC Beam-Column Joints Retrofitted Using Ferrocement Jackets" ***International Journal on Emerging Technologies 5(1): 212-219(2014) Scientific Journal Impact Factor 3.393, ISSN No. (Online): 2249-3255, ISSN No. (Print): 0975-8364***

4. **Varinder Singh***, Prem Pal Bansal, Maneek Kumar (2015). "Experimental studies on strength and ductility of Ferrocement jacketed reinforced concrete beam-column joints". ***International Journal of Civil and Structural Engineering****, Vol.5, No.3, 199-205, ISSN 0976-439*

5. **Varinder Singh***,PremPal Bansal, Maneek Kumar, S.K. Kaushik (2014) "**Experimental and FEM analysis of Ferrocement Jacketed RC Beam-Column Joints Using Different Layers of Wire Mesh"** ***(communicated)***

REFERENCES

A Manual of Earthquake Resistant Non-Engineered Construction, Book Published by Indian Society of Earthquake Technology, University of Roorkee, 1981: 155-161.

Abdullah, Mansur MA. Effect of mesh orientation on tensile response of Ferrocement. Journal of Ferrocement 2001; 31(4): 289-297.

Abhijit M, Mangesh J. Frpc reinforced concrete beam-column joints under cyclic excitation. Journal of Composite Structures 2004; 70 (2): 185-99.

ACI 318-08, Building Code Requirements for Structural Concrete and Commentary.

ACI- 352. Recommendation for design of beam-column joints in monolithic reinforced concrete structures (1976) American Concrete institute, Detroit, Michigan.

AIJ. Design guidelines for earthquake resistance reinforced concrete buildings based on inelastic displacement concept. AIJ; 1999; 440.

Akguzel U, Pampanin S. Assessment and design procedure for the seismic retrofit of reinforced concrete beam-column joints using FRP composite materials. Journal of Composites for Construction 2012; ASCE, 16(1): 21-34.

Akguzel U, Pampanin S. Effect of axial load variation on the retrofit of exterior reinforced concrete beam-column joints. Proceedings of 2010 NZSEE Conference, Christchurch, NZ, Paper No. 42.

Akhtarruzzama AKM, Pama RP. Cracking behavior of Ferrocement in tension. Proceeding of the Third International Symposium on Ferrocement 1988; 1-11.

Alcocer S, Jirsa JO. Strengthening of reinforced concrete frame connection rehabilitation by jacketing. ACI Structure Journal 1993; 90(3):249-61.

Al-Farabi MS, Baluch MH, Al-Sulaimani GJ, Basunbul IA. Repair of damaged RC beams using externally bonded fiber glass plates. Fourth International Conference Structural Failure, Durability and Retrofitting Singapore 1993; 621-628.

Al-Kubaisy MA, Nedwell PJ. Behavior and strength of Ferrocement rectangular beams. Journal of Ferrocement 1999; 29(1): 1-15.

Al-Kubaisy MA. Location of the critical diagonal crack in Ferrocement beams. Journal of Ferrocement 1998; 28(2): 135-146.

Al-Noury SI, Huq S. Ferrocement in axial tension. Journal of Ferrocement 1988; 18(2): 111-137.

Al-Rifaie WN, Trikha DN. Effect of arrangement and orientation of hexagonal mesh on the behavior of two- way Ferrocement slabs. Journal of Ferrocement 1990; 20(3): 219-230.

Alsayed SH, Al-Salloum YA, Almusallam TH, Siddiqui NA. Seismic response of FRP-upgraded exterior RC beam-column joints. Journal of Composites for Construction 2010; ASCE, 14(2): 195-208.

Al-Sulalmani, Basunbul IA. Behavior of Ferrocement material under direct shear. Journal of Ferrocement 1991; 21(2): 109-117. American Concrete Institute SP172-36 ,1997; 669-681.

American Concrete Institute. State- of -the -art report on Ferrocement. Report No. ACI 549, 88R, 1988; Detroit: 24.

American Concrete Institute. Guide for the design, construction, and repair of Ferrocement. Report No. ACI 549.1-88R, 1988; Detroit: 27.

Andrews G, Sharma AK. Repaired reinforced concrete beams. ACI, Concrete International, Detriot 1998; 47-50.

Antonopoulos CP, Triantafillou TC. Analysis of FRP - strengthened RC beam-column joints. Journal of Composites for Construction 2002; ASCE, 6(1): 41-51.

Antonopoulos CP, Triantafillou TC. Experimental investigation of FRP strengthened RC beam-column joints. Journal of Composites for Construction 2003; ASCE, 7(1): 39-49.

Anwar AW. Ferrocement for low-cost housing in Pakistan. Journal of Ferrocement1993; 23(2): 117-123.

Asha P, Sundarajan R. Strength and ductility of exterior beam- column joints with welded wire mesh. Journal of ICI 2006; 80 (2): 29-36.

Balagurusamy, Perumalsamy N, Naaman AE, Shah Surinder P. Analysis and behavior of Ferrocement in flexure. ASCE (Structural Division) 1997; 103(10): 1937-1951.

Bansal PP, Kumar M, Kaushik SK. Effect of initial stress levels on strength parameters of reinforced concrete beams retrofitted using Ferrocement jackets. Journal of Testing and Evaluation 2011; ASTM, 39(5): Paper ID: JTE102891.

Bansal PP, Kumar M, Kaushik SK. Effect of wire mesh orientation on strength of beams retrofitted using Ferrocement jackets. International Journal of Engineering 2008; 2(1): 8-19.

Bansal PP, Kumar M, Kaushik SK. Experimental study on retrofitting of stressed RC beams using GFRP jackets. Journal of Reinforced Plastics and Composites 2010; 29(2):190-200.

Barbato M. Efficient finite element modeling of reinforced concrete beams retrofitted with fiber reinforced polymers**.** Journal of Composite Structures 2009; 87: 167-176.

Basu PC. Seismic upgradation of buildings an overview. The Indian Concrete Journal 2002; The Associated Cements Companies Ltd. 461-475.

Basunbul IA, Husain M, Sharif AM. Al-Sulaimani GJ, Baluch MH. Repair of shear cracked r/c beams with bonded external steel plates1993; Fourth International Conference on Structural, Failure, Durability and Retro-fitting, Singapore 629-634.

Bhargava P, Bhowmick, R, Sharma U, and Kaushik SK, Three dimensional finite element analysis of confined high strength concrete columns. ACI SP on "Confined Concrete American Concrete Institute, Michigan, SP-238, 2006, pp. 480.

Bonacci JF, Maalej M. Behavioral trends of RC beams strengthened with externally bonded FRP. Journal of Composites for Construction 2001; 5(2): 102-103.

Bousselham A. State of research on seismic retrofit of RC beam-column joints with externally bonded FRP. Journal of Composites for Construction 2010; ASCE, 14(1): 49-61.

Buckhouse ER. External flexural reinforcement of existing reinforced concrete beams using bolted steel channels, Master's Thesis1997; Marquette University, Milwaukee, Wisconsin.

Buyukozturk Oral, Hearing Brain. Failure behavior of precraked concrete beams retrofitted with FRP. Journal of Composites for Construction 1998; 2(3): 138-144.

Camata G, Spacone E, Zarnic R. Experimental and non linear finite element studies of RC beams strengthened with FRP plates. Journal of Composite Part B 2007; 38: 277-288.

Cao Z, Li A, Wang YY, Zhang W, Yao Q. Experimental study on RC space beam-column joints strengthened with high strength steel wire mesh and polymer mortar. Journal of Southeast University 2007; 37(2): 235-39.

Cervenka Vladimir, Jendele Libor and Cervenka Jan, ATENA 3D theory manual, part 1.

Clarke RP, Sharma AK. The experimental behaviour of Ferrocement flat plate under biaxial flexure. Journal of Ferrocement1991; 21(2): 127-136.

Colotti Vincenzo, Spadea Giuseppe. Shear strength of rc beams strengthened with bonded steel and FRP plates. Journal of Structural Engineering 2001; 127(4): 367-373.

D'Ayala D, Penford A, Valentini S. Use of FRP fabric for strengthening of reinforced concrete beam-column joints. In: 10thInt conference on structural faults and repair. London: July 2003.

Desayi Prakash, Nandakumar N, A El-kholy Said. Shear stress of Ferrocement trough section elements. Journal of Ferrocement 1994; 24(4): 323-342.

Desia R. Field shake test programme at latur, western India. News letter, Earthquake Hazard Centre, New Zealand 1999, 3(2), 4-5.

Dowrick DJ. Earthquake risk reduction 2003; John Wiley & Sons Ltd., England.

El-Amoury T, GhobarahA. Seismic rehabilitation of beam-column joint using GFRP sheets. Engineering Structures 2002: The Journal of Earthquake, Wind and Ocean Engineering, 24(11):1397-1407.

Engindeniz M, Kahn LF, Zureick AH. Repair and strengthening of reinforced concrete beam-column joints: State of the Art. ACI Structural Journal 2005; 102(2): 187-197.

Fahmy, Ezzat H, Shaheen, Yoursy BI, Korany Yasse S. Use of Ferrocement laminates for reaping reinforced concrete slabs. Journal of Ferrocement 1997; 27(3): 219-232.

Fahmy, Ezzat H, Shaheen, Youysry BI, Korany Yasser S. Repairing reinforced concrete beams by Ferrocement. Journal of Ferrocement 1997;27(1): 19-32.

Fanning P. Nonlinear models of reinforced and post-tensioned concrete beams. Electronic Journal of Structural Engineering 2001; 2: 111-119.

Ferreira AJM. On the shear deformation theories for the analysis of concrete shells reinforced with external composite laminates. Strength Materials 2003; 35(2):128-35.

Paul BK, Pamma RP. Ferrocement, International Ferrocement information centre (IFIC), Bangkok, Thailand ; 1978

Ganga Rao, Hota VS, Vijay PV. Bending behavior of concrete beams wrapped with carbon fabric. Journal of Structural Engineering 1998; 124(1): 3-10.

Gergely I, Pantelides CP, Reaveley LD. Shear strengthening of bridge joints with carbon fiber composites. In: Proceedings of sixth US national conference on earthquake engineering, EERI Seattle, WA; 1998.

Gergely J, Pantelides CP, Reaveley LD. Shear Strengthening of RC T Joints using CFRP Composites. Journal of Composites for Construction 2000; ASCE, 4(2): 56-64.

Ghobarah A, Aziz TS, Biddah A. Rehabilitation reinforced concrete frame connections using corrugated steel jacketing. ACI Structures Journal 1997; 4(3):293-94.

Ghobarah A, EI-Amoury T. Seismic rehabilitation of deficient exterior concrete frame joints. ASCE 2005; 9(5):408-16.

Ghobarah A, Said A. Seismic rehabilitation of beam-column joints using FRP laminates. Journal of Earthquake Engineering 2001; 5(1): 113-129.

Ghobarah, A, Said A. Shear Strengthening of Beam-Column Joints. Engineering Structures 2002; The Journal of Earthquake, Wind and Ocean Engineering, 24(7): 881-888.

Haach VG, El Debs, AL,HdC, El Debs, MK. Evaluation of the influence of the column axial load on the behavior of monotonically loaded RC Exterior beam–column joints through numerical simulations. Engineering Structures 2008; 30: 965-975.

Hadi MNS. Retrofitting of shear failed reinforced concrete beams. Elsevier Composite Structures 2003; 62: 1-6.

Hakuto S, Park R, Tanaka H. Seismic load tests on interior and exterior beam-column joints with substandard reinforcing details. ACI Structural Journal 2000; 97(1):11-25.

Hegger J, Sherif A, Roeser W. Nonlinear finite element analysis of reinforced concrete beam-column connections. ACI Structure Journal 2004; 101(5): 604-614.

Hua PL, Shi SF. An experimental study on flexural behavior of reinforced concrete beams strengthened with high-performance Ferrocement. Advance Materials Research 2011; 163–67: 3772–76.

Hussin MW. Deflection and cracking of performance of fibrous Ferrocement thin sheets. Journal of Ferrocement 1992; 21(11): 31-41.

Ibrahim AM, and Mahmood MS. Finite element modeling of reinforced concrete beams strengthened with FRP laminates**.** Europe Journal *Scientific* Research 2009; 30 (4): 526-541.

IS 13920-1993. Indian standard code of practice ductile detailing of reinforced concrete structures subjected to seismic forces. Bureau of Indian Standards, New Delhi, 2002. Edition 1.2 (2002-03).

IS: 10262-2009. Recommended guidelines for concrete mix design. Bureau of Indian Standards, New Delhi.

IS: 13935-1993. Repair and seismic strengthening of buildings-guidelines. Bureau of Indian Standards, New Delhi.

IS: 1489 (Part 1)-1991, Portland-Pozzolana Cement specification Part 1, Fly Ash Based, Bureau of Indian Standards, New Delhi.

IS: 1786-1985. Specification for high strength deformed steel bars and wires for concrete reinforcement. Bureau of Indian Standards, New Delhi.

IS: 383-1970. Specification for coarse and fine aggregates from natural sources for concrete. Bureau of Indian Standards, New Delhi.

IS: 456-2000. Indian standard plain and reinforced concrete code of practice. Bureau of Indian Standards, New Delhi.

Johnston Colin D, Mattar Samir G. Ferrocement behavior in tension and compression. Journal of Structural Division1976; 102(ST5): 875-889.

Johnston Colin D, Mowat Dallas N. Ferrocement material behavior in flexure. Journal of Structural Division.1974; 100 (ST10): 2053-2069.

Kabir A, Ali S. Strengthening of damaged reinforced concrete beams with Ferrocement deep beams with Ferrocement overlays. International Seminar on Civil Engineering in the Twenty first Century, Roorkee1996; 1667-1677.

Kachlakev D, McCurry DD. Behavior of full-scale reinforced concrete beams retrofitted for shear and flexural with FRP laminates. Composites 2000; 31: 445-52.

Kachlakev M, Miller T, Solomon PE, Yim PE, Chansawat, Potisuk KT. Finite element modeling of reinforced concrete structures strengthened with FRP laminate**s.** Final Report ; 2001: OREGON Department of transportation.

Kamasewara Rao, CB, Kamasundara Rao A. Stress strain relation for Ferrocement in tension Journal of Ferrocement1994; 24(4): 309-321.

Karasudhi P, Mathew AG, Nimityongskul P. Fatigue of Ferrocement in flexure. Journal of Ferrocement1977;7, (2): 80-95.

Karayannis CG, Sirkelis GM. Strengthening and rehabilitation of RC beam-column joints using carbon FRP jacketing and epoxy resin injection. Earthquake Engineering and Structure Dynamics 2008; 37:769-90.

Karunasena W, Hardeo P, Bosnich G. Rehabilitation of concrete beams by externally bonding fiber composite reinforcement. In composite systems: macrocomposites, microcomposites, nanocomposites. In: Proceedings of the ACUN-4, international composites conference, 4th, Sydney, Australia: July 21-25 2002. P.222-26.

Kaushik SK, Dubey AK. Performance evaluation of RC Ferrocement composite beams. Proceedings of Fifth International Symposium1994;, UMIST:240-256.

Kaushik SK, Gupta VK, Anuj, Singh KK. Behavior and performance of composite Ferrocement brick slabs. Journal of Ferrocement1991; 21(3): 215-222.

Kaushik SK, Gupta VK, Rahman MK. Efficiency of mesh overlaps of Ferrocement elements. Journal of Ferrocement1987;17(4): 329-336.

Kaushik SK, Gupta VK, Singh KT. Behavior of composite slabs with lost formwork. Journal of Ferrocement 1991;21(3): 203-213.

Kaushik SK, Prakash A, Singh K K. Inelastic buckling of Ferrocement encased columns. Ferrocement: Proceedings of Fifth International Symposium1994, UMIST: 327-341.

Khalifa A, Nanni A. Rehabilitation of rectangular simply supported RC beams with shear deficiencies using CFRP composites. Construction & Building Materials 2002; 1:97-106.

Khalifa A, Tumialan G, Nanni A, Belarbi A. Shear strengthening of continuous RC beams using externally bonded CFRP sheets. ACI. In; Proceedings of the 4th international symposium on FRP for reinforcement of concrete struct, Baltimore, MD; Nov 1999.p.995-1008.

Khalifa Ahmed, Nanni Antonio. Improving shear capacity of existing RC T-section beams using cfrp composites. Cement and Concrete Composites 2000;22(2): 165-174.

Kumari B, Kwatra N. Finite element modeling of a multi-storeyed retrofitted reinforced concrete frame. IOSR Journal of Mechanical and Civil Engineering (IOSR-JMCE) 2013; 8(3): 8-22.

Lee WT, Chiou YJ, Shih MH. Reinforced concrete beam–column joint strengthened with carbon fiber reinforced polymer. Composite Structures 2010; 92: 48-60.

Li B, Chua HYG. Seismic performance of strengthened reinforced concrete beam-column joints using FRP composites. Journal of Structural Engineering2009; ASCE, 135(10): 1177-1190.

Li B, Lam Eddie SS. Strengthening of reinforced concrete beam-column joints using Ferrocement. Concrete Solutions 2012; 93:717-26.

Li J, Samali B, Ye L. Behaviour of concrete beam-column connections reinforced with hybrid frp sheet. Composite Structures 2002; 57 (1-4): 357-65.

Lim CTE, Paramasivam P. Ong KCG. Pushout shear strength of Ferrocement concrete interface. Journal of Ferrocement 2001; 31(4): 299-310.

Liu C. Seismic Behaviour of beam-column joint subassemblages reinforced with Steel fibers, Master's Thesis 2006: University of Canterbury, Christchurch, New Zealand.

Lorenzis DL, Nanni A. Bond between near surface mounted fiber reinforced polymer rods and concrete in structural strengthening. ACI Structural Journal, ACI, 2002; (2):123-132.

Ludovico DM, Manfredi G, Mola E, Negro P, Prota A. Seismic behavior of a full-scale RC structure retrofitted using GFRP laminates. Journal of Composites for Construction 2008; ASCE, 134(5): 810-821.

Mahini SS, Ronagh HR. A new method for improving ductility in existing RC ordinary moment resisting frames using FRPS. Asian Journal of Civil Engineering (Building and Housing); 8(6): 581-595.

Mahini SS, Isfahani AD, Ronagh,HR. Numerical modelling of cfrp retrofitted rc exterior beam column joints under cyclic loads. Fourth International Conference on FRP Composites in Civil Engineering 2008; Zurich, Switzerland.

Mahini SS, Ronagh, HR. Strength and ductility of frp web-bonded rc beams for the assessment of retrofitted beam–column joints. Composite Structures 2010; 92:1325-1332.

Mansur MA, Abdullah. Constitutive law of Ferrocement under biaxial tension compression. Journal of Ferrocement1998; 28(1): 1-25.

Mansur MA, Ong KCG. Shear strength of Ferrocement beams. ACI Structural Journal, 1987; 10-17.

Mansur MA, Ong KCG. Shear strength of Ferrocement I- beams. ACI Structural Journal1991; 458-464.

Mansur MA, Paramasivam P. Cracking behavior and ultimate strength of Ferrocement in flexure. Journal of Ferrocement1986; 16(4): 405-415.

Mansur MA, Tan KL, Naaman AE, Paramasivam P. Design charts for Ferrocement structural section in flexure. Journal of Ferrocement 2000; 30(4): 345-362.

Mansur MA, Tan KL, Naaman AE. Strength of bolted moment connections in Ferrocement construction. Cement Concrete Composite 2010; 32 (7): 532-43.

Martinola G, Meda A, Plizzari GA, Rinaldi Z. Strengthening and repair of RC beams with fiber reinforced concrete. Cement Concrete Composite 2010; 32(9): 731-39.

Mattone R. Ferrocement in low-cost housing: an application proposal (use of Ferrocement in rural housing projects) Journal of Ferrocement1992; 22(2): 181-187.

Mays GC, Barnes RA. Ferrocement permanent formwork as protection to reinforced concrete. Journal of Ferrocement 1995; 25(4): 331-345.

Mostofinejad D and Talaeitaba SB. Finite element modeling of RC connections strengthened with FRP laminates. Iranian Journal Science Tech Transaction B, Engineering 2006; 30 : 21-30.

Mourad SM, Shannag MJ. Repair and strengthening of reinforced concrete square columns using Ferrocement jackets. Cement Concrete Composite 2012; 34 (2): 288-94.

Mukherjee A, Joshi M. FRPC reinforced concrete beam-column joints under cyclic excitation. Composite Structures 2005; 70(2): 185-199.

Murty CVR, Rai DC, Bajpai KK, Jain SK. Effectiveness of reinforcement details in exterior reinforced concrete beam-column joints for earthquake resistance. ACI Structural Journal 2003; 100(2): 149-156.

Naaman AE. Ferrocement and thin fiber reinforced cement composite: Looking Back, Looking Ahead. Journal of Ferrocement 2001 31(4): 267-280.

Nanni, Antonio. Flexural behavior and design of rc members using FRP reinforcement. Journal of Structural Engineering 1993119(11) 3444-3459.

Nassif Hani H, Najm Husam. Experimental and analytical investigation of Ferrocement-concrete composite. Cement and Concrete Composite 2004, 26: 787-796.

Nedwell PJ, Nakass AS. High performance Ferrocement using steel mesh and high strength mortar. Journal of Ferrocement 1999; 29(3): 189-195.

Neelmani. Ferrocement construction technology and its applications – A Review; 2013

Non-Engineered Construction in Earthquake Prone Areas and Earthquake Mitigation with Special Reference of Pakistan, Project Report, Department of Civil Engineering, NED University of Engineering and Technology, Karachi, Pakistan,1988: 103.

Ohama Y, Shirai A. Durability of polymer-Ferrocement. Journal of Ferrocement1992; 22(1): 27-34.

Ong KCG, Paramasivamm P, Lim CTE. Flexure strengthening of reinforced concrete beams using Ferrocement laminate. Journal of Ferrocement 1992; 22(4): 331-42.

Pampanin S, Magenes G, Carr A. Modelling of shear hinge mechanism in poorly detailed RC beam-column joints. Proceedings of the FIB 2003 Symposium2003; Athens,Greece.

Pantazopoulou S, Bonacci J. Consideration of questions about beam- column joints. ACI Structural Journal1992; 89(1):27-36.

Pantelides CP, Gergly J, Reaveley LD, Volnyy VA. Retrofit of RC bridge pier with CFRP advanced composites. Journal of Structure Engg. 1999; 125(10):1094-9.

Paramasivam P, Lim CTE, Ong KCG. Ferrocement laminates for strengthening RC T- beams. Cement Concrete Composite 1994; 16 (2): 143-152.

Paramasivam P, Lim CTE, Ong KCG. Strengthening of RC beams with Ferrocement laminate. Cement and Concrete Composite 1998; (20): 53-65.

Paulay T, Priestley MJN. Seismic design of reinforced concrete and masonry buildings. A Wiley Inter Science Publication1992; 744.

Prota A, Nanni A, Manfredi G, Cosenza E. Selective upgrade of under designed reinforced concrete beam-column joints using carbon fiber-reinforced polymers. ACI Structural Journal 2004; 101(5): 699-707.

Ravi SR, Arulraj GP. Finite element modeling on behavior of reinforced concrete beam column joints retrofitted with carbon fiber reinforced polymer sheets. International Journal of Civil and Structural Engineering 2010; 1(3): 576-582.

Ravinderarajah RS, Paramasivam P. Effect of arrangement of reinforcement on mechanical properties of Ferrocement. ACI Structural Journal 1988, 1988: 3-11.

Ravinderarajah RS, Paramasivam P. Influence of weathering on Ferrocement properties. Journal of Ferrocement 1986; 16(1): 1-11.

Robert Ravi S, Prince Arulraj G. Experimental investigation on influence of development length in retrofitting reinforced concrete beam-column joints. NBMCW 2009; 4: 148-158.

Saadatmanesh, Hamid, Ehsani, Mohammad R. RC beams strengthened with FRP plates I: experimental study. Journal of Structural Engineering 1991; 117(11): 3417-3433.

Sasmal S. Performance evaluation and strengthening of deficient beam-column sub assemblages under cyclic loading 2009; University of Stuttgart.

Sehgal VK, Bhandari NM, Kaushik SK. Ferrocement box girder elements for roofs and floors. Proc. 3rd International Conference Ferrocement, Department of Civil Engineering, University of Roorkee, 1988; 551-560.

Senthil E, Murugenesan A, Thirugnaman. Experimental study on behavior of Retrofitted with FRP wrapped RC Beam-Column Exterior Joints Subjected to cyclic loading. International Journal of Civil and Structural Engineering 2010;1(1);2010

Seshu DR. Flexural behavior of Ferrocement confined reinforced concrete (FCRC) simply supported beams. Journal of Ferrocement 2000; 30(3): 261-273.

Shahawy MA, Arockiasamy TM, Beitelmant T, Sowrirajan R. Reinforced concrete rectangular beams strengthened with CFRP laminates. Composites 1996; 27:225-33.

Sharma A, Genesio G, Reddy GR, Eligehausen R, Pampanin S, Vaze, KK. (2010). Experimental investigations on seismic retrofitting of reinforced concrete beam- column joints. Proceedings of the 14th Symposium on Earthquake Engineering 2010; Indian Institute of Technology, Roorkee, India, Paper No. A007.

Shehata AEM, Cerqueira EC, Pinto CTM, Coppe. Strengthening of RC beams in flexure and shear using CFRP laminate. Fiber Reinforced Plastic Concrete Structures 2001; 1:97-106.

Sheikh Shamin A. Performance of concrete structures retrofitted with fiber reinforced polymers. Elsevier Engineering Structures 2002; 22: 869-879.

Singh KK, Kaushik SK, Prakash A. Strengthening of brick masonry columns by Ferrocement. Proceedings of the Third International Symposium on Ferrocement, University of Roorkee, 1998; 306-315.

Singh SK, Kaushik SK. Flexural strengthening of reinforced concrete beams by Ferrocement. Maharashtra India Chapter of ACI, 1997; 17-24.

Singh SP, Kaushik SK. Behavior of Ferrocement Composite Columns in Compression American Concrete Institute SP172-36, 1997; 669-681.

Singh V, Kumar M, Bansal PP, Kaushik SK. Experimental studies on strength and ductility of CFRP jackted reinforced concrete beam-column joints. Construction building Materials 2014;55:194-201.

Singh, K.K., Kaushik, S.K. and Prakash, Anand. Ferrocement Composite Columns, Proceedings of 3rd International Conference Ferrocement, Department of Civil Engineering, University of Roorkee, 1988, pp 296-305.

Singhal H. Finite element modeling of retrofitted RCC beams**,** M.E. Thesis 2009; Thapar University, Patiala.

Subrahmanyam BV, Abdul Karim E, Ganesh Babu,K. Ferrocement ribbon roofs for long spans. Bulletin of international Assoc for shell Structures. 74,1980,PP 39-47

Supaviriyakit T, Pornpongsaroj P, Pimanmas A, Finite element analysis of FRP strengthened RC beams**.** Songklanakarin Journal Science Technology 2004; 26(4): 497-507.

Takiguchi K, Abdullah. Ferrocement as strengthening and repairing material for r/c columns. Seventh International Symposium on Ferrocement and Thin Reinforced Cement Composites, National University of Singapore, 27-29, 2001; 441-452.

Tavárez FA. Simulation of behavior of composite grid reinforced concrete beams using explicit finite element methods, Master's Thesis 2001; University of Wisconsin- Madison, Madison, Wisconsin.

Teng JG, Chen JF, Smith ST. FRP Strengthened RC Structures. John Wiley Publications, 2002.

Teng JG, lam L, Chan W, Wang J. Retrofitting of deficient RC cantilever slabs using GFRP strips. Journal of Composites for Construction 2000; 4(2): 75-84.

Toutanji H, Zhao L, Zhang Y. Flexural behavior of reinforced concrete beams externally strengthened with CFRP sheets bonded with an inorganic matrix. Engineering Structures 2006; 28(March): 557-66.

Triantafillou, Thanasis C. Shear strengthening of reinforced concrete beams using epoxy-bonded FRP composites. ACI Structural Journal,1998; 95(2): 107-115.

Tsai, Hsiang-Chuan, Lin, Guan-Cheng. Optimum tuned-mass dampers for minimizing steady-state response of support-excited and damped system. Earthquake Engineering and Structural Dynamics 1993; Vol. 22: 957-973.

Tsonos AG. Cyclic load behavior of reinforced concrete beam-column subassemblages of modern structures. ACI Structural Journal 2007; 104(4): 468-478.

Turner M J, Clough R W, Martin H C, Topp LJ. Stiffness and deflection analysis of complex structures. Journal of the Aeronautical Sciences 1956**;** 23: 805-823.

Uma SR, Prasad AM. Department of Civil Engineering Indian Institute of technology Madras, Chennai, Document No. :: IITK-GSDMA-EQ31-V1.0 (2003)

Vidivelli B, Antiny Jayasehar C, Srividya PR. Repair and rehabilitation of reinforced concrete beams by Ferrocement. Seventh International Symposium on Ferrocement and Thin Reinforced Cement Composites, National University of Singapore, 27-29, June 2001: 465-471.

Wang YC. Analytical and experimental study on seismic performance of rc t-beams with design deficiency in steel bar curtailment. Elsevier Engineering Structures 2003; 25: 215-227.

Wasti ST, Erberik MA, Sucuoglu H. Kaur C. Studies on strengthening of rural structures damaged in the 1995 dinar earthquakes. Proceedings of the Eleventh European Conference on Earthquake Engineering Paris, France (1998).

White RN. Seismic Rehabilitation of Non-Ductile Reinforced Concrete Frames – A Summary of issues, Methods and Needs. Proceedings, Workshop on the Seismic Rehabilitation of Lightly Reinforced Concrete Frames, Gaithersburg, USA, June 12-13, National Institute of Standards and Technology1995; 39-71.

Willam KJ, Warnke EP. Constitutive model for triaxial behaviour of concrete, Proceedings of the International Association of Bridge and Structural Engineering1975, Bergamo, Italy.

Wolanski, AJBS. Flexural Behavior of Reinforced and Prestressed Concrete Beams Using Finite Element Analysis. Master's Thesis; 2004 Marquette University, Milwaukee, Wisconsin.

Xiong GJ, Singh G. Behavior of weld mesh Ferrocement composite under flexural cyclic loads. Journal of Ferrocement 1992; 22 (3): 237-48.

Xiong, Guangjing. Liu, Jinwei Xie, Huicai. Flexural behavior of reinforced concrete beams with unbonded repair patch. ACI Structural Journal 2000; 97(5): 783-786.

Yang ZJ, Chen JF, Proverbs D. Finite element modeling of concrete cover separation failure in FRP plated RC beams. Construction Building Materials 2003; 17: 3-13.

APPENDIX

Table 5.1: Load vs Deflection Data for Controlled Beam-Column Joint Specimens

S.No.	Beam-Column Joint Sample 1 (S1)		Beam-Column Joint Sample 2 (S2)		Beam-Column Joint Sample 3 (S3)		Average (S1+S2+S3)/3	
	Load (kN)	Deflection (mm)	Load (kN)	Deflection (mm)	Load (kN)	Deflection (mm)	Load (kN)	Deflection (mm)
1	0.0	0.0	0.0	0.0	0.0	0.0	0.0	0.0
2	2.0	0.6	2.0	0.4	2.0	0.2	2.0	0.4
3	4.0	0.7	4.0	0.9	4.0	0.7	4.0	0.8
4	6.0	1.6	6.0	1.8	6.0	1.3	6.0	1.5
5	8.0	2.6	8.0	2.4	8.0	2.5	8.0	2.5
6	10.0	3.0	10.0	3.4	10.0	2.7	10.0	3.1
7	12.0	4.7	12.0	4.8	12.0	4.8	12.0	4.8
8	14.0	5.5	14.0	5.2	14.0	6.2	14.0	5.6
9	16.0	6.1	16.0	5.8	16.0	6.4	16.0	6.1
10	18.0	6.9	18.0	6.7	18.0	7.6	18.0	7.1
11	20.0	8.8	20.0	8.5	20.0	7.8	20.0	8.4
12	22.0	19.5	22.0	19.2	22.0	19.6	22.0	19.4
13	22.4	23.0	23.3	22.8	22.4	23.9	22.7	23.2

Table 5.2: Load vs Deflection Data and Other Derived Parameters for Controlled Beam-Column Joints Sample

S.No	Average Load P (kN)	Average Deflection Δ (mm)	Moment M (kN-m)	Rotation (ϕ)	Normalised Load P/P_U	Normalised Deflection Δ/Δ_U
1	0.0	0.0	0.0	0.00	0.0	0.0
2	2.0	0.4	1.0	0.00	0.1	0.0
3	4.0	0.8	2.0	0.00	0.2	0.0
4	6.0	1.5	3.0	0.00	0.3	0.1
5	8.0	2.5	4.0	0.00	0.4	0.1
6	10.0	3.1	5.0	0.01	0.4	0.1
7	12.0	4.8	6.0	0.01	0.5	0.2
8	14.0	5.6	7.0	0.01	0.6	0.2
9	16.0	6.1	8.0	0.01	0.7	0.3
10	18.0	7.1	9.0	0.01	0.8	0.3
11	20.0	8.4	10.0	0.02	0.9	0.4
12	22.0	19.4	11.0	0.04	1.0	0.8
13	22.7	23.2	11.3	0.05	1.0	1.0

Table 5.3: Load vs Deflection Data for 100 percent Stressed at Free End of Beam-Column Joints Retrofitted with Ferrocement Jacket Reinforced with Two layers of Woven Wire Mesh

S.No	Beam-Column Joint Sample 1(S1)		Beam-Column Joint Sample 2 (S2)		Beam-Column Joint Sample 3 (S3)		Average (S1+S2+S3)/3	
	Load (kN)	Deflection (mm)	Load (kN)	Deflection (mm)	Load (kN)	Deflection (mm)	Load (kN)	Deflection (mm)
1	0.0	0.0	0.0	0.0	0.0	0.0	0.0	0.0
2	2.0	0.6	2.0	0.6	2.0	0.7	2.0	0.5
3	4.0	1.2	4.0	1.2	4.0	1.6	4.0	1.0
4	6.0	2.1	6.0	2.0	6.0	2.3	6.0	1.7
5	8.0	2.9	8.0	3.0	8.0	3.1	8.0	2.5
6	10.0	3.7	10.0	3.9	10.0	3.9	10.0	2.9
7	12.0	6.0	12.0	5.1	12.0	5.1	12.0	3.7
8	14.0	5.5	14.0	5.7	14.0	5.7	14.0	4.4
9	16.0	6.8	16.0	6.9	16.0	6.1	16.0	4.7
10	18.0	7.0	18.0	7.7	18.0	6.9	18.0	5.3
11	20.0	8.8	20.0	8.0	20.0	7.7	20.0	6.0
12	22.0	10.0	22.0	9.8	22.0	8.2	22.0	7.0
13	24.0	11.1	24.0	11.3	24.0	12.9	24.0	7.7
14	26.0	13.0	26.0	13.7	26.0	13.0	26.0	9.0
15	26.9	14.9	27.1	15.4	26.1	15.9	26.7	15.4

Table 5.4: Load vs Deflection Data and Other Derived Parameters for 100 Percent Stressed at Free End of Beam-Column Joints Retrofitted with Ferrocement Jacket Reinforced with Two Layers of Woven Wire Mesh

S.No.	Average Load P(kN)	Average Deflection Δ (mm)	Moment M(kNm)	Rotation (ϕ) Δ/L	Normalised Load P/P_U	Normalised Deflection Δ/Δ_U
1	0.0	0.0	0.0	0.00	0.0	0.0
2	2.0	0.6	1.0	0.00	0.1	0.0
3	4.0	1.2	2.0	0.00	0.2	0.1
4	6.0	2.0	3.0	0.00	0.3	0.1
5	8.0	3.0	4.0	0.01	0.4	0.1
6	10.0	3.7	5.0	0.01	0.4	0.2
7	12.0	5.1	6.0	0.01	0.5	0.2
8	14.0	5.7	7.0	0.01	0.6	0.3
9	16.0	6.8	8.0	0.01	0.7	0.3
10	18.0	7.7	9.0	0.02	0.8	0.3
11	20.0	8.8	10.0	0.02	0.9	0.4
12	22.0	9.9	11.0	0.02	1.0	0.4
13	24.0	11.3	12.0	0.02	1.1	0.5
14	26.0	13.7	13.0	0.03	1.2	0.6
15	26.7	15.4	13.4	0.03	1.2	0.7

Table 5.5: Load vs Deflection Data for 85 Percent Stressed at Free End of Beam-Column Joints Retrofitted with Ferrocement Jacket Reinforced with Two Layers of Woven Wire Mesh

S.No.	Beam-Column Joint Sample 1(S1)		Beam-Column Joint Sample 2(S2)		Beam-Column Joint Sample 3(S3)		Average (S1+S2+S3)/3	
	Load (kN)	Deflection (mm)	Load (kN)	Deflection (mm)	Load (kN)	Deflection (mm)	Load (kN)	Deflection (mm)
1	0.0	0.0	0.0	0.0	0.0	0.0	0.0	0.0
2	2.0	0.9	2.0	0.2	2.0	0.2	2.0	0.4
3	4.0	1.4	4.0	0.4	4.0	1.7	4.0	1.3
4	6.0	1.9	6.0	0.8	6.0	2.7	6.0	2.0
5	8.0	2.7	8.0	0.8	8.0	3.9	8.0	2.5
6	10.0	3.2	10.0	1.0	10.0	4.5	10.0	2.9
7	12.0	4.0	12.0	1.9	12.0	5.2	12.0	3.7
8	14.0	4.3	14.0	2.0	14.0	5.7	14.0	4.0
9	16.0	4.8	16.0	2.6	16.0	6.2	16.0	4.5
10	18.0	5.4	18.0	3.0	18.0	6.6	18.0	5.0
11	20.0	6.2	20.0	4.2	20.0	7.4	20.0	6.0
12	22.0	6.9	22.0	4.7	22.0	8.1	22.0	6.6
13	24.0	7.7	24.0	5.8	24.0	9.0	24.0	7.5
14	26.0	9.3	26.0	7.7	26.0	10.7	26.0	9.2
15	27.9	12.9	28.1	13.5	26.8	14.2	27.6	13.5

Table 5.6: Load vs Deflection Data and Other Derived Parameters for 85 Percent Stressed at Free End of Beam-Column Joints Retrofitted with Ferrocement Jacket Reinforced with Two Layers of Woven Wire Mesh

S.No.	Average Load P(kN)	Average Deflection Δ (mm)	Moment M(kNm)	Rotation (ϕ) Δ/L	Normalised Load P/P_U	Normalised Deflection Δ/Δ_U
1	0.0	0.0	0.0	0.00	0.0	0.0
2	2.0	0.4	1.0	0.00	0.1	0.0
3	4.0	1.3	2.0	0.00	0.2	0.1
4	6.0	2.0	3.0	0.00	0.3	0.1
5	8.0	2.5	4.0	0.00	0.4	0.1
6	10.0	2.9	5.0	0.01	0.4	0.1
7	12.0	3.7	6.0	0.01	0.5	0.2
8	14.0	4.0	7.0	0.01	0.6	0.2
9	16.0	4.5	8.0	0.01	0.7	0.2
10	18.0	5.0	9.0	0.01	0.8	0.2
11	20.0	6.0	10.0	0.01	0.9	0.3
12	22.0	6.6	11.0	0.01	1.0	0.3
13	24.0	7.5	12.0	0.01	1.1	0.3
14	26.0	9.2	13.0	0.02	1.2	0.4
15	27.6	13.5	13.8	0.03	1.2	0.6

Table 5.7: Load vs Deflection Data for 50 Percent Stressed at Free End of Beam-Column Joints Retrofitted with Ferrocement Jacket Reinforced with Two Layers of Woven Wire mesh

S.No.	Beam-Column Joint Sample 1(S1)		Beam-Column Joint Sample 2 (S2)		Beam-Column Joint Sample 3(S3)		Average (S1+S2+S3)/3	
	Load (kN)	Deflection (mm)	Load (kN)	Deflection (mm)	Load (kN)	Deflection (mm)	Load (kN)	Deflection (mm)
1	0.0	0.0	0.0	0.0	0.0	0.0	0.0	0.0
2	2.0	0.3	2.0	0.5	2.0	0.5	2.0	0.4
3	4.0	0.9	4.0	1.2	4.0	1.1	4.0	1.0
4	6.0	1.1	6.0	1.6	6.0	1.6	6.0	1.4
5	8.0	1.6	8.0	2.2	8.0	2.2	8.0	2.0
6	10.0	2.2	10.0	2.7	10.0	2.9	10.0	2.6
7	12.0	2.8	12.0	3.5	12.0	3.6	12.0	3.3
8	14.0	3.5	14.0	4.0	14.0	4.1	14.0	3.9
9	16.0	3.8	16.0	4.4	16.0	4.5	16.0	4.2
10	18.0	4.3	18.0	5.1	18.0	5.1	18.0	4.8
11	20.0	5.0	20.0	5.7	20.0	5.9	20.0	5.5
12	22.0	6.9	22.0	7.1	22.0	6.9	22.0	7.0
13	24.0	7.8	24.0	8.4	24.0	7.8	24.0	8.0
14	26.0	8.8	26.0	10.7	26.0	8.5	26.0	9.3
15	26.2	10.1	27.2	14.4	27.0	13.1	26.8	12.5

Table 5.8: Load vs Deflection Data and Other Derived Parameters for 50 Percent Stressed at Free End of Beam-Column Joints Retrofitted with Ferrocement Jacket Reinforced with Two Layers of Woven Wire Mesh

S.No.	Average Load P(kN)	Average Deflection Δ (mm)	Moment M(kN-m)	Rotation (ϕ) Δ/L	Normalised Load P/P_U	Normalised Deflection Δ/Δ_U
1	0.0	0.0	0.0	0.00	0.0	0.0
2	2.0	0.4	1.0	0.00	0.1	0.0
3	4.0	1.0	2.0	0.00	0.2	0.0
4	6.0	1.4	3.0	0.00	0.3	0.1
5	8.0	2.0	4.0	0.00	0.4	0.1
6	10.0	2.6	5.0	0.01	0.4	0.1
7	12.0	3.3	6.0	0.01	0.5	0.1
8	14.0	3.9	7.0	0.01	0.6	0.2
9	16.0	4.2	8.0	0.01	0.7	0.2
10	18.0	4.8	9.0	0.01	0.8	0.2
11	20.0	5.5	10.0	0.01	0.9	0.2
12	22.0	7.0	11.0	0.01	1.0	0.3
13	24.0	8.0	12.0	0.02	1.1	0.3
14	26.0	9.3	13.0	0.02	1.2	0.4
15	26.8	12.5	13.4	0.03	1.2	0.5

Table 5.9: Load vs Deflection Data for 100 percent Stressed at Free End of Beam-Column Joints retrofitted with Ferrocement jacket Reinforced with Four Layers of Woven Wire Mesh

S.No.	Beam-Column Joint Sample 1 (S1)		Beam-Column Joint Sample 2 (S2)		Beam-Column Joint Sample 3 (S3)		Average (S1+S2+S3)/3	
	Load (kN)	Deflection (mm)	Load (kN)	Deflection (mm)	Load (kN)	Deflection (mm)	Load (kN)	Deflection (mm)
1	0.0	0.0	0.0	0.0	0.0	0.0	0.0	0.0
2	2.0	0.4	2.0	0.3	2.0	0.4	2.0	0.4
3	4.0	0.8	4.0	0.8	4.0	0.8	4.0	0.8
4	6.0	1.7	6.0	1.3	6.0	1.6	6.0	1.5
5	8.0	2.6	8.0	1.9	8.0	2.4	8.0	2.3
6	10.0	2.9	10.0	2.5	10.0	2.9	10.0	2.8
7	12.0	3.9	12.0	3.3	12.0	3.6	12.0	3.6
8	14.0	4.4	14.0	3.9	14.0	4.4	14.0	4.2
9	16.0	4.9	16.0	4.2	16.0	4.5	16.0	4.5
10	18.0	5.5	18.0	4.9	18.0	5.2	18.0	5.2
11	20.0	6.5	20.0	5.3	20.0	5.8	20.0	5.9
12	22.0	7.1	22.0	6.0	22.0	6.5	22.0	6.6
13	24.0	8.0	24.0	6.8	24.0	7.4	24.0	7.4
14	26.0	9.9	26.0	7.2	26.0	7.6	26.0	8.2
15	28.0	10.5	28.0	8.8	28.0	8.8	28.0	9.4
16	30.4	14.1	30.0	14.7	30.2	14.4	30.2	14.4

Table 5.10: Average, Load vs Deflection Data and Other Derived Parameters for 100 Percent Stressed at Free End of Beam-Column Joints Retrofitted with Ferrocement Jacket Reinforced with Four Layers of Woven Wire Mesh

S.No.	Average Load P(kN)	Average Deflection Δ (mm)	Moment M(kNm)	Rotation (ϕ) Δ/L	Normalised Load P/P_U	Normalised Deflection Δ/Δ_U
1	0.0	0.0	0.0	0.00	0.0	0.0
2	2.0	0.4	1.0	0.00	0.1	0.0
3	4.0	0.8	2.0	0.00	0.2	0.0
4	6.0	1.5	3.0	0.00	0.3	0.1
5	8.0	2.3	4.0	0.00	0.4	0.1
6	10.0	2.8	5.0	0.01	0.4	0.1
7	12.0	3.6	6.0	0.01	0.5	0.2
8	14.0	4.2	7.0	0.01	0.6	0.2
9	16.0	4.5	8.0	0.01	0.7	0.2
10	18.0	5.2	9.0	0.01	0.8	0.2
11	20.0	5.9	10.0	0.01	0.9	0.3
12	22.0	6.6	11.0	0.01	1.0	0.3
13	24.0	7.4	12.0	0.01	1.1	0.3
14	26.0	8.2	13.0	0.02	1.2	0.4
15	28.0	8.6	14.0	0.02	1.2	0.4
16	30.2	14.4	15.1	0.02	1.3	0.6

Table 5.11: Load vs Deflection Data for 85 Percent Stressed at Free End of Beam-Column Joints Retrofitted With Ferrocement Jacket Reinforced With Four Layers of Woven Wire Mesh

S.No.	Beam-Column Joint Sample 1(S1)		Beam-Column Joint Sample 2(S2)		Beam-Column Joint Sample 3(S3)		Average (S1+S2+S3)/3	
	Load (kN)	Deflection (mm)	Load (kN)	Deflection (mm)	Load (kN)	Deflection (mm)	Load (kN)	Deflection (mm)
1	0.0	0.0	0.0	0.0	0.0	0.0	0.0	0.0
2	2.0	0.5	2.0	0.3	2.0	0.5	2.0	0.4
3	4.0	0.9	4.0	0.9	4.0	0.8	4.0	0.8
4	6.0	1.5	6.0	1.4	6.0	1.6	6.0	1.3
5	8.0	2.1	8.0	1.9	8.0	1.8	8.0	2.0
6	10.0	2.9	10.0	2.4	10.0	2.4	10.0	2.6
7	12.0	3.5	12.0	2.7	12.0	2.4	12.0	2.9
8	14.0	4.2	14.0	3.4	14.0	2.9	14.0	3.5
9	16.0	4.4	16.0	3.8	16.0	2.9	16.0	3.7
10	18.0	5.1	18.0	4.4	18.0	3.4	18.0	4.3
11	20.0	5.6	20.0	5.2	20.0	4.0	20.0	4.9
12	22.0	6.2	22.0	6.0	22.0	4.5	22.0	5.5
13	24.0	7.4	24.0	7.8	24.0	4.9	24.0	6.2
14	26.0	7.8	26.0	7.6	26.0	5.3	26.0	6.8
15	28.0	8.0	28.0	9.9	28.0	5.2	28.0	7.7
16	29.1	14.0	29.6	12.5	29.5	10.4	29.4	10.4

Table 5.12: Load vs Deflection Data and Other Derived Parameters for 85 Percent Stressed at Free End of Beam-Column Joints Retrofitted with Ferrocement Jacket Reinforced with Four Layers of Woven Wire Mesh

S.No.	Average Load P(kN)	Average Deflection Δ (mm)	Moment M(kNm)	Rotation (ϕ) Δ/L	Normalised Load P/P_U	Normalised Deflection Δ/Δ_U
1	0.0	0.0	0.0	0.00	0.0	0.0
2	2.0	0.4	1.0	0.00	0.1	0.0
3	4.0	0.8	2.0	0.00	0.2	0.0
4	6.0	1.3	3.0	0.00	0.3	0.1
5	8.0	2.0	4.0	0.00	0.4	0.1
6	10.0	2.6	5.0	0.01	0.4	0.1
7	12.0	2.9	6.0	0.01	0.5	0.1
8	14.0	3.5	7.0	0.01	0.6	0.2
9	16.0	3.7	8.0	0.01	0.7	0.2
10	18.0	4.3	9.0	0.01	0.8	0.2
11	20.0	4.9	10.0	0.01	0.9	0.2
12	22.0	5.5	11.0	0.01	1.0	0.2
13	24.0	6.2	12.0	0.01	1.1	0.3
14	26.0	6.8	13.0	0.01	1.2	0.3
15	28.0	7.7	14.0	0.02	1.2	0.3
16	29.4	10.4	14.7	0.02	1.3	0.4

Table 5.13: Load vs Deflection Data for 50 Percent Stressed at Free End of Beam-Column Joints Retrofitted with Ferrocement Jacket Reinforced with Four Layers of Woven Wire Mesh

S.No.	Beam-Column Joint Sample 1(S1)		Beam-Column Joint Sample 2(S2)		Beam-Column Joint Sample 3(S3)		Average (S1+S2+S3)/3	
	Load (kN)	Deflection (mm)	Load (kN)	Deflection (mm)	Load (kN)	Deflection (mm)	Load (kN)	Deflection (mm)
1	0.0	0.0	0.0	0.0	0.0	0.0	0.0	0.0
2	2.0	0.6	2.0	0.2	2.0	0.1	2.0	0.3
3	4.0	1.0	4.0	0.6	4.0	0.3	4.0	0.8
4	6.0	1.6	6.0	1.0	6.0	0.6	6.0	1.2
5	8.0	2.7	8.0	1.4	8.0	1.2	8.0	1.5
6	10.0	3.5	10.0	2.0	10.0	1.3	10.0	2.3
7	12.0	4.3	12.0	2.7	12.0	1.6	12.0	2.9
8	14.0	4.8	14.0	3.2	14.0	1.9	14.0	3.3
9	16.0	5.2	16.0	3.5	16.0	2.0	16.0	3.6
10	18.0	5.9	18.0	3.9	18.0	2.1	18.0	4.0
11	20.0	7.5	20.0	4.0	20.0	2.3	20.0	4.5
12	22.0	8.0	22.0	4.9	22.0	3.0	22.0	5.3
13	24.0	8.8	24.0	5.7	24.0	3.3	24.0	6.0
14	26.0	9.5	26.0	6.8	26.0	3.4	26.0	6.6
15	28.0	13.7	28.2	10.3	29.0	9.9	28.4	11.3

Table 5.14: Load vs Deflection Data and Other Derived Parameters for 50Percent Stressed at Free End of Beam-Column Joints Retrofitted with Ferrocement Jacket Reinforced with Four Layers of Woven Wire Mesh

S.No.	Average Load P(kN)	Average Deflection Δ (mm)	Moment M(kNm)	Rotation (ϕ) Δ/L	Normalised Load P/P_U	Normalised Deflection Δ/Δ_U
1	0.0	0.0	0.0	0.00	0.0	0.0
2	2.0	0.3	1.0	0.00	0.1	0.0
3	4.0	0.8	2.0	0.00	0.2	0.0
4	6.0	1.2	3.0	0.00	0.3	0.1
5	8.0	1.5	4.0	0.00	0.4	0.1
6	10.0	2.3	5.0	0.00	0.4	0.1
7	12.0	2.9	6.0	0.01	0.5	0.1
8	14.0	3.3	7.0	0.01	0.6	0.1
9	16.0	3.6	8.0	0.01	0.7	0.2
10	18.0	4.0	9.0	0.01	0.8	0.2
11	20.0	4.5	10.0	0.01	0.9	0.2
12	22.0	5.3	11.0	0.01	1.0	0.2
13	24.0	6.0	12.0	0.01	1.1	0.3
14	26.0	6.6	13.0	0.01	1.2	0.3
15	28.4	11.3	14.2	0.02	1.3	0.5

Table 5.15: Load vs Deflection Data for 100 Percent Stressed at Free End of Beam-Column Joints Retrofitted with Ferrocement Jacket Reinforced with Six Layers of Woven Wire Mesh

S.No.	Beam-Column Joint Sample 1(S1)		Beam-Column Joint Sample 2(S2)		Beam-Column Joint Sample 3(S3)		Average (S1+S2+S3)/3	
	Load (kN)	Deflection (mm)	Load (kN)	Deflection (mm)	Load (kN)	Deflection (mm)	Load (kN)	Deflection (mm)
1	0.0	0.0	0.0	0.0	0.0	0.0	0.0	0.0
2	2.0	0.3	2.0	0.3	2.0	0.2	2.0	0.3
3	4.0	0.9	4.0	0.7	4.0	1.0	4.0	0.7
4	6.0	1.3	6.0	0.7	6.0	1.7	6.0	1.2
5	8.0	1.9	8.0	1.5	8.0	2.7	8.0	2.0
6	10.0	2.6	10.0	2.3	10.0	3.4	10.0	2.8
7	12.0	3.1	12.0	3.1	12.0	4.3	12.0	3.5
8	14.0	3.5	14.0	3.5	14.0	5.0	14.0	4.0
9	16.0	3.9	16.0	3.9	16.0	5.4	16.0	4.4
10	18.0	4.4	18.0	4.6	18.0	6.4	18.0	5.1
11	20.0	5.1	20.0	4.9	20.0	7.0	20.0	5.6
12	22.0	5.5	22.0	5.2	22.0	7.3	22.0	6.2
13	24.0	6.1	24.0	5.5	24.0	8.8	24.0	6.8
14	26.0	6.8	26.0	5.6	26.0	9.0	26.0	7.4
15	28.0	7.0	28.0	5.2	28.0	11.8	28.0	8.0
16	30.0	8.0	30.0	5.5	30.0	12.4	30.0	8.6
17	32.0	9.4	32.0	6.1	32.0	12.8	32.0	19.3

Table 5.16: Load vs Deflection Data and Other Derived Parameters for 100Percent Stressed at Free End of Beam-Column Joints Retrofitted with Ferrocement Jacket Reinforced with Six Layers of Woven Wire Mesh

S.No.	Average Load P(kN)	Average Deflection Δ (mm)	Moment M(kNm)	Rotation (ϕ) Δ/L	Normalised Load P/P_U	Normalised Deflection Δ/Δ_U
1	0.0	0.0	0.0	0.00	0.0	0.0
2	2.0	0.3	1.0	0.00	0.1	0.0
3	4.0	0.7	2.0	0.00	0.2	0.0
4	6.0	1.2	3.0	0.00	0.3	0.1
5	8.0	2.0	4.0	0.00	0.4	0.1
6	10.0	2.8	5.0	0.01	0.4	0.1
7	12.0	3.5	6.0	0.01	0.5	0.2
8	14.0	4.0	7.0	0.01	0.6	0.2
9	16.0	4.4	8.0	0.01	0.7	0.2
10	18.0	5.1	9.0	0.01	0.8	0.2
11	20.0	5.6	10.0	0.01	0.9	0.2
12	22.0	6.2	11.0	0.01	1.0	0.3
13	24.0	6.8	12.0	0.01	1.1	0.3
14	26.0	7.4	13.0	0.01	1.2	0.3
15	28.0	8.0	14.0	0.02	1.2	0.3
16	30.0	8.6	15.0	0.02	1.3	0.4
17	32.0	19.3	16.0	0.02	1.4	0.8

Table 5.17: Load vs Deflection Data for 85 Percent Stressed at Free End of Beam-Column Joints Retrofitted with Ferrocement Jackets Reinforced with Six Layers of Woven Wire Mesh

S.No.	Beam-Column Joint Sample 1(S1)		Beam-Column Joint Sample 2(S2)		Beam-Column Joint Sample 3(S3)		Average (S1+S2+S3)/3	
	Load (kN)	Deflection (mm)	Load (kN)	Deflection (mm)	Load (kN)	Deflection (mm)	Load (kN)	Deflection (mm)
1	0	0.0	0.0	0.0	0.0	0.0	0.0	0.0
2	2	0.3	2.0	0.6	2.0	0.3	2.0	0.4
3	4	0.9	4.0	1.3	4.0	0.9	4.0	1.0
4	6	1.4	6.0	2.0	6.0	1.6	6.0	1.6
5	8	1.8	8.0	2.5	8.0	2.1	8.0	2.2
6	10	2.3	10.0	3.1	10.0	2.7	10.0	2.7
7	12	2.8	12.0	3.6	12.0	3.5	12.0	3.3
8	14	3.6	14.0	4.5	14.0	4.0	14.0	4.0
9	16	4.1	16.0	5.1	16.0	4.3	16.0	4.5
10	18	4.8	18.0	6.0	18.0	4.9	18.0	5.2
11	20	5.5	20.0	6.7	20.0	5.7	20.0	6.0
12	22	6.2	22.0	7.9	22.0	5.6	22.0	6.6
13	24	7.3	24.0	9.2	24.0	6.3	24.0	7.6
14	26	7.4	26.0	11.5	26.0	6.3	26.0	8.4
15	28	8.8	28.0	12.8	28.0	7.0	28.0	9.5
16	30	10.2	30.0	13.7	30.0	8.1	30.0	10.7
17	31	18.9	31.0	18.0	31.0	18.5	31.0	18.5

Table 5.18: Average, Load vs Deflection Data and Other Derived Parameters for 85 Percent Stressed at Free End of Beam-Column Joints Retrofitted with Ferrocement Jacket Reinforced with Six Layers of Woven Wire Mesh

S.No.	Average Load P(kN)	Average Deflection Δ (mm)	Moment M(kNm)	Rotation (ϕ) Δ/L	Normalised Load P/P_U	Normalised Deflection Δ/Δ_U
1	0.0	0.0	0.0	0.00	0.0	0.0
2	2.0	0.4	1.0	0.00	0.1	0.0
3	4.0	1.0	2.0	0.00	0.2	0.0
4	6.0	1.6	3.0	0.00	0.3	0.1
5	8.0	2.2	4.0	0.00	0.4	0.1
6	10.0	2.7	5.0	0.01	0.4	0.1
7	12.0	3.3	6.0	0.01	0.5	0.1
8	14.0	4.0	7.0	0.01	0.6	0.2
9	16.0	4.5	8.0	0.01	0.7	0.2
10	18.0	5.2	9.0	0.01	0.8	0.2
11	20.0	6.0	10.0	0.01	0.9	0.3
12	22.0	6.6	11.0	0.01	1.0	0.3
13	24.0	7.6	12.0	0.02	1.1	0.3
14	26.0	8.4	13.0	0.02	1.2	0.4
15	28.0	9.5	14.0	0.02	1.2	0.4
16	30.0	10.7	15.0	0.02	1.3	0.5
17	31.0	18.5	15.5	0.02	1.4	0.8

Table 5.19: Load vs Deflection Data for 50 Percent Stressed at Free End of Beam-Column Joints Retrofitted With Ferrocement Jackets Reinforced with Six Layers of Woven Wire Mesh

S.No.	Beam-Column Joint Sample 1(S1)		Beam-Column Joint Sample 2(S2)		Beam-Column Joint Sample 3(S3)		Average (S1+S2+S3)/3	
	Load (kN)	Deflection (mm)	Load (kN)	Deflection (mm)	Load (kN)	Deflection (mm)	Load (kN)	Deflection (mm)
1	0.00	0.00	0.00	0.00	0.00	0.00	0.00	0.00
2	2.00	0.37	2.00	0.48	2.00	0.42	2.00	0.42
3	4.00	0.80	4.00	0.82	4.00	0.90	4.00	0.84
4	6.00	1.27	6.00	1.41	6.00	1.43	6.00	1.37
5	8.00	1.67	8.00	1.87	8.00	1.98	8.00	1.84
6	10.00	2.19	10.00	2.25	10.00	2.50	10.00	2.32
7	12.00	2.59	12.00	2.56	12.00	3.06	12.00	2.74
8	14.00	3.20	14.00	2.87	14.00	3.40	14.00	3.16
9	16.00	3.55	16.00	2.97	16.00	3.75	16.00	3.42
10	18.00	4.03	18.00	3.41	18.00	4.24	18.00	3.90
11	20.00	4.62	20.00	3.81	20.00	4.83	20.00	4.42
12	22.00	5.11	22.00	4.01	22.00	5.73	22.00	4.95
13	24.00	5.81	24.00	4.52	24.00	6.73	24.00	5.68
14	26.00	7.17	26.00	4.47	26.00	7.94	26.00	6.53
15	28.00	8.26	28.00	4.97	28.00	8.88	28.00	7.37
16	30.00	9.08	30.00	5.86	30.6	9.85	30.2	13.48

Table 5.20: Load vs Deflection Data and Other Derived Parameters for 50 Percent Stressed at Free End of Beam-Column Joints Retrofitted with Ferrocement Jacket Reinforced with Six Layers of Woven Wire Mesh

S.No.	Average Load P(kN)	Average Deflection Δ (mm)	Moment M(kNm)	Rotation (ϕ) Δ/L	Normalised Load P/P_U	Normalised Deflection Δ/Δ_U
1	0.0	0.0	0.0	0.00	0.0	0.0
2	2.0	0.4	1.0	0.00	0.1	0.0
3	4.0	0.8	2.0	0.00	0.2	0.0
4	6.0	1.4	3.0	0.00	0.3	0.1
5	8.0	1.8	4.0	0.00	0.4	0.1
6	10.0	2.3	5.0	0.00	0.4	0.1
7	12.0	2.7	6.0	0.01	0.5	0.1
8	14.0	3.2	7.0	0.01	0.6	0.1
9	16.0	3.4	8.0	0.01	0.7	0.2
10	18.0	3.9	9.0	0.01	0.8	0.2
11	20.0	4.4	10.0	0.01	0.9	0.2
12	22.0	5.0	11.0	0.01	1.0	0.2
13	24.0	5.7	12.0	0.01	1.1	0.2
14	26.0	6.5	13.0	0.01	1.2	0.3
15	28.0	7.4	14.0	0.01	1.2	0.3
16	30.2	13.5	15.1	0.02	1.3	0.6

Table 5.23: Load vs Deflection Data for 100 percent Stressed at Free End of Beam-Column Joints Retrofitted with Two Layers of CFRP Jacket

S.No.	Beam-Column Joint Sample 1(S1)		Beam-Column Joint Sample 2 (S2)		Average (S1+S2)/2	
	Load (kN)	Deflection (mm)	Load (kN)	Deflection (mm)	Load (kN)	Deflection (mm)
1	0.0	0.0	0.0	0.0	0.0	0.0
2	2.0	1.1	2.0	0.9	2.0	1.0
3	4.0	2.6	4.0	2.2	4.0	2.4
4	6.0	3.7	6.0	3.5	6.0	3.6
5	8.0	5.3	8.0	4.8	8.0	5.0
6	10.0	6.1	10.0	5.9	10.0	6.0
7	12.0	7.4	12.0	7.0	12.0	7.2
8	14.0	7.9	14.0	7.5	14.0	7.7
9	16.0	8.6	16.0	8.3	16.0	8.4
10	18.0	9.6	18.0	9.2	18.0	9.4
11	20.0	10.5	20.0	10.3	20.0	10.4
12	22.0	11.7	22.0	11.5	22.0	11.6
13	24.0	15.1	24.0	14.8	24.0	14.8
14	25.2	22.4	24.4	21.6	24.8	22.0

Table 5.24: Load vs Deflection Data and Other Derived Parameters for 100 Percent Stressed at Free End of Beam-Column Joints Retrofitted with Two Layers of CFRP Jackets

S.No	Average Load P (kN)	Average Deflection Δ (mm)	Moment M (kN-m)	Rotation (ϕ)	Normalised Load P/P_U	Normalised Deflection Δ/Δ_U
1	0.0	0.0	0.0	0.0	0.0	0.0
2	2.0	1.0	1.0	0.0	0.1	0.0
3	4.0	2.4	2.0	0.0	0.2	0.1
4	6.0	3.6	3.0	0.0	0.3	0.2
5	8.0	5.0	4.0	0.0	0.4	0.2
6	10.0	6.0	5.0	0.0	0.4	0.3
7	12.0	7.2	6.0	0.0	0.5	0.3
8	14.0	7.7	7.0	0.0	0.6	0.3
9	16.0	8.4	8.0	0.0	0.7	0.4
10	18.0	9.4	9.0	0.0	0.8	0.4
11	20.0	10.4	10.0	0.0	0.9	0.5
12	22.0	11.6	11.0	0.0	1.0	0.5
13	24.0	14.8	12.0	0.0	1.1	0.6
14	24.8	22.0	12.4	0.0	1.1	1.0

Table 5.25: Load vs Deflection Data for 85 percent Stressed at Free End of Beam-Column Joints Retrofitted with Two Layers of CFRP Jacket

S.No.	Beam-Column Joint Sample 1(S1)		Beam-Column Joint Sample 2 (S2)		Average (S1+S2)/2	
	Load (kN)	Deflection (mm)	Load (kN)	Deflection (mm)	Load (kN)	Deflection (mm)
1	0.0	0.0	0.0	0.0	0.0	0.0
2	2.0	0.7	2.0	0.7	2.0	0.7
3	4.0	2.3	4.0	2.3	4.0	2.3
4	6.0	3.3	6.0	3.3	6.0	3.3
5	8.0	4.3	8.0	4.3	8.0	4.3
6	10.0	5.3	10.0	5.3	10.0	5.3
7	12.0	6.7	12.0	6.6	12.0	6.7
8	14.0	7.6	14.0	7.1	14.0	7.3
9	16.0	8.2	16.0	8.1	16.0	8.2
10	18.0	9.3	18.0	8.7	18.0	9.0
11	20.0	9.7	20.0	9.6	20.0	9.7
12	22.0	10.7	22.0	10.7	22.0	10.7
13	24.0	16.8	24.0	16.5	24.0	16.7
14	25.2	23.9	25.6	23.5	25.4	23.7

Table 5.26: Load vs Deflection Data and Other Derived Parameters for 85 Percent Stressed at Free End of Beam-Column Joints Retrofitted with Two layers of CFRP Jackets

S.No	Average Load P (kN)	Average Deflection Δ (mm)	Moment M (kN-m)	Rotation (ϕ)	Normalised Load P/P_U	Normalised Deflection Δ/Δ_U
1	0.0	0.0	0.0	0.00	0.0	0.0
2	2.0	0.7	1.0	0.00	0.1	0.0
3	4.0	2.3	2.0	0.00	0.2	0.1
4	6.0	3.3	3.0	0.01	0.3	0.1
5	8.0	4.3	4.0	0.01	0.4	0.2
6	10.0	5.3	5.0	0.01	0.4	0.2
7	12.0	6.7	6.0	0.01	0.5	0.3
8	14.0	7.3	7.0	0.01	0.6	0.3
9	16.0	8.2	8.0	0.02	0.7	0.4
10	18.0	9.0	9.0	0.02	0.8	0.4
11	20.0	9.7	10.0	0.02	0.9	0.4
12	22.0	10.7	11.0	0.02	1.0	0.5
13	24.0	16.7	12.0	0.03	1.1	0.7
14	25.4	23.7	12.7	0.05	1.1	1.0

Table 5.27: Load vs Deflection Data for 50 percent Stressed at Free End of Beam-Column Joints Retrofitted with Two Layers of CFRP Jacket

S.No.	Beam-Column Joint Sample 1(S1)		Beam-Column Joint Sample 2 (S2)		Average (S1+S2)/2	
	Load (kN)	Deflection (mm)	Load (kN)	Deflection (mm)	Load (kN)	Deflection (mm)
1	0.0	0.0	0.0	0.0	0.0	0.0
2	2.0	0.9	2.0	0.9	2.0	0.9
3	4.0	2.1	4.0	2.1	4.0	2.1
4	6.0	3.0	6.0	2.9	6.0	3.0
5	8.0	3.8	8.0	3.8	8.0	3.8
6	10.0	4.7	10.0	4.7	10.0	4.7
7	12.0	5.9	12.0	5.9	12.0	5.9
8	14.0	6.6	14.0	6.6	14.0	6.6
9	16.0	7.1	16.0	7.1	16.0	7.1
10	18.0	8.5	18.0	8.5	18.0	8.5
11	20.0	9.8	20.0	9.7	20.0	9.7
12	22.0	11.1	22.0	11.1	22.0	11.1
13	24.0	19.2	24.0	19.0	24.0	19.1
14	24.6	20.2	24.3	20.0	24.4	20.1

Table 5.28: Load vs Deflection Data and Other Derived Parameters for 50 Percent Stressed at Free End of Beam-Column Joints Retrofitted with Two layers of CFRP Jackets

S.No	Average Load P (kN)	Average Deflection Δ (mm)	Moment M (kN-m)	Rotation (ϕ)	Normalised Load P/P_U	Normalised Deflection Δ/Δ_U
1	0.0	0.0	0.0	0.00	0.0	0.0
2	2.0	0.9	1.0	0.00	0.1	0.0
3	4.0	2.1	2.0	0.00	0.2	0.1
4	6.0	3.0	3.0	0.01	0.3	0.1
5	8.0	3.8	4.0	0.01	0.4	0.2
6	10.0	4.7	5.0	0.01	0.4	0.2
7	12.0	5.9	6.0	0.01	0.5	0.3
8	14.0	6.6	7.0	0.01	0.6	0.3
9	16.0	7.1	8.0	0.01	0.7	0.3
10	18.0	8.5	9.0	0.02	0.8	0.4
11	20.0	9.7	10.0	0.02	0.9	0.4
12	22.0	11.1	11.0	0.02	1.0	0.5
13	24.0	19.1	12.0	0.04	1.1	0.8
14	24.4	20.1	12.2	0.04	1.1	0.9